Effect of Particle Size and Relative Density on Dynamic Resistance and Subgrade Modulus of Clean Sand

by

Md. Assaduzzaman

A thesis submitted to the Department of Civil Engineering,
Bangladesh University of Engineering and Technology,
Dhaka, in partial fulfillment of the degree of

MASTER OF SCIENCE IN CIVIL ENGINEERING (Geotechnical)

DEPARTMENT OF CIVIL ENGINEERING
BANGLADESH UNIVERSITY OF ENGINEERING AND TECHNOLOGY
DHAKA

AUGUST, 2014

The project titled **"Effect of Particle Size and Relative Density on Dynamic Resistance and Subgrade Modulus of Clean Sand"** Submitted by **Md. Assaduzzaman,** Roll No. **0412042238(F),** Session **April 2012,** has been accepted as satisfactory in partial fulfillment of the requirement for the degree of **Master of Science in Civil Engineering (Geotechnical)** on **August 16, 2014**.

BOARD OF EXAMINERS

____

Dr. Md. Jahangir Alam — Chairman (Supervisor)
Associate Professor
Department of Civil Engineering
BUET, Dhaka - 1000.

____

Dr. A. M. M. Taufiqul Anwar — Member
Professor & Head
Department of Civil Engineering
BUET, Dhaka - 1000

____

Dr. Mehedi Ahmed Ansary — Member
Professor
Department of Civil Engineering
BUET, Dhaka-1000

____

Dr. Md. Rokonuzzaman — Member (External)
Associate Professor
Department of Civil Engineering
KUET, Khulna- 9203

Candidate's Declaration

It is hereby declared that this project or any part of it has not been submitted elsewhere for the award of any degree or diploma.

August, 2014

(Md. Assaduzzaman)

TABLE OF CONTENTS

LIST OF FIGURES

List of Tables

Notations

CBR	= California Bearing Ratio;
CPT	= Cone penetration test;
DCP	= Dynamic cone penetrometer;
DP	= Dynamic probing;
DPL	= Dynamic probing light;
DPM	= Dynamic probing medium;
DPH	= Dynamic probing heavy;
DPSH	= Dynamic probing super heavy;
DS	= Deviator stress;
E	= Modulus of elasticity;
$E_{PLT(i)}$	= Initial tangent modulus;
$E_{PLT(R2)}$	= Reloading stiffness modulus;
FWD	= Falling weight deflectometer;
g	= Acceleration of gravity;
H	= Height of fall;
K_s	= Modulus of subgrade reaction;
M	= Mass of hammer;
MS	= Mild steel;
MSP	= Multiple sieving pluviation;
N_{10}	= Number of blow required for 10 cm penetration of cone;
P	= Applied load;
P_{index}	= Penetration Index (rate of penetration in mm/blow);
R	= Radius of plate;
D_r	= Relative Density;
SS	= Stainless steel;
SPT	= Standard penetration test;
TRL	= Transportation Research Laboratory
UCS	= Unconfined compressive strength;
γ_{max}	= Maximum index dry density;
γ_{min}	= Minimum index dry density;
γ_d	= Field dry density;
δ	= Deflection of plate;

Acknowledgement

The author wishes to express his deep appreciation to the almighty Allah for allowing him to bring an end of this thesis. Then he desires to convey his admiration to his supervisor Dr. Md Jahangir Alam, Associate Professor, Department of Civil Engineering, Bangladesh University of Engineering and Technology (BUET), for his keen interest, valuable suggestions, proper guidance, cordial association and supervision throughout the project work. In the different stages of study and report making, his appropriate opinion and suggestions helped to avoid omissions, confusions and inconsistency. Without his profuse help throughout the time of the research work, this thesis work could not have been completed

The author gratefully acknowledges the construction criticisms and valuable suggestions made by Professor Dr. Mehedi Ahmed Ansary and Associate Professor Dr. Md. Rokonuzzaman.

Thanks are extended to Mr. Ziaur Rahman who started to develop this correlation as a part of his undergraduate thesis and Mr. Abul kalam Azad who made a correlation between Relative Density and N_{10} for Sylhet sand and Jamuna sand using DCP and DPL in his M.Sc. Engineering thesis.

Thanks are also extended to Mr. Shahabuddin, Mr. Khokon from geotechnical lab and Mr. Golam Rabbani from strength materials lab for their helps and assistance during experimental works.

Last but not the least, the author gratefully acknowledges his parents’ patience and encouragement during two years of his M. Sc. Engineering study in BUET.

Abstract

The present study was aimed at developing an alternative indirect method which can be used to determine Relative Density, Initial Tangent Modulus and Modulus of Subgrade Reaction for clean sand of any particle size. To know the height of fall and hole diameter of sand discharging bowl for a desired Relative Density of a specific sand, the air pluviation method was calibrated in the first stage. Then in the second stage sand deposits of different relative densities were prepared in calibration chamber and Dynamic Probing Light (DPL), Dynamic Cone Penetrometer (DCP) tests and Plate Load Test (PLT) were performed on the prepared sand deposit. Correlation between P_{index} (rate of penetration in mm/blow) and Relative Density was made from the test results in calibration chamber. Based on the test results, resistance of sand increase exponentially with increasing Relative Density for different mean diameter (D_{50}) of particles but the larger mean diameter of particles of sand shows the higher resistance at same Relative Density than the smaller mean diameter of particles. Correlation among Initial Tangent Modulus ($E_{PLT(i)}$), Subgrade Modulus (K_s), Relative Density and P_{index} was made from the test result in calibration chamber. It was found that Initial Tangent Modulus ($E_{PLT(i)}$) and Subgrade Modulus (K_s) increases with increasing Relative Density. On the other hand, mean diameter (D_{50}) of particles has large effect on the Initial Tangent Modulus ($E_{PLT(i)}$) and Subgrade Modulus (K_s). Larger mean diameter (D_{50}) of particle shows the higher value of Initial Tangent Modulus ($E_{PLT(i)}$) and Subgrade Modulus (K_s) at same Relative Density. Therefore, Initial Tangent Modulus ($E_{PLT(i)}$) and Subgrade Modulus (K_s) decrease exponentially with increasing P_{index} for different mean diameter of particle. In the third stage, the correlation was verified for three dredge fill sites where DCP and DPL results were compared with the result from Sand Cone Method. At the last stage, CBR test was performed at laboratory at field density to make the correlation among CBR value, Relative Density (%) and field P_{index} for DPL and DCP. CBR value decreases exponentially with increasing P_{index} value for both DPL and DCP. A generalized correlation between P_{index} and Relative Density for clean sand of any particle size was found from this study. To determine in situ Relative Density of sand deposit, it is concluded that the proposed method (DCP and DPL) can be used as an alternative indirect method which is suitable up to 2 m depth.

CHAPTER 1
INTRODUCTION

1.1 General

The density of granular soils varies with the shape and size of grains, the gradation and the manner in which the mass is compacted. The term used to indicate the strength characteristics in a qualitative manner is Relative Density (D_r)(Murthy, 1993) which describes the state condition in cohesionless soils. It is commonly used to identify liquefaction potential under earthquake or other shock-type loading (Seed and Idris, 1971). So Relative Density is a very important index for a sandy soil. Relative Density is 0% for loosest condition of sand and 100% for densest condition of sand. If maximum index density and minimum index density of sand is determined in laboratory as per ASTM D4253 and D4254, and field dry density is determined by any one of the methods such as Sand Cone Method (ASTM D1556), Sleeve Method (ASTM D4564), Rubber Balloon Method (ASTM D2167), and Drive-Cylinder Method (ASTM D2937), Relative Density can be calculated using the following formula.

$$D_r(\%) = \left(\frac{\gamma_d - \gamma_{\min}}{\gamma_{\max} - \gamma_{\min}}\right) \cdot \left(\frac{\gamma_{\max}}{\gamma_d}\right) .100 \text{ ------------------------------ } 1.1$$

Where,

γ_d = field dry density of sand deposit

$\gamma_{\max}$ = maximum index density

$\gamma_{\min}$ = minimum index density

Relative Density can be expressed in terms of void ratio as follows:

$$D_r(\%) = \left(\frac{e_{\max} - e}{e_{\max} - e_{\min}}\right) .100 \text{ ---------------------------------- } 1.2$$

Where,

e_{max}=Maximum possible void ratio

e_{min}=Minimum possible void ratio

e = void ratio in natural state of soil

Sand fill are required for many purposes, for example, backfill of earth retaining structures, backfill in foundation trenches, reclamation of low lands etc. In all these situations good compaction of fill should be ensured to avoid future subsidence, failure of foundation and moreover liquefaction. Relative Density is the most appropriate index to control the compaction of sand fill. Depending on the importance of structure, minimum Relative Density generally be specified as 70% to 95%.

The method of performing plate load test (PLT) on soils and flexible pavement is described by ASTM D1195-93. In this method, the PLT test should continue until a peak load is reached or until the ratio of load increment to settlement increment reaches a minimum, steady magnitude. Generally, a load increment is applied when the rate of deformation has approached about 0.001 inch/min. As in the case for other stress-strain tests, different elasticity moduli can be obtained from the PLT. Soil elasticity moduli can be defined as: (1) the initial tangent modulus; (2) the tangent modulus at a given stress level; (3) reloading and unloading modulus and; (4) the secant modulus at a given stress level. In this study, the initial tangent modulus and reloading modulus were determined for all plate load tests.

1.2 Background of the Study

To develop low lands, dredge fill sand is usually used which meet the need of growing people to construct many facilities like model towns, inland container terminal, deep sea-port etc. It is proved that dredge fill sand is liquefiable from several case studies of earthquakes. In earthquake when seismic liquefaction occurs, even pile foundations could not save the structure from damage in many cases. To make the sand fill non liquefiable it should be well compacted. Mitigation measures become very expensive if a structure is constructed on liquefiable soil and it would be damaged during earthquake. So, it is very important to control the quality of sand fill.

In our country, quality control of sand fill is done by determining field density near the top surface of fill using Sand Cone Method (ASTM D1556-90, 2006). It has limitations because it is a direct method of determining field density and Relative Density of sand fill. This method is very difficult to perform at deeper locations. Sand Cone Method has to be applied to control the quality of sand fill after compaction/densification of each layer of fill. For this reason it is time consuming and expensive to use Sand Cone Method. Sand Cone Method cannot be applied in saturated sand or where water table is high. To determine Relative Density of sand fill easily, it is necessary to develop an indirect method which can be performed in all seasons and in any location. In road construction, there is a need to assess the adequacy of a subgrade to behave satisfactorily beneath a pavement. Proper pavement performance requires satisfactorily performing subgrade. Therefore further study is necessary to understand the effect of particle size and relative density on penetration index, initial tangent modulus and subgrade modulus.

1.3 Objectives of this Study

The main objectives of the study areas follow

I. To calibrate the DCP and DPL in a calibration chamber so that a correlation can be made between Penetration Index (P_{index}) and Relative Density (D_r) for sand by using of different mean diameter sand having D_{50}=0.70 mm and 0.35 mm respectively.

II. To develop a relationship between Subgrade Modulus (K_s) and Relative Density (D_r); Subgrade Modulus (K_s) and Penetration Index (P_{index}); Initial Tangent Modulus ($E_{PLT(i)}$)and Relative Density (D_r); Initial Tangent Modulus ($E_{PLT(i)}$) and Penetration Index (P_{index}).

III. To develop a relationship between CBR value and Relative Density ($D_{r)}$; CBR value and Penetration Index (P_{index}).

1.4 Methodology

The present study was carried out in three stages.

The air pluviation method was calibrated to know the height of fall and hole diameter and spacing of discharging bowl for a desired Relative Density of specific sand in the first stage.

In the second stage using this relation between Relative Density and height of fall, sand deposits of different relative densities were prepared in calibration chamber. On the prepared sand deposit DPL, DCP and Plate Load tests were performed.

Penetration of cone was recorded for every blow of hammer. N_{10} and P_{index} value of DCP and DPL tests were determined. N_{10} is the number of blows per 10 cm of penetration of dynamic cone and P_{index} is the penetration rate of cone in mm/blow. To get a generalized correlation for various sizes of sand, P_{index} values were normalized by multiplying it with $D_{50}^{0.75}$. Then a generalized correlation between Relative Density and $P_{index}D_{50}^{0.75}$ were found in DPL and DCP for clean sand of any particle size. It is not worthy that DCP and DPL test data of Hossain, M. S., (2009) was also used to get the generalized correlation.

In Plate Load Test (PLT), ASTM-D1196 method was followed to perform the plate load test. In Plat Load test, plate diameter, applied load increments and the corresponding deflections were recorded for each load increment. Each increment of load was maintained until the rate of deflection became less than 0.001 inch/min for three consecutive minutes. Each sample was loaded to failure or until load capacity of the loading frame has been reached. Settlement of the plate for each load increment was recorded during the test. These values are then used to plot soil pressure settlement relationship.

A tangent was drawn to the initial portion of the curve to determine the load and corresponding settlement that will be used in order to obtain the initial tangent modulus ($E_{PLT(i)}$) and modulus of subgrade reaction(K_s) of the test layer.To get a universal correlation for various sizes of sand in PLT, Relative Density values were normalized by multiplying it with $D_{50}^{0.20}$. Then a generalized correlation between Initial tangent modulus $E_{PLT(i)}$ and D_r $D_{50}^{0.20}$subgrade reaction was determined from the soil pressure and settlement curve.

In the third stage, the generalized correlation between Relative Density and penetration index (P_{index}) was verified from the test results in three dredge fill sites. At the same location Relative Density was determined using Sand Cone Method and dynamic cone resistance data. This data helped to improve the generalized correlation by incorporating depth correction factor (R_d) and fines correction factor (R_{FC}).

Finally, California Bearing Ratio (CBR) test was performed in laboratory at the field density to develop the correlation between CBR value and Relative Density, CBR value and penetration index (P_{index}).

1.5 Organization of the Thesis

The thesis consists of five chapters and two appendices. In Chapter One, background and objectives of the research is described. Chapter Two contains the literature review where history, use and researches on DCP are described. In this chapter description of apparatus DCP, DPL, Hydraulic Jack and load frame are given. Chapter Three describes the testing arrangement and program. Chapter Four contains results and discussion. Chapter Five contains Regression Model Analysis by SPSS. Chapter Six contain the conclusions and recommendations for further research. All graphs of DCP, DPL and Plate load tests in calibration chamber are presented in Appendix A.

CHAPTER 2
LITERATURE REVIEW

2.1 Introduction

The literature review given here is consisting of (a) Principles of Dynamic Cone Penetrometer (DCP) test and Dynamic Probing, (b) Description of DCP and DPL,(c) researches on DCP, (d) Application of DCP, (e) Factors affecting DCP and DPL result, (f) Static Plate Load test (SPLT) and (g) California Bearing Ratio (CBR) test.

2.2 General Principle of Dynamic Probing

To drive a pointed probe (cone), a hammer of mass M and a height of fall H are used. Typical arrangement of Dynamic Probing is shown in Fig. 2.1. The hammer strikes on anvil which is rigidly attached to extension rods. The penetration resistance is defined as the number of blows required to drive the probe a defined distance. The energy of a blow is the mass of the hammer times the acceleration of gravity and times the height of the fall. Dynamic probing is mainly used in cohesionless soils. In interpreting the test results obtained in cohesive soils and in soils at great depth, caution has to be taken when friction along the extension rod is significant. Dynamic probing can be used to detect soft layers and to locate strong layers as, for example, in cohesion less soils for end bearing piles (DPH, DPSH). In connection with key borings, soil type and cobble and boulder contents can be evaluated under favourable conditions. After proper calibration, the results of dynamic probing can be used to get an indication of engineering properties, e.g. Relative Density, compressibility, shear strength, consistency etc. For the time being, quantitative interpretation of the results including predictions of bearing capacity remains restricted mainly to cohesionless soils; it has to be taken into account that the type of cohesionless soil (grain size distribution, etc.) may influence the test result.In order to run the Dynamic Cone Penetration (DCP) or DPL test, two operators are required. One person drops the hammer and the other records measurements. The first step of the test is to put the cone tip on the testing surface. The lower shaft containing the cone moves independently from the reading rod sitting on the testing surface throughout the test reading is counted as initial penetration corresponding to blow 0. Fig. 2.2 shows the penetration result. The initial reading is not usually equal to 0 due to the disturbed loose state of the ground surface and the self weight of the testing equipment. The value of the initial from the first drop of the hammer. Hammer blows are repeated and the penetration depth is measured for each hammer drop. This process is continued until a desired penetration depth is reached. As shown in Fig. 2.3, DCP test results consist of number of blow counts versus penetration depth. Since the recorded blow counts are cumulative values, results of DCP test in general are given as incremental values defined as follows:

$$P_{index} = \frac{\Delta D_{p2}}{\Delta BC} \text{------------------------------------} 2.1$$

Where,

P_{index} = DCP/DPL penetration index in units of length divided by blow count;

ΔD_p= incremental penetration depth;

ΔBC = blow counts corresponding to incremental penetration depth ΔD_p.

As a result, values of the penetration index (P_{index}) represent DCP test characteristics at certain depths.

2.3 Various Types of Dynamic Probing

To indicate that a continuous record is obtained from the test in contrast to the expression probing is used, for example, the Standard Penetration Test (SPT). This is a simple test consisting of driving a rod with an oversize point at its base into the ground with a uniform hammer blow. Dynamic Probing (DP) is carried out as per BS 1377: 1990. The test involves driving a solid steel 90 degree cone into the bottom of the bore hole. The blow count is recorded for every 10 cm of driving (N_{10}) and the results presented as a plot of blow count against depth. Four different probing types, DPL, DPM, DPH and DPSH are available to fit different topographic and geological conditions and various purposes of investigation. In Table 2.1 Differences among these four types of probing are summarized.

Dynamic Probing Light (DPL): Representing the lower end of the mass range of dynamic cone used the world wide, the investigation depth usually is not larger than about 8 m if reliable results are to be obtained.

Dynamic Probing Medium (DPM): Representing the medium mass range; the investigation depth usually is not larger than about 20 to 25 m.

Dynamic Probing Heavy (DPH): Representing the medium to very heavy mass range; the investigation depth usually is not larger than about 25 m.

Dynamic Probing Super Heavy (DPSH): Representing the upper end of the mass range and simulating closely the dimensions of the SPT; the investigation depth can be larger than 25 m.

There are four different methods for dynamic probing DPC: DPL, DPM, DPH and DPSH. The abbreviation L, M, H and SH stand for the weight of the equipment, which is described as Light, Medium, Heavy and Super Heavy, respectively. The input energy for each type of probing is dependent upon the weight of the hammer and the drop height. According to the specific energy per blow, the blow count of the dynamic probing of any weight category can be converted by the ratios of specific energy per blow to the Super Heavy dynamic probing blow using the Equation 2.2.

$$N(SH) = 0.7\,N(H) = 0.63\,N(M) = 0.21\,N(L) \quad -------------------2.2$$

2.4 Specification of Dynamic Probing Light (DPL)

Dimensions and masses of DPL are given in Fig. 2.4 and Table 2.2. The driving device consists of the hammer, the anvil and the guide rod.

Anvil: Fig. 2.5 shows the anvil of DPL which is rigidly connected to the extension rod. The diameter of the anvil shall not be less than 100 mm and not more than the half the diameter of the hammer. The axis of the anvil, guide rod and extension rod shall be straight with a maximum deviation of 5 mm per meter. Total of mass of anvil and guide rod is 6 kg.

Hammer: The weight of hammer used here is 10 kg. The dimensions of the hammer are shown in Fig. 2.6. The hammer shall be provided with an axial hole with a diameter which is about 3 to 4 mm larger than the diameter of the guide rod. The ratio of the length to the diameter of the cylindrical hammer shall be between 1 and 2. The hammer shall fall freely and not be connected to any object which may influence the acceleration and deceleration of the hammer. The velocity shall be negligible when the hammer is released in its upper position.

Extension Rod: The extension rod material should have high toughness at low temperatures and high fatigue strength. It also should be of high-strength steel with high resistance to wear. Permanent deformation must be capable of being corrected. The rods shall be straight. Solid rods can be used; hollow rods should be preferred in order to reduce the weight of the rod. Joints shall be flush with the rods. The deflection (from a straight line through the ends) at the midpoint of 1-m push rod shall not exceed 0.5 mm for the five lowest push rods and 1 mm for the remainder.

Cone: In Fig. 2.7, it shows a typical cone of DPL. The dimensions of cone are given in Table 2.2. The cone consists of a conical part (tip), a cylindrical extension, and a conical transition with a length equal to the diameter of the cone between the cylindrical extension and the rod. The cone, when new, shall have a tip with an apex angle of 90°. The tip of the cone may be cut (e.g. by wear) about less than 10% of the diameter from the theoretical tip of the cone. The maximum permissible wear of the cone is given in Table 2.2. The cone shall be attached to the rod in such a manner that it does not loosen during driving. Fixed or detachable cones can be used.

2.4.1 Research by dynamic probing light (DPL)

The test with the DPL is summarized by the penetration of a cone with 10 cm^2 of area coupled to a set of threaded rods 1 m in length. In the top there is an anvil that receives the impact of a hammer in a free fall manner, which mass is corresponding to 98.1 N. Each 10 cm of penetration is marked by the number of blows known as N_{10}. Most of the background research on the DPL has been basically targeted on comparisons between the SPT and the CPT test.

Nilsson & Cunha (2004) conducted studies with the DPL for estimating load capacity of piles for a tropical soil with the presence of a particular “porous clay”, as it is colloquially known in Brasília city. The authors assumed that the possible measurement of torque (a new feature) obtained in DPL tests could provide lateral friction resistances by the advancing tip and body of the DPL, which obviously can be associated with the lateral friction of a driven pile. Accordingly, these authors adopted an energy derived formula for pile driving, as the Hiley equation, and a simple moment equation for the measured torque, in order to derive the lateral DPL lateral resistance. As explained by these authors, such resistance could be further calibrated, via field pile loading tests, to consider into the equations a possible pile scale effect and the construction methodology, hence to be further employed into real pile analyses. Although it is particularly not a Brazilian research, Martins & Miranda (2005) conducted several tests with the aim to obtain correlations between various penetrometers focusing their comparisons between DPL and CPT tests in granitic soils from several urban locations in the North of Portugal, i.e. Essentially Porto, Braga and Guimaraes. The authors found good correlations between the CPT resistance and the DPL.

Sousa & Fonseca (2006) made correlations of the DPL with the SPT and the CPT, based on results of plate load tests and the use of various methods of load forecasting for shallow foundations, including the methods of Burland & Burbidge (1985) and Anagnastopoulos et al. (1991). The soils chosen by these authors were a granite residual soil, a schist soil, a massive natural residual soil of granite, and a soil of volcanic origin. The authors compared the prediction results, and showed that there was a good agreement of the DPL with other penetrometers, with the exception of the case of the granite residual soil.

Azevedo & Guimarães (2010) made a direct correlation between the N_{30} of the SPT test and the N_{10} of the DPL. The field experiment was conducted in a stretch of an electrical transmission line in the state of Acre, in Brazil and the authors warned that more studies on this particular correlation would be necessary. It is noticed that the geotechnical literature often fails to show a good agreement between the DPLand the SPT testing results. Nilsson (2004), Ávila & Conciani (2005) and Ribeiro Junior et al. (2007) made valuable observations about the inadequacies of these comparisons.

Nilsson (2004) made several considerations about the differences between the DPL test and the SPT. This latter author stated that by using these two tests simultaneously for situations where each one is more effective, one could surely obtain better correlations and results improving the efficiency of the design.

Ávila & Conciani (2005) concluded that for soils of low resistance in Mato Grosso, the SPT and the DPL do not correlate well. According to Ribeiro Júnior et al. (2007), the SPT test is best suited for granular soils, with SPTs (N_{30}) above 5, where the deep foundation generally has a length greater than 5 m, whereas the DPL test is more useful in fine-grained soils of low resistance, where it could be used for the prediction of deep foundation capacity loads in buildings up to 5 m high (2 stores). It is worthwhile to say that the DPL test is extremely sensitive to small variations to stratifications within the soil deposit, feature generally not found in SPT tests.

In addition to that, some studies have been conducted to compare different DPL configurations. Ávila et al. (2006) in a comparative study between two types of DPLs (DPL Nilsson, and DPL CEFET) concluded that the configuration of the equipment do influence directly on the efficiency of the test. However, Souza et al. (2008) concluded that the density of the rods have little influence on the results. Thus, the choice between a thicker or thinner than normal rod should solely affect the durability of the device.

2. 5 Dynamic Cone Penetration (DCP)

For the rapid in situ measurement of the structural properties of existing road pavements with unbound granular materials the Transportation Research Laboratory Dynamic Cone Penetration (TRL-DCP) test apparatus is designed. Continuous measurements can be made to a depth of 800 mm or to 1200 mm when an extension rod is fitted. The underlying principle of the DCP is that the rate of penetration of the cone, when driven by a standard force, is inversely related to the strength of the material as measured by the California Bearing Ratio (CBR) test where the pavement layers have different strength, the boundaries between the layers can be identified and the thickness of the layers are determined.

Three operators are needed to operate the DCP; one to hold the instrument, one to raise and drop the weight and a technician to record the results. The instrument is held vertical; the weight is carefully raised up to the handle; then the weight is dropped on anvil freely. Care should be taken to ensure that the weight is touching the handle, but not lifting the instrument before it is allowed to drop. The operator lets the weight fall freely and does not lower it with his hand. If, during the test, the DCP tilts from the vertical, no attempt should be made to correct this as contact between the shaft and the sides of the hole will give rise to erroneous results. The test should be abandoned if the angle of the instrument becomes worse, causing the weight to slide on the hammer shaft and not fall freely. A reading should be taken at increments of penetration of about 10 mm is recommended. However it is usually easier to take readings after a set numbers blows. It is therefore necessary to change the number of blows between readings according to the strength of the layer being penetrated.

2.5.1 History of dynamic cone penetration (DCP)

The Dynamic Cone Penetration test (DCPT) was developed in Australia by Scala (1956). The current model was developed by the Transvaal Roads Department in South Africa (Luo, 1998). The mechanics of the DCPT shows features of both the CPT and SPT. The DCPT is performed by dropping a hammer from a certain fall height measuring penetration depth per blow for a certain depth. Therefore it is quite similar to the procedure of obtaining the blow count N using the soil sampler in the SPT. In the DCPT, however, a cone is used to obtain the penetration depth instead of using the split spoon soil sampler. In this respect, there is some resemblance with the CPT in the fact that both tests create a cavity during penetration and generate a cavity expansion resistance. In road construction, there is a need to assess the adequacy of a subgrade to behave satisfactorily beneath a pavement. Proper pavement performance requires a satisfactorily performing subgrade. A recent Joint Transportation Research Program project by Luo (1998) was completed showing that the DCPT can be used to evaluate the mechanical properties of compacted subgrade soils.

DCP was developed in 1956 in South Africa as in situ evaluation of pavement layer strength (Scala, 1956) which is also known as the Scala penetrometer. Since then, this device has been extensively used in South Africa, the United Kingdom, the United

States, Australia and many other countries, because of its portability, simplicity, cost effectiveness, and the ability to provide rapid measurement of in situ strength of pavement layers and subgrades. Later, DCP is standardized by ASTM (ASTM D 6951-03). The DCP has also been proven to be useful during pavement design and quality control program. The DCP, however, was not a widely accepted technique in the United States in the early 1980s (Ayers et. al., 1989). De Beer (1991), Burnham and Johnson (1993), Burnham (1997), Newcomb et al (1994) and Hasan (1996) have shown considerable interest in the use of the DCP for several reasons. Firstly, the DCP is adaptable to many types of evaluations. Secondly, there are no other available rapid evaluation techniques and finally DCP test is economical.

2.5.2 Parts of DCP

The design specification of the parts has a tremendous impact on the results collected from the tests so various parts of the DCP are very important. The schematic diagram of DCP instrument is shown in Fig. 2.8. The instrument is made by Stainless Steel for better efficiency and longer life time. The various parts of DCP are described in the following paragraphs.

Probing Cone: The most important part of the DCP instruments is Probing cone. Probing cone enters through the sand as test starts. So the design of the probing cone must be perfect according to the standards. We use a probing cone of 1.95 cm high and the angle of the cone is 60°. The diameter of the probing cone at the edge is 2.25 cm. The cone size can affect the results significantly. The various dimensions of cone are shown in Fig. 2.9.

Anvil: Another important part of DCP is Anvil. The hammer falls on the anvil each time a data is intended to collect. The anvil is connected to the extension rod. It is also made of stainless steel. Anvil also contains the clamp which holds the scale in position shown in Fig. 2.11.

Guide Rod: Guide rod is used for guiding the hammer to fall on the anvil. It is made of stainless steel and the diameter of the guiding rod is 1.6 cm. The length of the guide rod without thread is 81.4 cm.

Hammer: In the DCP an 8 kg hammer is used. The hammer moves along the guide rod. The dimensions are given in Fig. 2.12.

Extension Rod: We can join extension rod one after another with each other and make a long rod for larger depth. Extension rods are 100 cm long and its diameter is 1.6 cm.

Handle: On the top of a guide rod a handle is attached. It helps the operator to hold the instrument in place and also a guide for the operator to move the hammer up to that level. The dimensions are shown in Fig. 2.13.

Damping Washer: Damping washer is put in the junction of hammer and the anvil. It lessens the collision sound and also extends the longevity of the instrument. It may be a piece of geo-textile or any damping material.

1 m Scale: For taking the reading of the penetrated rod in mm per blow a one meter stainless steel scale is also used.

2.5.3 Correlations with DCP

Researchers tried to establish correlation between other test parameters and DCP test results. In this section brief review of those correlations are presented.

2.5.3.1 Relationship between penetration index (P_{index}) and CBR values

Several authors have investigated relationships between the DCP penetration index P_{index} and California Bearing Ratio (CBR). CBR values are often used in road and pavement design. Two types of equations have been considered for the correlation between the P_{index} and CBR. Those are the log-log and inverse equations.
The log-log and inverse equations for the relationship can be expressed as the following general forms

log-log equation: $$M_R = 235.3P_{index}^{-0.475} \text{--------------------} 2.3$$

Inverse equation: $$(CBR) = D(P_{index})E + F \text{---------------------} 2.4$$

Where,

CBR = California Bearing Ratio;

P_{index}= penetration index obtained from DCPT in units of mm/blow or in/blow; A, B, C, D, E, and F = regression constants for the relationships.

Extensive research has been performed to develop empirical relationships between DCP penetration resistance and CBR measurements (e.g., Kleyn, 1975; Harison,1987; Livneh, 1987; Livneh and Ishai, 1988; Chua, 1988; Harison, 1983; Van Vuuren,1969; Livneh, et. al., 1992; Livneh and Livneh, 1994; Ese et. al., 1994; and Coonse,1999).For example, Livneh (1987) and Livneh, M. (1989) proposed the following relationships based on field and laboratory tests:

$$\text{Log(CBR)} = 2.20 - 0.71(\log P_{index})^{1.5} \quad \text{------------------------------} \; 2.5$$

$$\text{Log(CBR)} = 2.14 - 0.69(\log P_{index})^{1.5} \quad \text{------------------------------} \; 2.6$$

After further examination of results by other authors, Livneh et al. (1994) proposed the following equation as the best correlation.

$$\text{Log(CBR)} = 2.46 - 1.12(\log P_{index}) \quad \text{------------------------------} \; 2.7$$

In 1983, Smith and Pratt (1983) proposed the correlation between CBR and Penetration Index.

$$\text{Log(CBR)} = 2.56 - 1.15(\log P_{index}) \quad \text{------------------------------} \; 2.8$$

It can be seen that Harrison’s correlation is almost the same as the Smith and Pratt’s correlation, which suggests a higher level of confidence for both correlations. Another DCP versus CBR correlation, which is available in the literature is the correlation suggested by the Army Corps of Engineers.

$$\text{CBR} = \frac{292}{P_{index}^{1.12}} \quad \text{--------------------------------------} \; 2.9$$

Where, P_{index} is in mm/blow.

After further testing at the Waterways Experiment Station (WES), it was found that the data for CBR with values less than 10% and the data for fat clay do not agree with

Equation 2.12. The following correlations were then developed for soils with CBR values less than 10% (Webster et al., 1992).

If CBR < 10%

$$CBR = \frac{1}{(0.017019 P_{index})^2} \text{------------------------------} 2.10$$

For fat clays (CH)

$$CBR = \frac{1}{(0.002871 P_{index})} \text{------------------------------} 2.11$$

A summary of some of these correlations is presented in Table 2.3

2.5.3.2 *Relationship between penetration index (P_{index}) and resilient modulus (MR)*

Several researchers have developed correlations between Resilient Modulus (MR) and DCPI. Hassan (1996) indicated that the correlation of MR with the DCPI significant at optimum moisture content but insignificant at optimum moisture content + 20%. He developed a simple regression model in the following form:

$$MR\,(psi) = 7013.065 - 2040.783 \ln (P_{index}) \text{------------------------------} 2.12$$

Where, P_{index} is in inches/blow

Chai and Roslie (1998) used the results of CBR-DCP relationships and the DCP tests to determine in situ subgrade modulus in the following form:

$$E(MN/m^2) = 17.6 \left(\frac{269}{DCP}\right)^{0.64} \text{------------------------------} 2.13$$

Where, DCP = blows/300mm penetration.

They also developed a relationship between the back calculated modulus and the DCP value in the following form:

$$E(back) = 2224\, DCP^{-0.996} \text{------------------------------} 2.14$$

Where, E(back) = Back calculated subgrade modulus (MN/m^2),
Jianzhou et al. (1999) found that there was a strong relationship between DCP and the FWD-back calculated moduli in the following form:

$$E(back) = 338P_{index}^{-0.39} \text{-------------------------------------} 2.14$$

Where, P_{index} is in inches/blow

George and Uddin (2000) developed relationships between MR and DCPI as a function of moisture content, liquid limit, and density. Due to the MDOT requirements for being able to correlate MR in real time, they also provided simpler one to one relationships between P_{index} (DCP) and MR. For fine grained soils the following relationship was developed.

$$M_R = 532.1P_{index}^{-0.492} \text{-------------------------------------} 2.15$$

The relationship for coarse-grained soils is of the following form:

$$M_R = 235.3P_{index}^{-0.475} \text{-------------------------------------} 2.16$$

2.5.3.3 Application of DCP in unconfined compressive strength evaluation of lime-stabilized subgrade

McElvaney and Djatnika (1991), based on laboratory studies, have concluded that PI values can be correlated to the Unconfined Compressive Strength (UCS) of soil lime mixtures. They considered both individual and combined soil types in their analysis. They have also concluded that the inclusion of data on mixtures from material with zero lime content has negligible effects on the correlation equations, indicating that the correlation is mainly a function of strength and not the way in which strength is achieved.

This observation was valid only for lower range of strain values. For the combined data, three relationships, with each model permitting estimated unconfined compressive strength to a predetermined reliability level, were developed. Their first relationship was a best fit for 50 percent line, which implies that there is a 50 percent probability that the value of UCS determined from the measured PI value using the regression equation will underestimate the .real value. They also developed relationships such that with different degrees of confidence (96 and 99 percent), the probability of underestimation is reduced to 15 percent. These relationships are summarized below.

50% probability of underestimation

$$\text{Log UCS} = 3.56 - 0.807 \ \text{Log}(P_{index}) ------------------------- 2.16$$

95% confident that probability of under estimation will not exceed 15 percent

$$\text{Log UCS} = 3.29 - 0.809 \ \text{Log}(P_{index}) ------------------------- 2.17$$

99% confident that probability of under estimation will not exceed 15 percent

$$\text{Log UCS} = 3.21 - 0.809 \ \text{Log}(P_{index}) ------------------------- 2.18$$

Where, UCS = unconfined compressive strength (kPa).

In addition, the DCP, through its correlations with CBR, has been used to characterize stabilized bases and subgrades in isolated projects, but no consistent methodologies have been proposed (Little, et al., 1995). The DCP has also been used to verify Falling Weight Deflectometer (FWD) measurements and consequently, moduli back calculation derived from FWD deflection data for stabilized bases and subbases.

2.5.3.4 Relationships between DCP penetration index (P_{index}) and shear strength of cohesionless materials

Ayers et al (1989) carried out a laboratory study to determine relationships between Penetration Index and the shear strength properties of cohesionless granular materials. Prediction equations are of' the form:

$$DS = A - B(P_{index}, DCP) ------------------------------ 2.19$$

Where,

DS =Deviator stress at failure for confining pressures of 5, 15, and 30 psi (35, 103, and 207 kPa).

The selection of the appropriate prediction equation requires an estimate of the confining pressure under field loading conditions, which was stated to require further investigation.

2.5.3.5 Relationships between DCP penetration index (P_{index}) and standard penetration resistance

Sowers and Hedges (1966), and later Livneh and Ishai (1988), developed a correlation between Penetration Index ($P_{index,\ DCP}$) and rate of penetration ($P_{index,\ SPT}$) in SPT sampler (ASTM D1586-64). By Penetration Index ($P_{index,\ DCP}$) they meant rate of penetration of DCP cone in mm/blow. They also expressed rate of penetration of SPT sampler ($P_{index,\ SPT}$) in mm/blow. Their correlation, which is valid for SPT < 0.40 inches/blow or 10 mm/ blow, is

$$\text{Log}\,(P_{\text{Iindex, DCP}}) = -A + B\text{Log}(P_{\text{index, SPT}}) ----------------------- 2.20$$

Where,

$P_{index,\ DCP}$ = Penetration Index in mm/blow

$P_{index,\ SPT}$ = SPT sampler penetration rate in mm/blow

This correlation is shown in Fig. 2.14.

2.5.3.6 Equations to relate CBR to modulus

One of the most commonly required inputs in pavement design is the modulus value. Thus, the relationship between CBR and modulus becomes essential to implement the DCP in pavement evaluation. The AASHTO Guide for Design of Pavement Structures adopted Equation 2.21 for calculating moduli (E), which was proposed by Huekelom and Klomp (1962)

$$E(psi) = 1500\,CBR \quad \text{or} \quad E(MPa) = 10.34\,CBR \text{ ------------------- } 2.21$$

The moduli from which this correlation RVAS developed ranged from 750 to 3000 times the CBR. Also, the formula is limited to fine-grained soil with a soaked CBR of 10 or less. Porvell el al.(1984) indicated a relationship between modulus and CBR as

$$E(psi) = 2500 CBR^{0.64} \quad \text{or} \quad E(MPa) = 17.58\ CBR^{0.64} \text{ --------------- } 2.22$$

Equation 2.22 was selected to compute modulus values in this study. A relationship between CBR and modulus has been reported by Van Til et al. (1972). This study also compared the moduli obtained from all CBR-Modulus relationship.

The modulus is one of the most common parameters in pavement design. The American Association of State Highway and Transportation Officials (AASHTO) Design Guide suggests the use of the following equation, which was developed by Shell, to convert a CBR value to a Young's modulus value (E)in English units (psi) or metric units (MPa).

$$E(psi) = 2500\ CBR \quad \text{or} \quad E(MPa) = 10.34\ CBR \text{ ---------------- } 2.23$$

Other common conversion equations follow:
From the U.S. Army Corps of Engineers Research and Development Center Waterways Experiment Station:

$$E(psi) = 5409\ CBR^{0.711} \quad \text{or} \quad E(MPa) = 37.3\ CBR^{0.711} \text{ -------------- } 2.24$$

From the Transport & Road Research Laboratory (TRRL) in the United Kingdom:

$$E(psi) = 2500\ CBR^{0.64} \quad \text{or} \quad E(MPa) = 17.6\ CBR^{0.64} \text{ ---------------- } 2.25$$

From the Danish Road Laboratory:

$$E(psi) = 1500\ CBR^{0.73} \quad \text{or} \quad E(MPa) = 10\ CBR^{0.73} \text{ ---------------- } 2.26$$

Once the CBR value is determined from Equation 2.21and is input into one of Equations 2.23 through 2.26, a modulus is calculated. Results from these equations are quite different. Figure 2.21 illustrates the differences among these equations. As one can see from the variety of conversion equations, groups tend to develop their own equations suited for local conditions. The variety among the local soils tested by the groups is a likely factor contributing to the differences among Equations 2.23 to 2.26. The AASHTO equation (Equation 2.23) reflects a middle of the road number. The U.S. Army Engineer Research and Development Center Waterways Experiment Station is in Vicksburg, Mississippi, and the equation (Equation 2.24) developed there likely reflects soils in that region. The TRRL is in the United Kingdom, and the Danish Road Lab is in Denmark.

ORITE conducted a federally funded experiment on U.S. Route 35 to compare the stiffness determined by DCP testing, the stiffness gauge, German plate, FWD and laboratory data. The experiment was conducted during construction. The first series of non-destructive tests were performed when the subgrade was finished, and the second series of tests were performed when the base was completed. The project was successfully concluded and the report was provided the Federal Highway Administration (FHWA) and ODOT. Currently, ORITE is preparing a technical note from that report.

De Villiers (1980) developed an equation representing the relationship between DCP readings and Unconfined Compressive Strength (UCS) and found reasonably good correlation. Kleyn and Savage (1982) suggested that analyzing to a depth of 800 mm (31.5 in) beneath the surface is sufficient for pavement structure investigation. Therefore, DSN800 is considered the pavement structural number. Based on heavy vehicle simulator results (rut criteria), equations expressing the relationship between sustainable axle load and DSN800 were developed. Chen et al. (Chen, Lin, Liau, and Bilyeu, 2005) tried to estimate modulus based on DCP testing results. After eliminating outlier data, they developed a correlation equation as follows:

$$E\ (\mathrm{ksi}) = 78.05 P_{index}^{-06645} \quad \text{or} \quad E\,(\mathrm{MPa}) = 537.76\ P_{index}^{-0.6645} \text{------------} 2.27$$

Where,

E= Young’s Modulus and

P_{index}= the penetration rate of the DCP in mm/blow.

To assess in-situ test methods, Abu-Farsakh et al. (Abu-Farsakh, Alshibli, Nazzal and Seyman, 2004) developed equations showing the correlations between the DCP (P_{index}) data and Static Plate Load (SPL) test, Falling Weight Deflectometer (FWD) test, and CBR test data collected in the field. The correlations between the PR and both the initial modulus and the reloading stiffness of the SPL test are as follows:

For initial modulus,

$$E_i(MPa) = \frac{17421.2}{P_{index}^{2.05} + 62.53} - 5.71 \quad \text{or} \quad E_i(Ksi) = \frac{2526.7}{P_{index}^{2.05} + 62.53} - 0.828 ----- 2.28$$

And for reloading modulus,

$$E_R(MPa) = \frac{5142.61}{P_{index}^{1.57} + 14.8} - 3.49 \quad \text{or} \quad E_R(Ksi) = \frac{745.873}{P_{index}^{1.57} - 14.8} - 0.506 ------ 2.29$$

The correlation between the PR and back-calculated modulus from a FWD test is:

$$\ln(M_{AFWD}) = 2.35 + \frac{5.21}{\ln(P_{index})} ------------------------------ 2.30$$

And the correlation between the PR and CBR is:

$$CBR = \frac{5.1}{P_{index}^{0.2} - 1.41} ---------------------------------- 2.31$$

Abu-Farsakh et al. concluded that the values calculated using DCP results are more consistent and correct than values calculated based on data from either a Geogauge or a Light Falling Weight Deflectometer (LFWD). The DCP is an effective tool for identifying layers and can take deep measurements than the other devices. In particular, this study showed that the DCP readings correlate better with CBR values than data gathered using the other two devices. Therefore, DCP test results can be used to profile in-situ CBR values or the modulus of the base and subgrade. Good correlations between PR and other common soil property parameters indicate that DCP testing is a reliable means of measuring base and subgrade stiffness. DCP testing should therefore be accepted as an alternative means of doing so, and the engineer should be able to present the in-situ stiffness of base and subgrade directly in terms of penetration rate.

2.6 Procedure of DCP and DPL Uses

All DCP and DPL tests were performed by two operators. One person operated the hammer, while the other person reads and records the penetrations. Before each test, the tip of the ruler used to measure the penetrations was placed to a marked reference point on the surface. The person who took the readings was responsible to ensure that the ruler was kept parallel to the penetrating rod while taking measurements. Friction between the rod and the tested material has negative effects on the results. In order to minimize the friction of the rod with surrounding soil, the DCP and DPL must be kept vertical during penetration. If the DCP and DPL deviates from vertical position and operator continues to test, the device might be damaged and the results obtained for that test will not be reliable.

Removing the DCP and DPL after the test is completed may be difficult for certain soils. Striking the hammer gently against the handle is an effective method but striking forcefully may damage the DCP and DPL. For testing of stiff soils, disposable cones were preferred over standard cones in order to eliminate the difficulty in retrieving the device from the soil. Disposable cones are designed for one time use. They mount on an adapter which is screwed into the penetration rod to replace the standard cone. At the end of the test, the disposable cone slides off the cone adapter, allowing the operator to easily remove the rod from the soil with minimum effort.

2.7 Applications of DCP

DCP testing can be applied to the characterization of subgrade and base material properties in many ways. Perhaps the greatest, strength of the DCP device lies in its ability to provide a continuous record of relative soil strength with depth. By plotting a graph of penetration index (P_{index}) versus depth below the testing surface, a user can observe a profile showing layer depths, thicknesses and strength conditions. This can be particularly helpful in cases where the original as built plans for a project were lost, never created, or found to be inaccurate. In confined areas such as inside buildings to evaluate foundation settlements, or used on congested sites (trees, steep topography, soft soils, etc.) that would prevent larger testing equipment from being used. The DCP is ideal for testing through core holes in existing pavements. The DCP other strength lies in its small and relatively light weight design. It can be used the following applications outline either existing or proposed uses of DCP testing.

2.7.1 Application in weakly cemented sands

Naturally cemented deposits are very common throughout many parts of the world. These deposits are often characterized by their ability to withstand steep natural slopes. Some studies have indicated that the static cone penetrometer can locate sand layers with very low cementation. Correlations have also been developed between the cone resistance and the strength parameters for very weakly cemented sands (e.g., Puppala, et al., 1995; and Day, 1996). Their results have also demonstrated the significance of incorporating the effect of any cementation in estimating the strength parameters of sands.

2.7.2 Application in soil classification and estimation of soil properties and relative density

Because of its simple and economical design DCP is being applied in the field to characterize the subgrade and base materials in several ways. One of the greatest advantages of the DCP device lies in its ability to provide a continuous record of relative soil strength with the depth. By plotting a graph of penetration index versus depth, one can observe the profile showing layer depths and strength conditions as shown in Fig. 2.21.

2.7.2.1 Soil classification

One of the main applications of the static cone penetrometer is for stratiographic profiling. There is considerable experience related to the identification and classification of the soil using the cone penetration test (e.g., Douglas and Olsen, 1981; Olsen and Farr, 1986; and Roberston, 1990).Robertson (1990) reported a soil classification system based on CPT using normalized cone penetration test results with pore pressure measurements. Using normalized parameters and the available extensive CPT database, new charts were developed to represent a three dimensional classification system. Factors such as changes in stress history, in situ stresses, sensitivity, stiffness, macrofabric and void ratio were included in the development of the charts. From an investigation of a series of case histories in Herfordshire, U.K., in which the DCP has been used, Huntley (1990) suggested a tentative classification system of soil based on penetration resistance; n in blows per 100 mm as illustrated in Tables 2.4 and 2.5. However he recommended the use of classification tables with considerable caution until a better understanding of the mechanics of skin friction on the upper drive rod is established.

2.7.2.2 Soil parameters

The cone resistance has been correlated to soil friction angle of granular soils and also to the consistency of cohesive soils (e.g., DeMello, 1971). Robertson, et al. (1982) correlated the cone resistance to the mean grain size (D_{50}) of the soil, which covered a wide range of soil types**.**

2.7.2.3 Relative density

Several investigators including Schmertmann (1978), Villet and Mitchell (1981), Baldi et al. (1982, 1986), Robertson and Campanella (1983), Jamiolkowski et al. (1985, 1988), Puppala et al. (1995), and Juang et al. (1996) have developed correlations for the relative density (D_r) as a function of quality control (qc) for sandy soils. These relationships are also functions of vertical effective stress. A more rational theory for the correlations, which can be used for general conditions, has been developed by Salgado et al. (1997). The reader may refer to these papers for further information.

2.7.3 Preliminary soil surveys

DCP testing can be done during; preliminary soil investigations to quickly map out areas of weak material. Some have used it to locate potentially collapsible soils. By running an initial DCP test, and then flooding the 1ocation with water and running another test, a noticeable increase in the P_{index} (less shear strength) might indicate a potentially collapsible, or moisture sensitive soil that would warrant a more detailed investigation.

2.7.4 Construction control

The DCP is an ideal tool for monitoring all aspects of the construction of a pavement subgrade and base. It can be used to verify the level and. uniformity of compaction over a project. It can also be used to define problem areas that develop due to unavoidable soil conditions brought on by inclement weather. Some have suggested it would be a good tool to use in lieu of test rolling on projects that are too short (to justify expense of test; rolling) or have shallow utilities (which would prevent test rolling), An excellent, example of the use fines of DCP testing was demonstrated in 1989 during the construction of a heavy cargo apron on the southeast, side of the Greater Peoria Regional Airport in Illinois. It was determined that lime modification (not stabilization) was necessary to obtain adequate compaction of the grade. The lime was applied to the upper 12 inches (30.5 cm) of the grade, but heavy rains prevented hauling traffic from reaching the treated areas, so they remained undisturbed for several weeks. When construction resumed those areas, the subgrade was found to be yielding under construction traffic. To test whether the lime modification was effective, eight DCP tests were run. It was found that the lime had modified the upper 12 inches soil and the actual cause of the rutting was a very soft layer 30 to 40 inches traffic.

2.7.5 Structural evaluation of existing pavements

One of the major applications of DCP testing has been in the structural evaluation of' existing pavements. South Africa has used DCP testing extensively in conjunction with their Heavy Vehicle Simulator (HVS) to investigate both shallow and deep pavements with light cementations gravel layers. The effects of traffic molding caused by HVS loading were also evaluated by DCP tests. Prior to this study, De Beer et al., had developed a pavement strength balance classification system based on Standard Pavement Balance Cunres (SPBCs) as determined from DCP testing. Kleyn describes the strength balance of a pavement as "the change in the strength of the pavement layers with depth. Normally, the strength decreases with depth and if this decrease is smooth and without discontinuities and conforms to one of the SPBCs, the pavement is regarded as balanced or in a state of balance. Thompson and Herrin reported (on the use of DCP testing in a 1988 non-destructive rehabilitation study at Illinois'

Palwaukee Municipal Airport. In the study DCP testing was conducted following Falling Weight Deflectometer (FWD)) testing to further evaluate "weak" areas that were found. FWD testing showed the northern 1000 feet of one runway to have weaker pavement sections than the rest. Since this weaker area was near a drainage ditch, a subsurface investigation, including DCP testing, was conducted both soil boring and DCP results indicated weaker granular material was underlying the pavement near the ditch. Based on these findings, properly designed bituminous overlays were then determined following the FAA design procedure.

2.7.6 Application of DCP in quality control of compaction

Soil compaction quality control is currently accomplished by determining the in Place compacted dry unit weight and comparing it with the maximum dry unit weight obtained from a standard laboratory compaction test.

INDOT (Indian Department of Transportation) requires that the in place dry unit weight for compacted soil be over 95% of the laboratory maximum dry unit weight. In order to determine the in place dry unit weight, INDOT engineers generally use the nuclear gauge, which is hazardous and also cumbersome due to strict safety requirements.

2.7.6.1 For cohesive and select backfill materials

Historically, the compaction levels of pavement subgrade and base layers have been determined by means of in-place density testing. In an effort to determine whether there is a reasonable correlation between the DCP index (P_{index}) and in place compaction density of cohesive and select backfill materials, some testing has been recently performed on these materials to determine if such a correlation exits. Most results of DCP testing have indicated too much variability in DCP results to practically apply a correlation (Burnham, 1997).

Siekmeier et al. (1999), as part of the Minnesota Department of Transportation study, investigated the correlation between DCP results and compaction of soils consisting of mixture of clayey and silty sand fill. They first correlated P_{index} (DCP) to the CBR.CBR was then related to the modulus using published relationships. They examined the relations between the modulus and percent compaction. It was concluded that a good correlation did not exist between the DCP results and percent compaction, partly because a typical range of soil mixtures at the site was not truly uniform.

2.7.6.2 Quality control of granular base layer compaction

The Minnesota Department of Transportation suggests this application to reduce testing time and effort while providing more consistent quality control of base layer compaction (Burnham, 1977). Using this procedure, immediately after the compaction of each layer of granular base material, DCP tests are conducted to insure that the P_{index} is less than 19 mm per blow (0.75 inches per blow). The P_{index} limiting value is valid for all freshly compacted base materials. The P_{index} dramatically decreases as the materials setup time increases and under traffic loading. Using this method, the DCP testing will only indicate those adequately compacted base layers that ”pass” Test failure, however, must be confirmed by other methods such as the nuclear gauge or the sand cone density method. Based on general agreement between the P_{index} and percent compaction, the Minnesota Department of Transportation has revised the limiting penetration rate to the following (Siekmeier et al., 1998):

a) 15 mm/blow in the upper 75 mm (3 in);

b) 10 mm/blow at depths between 75 and 150 mm (3 and 6 in); and

c) 5 mm/blow at depths below 150 mm (6 in).

They concluded that the penetration rate is a function of moisture content, set-uptime, and construction traffic, and that accurate and repeatable tests depend on seating the cone tip properly and beginning the test consistently. They recommended the following: a) the test be performed consistently and not more than one day after compaction while the base material is still damp; b) the construction traffic be distributed uniformly by requiring haul trucks to vary their path; and c) at least two dynamic cone penetrometer tests be conducted at selected sites within each 800 cubic meters of constructed base course. They proposed a Penetration Index Method (Trial Mn/DOT Specifications 2211.3C4) which described a step by step procedure for determining the “pass” and “fail” tests (Siekmeier, et al. 1998).

Siekmeier et al. (1999), as part of the Minnesota Department of Transportation study, studied the correlation between DCP results and compaction of soils consisting of sand and gravel mixture with less than 10 percent fine. They first correlated DCP index (P_{index}) to the CBR. CBR was then correlated to the modulus using published relationships. They examined the relations between the modulus and percent compaction. It was concluded a good correlation existed between the DCP results and percent compaction.

2.7.7 Application for granular materials around utilities

Many transportation agencies use granular soils as backfill and embedment materials in the installation of underground utility structures, including the thermoplastic pipe used in gravity flow applications. The granular backfill relies on proper compaction to achieve adequate strength and stiffness and to ensure satisfactory pipe performance. The commonly used standard proctor test cannot be used because it does not provide a well- defined moisture-density relationship. In addition, this approach requires density measurements on each lift of the compacted fill for the entire length of the pipe. Recent studies indicate that DCP blow count profiles provide a basis for comparison between compaction equipment, level of compaction energy, and materials. But, it should be noted that these data alone do not reveal what level of compaction must be achieved with each type of backfill material in order to achieve the specific performance criteria. The results have also indicated that the DCP index (P_{index}) values are very sensitive to the depth of measurements (Jayawickrama, et al., 2000).

2.7.8 Application during backfill compaction of pavement drain trenches

The Minnesota Department of Transportation has indicated that the DCP testing is reliable and effective in improving the compaction of these trenches. Using this procedure, immediately after installation of the pavement edge drainpipe and fine filter granular backfill material, DCP testing is conducted to insure that the P_{index} is less than 75 mm per blow (3 inches per blow). In this approach, each 150 mm (6 inches) of compacted backfill material is tested for compliance (Burnham, 1997).

2.7.9 Application of DCP in performance evaluation of pavement layers

Performance evaluation of pavement layers is needed on a regular basis in order to categorize the implementation of rehabilitation measures (e.g., Kleyn, et al., 1982).The Minnesota Department of Transportation, based on the analysis of Mn/Road DCP testing, has recommended the following limiting values for DCP index during a rehabilitation study (Burnham, 1997).

a) Silty/Clayey material: DCP index less than 25 mm/blow (1.0 in/blow)

b) Select granular material: DCP index less than 7 mm/blow (0.28 in/blow) and

c) Mn/Road Class 3 special gradation requirements: DCP index less than 5 mm/blow (0.2 in/blow)

The above values are based on the assumption that adequate confinement exists near the testing surface. In the event that higher values than the above mentioned limiting values are encountered, additional testing methods are needed. It should be noted that the above values are independent of the moisture content. Moisture content can cause large variability in DCP test results. Nevertheless, a limiting value was recognized. Gabr et al. (2000) proposed a model by which the DCP data are utilized to evaluate the pavement distress state. They proposed a model to predict the distress level of pavement layers using penetration resistance of the subgrade and aggregate base course (ABC) layers based on coupled contribution of the subgrade and the ABC materials. They provided a step by step procedure, based on the correlation of the DCP index with CBR, by which the DCP data can be used to evaluate the pavement distress state for categorizing the need for rehabilitation measures. Although their pavement stress model was specific in this study regarding the type of the ABC material tested, the frame work of the procedure can be used at other sites.

2.7.10 Application of DCP to obtain layer thickness

DCP can also be used effectively to determine the soil layer thickness from the changing slope of the depth versus the profile of the accumulated blows. Livneh (1987) showed that the layer thickness obtained from DCP tests correspond reasonably well to the thickness obtained from the test pits. It was concluded that the DCP test is a reliable alternative for project evaluation.

2.7.10.1 Complementing FWD during back calculation

It has been shown that the DCP is very useful when the moduli back calculated from Falling Weight Deflectometer (FWD) data are in question, such as when the asphalt concrete is less than 76 mm (3 inches) or when shallow bedrock is present (e.g., Little et al., 1995). These two situations often cause a misinterpretation of FWD data. The DCP can be readily applied in these two situations to increase the accuracy of the stiffness measurement. In addition, it is not possible to conduct a FWD test directly on weak subgrade or base layers because of the large deflections that can exceed the equipment's calibration limit.

2.7.10.2 Identifying weak spots in compacted layers

Many studies aimed to determine reasonable correlations between DCP's penetration rate and in-place compaction density failed to find such correlations. Most of the results that are based on cohesive and granular materials showed too much variability to practically apply a correlation. However properly compacted sections exhibit very uniform penetration rate values, so it is suggested to use DCP to map out weak spots in presumed to be uniform compacted material.

2.7.10.3 Locating layers in pavement structures

The DCP is an effective tool for evaluating pavement base, subbase and subgrade layers. Plotting the penetration rate versus depth enables engineers to analyze different layers of pavement materials with depth. It can penetrate to depths greater than the radius of influence of the geogauge, LFWD and plate load test. When DCP is used in the assessment of the surface layer strength without confinement, the penetration rate, after some required depth, should be calculated to determine the actual strength of the soil layer. The required depth depends on the type of the soil. Webster et al. (1992) reported the average required depths for different types of soils (Table 2.6) based on their field experiences at U.S Army Waterways Experiment Station, MS. In order to be able to use DCP as a more effective tool for rehabilitation studies and compaction evaluation, Mn/DOT suggested defining limiting penetration rate value for each particular subgrade soil and base type. After conducting more than 700 DCP tests on the Mn/ROAD project, they were able to recommend the PR values listed in Table 2.7 for use when analyzing DCP test results. These recommended values are based on assuming adequate confinement near the testing surface. The recommended values do not cover all types of materials; by conducting similar research Table 2.7 can be extended to include other classes of base courses.

2.7.10.4 Monitoring effectiveness of stabilization

Measuring density is not an effective method to monitor the strength gain with time for soil stabilization with additives. Densities of such materials do not increase in accordance with the strength gain. Since DCP's working principle is directly based on tested material's resistance for the cone to penetrate, decrease in the penetration resistance values as strength increases can be used to monitor effectiveness of stabilization with time.

2.7.11 Using as a quality acceptance testing tool

DCP is an efficient quality assurance testing tool for performance based specifications. The device already took its place in the Minnesota Department of Transportation's specification for pavement edge drain backfill and granular base compaction. DCP penetration rate of 3 inches/blow or less indicates satisfactory compaction according to Mn/DOT Subsurface Drain Installation Specifications.

2.7.12 To Control quality of roadway compaction and construction

Based on the experimental program undertaken to assess the Dynamic Cone Penetration Test (DCPT), DCP criteria for compaction quality control were suggested by dividing the soils considered into three groups based on the AASHTO soil classification. In addition, the statistical variability of the test results was considered in the development of the DCP criteria for compaction quality control. Based on the analysis of the data collected, the following equations are proposed by INDOT Office of Research and Development.

(a) A-3 soils: The minimum required blow count $(NDCP)_{req|0\sim12}$ for 0-12" penetration varies from 7 to 10; it is a function of the Coefficient of Uniformity (C_u). The following equation was proposed for A-3 soils:

$$(NDCP)_{req|0\sim12=}\ 4.0\ln(C_u) + 2.6$$

The $(NDCP)_{req|0\sim12}$ is the minimum required blow count for 0-to-12 inch penetration that implies an RC of 95% with high probability.

(b) "Granular" soil (A-1 and A-2 soils, except soils containing gravel): The minimum required blow count $(NDCP)_{req|0\sim12}$for this type of soil is influenced by the fine particles that are present in the soil. Since the plasticity index and the amount of fine particles contained in the "granular" soil correlate with the OMC, the minimum required blow count for "granular" soils is suggested as a function of the OMC as follows:

$$(NDCP)_{req|0\sim12}= 59\exp(-0.12w_{copt})$$

Where, w_{copt}= Optimum Moisture Content. The $(NDCP)_{req|0\sim12}$ is the minimum required blow count for 0 to 12 inch penetration that implies an RC of 95% with high probability.

(c) Silty, clayey soils: The minimum required blow count correlates with the plasticity index and the percentage of soil by weight passing the #40 sieve. Thus, we propose the minimum required blow count $(NDCP)_{req}$ for silty clay soils as a function of the plasticity index and the percentage of soil by weight passing the #40 sieve (F40) according to:

$$(NDCP)_{req|0\sim6}= 17\exp[-0.07PI(F40/100)]$$

Where $(NDCP)_{req|0\sim6=}$ Minimum required blow count for 0-to-6 inch penetration that implies an RC of 95% with high probability, PI = Plasticity Index, and F40 = % passing the # 40 sieve; and

$$(NDCP)_{req|6\sim12} =27\exp[-0.08PI(F40/100)]$$

Where $(NDCP)_{req|6\sim12}$= Minimum required blow count for 6 to 12 inch penetration that implies an RC of 95% with high probability.

2. 8 Factors Affecting DCP and DPL Results

Over the past years many researchers have studied the effects of several factors like density, gradation, soil type, moisture content and maximum aggregate size that affect the DCP test results. George et al. (2000) reported that maximum aggregate size and coefficient of uniformity were important factors affecting the DCP index of granular materials.

2.8.1 Material effects

Several investigators have studied the influence of several factors on the P_{index}. Kleyn and Savage (1982) indicated that moisture content, gradation, density and plasticity were important material properties influencing the DCP. Hassan (1996) performed a study on the effects of several variables on the DCP. He concluded that for fine-grained soils, moisture contents, soil classification, dry density and confining pressures influence the DCP. For coarse-grained soils, coefficient of uniformity and confining pressures were important variables.

2.8.2 Vertical confinement effect

Livneh, et al. (1995) performed a comprehensive study of the vertical confinement effect on Dynamic Cone Penetrometer strength values in pavement and subgrade evaluations. The results have shown that there is no vertical confinement effect by rigid pavement structure or by upper cohesive layers on the DCP values of lower cohesive subgrade layers. In addition, their findings have indicated that no vertical confinement effect exists by the upper granular layer on the DCP values of the cohesive subgrade beneath them. There is, however, vertical confinement effect by the upper asphaltic layers in the DCP values of the granular pavement layers. These confinement effects usually result a decrease in the DCP values. Any difference between the confined and unconfined values in the rigid structure or in the case of granular materials is due to the friction developed in the DCP rod by tilted penetration or by a collapse of the granular material on the rod surface during penetration.

2.8.3 Another effect

Several investigators have studied the influence of several factors on the DCP. Kleyn and Savage (1982) indicated that moisture content, gradation, density and plasticity were important material properties influencing the DCP. Hassan (1996) performed a study on the effects of several variables on the DCP. He concluded that for fine-grained soils, moisture contents, soil classification, dry density and confining pressures influence the DCP. For coarse-grained soils, coefficient of uniformity and confining pressures were important variables.

2.8.4 Side friction effect

Because the DCP device is not completely vertical while penetrating through the soil, the penetration resistance would be apparently higher due to side friction. This apparent higher resistance may also be caused when penetrating in a collapsible granular material. This effect is usually small in cohesive soils. Livneh (2000) suggested the use of a correction factor to correct the DCP/CBR values for the side friction effect.

2. 9 Static Plate Load Test (SPLT)

The PLT has been a useful site investigation tool for many years and has been used for proof testing pavement structure layers in many European countries. Currently, it is used for both rigid and flexible pavements. The test consists of loading a circular plate that is in contact with the layer to be tested and measuring the deflections under load increments. The plates used for roads are usually 30.5 cm (12 in.) in diameter. The load is transmitted to the plates by a hydraulic jack, acting against heavy mobile equipment as a reaction plate. The PLT can be conducted using different procedures depending on the information desired. In all cases, a load-deformation curve following the general relationship shown in Fig. 2.24 and Fig. 2.25will be obtained. The load must be sustained on the plate until all measured settlement has diminished so that the true deflection for each load increment is obtained. The time required for settlement is determined by plotting a time-deformation curve while the test is in progress, and identifying where this curve essentially becomes horizontal.

Generally, a load increment is applied when the rate of deformation has approached about 0.001 inch/min. The method of performing PLT test on soils and flexible pavement is described by ASTM D1195-93. In this method, the PLT test should continue until a peak load is reached or until the ratio of load increment to settlement increment reaches a minimum, steady magnitude. The influence depth of the PLT is about two times its diameter. Since the tested layers' thicknesses usually ranged from 6 to 12 inch, the influence zone of PLT reached the underlying layer. Therefore, the modulus obtained from PLT reflects the composite modulus rather than the true modulus of the tested layer. In this study, the Odemark method, referred to as the Method of Equivalent Thickness (MET), was used to back-calculate the PLT moduli on multi-layer systems. In this method, layers of different stiffness's are first transformed to an equivalent layer of same stiffness, such that Boussinesq's equations for homogeneous elastic half-space media can be used to predict stresses and deflections. For example, for a two layered system with $E_1$and E_2as the stiffness moduli of the first and second layers, the following equation is used to transform the first layer into an equivalent layer with stiffness modulus E_2. Where h_e is the equivalent thickness of layer one, $h_1$is thickness of layer one, and f is an adjustment factor, taken to be 0.9 for a two layer system, and 1.0 for a multilayer system

$$\mathrm{h_e} = f h_1 \sqrt[3]{\frac{E_1}{E_2}} \text{ ---------------------------------- } 2.32$$

Since FWD is capable of testing multi-layer systems due to the presence of several geophone sensors, this study assumed that the E_1/E_2ratios for PLT and FWD are the same for the two layer system.

2.9.1 Moduli from plate load test

Plate loading tests can be used to estimate the modulus of subgrade reaction (K_s).Determination of the modulus of subgrade reaction is made in the field on the selected subgrade soil at its natural moisture content. This test is conducted by subjecting the subgrade to a known stress at a predetermined rate of speed using a loading system and recording the resulting settlement. The modulus of subgrade reaction can be calculated using the following relation (Yoder and Witczak, 1975):

$$K_S = \frac{P}{\delta} -------------------------------------2.33$$

Where,

P= unit load on plate.

δ = deflection of the plate.

In addition the PLT can be used to determine the elastic stiffness modulus of different pavement layers. Usually, the load is often cycled several times to measure a more stable elastic stiffness (Fleming et al. 2001). The general equation used to determine the elastic static modulus for the PLT as follow (Yoder and Witczak, 1975).

$$E_{plt} = \frac{1.188PR}{\delta} -------------------------------------2.34$$

Where,

E_{plt} =plate load elastic modulus

P=applied pressure/ stress

R= radius of plate

δ = deflection at pressure, P and 1.18= factor for rigid plate

The factor of 1.18 in Equation 2.28 is based on a Poisson's ratio of 0.5. It has been noted that the materials used in roadway construction have Poisson's ratios typically ranging from 0.25 to 0.4, which might introduce some error with these types of materials (Horhota, 1996).The Plate Load test (PLT) is a well-known method of estimating the bearing capacity of soils and evaluating the strength of flexible pavement systems. The test has been somewhat discredited due to its destructive nature and time consuming testing procedure. The 10 inch in diameter plate was preferred in order to have enough loading increments, especially for cases where the test layer cannot handle high stresses. The PLT was used as a reference test to obtain the strength characteristics of the layers.As in the case for other stress-strain tests, different elasticity moduli can be obtained from the PLT. Soil elasticity moduli can be defined as: (1) the initial tangent modulus; (2) the tangent modulus at a given stress level; (3) reloading and unloading modulus and; (4) the secant modulus at a given stress level. In this study, the initial tangent modulus was determined for all plate load tests. To determine the initial modulus, a line was drawn tangent to the initial segment of the stress-strain curve; then an arbitrary point was chosen on this line and the stress and deflection corresponding to this point was used to determine the initial modulus. A tangent was drawn to the initial portion of the curve to determine the load and corresponding settlement that will be used in Equation 2.35 in order to obtain the initial tangent modulus ($E_{PLT(i)}$) of the test layer. Figure 2.25 describe the deflection and stress used for determining $E_{PLT(i)}$ from $\delta_1$andP.

German Code for the design of flexible pavement structures specifies performing in-situ plate-bearing tests on constructed pavement layers. For the second cycle of the regular plate bearing test, the German Code defines a reloading stiffness modulus called $E_{PLT(R2)}$ using the following Equation 2.35:

$$E_{PLT} = \frac{2P(1-\nu^2)}{\Pi R\delta} \quad \text{------------------------------------} \quad 2.35$$

Where,

P=applied stress/pressure,

δ =plate deflection and

ν = the poison's ratio.

Reloading lines were drawn from the beginning of reloading portion of the curve to the point where reloading portion of the curve reaches to the load, where un loading was started. Reloading modulus ($E_{PLT(R2)}$) is calculated with the load and corresponding change in the settlement that is obtained from the reloading line in the second cycle, using Equation 2.35.

2.10 California Bearing Ratio (CBR)

The California Bearing Ratio (CBR) test is a relatively simple test that is commonly used as an indicator of the strength of a subgrade soil, subbase and base course material in highways and airfield pavement systems. The test is described in ASTM D1883-99 standard.

The CBR test is used primarily to empirically determine the required thicknesses of flexible pavements. It is normally performed on remolded (compacted) specimens, although they may be conducted on undisturbed soils or on soils in the field. Remolded specimens may be compacted to their maximum unit weights at their optimum moisture contents if the CBR is desired at 100% maximum dry unit weight and optimum moisture content. CBR tests can also be performed at the desired unit weights and moisture contents. Soil specimens are tested by placing them in water for 96 hours in order to simulate very poor soil conditions. The CBR is defined as the ratio (expressed as a percentage) obtained by dividing the penetration stress required to cause a piston with a diameter of 49 mm (1.95 inch) to penetrate 0.10 inch into the soil by a standard penetration stress of 1,000 psi. This standard penetration stress is roughly what is required to cause the same piston to penetrate 0.10 inch into a mass of crushed rock. The CBR may be thought of as an indication of the strength of the soil relative to that of crushed rock.

It should be noted that the 1,000 psi in the denominator is the standard penetration stress for 0.10 inch penetration. If the bearing ratio based on a penetration stress required to penetrate 0.20 inch with a corresponding standard penetration stress of 1,500 psi is greater than the one for a 0.10 inch penetration, the test should be repeated, and if the result is still similar, the ratio based on the, 0.20 inch penetration should be reported as the CBR value.

$$CBR = \frac{\text{pentration stress (psi) required to penetrate 0.10 inch}}{1000 \text{ psi.}} 100 \quad ----2.36$$

According to the procedure described in ASTM D1883-99, if the CBR is desired at an optimum water content and some percentage of maximum dry unit weight, three specimens should prepared and tested from soil to within ±0.5% of the optimum water content and using a different compactive effort for each specimen such that the dry unit weights of these specimens varies above and below the desired value. Then the CBR for the three specimens should be plotted against their corresponding dry unit weight, and from this plot the CBR for the desired dry unit weight can be determined. The CBR test is sensitive to the texture of the soil, its water content and the compacted density. The result of a CBR test also depends on the resistance to the penetration of the piston. Therefore, the CBR indirectly estimates the shear strength of the material being tested (Rodriguez et al. 1988).

Table 2.1: Technical data of the equipment used in Dynamic Probing

Factor	DPL	DPM	DPH	DPSH
Hammer mass, kg	10	30	50	63.5
Height of fall, m	0.5	0.5	0.5	0.75
Mass of anvil and guide rod (max), kg	6	18	18	30
Extension rod outer diameter, mm,	22	32	32	32
Extension rod inner diameter, mm	6	9	9	-
Cone diameter, mm	35.7	35.7	43.7	50.5
Apex angle, deg.	90	90	90	90
Cone taper angle, upper, deg.	11	11	11	11
Number of blows per cm penetration	10 cm; N_{10}	10 cm; N_{10}	10 cm; N_{10}	20cm; N_{20}
Standard range of blows	3 – 50	3 – 50	3 – 50	5 – 100

Note : DPL = Dynamic Probing Light,

DPM = Dynamic Probing Medium,

DPH = Dynamic Probing Heavy,

DPSH = Dynamic Probing Super Heavy.

Table 2.2: Specification of Dynamic Probing Light

Factor	DPL
Hammer mass, kg	10 ± 0.1
Height of fall, m	0.5 ± 0.01
Mass of anvil and	
Guide rod (max), kg	6
Rebound(max),	50
Length of the diameter(D)	≥ 1 ≤ 2
Ratio(hammer)	
Diameter of anvil(d), mm	100<d<0.5d
Rod length, m	1 ± 0.1
Maximum mass of rod, kg/m	3
Rod deviation(max),	1.0
First 5m	
Rod deviation(max),	2.0
Below 5 m,	
Rod eccentricity(max), mm	0.2
Rod OD, mm	22 ± 0.2
Rod ID, mm	6 ± 0.2
Apex angle, deg.	90
Nominal are of cone, cm^2	10
Cone diameter, new, mm	35.7 ± .3
Cone diameter, (min), worn, mm	34
Mantle length of cone, mm	35.7 ± 1
Cone taper angle,	11
Upper, deg.	
Length of cone tip, mm	17.9 ± 0.1
Max wear of cone tip	3
Length, mm	
Number of blows	10 cm, N_{10}
Per cm penetration	
Standard range of blows	3 - 50
Specific work per blow:	50
Mgh/A, KJ/m^2	

Table 2.3: Correlations between CBR and PI (Datta, T. 2011)

Author	**Correlation**	**Field or laboratory based study**	**Material tested**
Kleyn (1975)	log (CBR) = 2.62 - 1.27 log(PI)	Laboratory	Unknown
Harison (1987)	log (CBR) = 2.56 - 1.16 log(PI)	Laboratory	Cohesive
Harison (1987)	log (CBR) = 3.03 - 1.51· log(PI)	Laboratory	Granular
Webster et al. (1992)	Log (CBR)= 2.46. -1.12 log (DCPI)	Laboratory	Various soil types
Livneh et al. (1994)	log (CBR) = 2.46 - 1.12· log(PI)	Field and laboratory	Granular and cohesive
Ese et al. (1994)	log (CBR) = 2.44 - 1.07· log(PI)	Field and laboratory	ABC*
NCDOT Pavement (1998)	Log (CBR)= 2.60. -1.07 log(PI)	Field and laboratory	ABC* and cohesive
Coonse (1999)	log (CBR) = 2.53 - 1.14· log(PI)	Laboratory	Piedomont residual soil
Gabr (2000)	log (CBR) = 1.40 – 0.55· log(PI)	Field and laboratory	ABC*
Shongtao Dai and Charlie Kremer (2006)	Log CBR= 2.438-1.065 x log(PI) $_{field.}$	Field and laboratory	Granular material
Varghese George (2009)	CBR = 88.37(DCPI) -1.08	Laboratory	Unsoaked blended soils

*Aggregate base course

Table 2.4: Suggested classification for granular soils using DCP (Huntley, 1990)

Classification	n Value Range		
		Sand	Gravelly sand
Very loose	<1	<1	<3
Loose	1-2	2-3	3-7
Medium Dense	3-7	4-10	8-20
Dense	8-11	11-17	21-33
Very Dense	>11	>17	>33

Table 2.5: Suggested classification for cohesive soils using DCP (Huntley, 1990)

Classification	n Value Range
Very soft	<1
Soft	1-2
Firm	3-4
Stiff	5-8
Very stiff to hard	>8

Table 2.6: DCP depth required to measure unconfined layer strength (Webster et al., 1992)

Soil Type	Average Required Penetration Depth (inch)
CH	1
CL	3
SC	4
SW-SM	4
SM	5
GP	5
SP	11

Table 2.7: Limiting DCP penetration rates by MNDOT (Burnham, 1997)

Material Type	**Limiting PR (mm/blow)**
Silty /Clay subgrade	<25
Select granular subgrade	<7
Class 3 special gradation granular base materials	<5

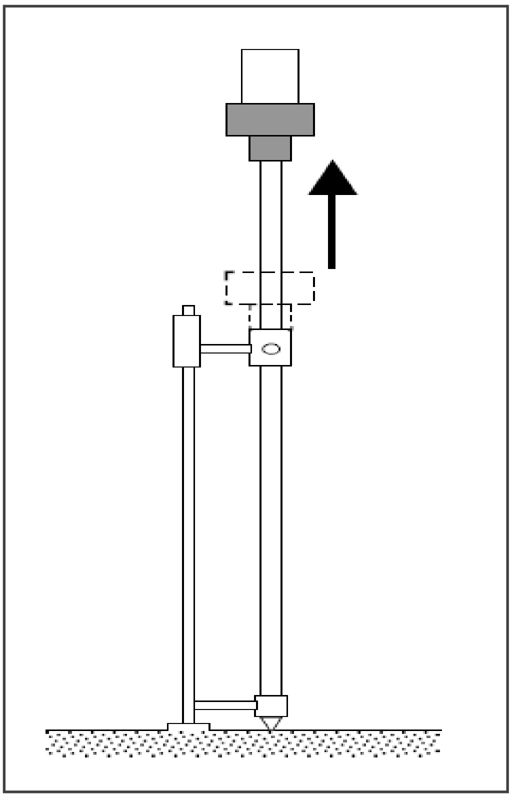

(a) Before hammer dropping

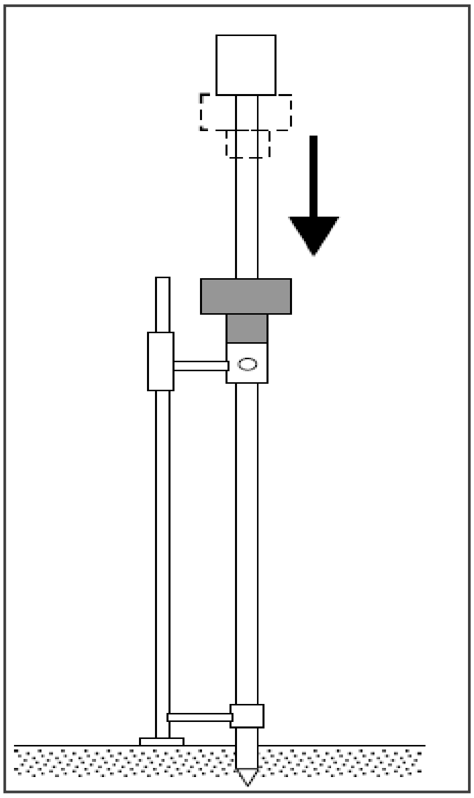

(b) After hammer dropping

Fig. 2.1: Dynamic Cone Penetration Test

.

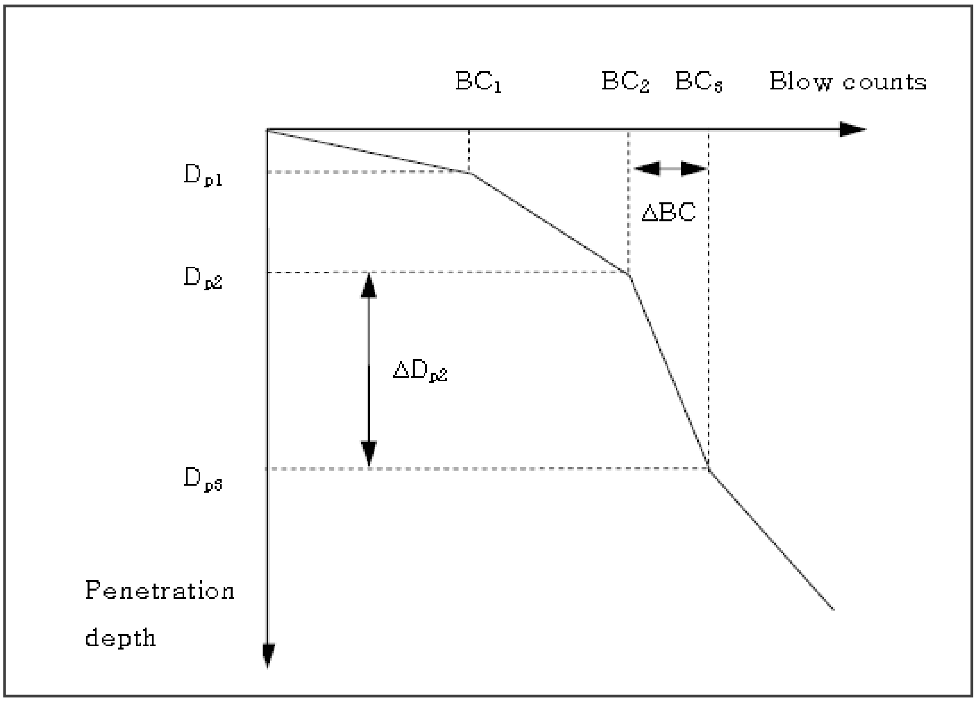

Fig. 2.2: Typical DCP and DPL results

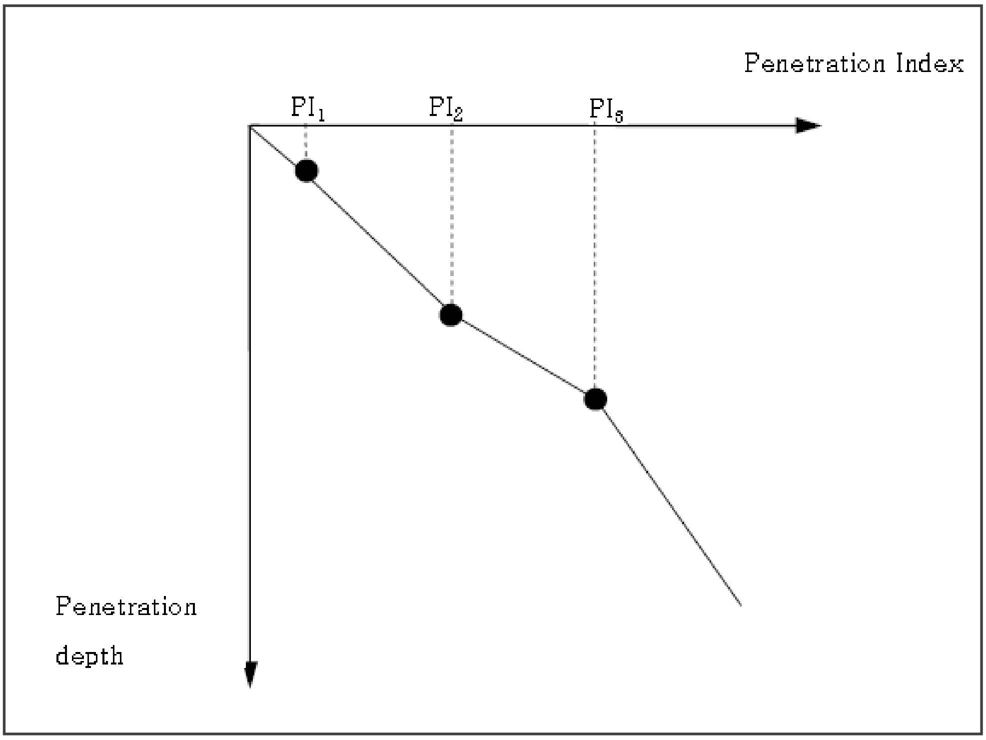

Fig. 2.3: Typical DCP and DPL results

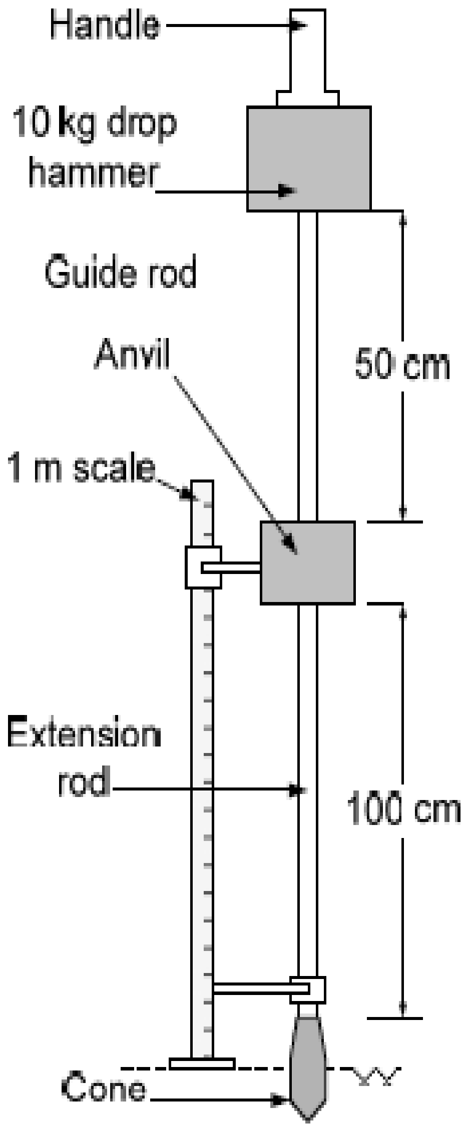

Fig. 2.4: Schematic diagram of Dynamic Probing Light (DPL).

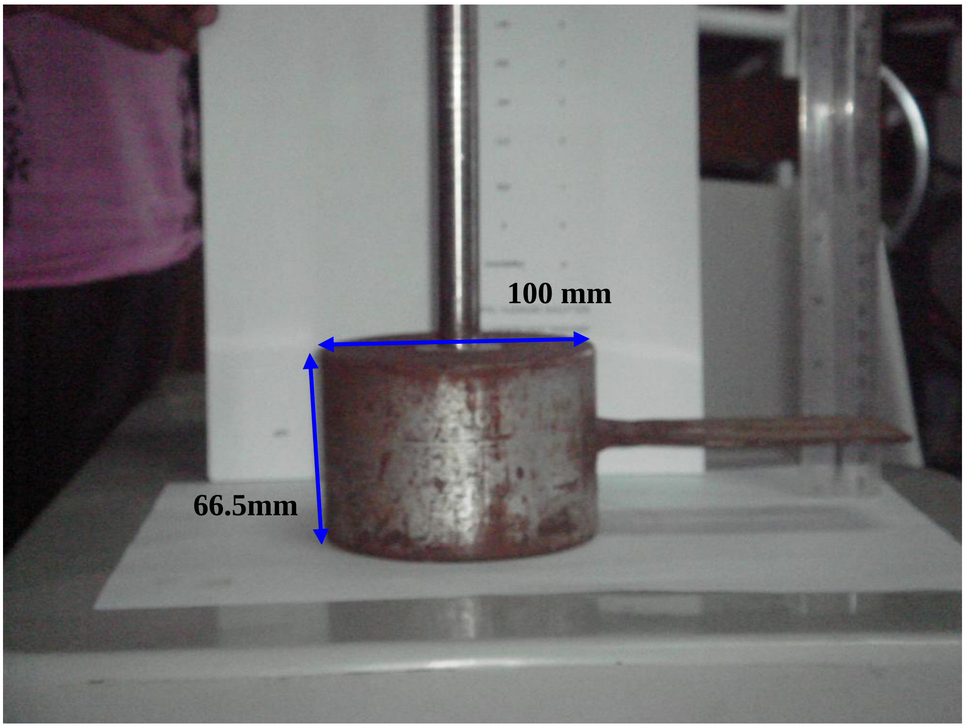

Fig. 2.5: The dimensions of 6 kg anvil of DPL (Azad, A.K., 2008)

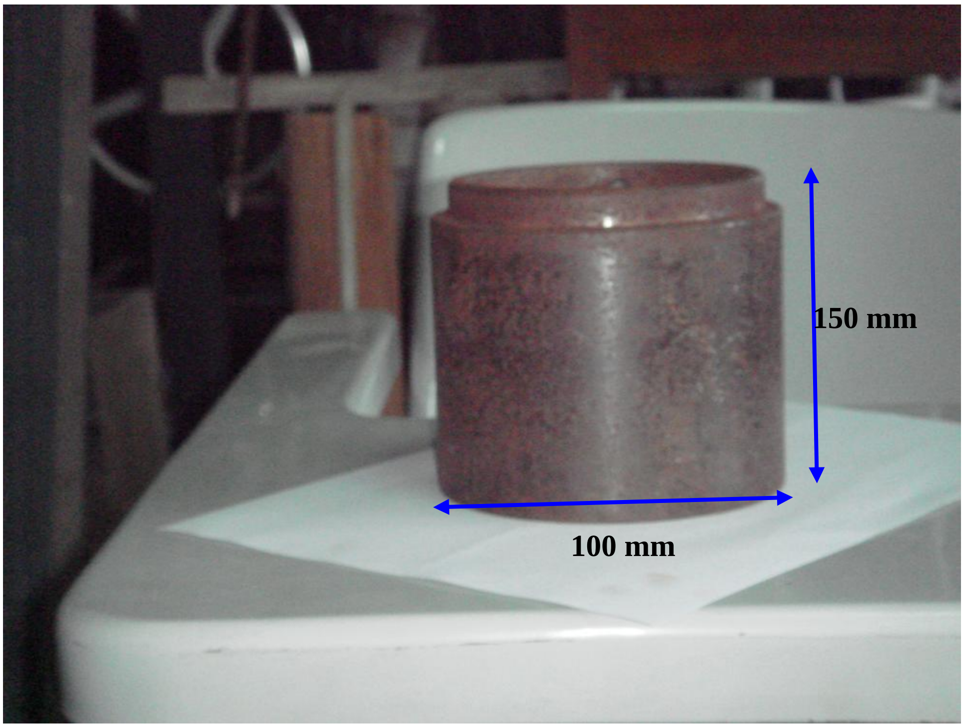

Fig. 2.6: Dimensions of 10 kg hammer of DPL (Azad, A.K., 2008)

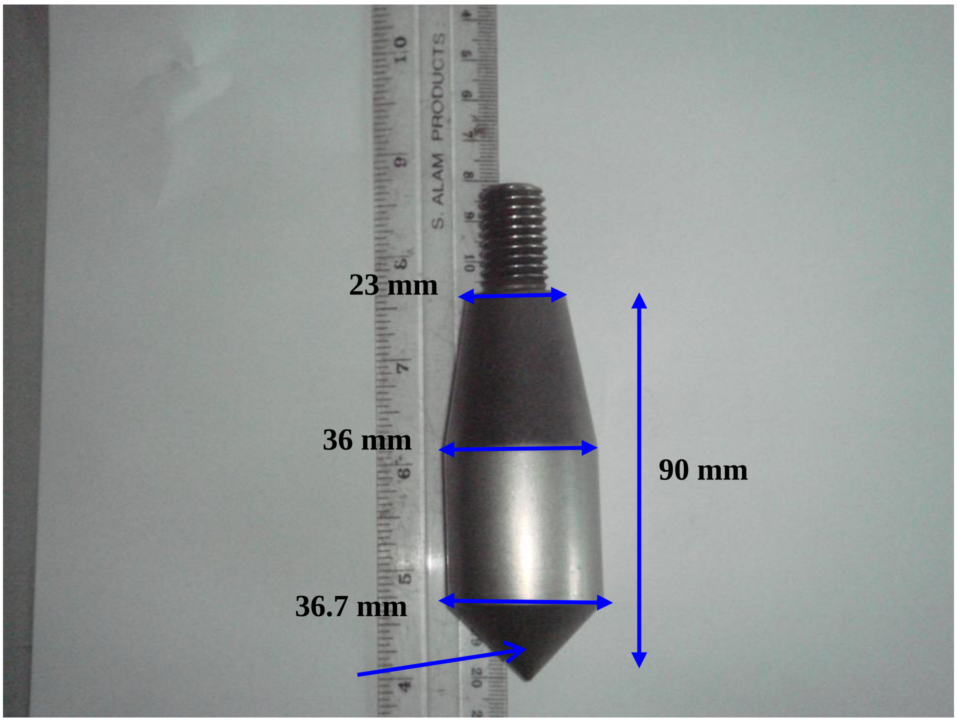

Fig. 2.7: Dimensions of Probing cone of DPL (Azad, A.K., 2008)

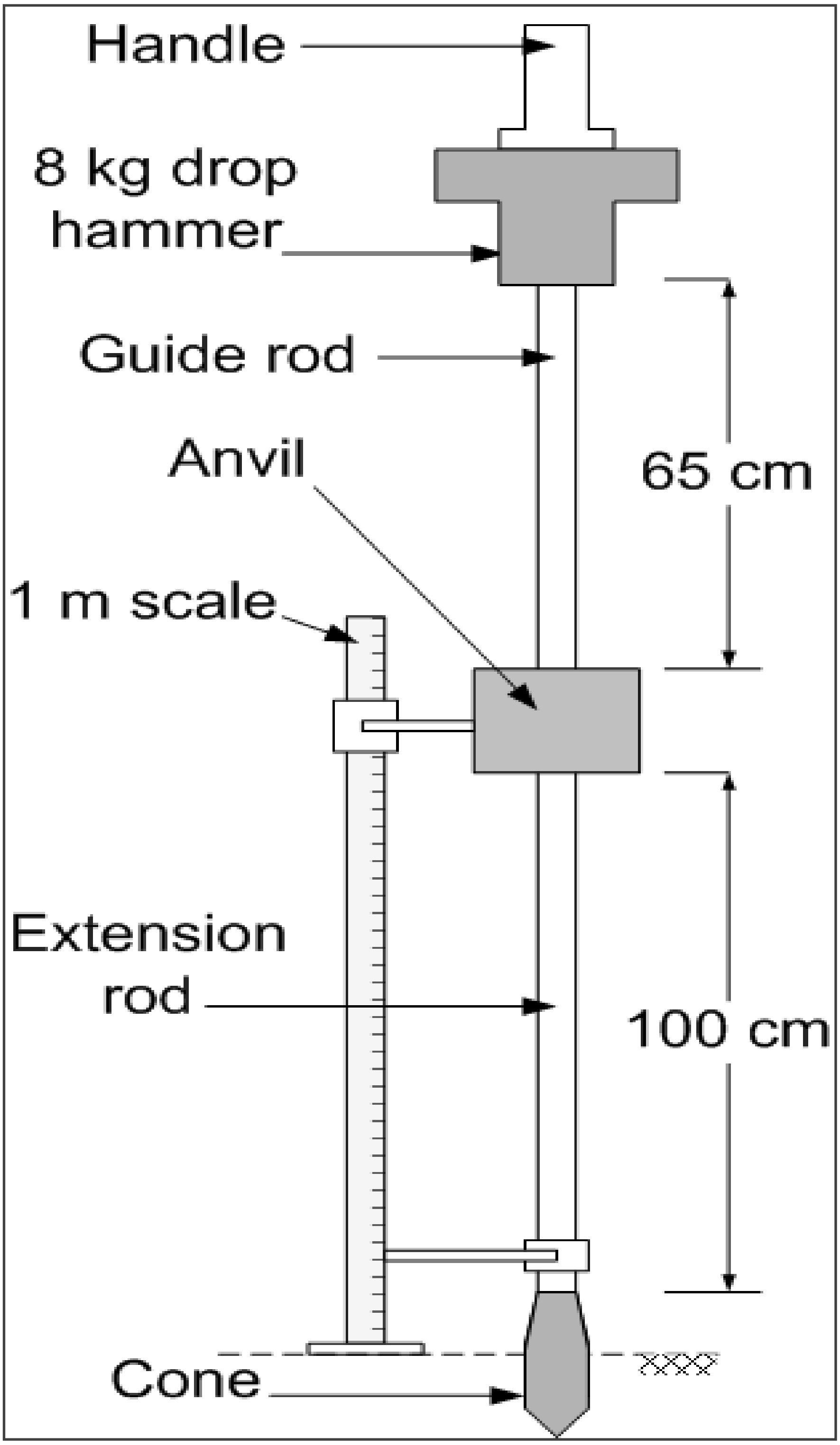

Fig.2.8: Schematic diagram of Dynamic Cone Penetration (DCP) test

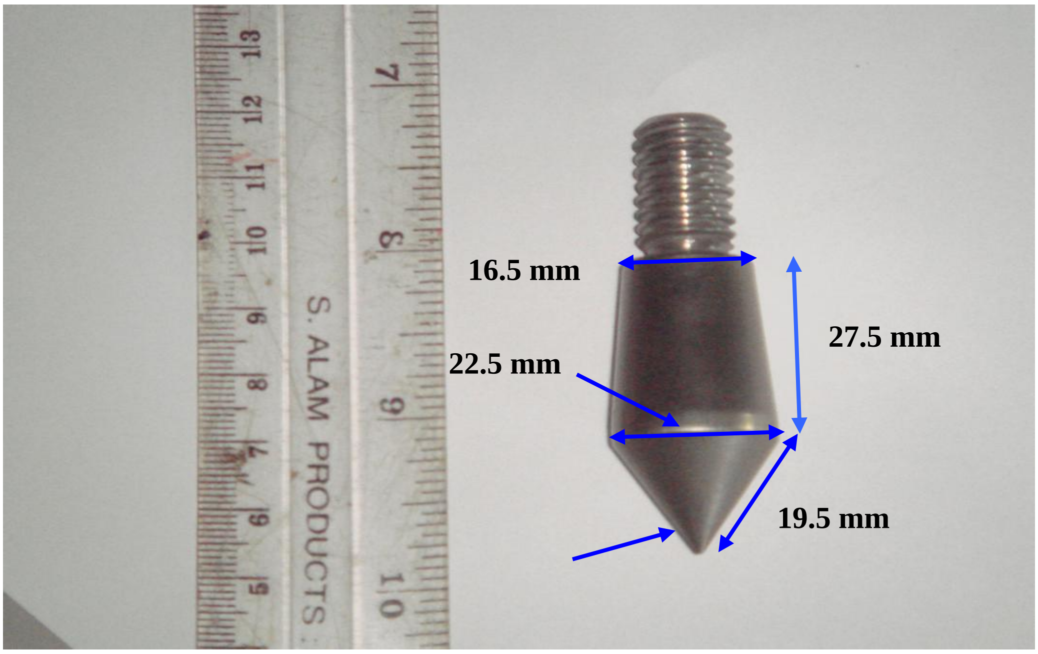

Fig. 2.9: Different dimensions of probing cone of DCP (Azad, A.K., 2008)

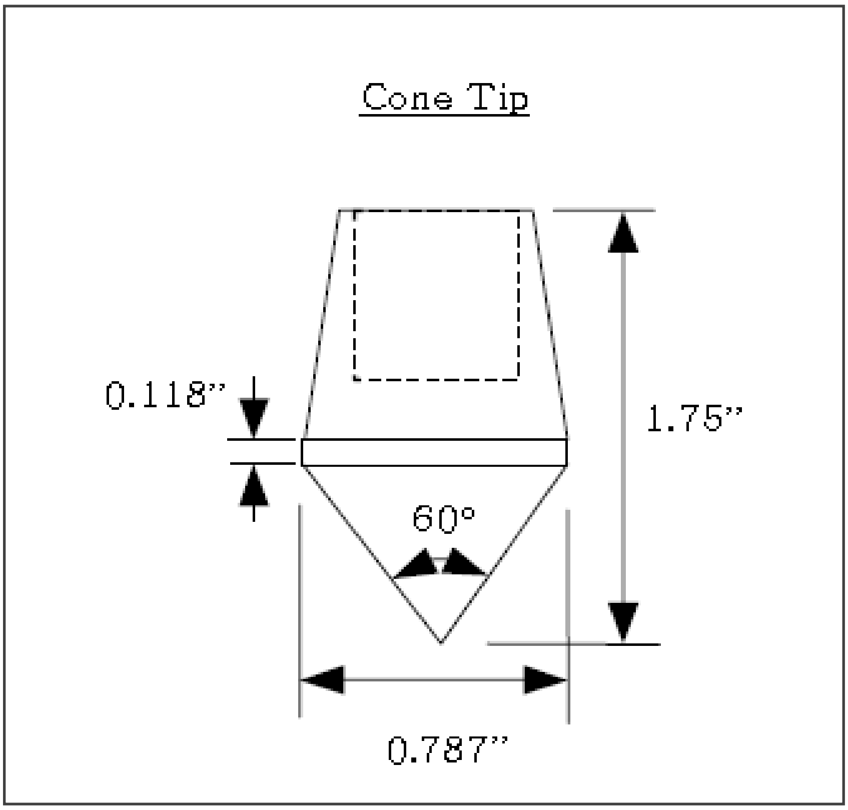

Fig. 2.10: Dimensions of probing cone of DCP.

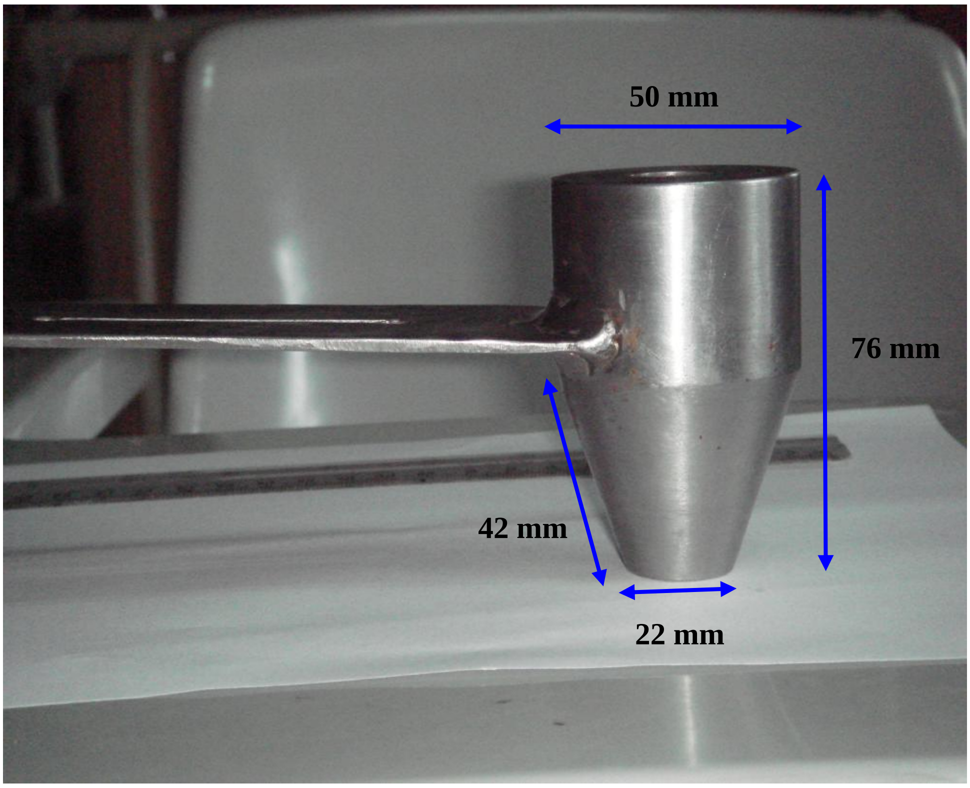

Fig. 2.11: Different dimensions of Anvil of DCP (Azad, A.K., 2008)

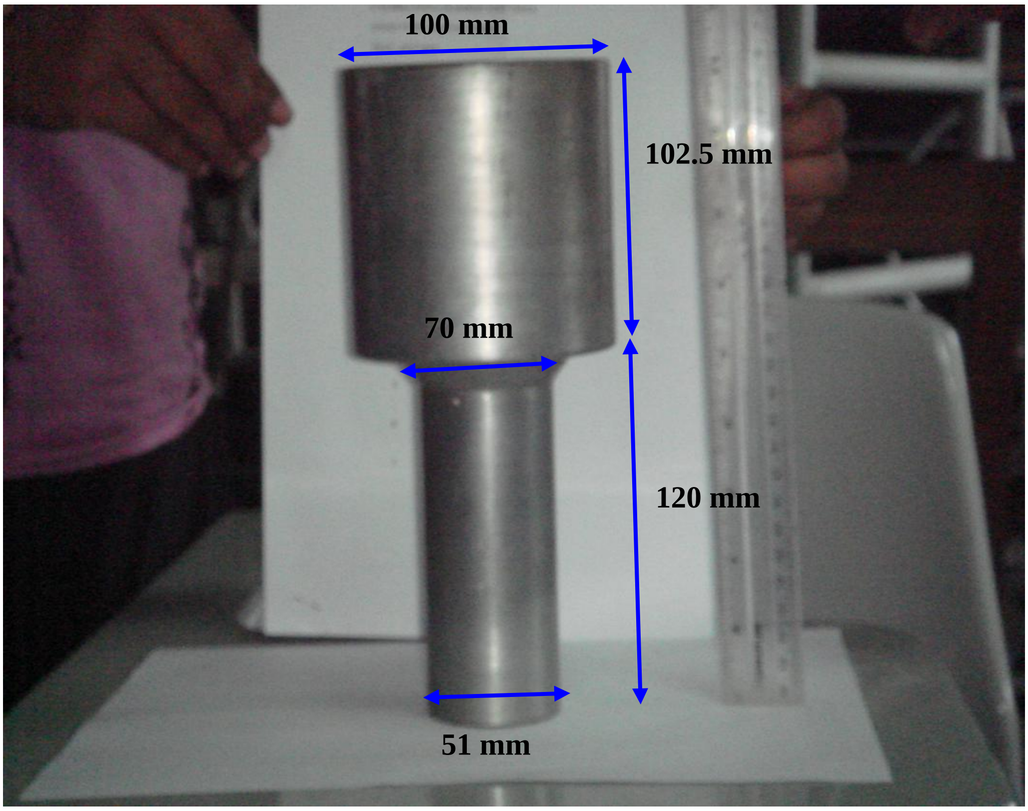

Fig. 2.12: Dimensions of 8 kg hammer of DCP (Azad, A.K., 2008)

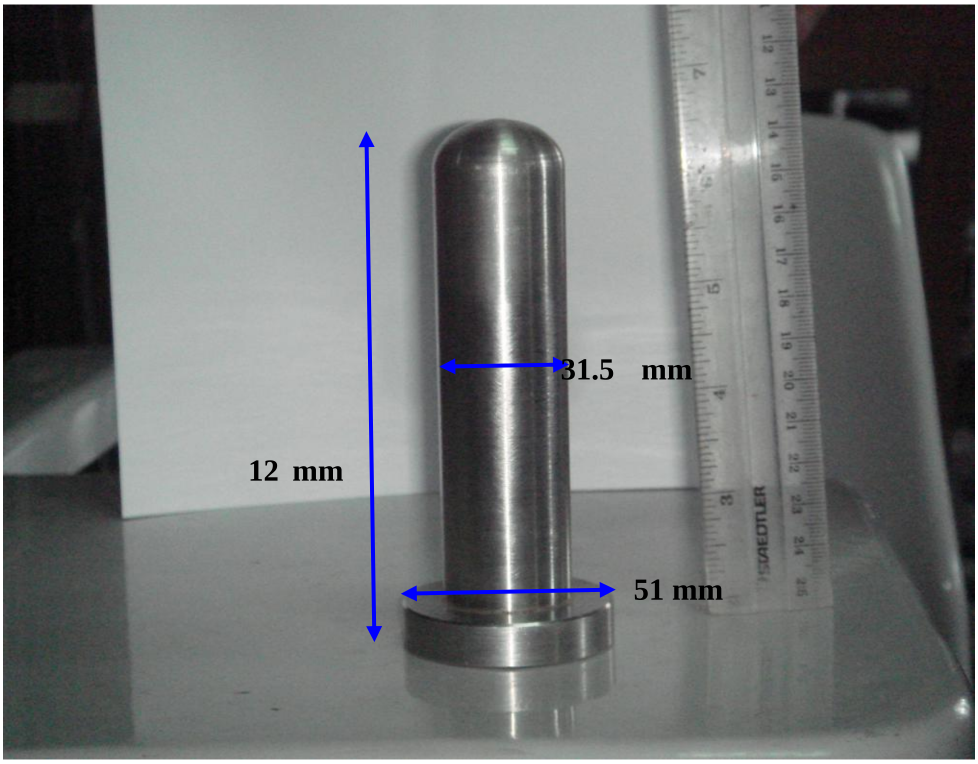

Fig. 2.13: Handle to hold DCP during test (Azad, A.K., 2008)

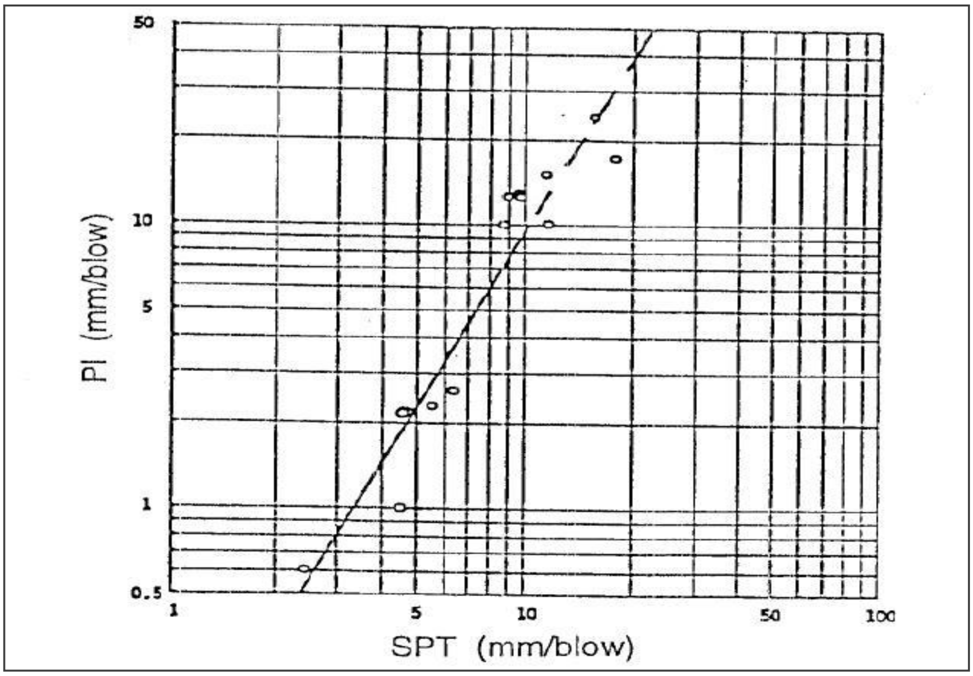

Fig. 2.14: Relationship between PI and SPT

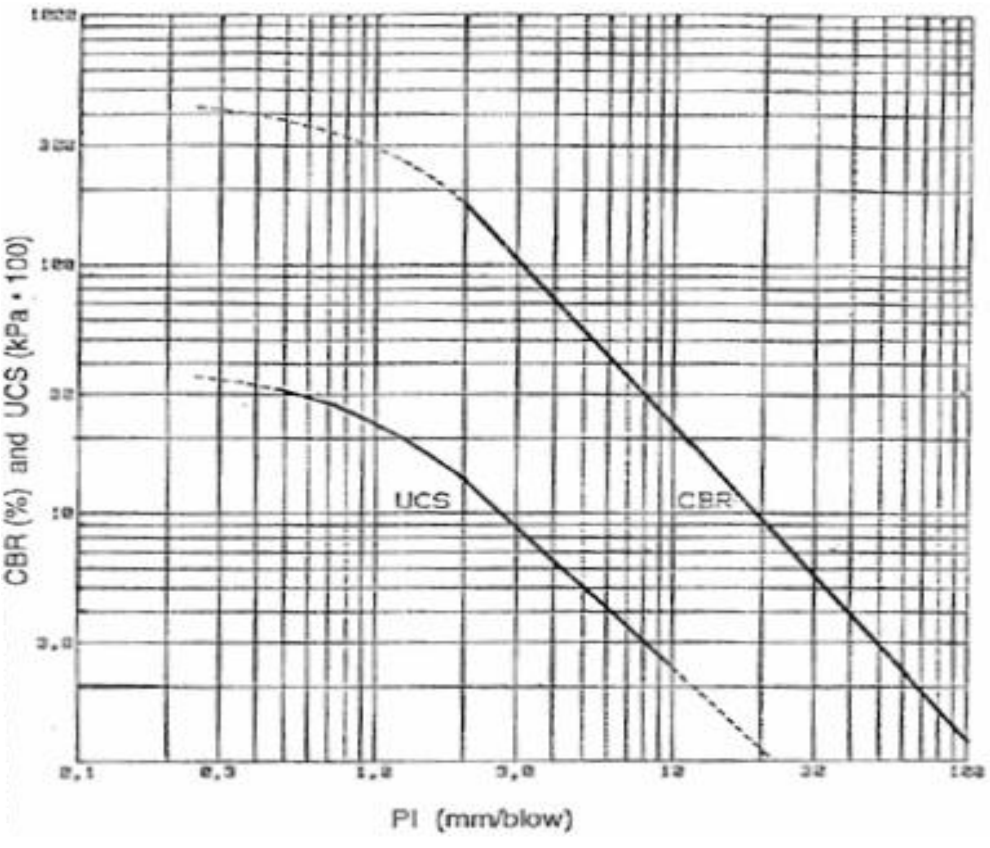

Fig. 2.15: Plot of California Bearing Ratio, Unconfined Compression Strength vs. Penetration Index (Tom Burnham, 1993)

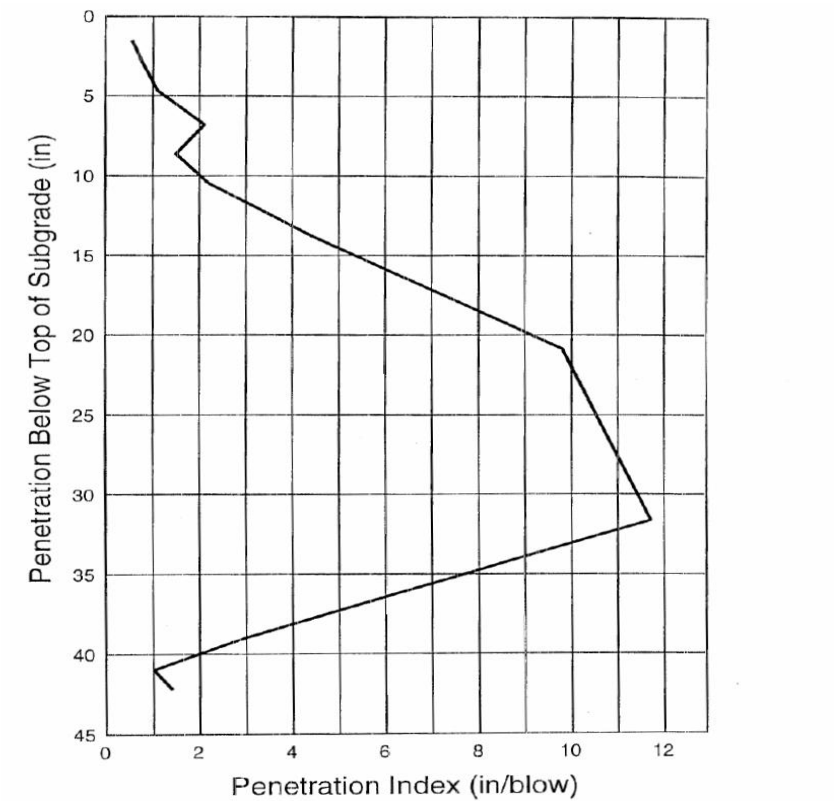

Fig. 2.16: The weak spot in subgrade bridge embankment (Tom Burnham, 1993)

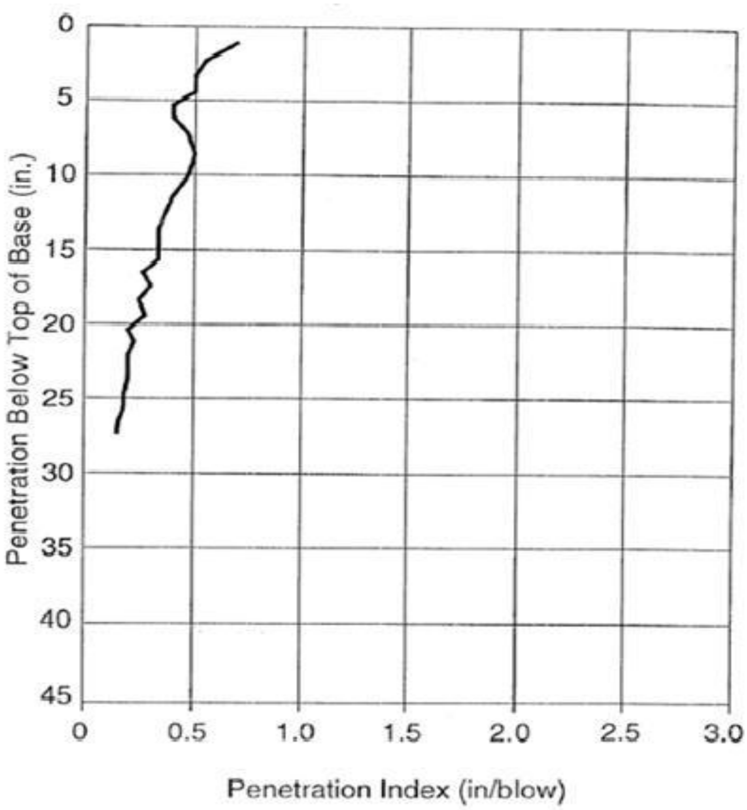

Fig. 2.17: Locating high strength layers in pavement structure (Tom Burnham, 1993)

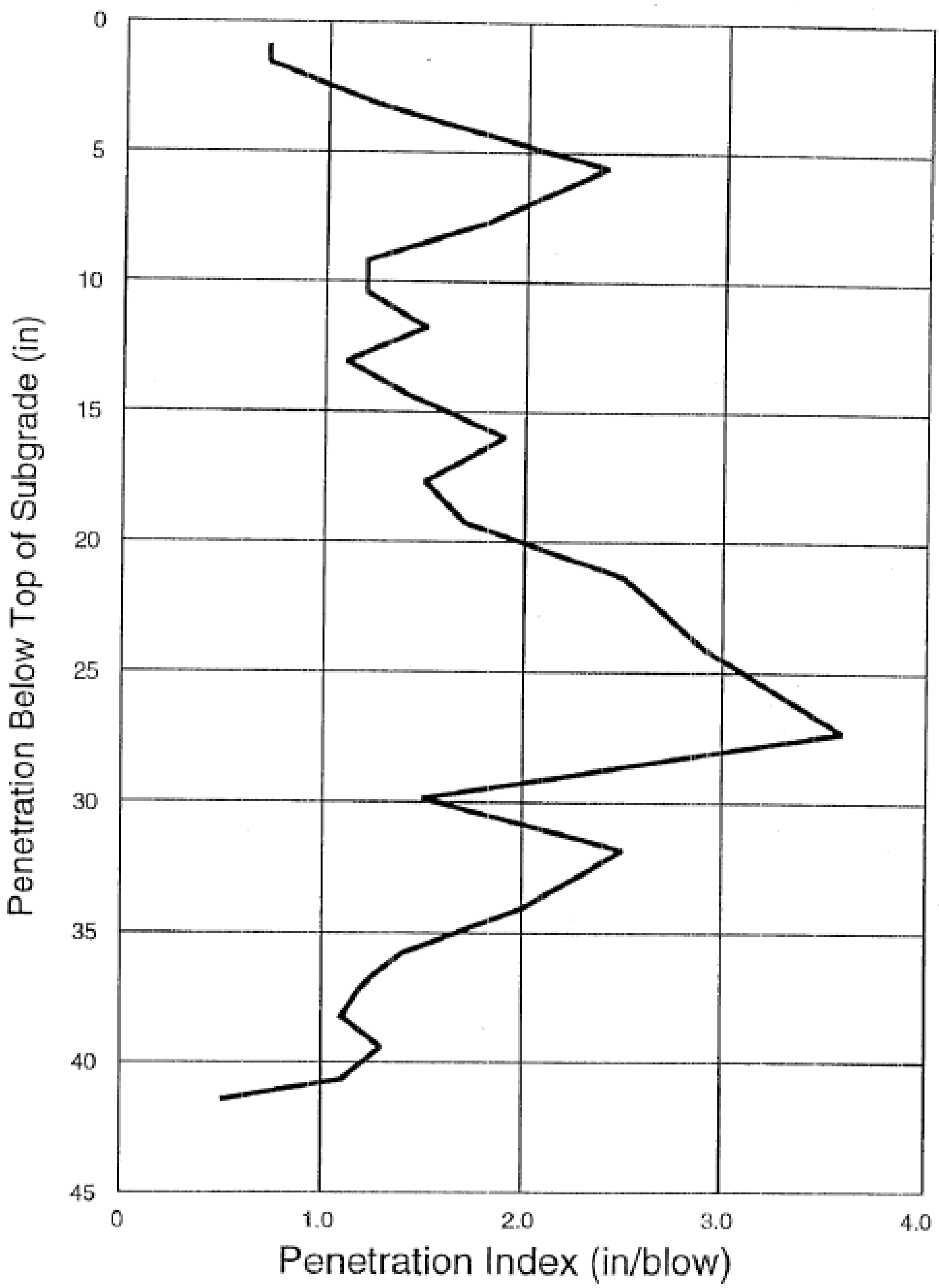

Fig. 2.18: The weak spot in subgrade bridge embankment (Tom Burnham, 1993).

Note: One test (Fig. 2.18) depicted an embankment with an average PI of about 2 inches (51 mm) per blow with a. range from .5 to 3.6 inches (1.3 to 91.mm) per blow.

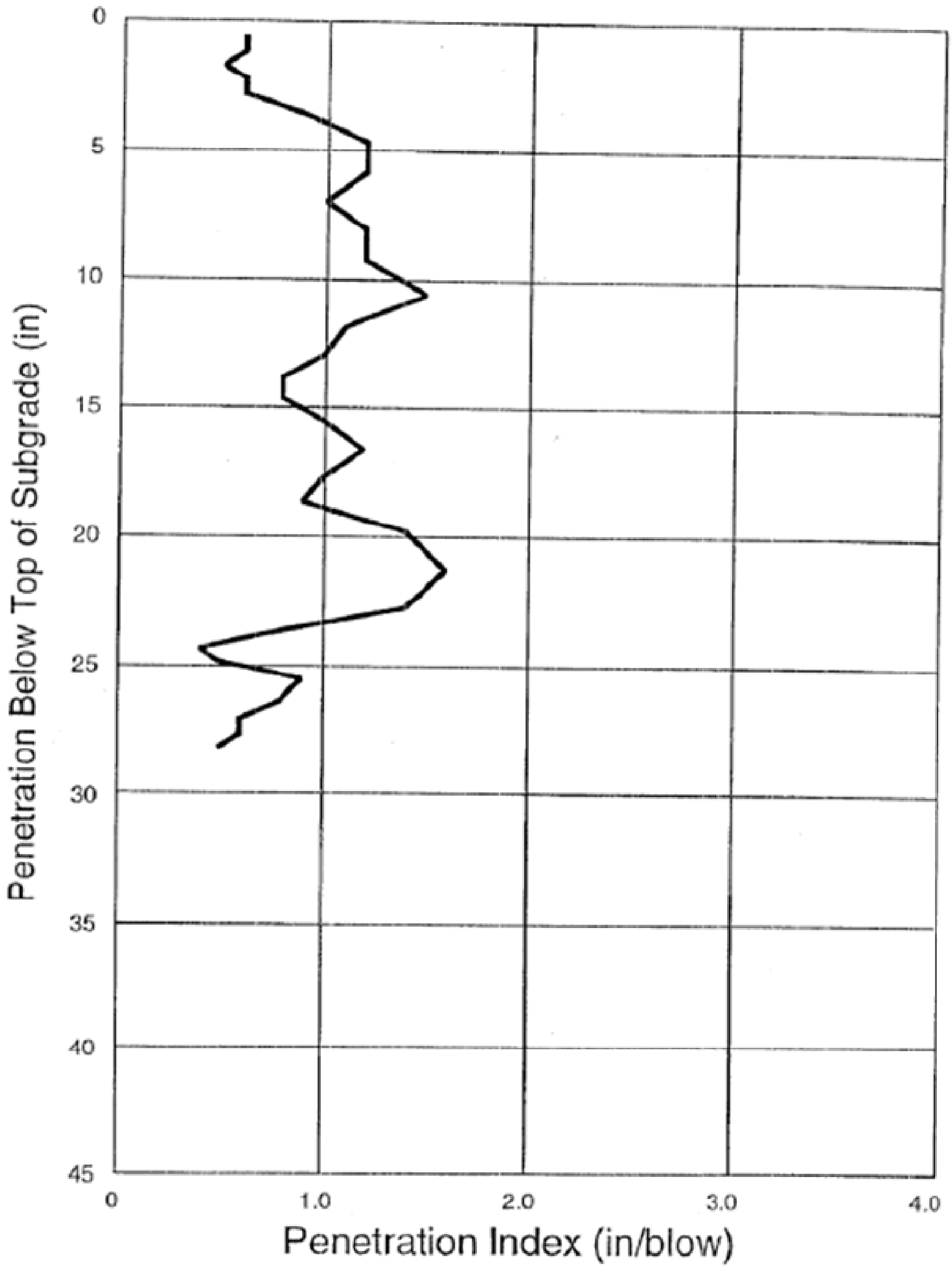

Fig. 2.19: The weak spot in subgrade bridge embankment (Tom Burnham, 1993)

Note: A nearer 40 feet (12 m) away (Fig. 2.19) the average PI was about 1 inch. (25 mm) per blow with a range from. 0.4 to 1.6 inches (10 to 41mm) per blow.

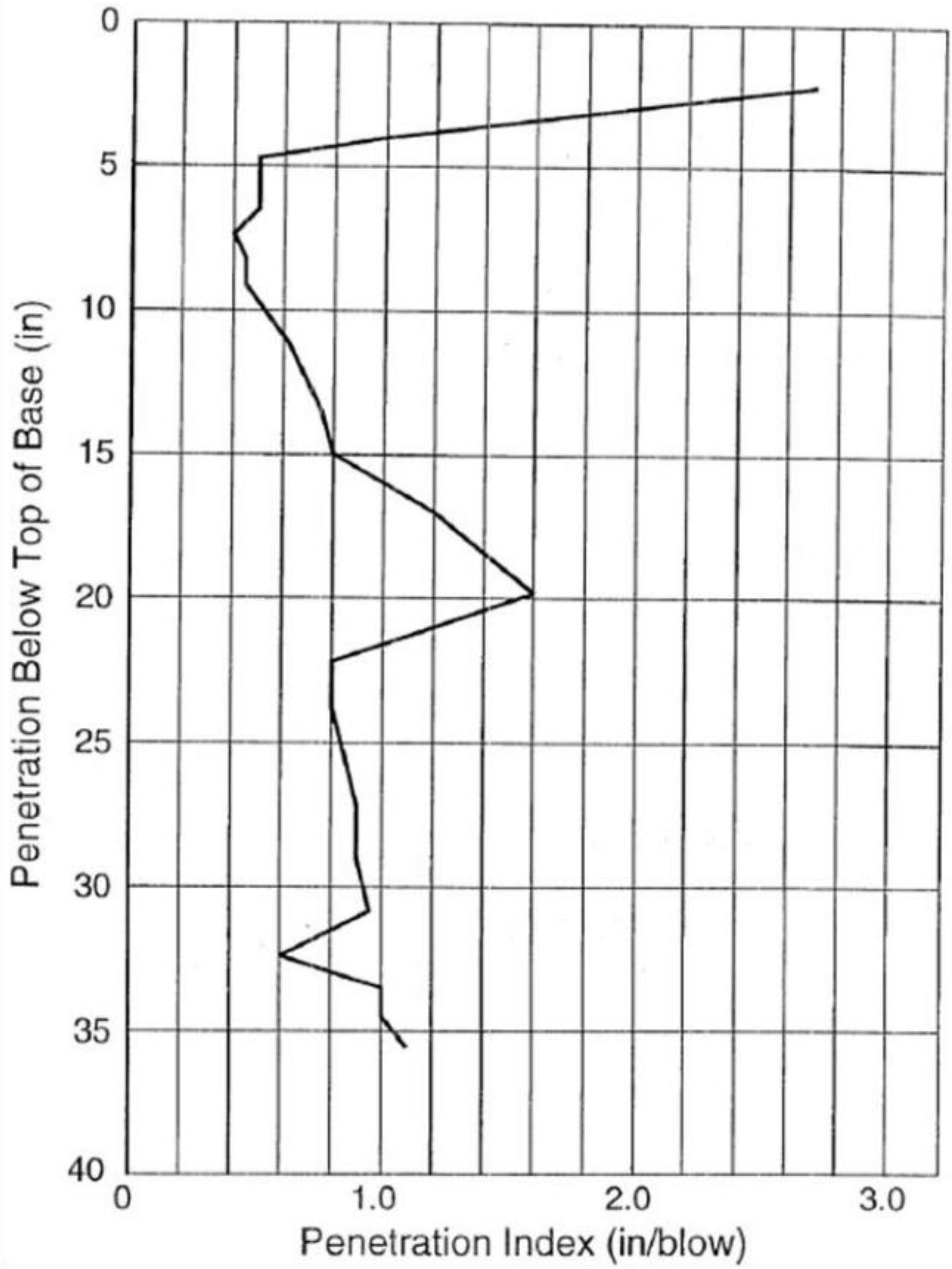

Fig. 2.20: Measuring the uniformity of in situ base material

Note: PI'S were as high as an astounding 11.7 inches (297 mm) per blow ;at a depth of 30 inches (762 mm) while PI'S near the surface averaged under 2 inches (51 mm.) per blow (Fig. 2.20)

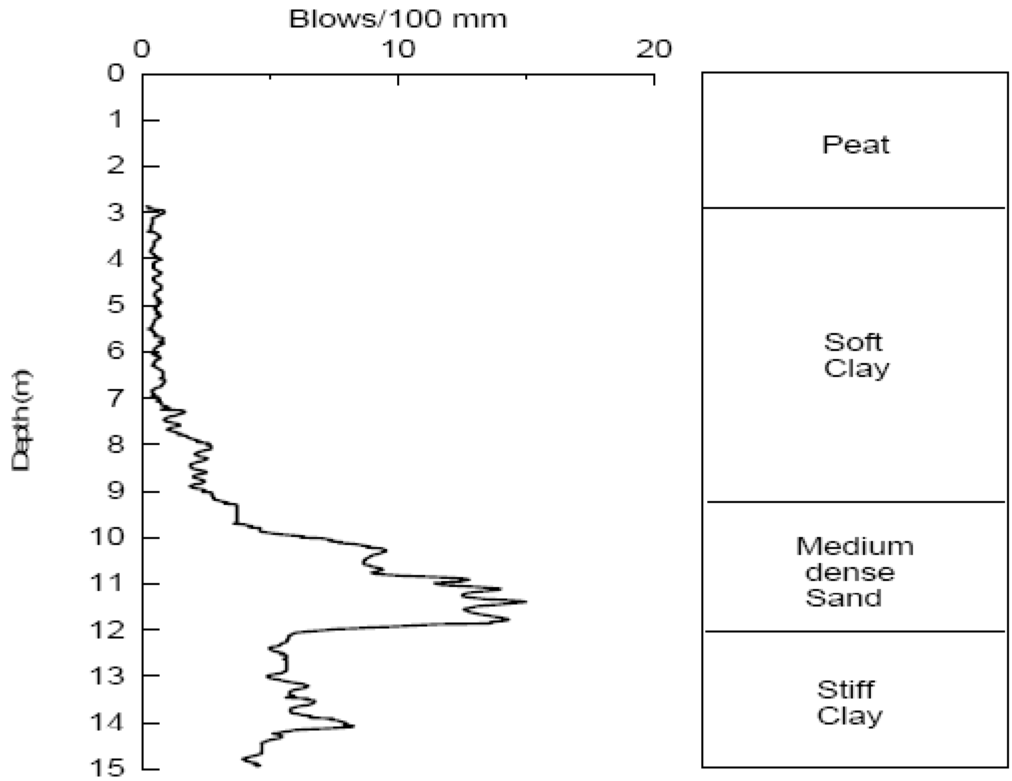

Fig. 2.21: Typical test profiles of DCP (Gudishala, R., 2004)

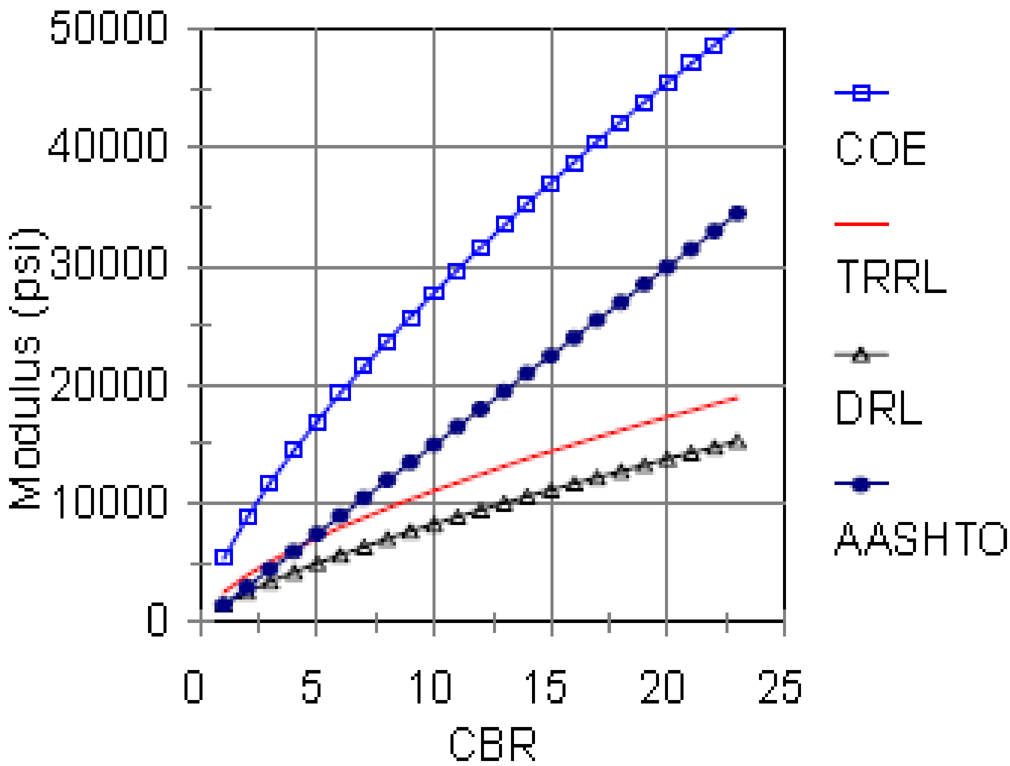

Fig. 2.22: Comparing different CBR-modulus relationships

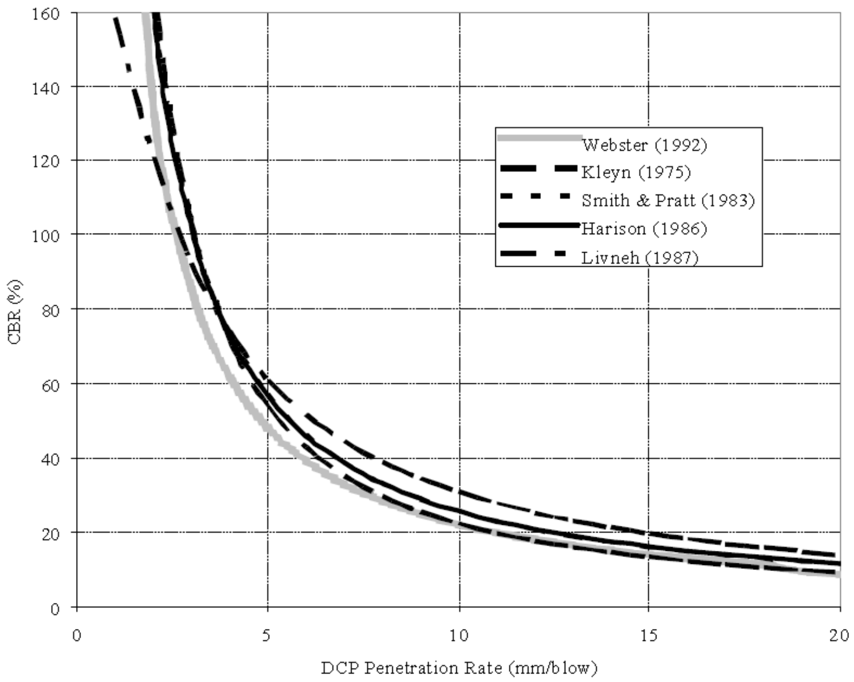

Fig. 2.23: Comparison of different CBR vs.DCP correlations

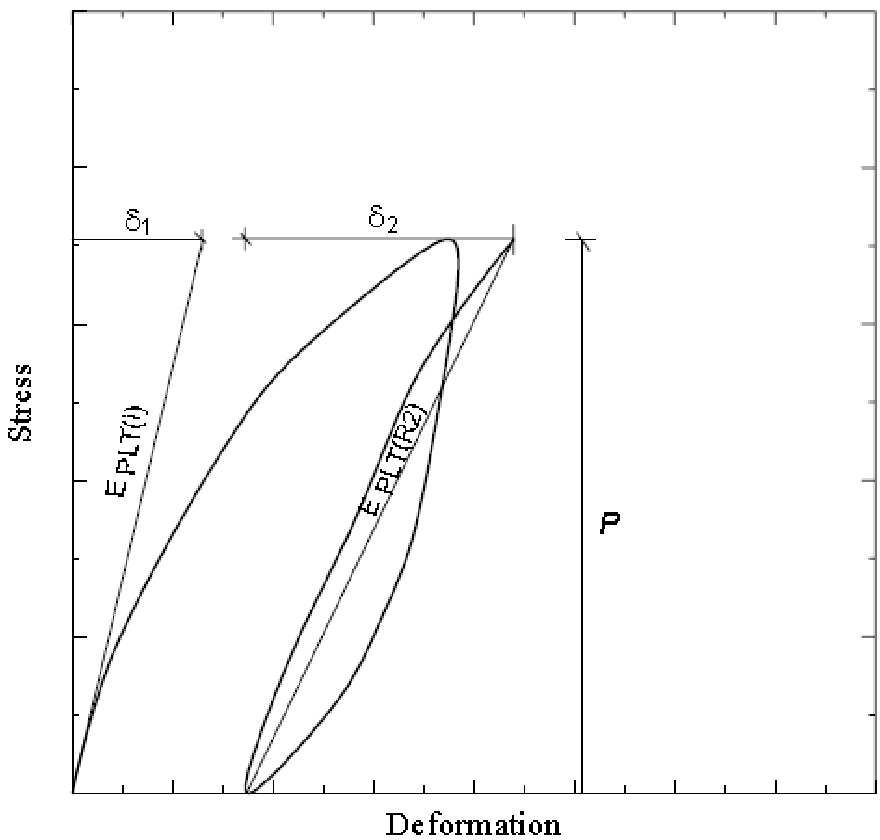

Fig. 2.24: Definition of modulus from PLT

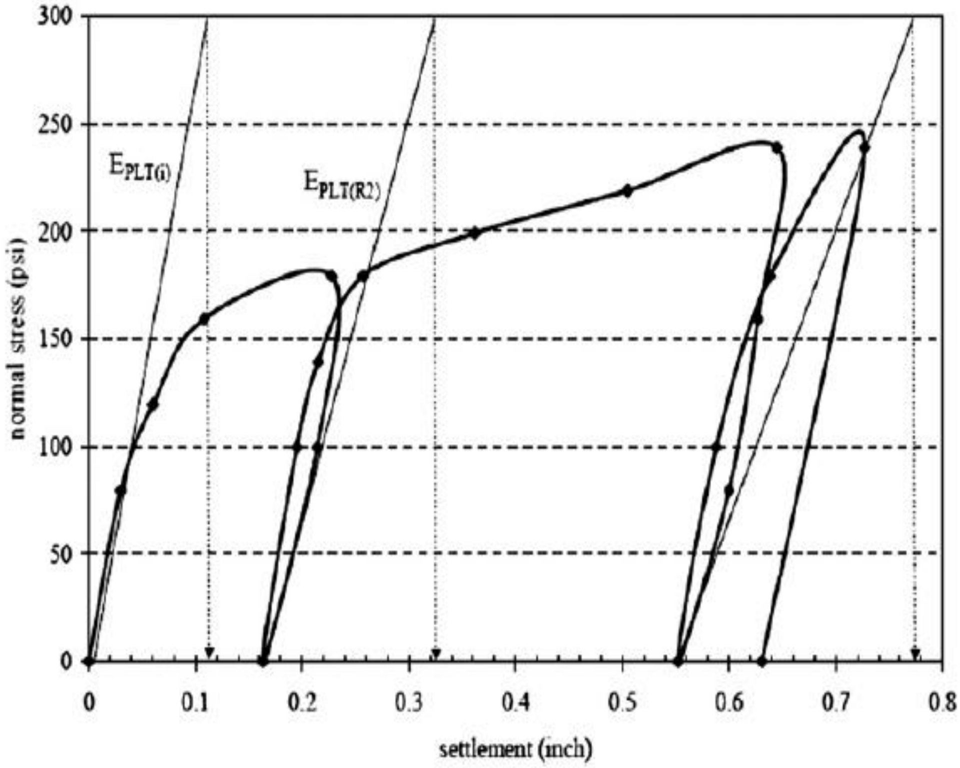

Fig.2.25: Definition of modulus from PLT (Abu-Farsakh et al., 2004).

CHAPTER 3
INSTRUMENTAION, TEST PROGRAM AND PROCEDURE

3.1General

This chapter describes the overall program including designing and fabricating the potable dynamic cone penetrometers and dynamic probabing light, plate load test, experimental setup and all the test procedure with necessary sample calculation.This chapter describes the experimental program. The experimental program consists of four stages.

In the first stage sample was prepared for required mean diameter (D_{50}). Sylhetsand was collected from local market. Mean diameter (D_{50}) value of test sample is 0.70 mm that was achieved by sieving thoroughly No. 4 passing and No. 200 retained sand collecting. Similarly same procedure was followed to achieve mean diameter value 0.35 mm of test sample by sieving thoroughly No.30 passing and No. 200 retained sand collecting.

In the second stage the air pluviation method was calibrated to know the height of fall and hole diameter of sand discharging bowl for different relative densities of two types of sand having mean diameter (D_{50}) is 0.70mm and 0.35 mm.

In the third stage sand deposits of different relative densities were prepared in calibration chamber where DCP, DPL and PLT test were performed. To obtain data for analysis, many laboratory tests were performed. It contained physical and index properties for strength properties determination. All the tests have standard procedure. But due to limited laboratory facilities, sometimes it becomes quite difficult to maintain the standard procedure. So slight deviation is very much possible. So it is necessary to mention the entire procedure with detailed sample calculation to show how the work was actually carried out in laboratory and up to results. Correlation between Penetration Index (P_{index}) and relative density was made from the test result in calibration chamber.

In the fourth stage, DPL and DCP tests were performed in dredge fill sites to verify the correlation.

3.2 Calibration of Air Pluviation Method

By controlling height of fall & rate of sand discharge, sand of desired density can be prepared by Multiple Sieve Method and air pluviation method. Multiple sieving pluviation apparatus used by Miura and Toki (1982) is shown in Fig. 3.1. A simple air pluviation method was developed in the Geotechnical Laboratory to prepare sand deposit of desired density. Plastic bowls, shown in Fig. 3.2 has been used for this purpose. Holes of different diameters (3.5 mm, 4.0 mm, 5.0 mm and 6.0 mm) are punched into the plastic bowl. Hole to hole triangle distance was 35 mm as shown in Fig. 3.7. A CBR mold was filled up by discharging sand from these holed bowls (hereafter called discharging bowl) maintaining fixed height of fall. Then density of sand was determined by weighing sand in CBR mold. This procedure was repeated for different height fall to get different densities for a specific type of sand. Two types of sand were calibrated by this procedure having mean diameter D_{50}=0.70 mm and D_{50}=0.35 mm. Index properties of these sands are shown in Table 3.1. Grain size distributions of these two sands are shown in Fig. 3.5 to Fig. 3.6 and scanning electro microscopic view are shown in Figs. 3.7 to 3.8. Air pluviation calibration data are tabulated in Tables 3.2 to 3.5.

3.3DCP, DPL and Plate Load Tests in Calibration Chamber

To perform the DCP and DPL test a steel cylinder of diameter 0.5 m and height 1 m was used as a calibration chamber. The thickness of calibration chamber wall was 13 mm.

3.3.1 Preparation of sand deposit

The calibration chamber was placed on a level ground. Sands were air dried by spreading them on dry floor. Then sand deposit of desired density was prepared by air pluviation method described in section 3.2. Height of fall was maintained by suspending a small weight from the discharging bowl through a fixed length of rope. Dry deposition of sand is shown in Fig. 3.9 and Fig. 3.10. Sand deposit of various relative densities was prepared using this method.

To get higher Relative Density sand deposit was prepared by filling sand into chamber in 4 layers. Each layer was densified using some sand bags were placed top of the chamber with striking the chamber body with hammer. Then DCP, DPL and PLT test was performed on the prepared sand deposit. The total weight of sand was measured to determine the density of sand deposit.

3.3.2 DCP and DPL tests in calibration chamber

The calibration chamber was filled up by discharging sand from the discharging bowls maintaining fixed height of fall. After filling the calibration chamber, every time DPL and DCP tests were performed and for each blow the penetration of cone was recorded. It is important to note that DCP and DPL has similar features except differences in cone size, weight of anvil, weight of drop hammer and height of fall. Table 3.6 shows the differences between DCP and DPL.

All DCP and DPL tests were performed by two operators. One person operated the hammer, while the other person reads and records the penetrations. Before each test, the tip of the ruler used to measure the penetrations was placed to a marked reference point on the surface. The person who took the readings was responsible to ensure that the ruler was kept parallel to the penetrating rod while taking measurements. Friction between the rod and the tested material has negative effects on the results. In order to minimize the friction of the rod with surrounding soil, the DCP and DPL must be kept vertical during penetration. If the DCP and DPL deviates from vertical position and operator continue to test, the device might be damaged and the results obtained for that test will not be reliable. In both cases, N_{10} is the number of blows required for 10 cm penetration of the cone. Figure 3.11 show starting of a DCP test after filling calibration. After completion of tests, sands were taken out from the calibration chamber and weighed by digital balance to check the density and Relative Density of sand deposit.

3.3.3 Plate Load test incalibration chamber

The plate loading test (PLT) is a well known method of estimating the bearing capacity of soils and evaluating the strength of flexible pavement systems. The test has been somewhat discredited due to its destructive nature and time consuming testing procedure. Round plates with 10 inches in diameter was used in this study. The 10 inch in diameter plate was preferred in order to have enough loading increments, especially for cases where the test layer cannot handle high stresses. A loading frame as shown in Fig.3.23, that was designed to fit to the calibration chamber, was used as a support for the Plate Load Test are shown in Figs.3.17 to Figs. 3.22. Bearing plate of the selected diameter, dial gauges capable of recording a maximum deformation of 1 mm with 0.01 mm resolution as shown in Fig. 3.13 and the hydraulic jack were carefully placed at the center of the samples under the loading frame is shown in Fig.3.25a and Fig.3.25b.

A 50 tones capacity hydraulic jack that was used for loading the plate has a resolution of 0.5 ton is shown in Fig. 3.12.In this plate load test, hydraulic pump and jack gauge was used that is shown in Fig. 3.14.Before plate load test, hydraulic jack load calibration test was performed in the strength material laboratory of BUET, is shown in Fig. 3.16. Hydraulic jack calibration chart are shown in the Table 3.7 and Table 3.8.To achieve this purpose load column was used that capacity 500 kN (Model No. 1052-12-1085), are shown in Fig. 3.15.ASTM-D1196 method was followed to perform the plate load test. Plate diameter, applied load increments and the corresponding deflections were recorded for each load increment. Each increment of load was maintained until the rate of deflection became less than 0.001 inch/min for three consecutive minutes. Each sample was loaded up to failure or until load capacity of the loading frame has been reached.

Each sample was unloaded and reloaded at least once in order to be able to determine the reloading modulus of the two samples having mean diameter is 0.70 mm and 0.35 mm at different relative density in addition to the initial loading modulus. Settlement of the plate for each load increment was recorded during the test. These values are then used to plot load settlement relationship. A tangent was drawn to the initial portion of the curve to determine the load and corresponding settlement that will be used in order to obtain the initial tangent modulus ($E_{PLT(i)}$)of the test layer. Reloading lines were drawn from the beginning of reloading portion of the curve to the point where reloading portion of the curve reaches to the load, where unloading was started. Reloading modulus ($E_{PLT(R2)}$) is calculated with the load and corresponding change in the settlement that is obtained from the reloading line in the second cycle

3.3.4 California bearing ratio test

To find the unsoaked CBR value at in situ density, the specimens were prepared in the laboratory by varying the number of blows at different compaction levels. In t his study, four compaction levels i.e. 10, 25, 35 and 45 blows were adopted for different percentage of water. The in situ densities were calculated for the different compaction levels and the graph is plotted between the in situ density and number of blows. Hence, the number of blows calculated from that graph corresponding to the desired in situ density was used to prepare the sample in the CBR mould. The dry density and the number of blows and the similar results were obtained for the different locations also.

ASTM D1883 method was followed to perform the CBR tests. CBR samples representing the materials tested in the boxes were prepared according to the moisture content measured using the nuclear density gauge. Standard mold with 6 inch diameter and 7 inch height was used for preparation. Since it is not possible to prepare samples with the exact same density measured using the nuclear density gauge; at least four samples with different compaction levels were prepared with the some required moisture content. Specimens were compacted at five layers. An automatic compactor with a 10 lbs hammer was used.

Table 3.1: Properties of two types of sand

Properties	Type 1	Type 2
Fineness Modulus, F.M	3.74	2.58
D_{10} (mm)	0.32	0.18
D_{25}(mm)	0.46	0.25
D_{30} (mm)	0.50	0.28
D_{50} (mm)	0.70	0.35
D_{60} (mm)	0.85	0.40
D_{75}(mm)	1.005	0.45
Coefficient of uniformity, C_u	2.66	2.22
Coefficient of curvature, C_c	0.92	1.08
Maximum void ratio, e_{max}	0.67	0.95
Minimum void ratio, e_{min}	0.48	0.57
Maximum index density, γ_{max} (kN/m^3)	17.50	16.52
Minimum index density, γ_{min} (kN/m^3)	14.54	13.30
Fines (%)	0	0
Types (Unified Soil Classification)	SP (Clean Sand)	SP (Clean Sand)

Note: D_{10} (mm) = particle size corresponding to 10% finer,
D_{50} (mm) = mean diameter of sand.

Table 3.2: Calibration of air pluviation method for sand (D_{50}=0.70 mm, γ_{max}= 17.50 kN/m^3 and γ_{min} =14.54 kN/m^3) (Opening of discharging bowl=5.0mm)

Height of fall (cm)	**Dry density (kN/m^3)**	**Relative density Dr (%)**
15	15.92	51.40
25	16.03	54.89
36	16.13	58.35
46	16.27	62.88
56	16.40	67.34
66	16.44	68.44
76	16.53	71.18
86	16.56	72.27
97	16.61	73.89
107	16.65	75.08
117	16.68	76.04
127	16.72	77.11
137	16.73	77.53
147	16.73	77.53
158	16.73	77.53

Table 3.3: Calibration of air pluviation method for sand (D_{50}=0.70 mm, γ_{max}=17.50 kN/m^3 and γ_{min} =14.54 kN/m^3)**(**Opening of discharging bowl= 6.0mm)

Height of fall (cm)	**Dry density (kN/m^3)**	**Relative density, Dr (%)**
15	15.70	43.66
25	15.84	48.56
36	15.97	53.15
46	16.12	58.12
56	16.34	65.12
66	16.39	66.79
76	16.49	70.09
86	16.54	71.73
97	16.59	73.35
107	16.63	74.43
117	16.63	74.43
127	16.65	74.97
137	16.68	76.04
147	16.70	76.57
158	16.70	76.57

Table 3.4: Calibration of air pluviation method for sand (D_{50}=0.35 mm, γ_{max}=16.52 kN/m^3 and γ_{min}=13.30 kN/m^3) (Opening of discharging bowl=3.5mm)

Height of fall (cm)	**Dry density (kN/m^3)**	**Relative density, Dr (%)**
15	14.66	47.67
25	14.96	56.92
36	15.17	63.26
46	15.39	69.63
56	15.51	73.09
66	15.54	74.07
76	15.59	75.53
86	15.66	77.47
97	15.70	78.52
107	15.70	78.52
117	15.74	79.48
127	15.80	81.38
137	15.80	81.38
147	15.80	81.38
158	15.80	81.38

Table 3.5: Calibration of air pluviation method for sand (D_{50}=0.35 mm γ_{max}=16.52 kN/m^3 and γ_{min} =13.30 kN/m^3) (Opening of discharging bowl= 4.0mm)

Height of fall (cm)	**Dry density (kN/m^3)**	**Relative density, Dr (%)**
25	14.73	43.79
36	15.07	49.74
46	15.27	60.17
56	15.46	66.12
66	15.59	71.62
76	15.63	75.53
86	15.66	76.50
97	15.71	77.47
107	15.75	78.90
117	15.77	79.86
127	15.78	80.81
137	15.78	80.33
147	15.78	80.33
158	15.78	80.33

Table 3.6: Basic differences between DCP and DPL

Parameters	DCP	DPL
Hammer Weight (Kg)	8	10
Height of Fall (m)	0.66	0.50
Mass of anvil and Guide Rod (kg)	--	6
Cone diameter (mm)	22.5	35.7
Cross sectional Area of cone (mm^2)	397.60	1000.98
Volume of cone, (mm^3)	2111.30	5955.85
Apex angel of cone (degree)	60	90
Energy per blow, (J)	51.80	49.05
Energy per blow (J)/ Cone Diameter (mm)	2.30	1.37
Energy per blow(J)/ Cross sectional area of cone (mm^2)	0.130	0.050
Energy per blow(J)/ Volume of cone (mm^3)	0.0245	0.00823

Table 3.7: Calibration of Load Column
(Used Load Column=500 kN, Model No. 1052-12-1085)

500 kN (No. 1052-12-1085) Load Column Calibration					
Orientation	0^o	0^o	120^o	240^o	Unbiased Estimate of Mean
Force (kN)	Deflectometer Reading (Divisions)				
	Test 1	Test 2	Test 3	Test 4	
50	130.2	130.3	130.2	130.2	130.2
100	257.5	257.7	257.7	257.7	257.7
150	389.4	389.6	389.6	389.6	389.5
200	516.8	516.8	516.8	516.8	516.8
250	644.8	644.9	644.8	644.8	644.8
300	773.5	773.7	773.5	773.5	773.5
350	901.5	901.5	901.4	901.4	901.4
400	1029.5	1029.5	1029.6	1029.6	1029.6
450	1155.4	1155.3	1155.3	1155.2	1155.3
500	1282.8	1282.6	1282.6	1282.7	1282.7

Table 3.8: Calibration Chart of Hydraulic Jack (Used Load Column = 500 kN, Model No. 1052-12-1085)

Used Load Column = 500 kN (Model No. 1052-12-1085)				
Hydraulic Jack Capacity= 50 tones				
Gauge Reading Load (Kg/cm^2)	Load Column Reading (Divisions)		Average Column Reading (Divisions)	Observed Load (kN)
	Test 1	Test 2		
60	68	67	67.5	24.953
100	175	172	173.5	66.293
160	322	321	321.5	124.013
200	425	428	426.5	164.963
260	575	578	576.5	223.463
300	672	673	672.5	260.903
360	827	820	823.5	319.793
400	925	924	924.5	359.183
460	1073	1062	1067.5	414.953

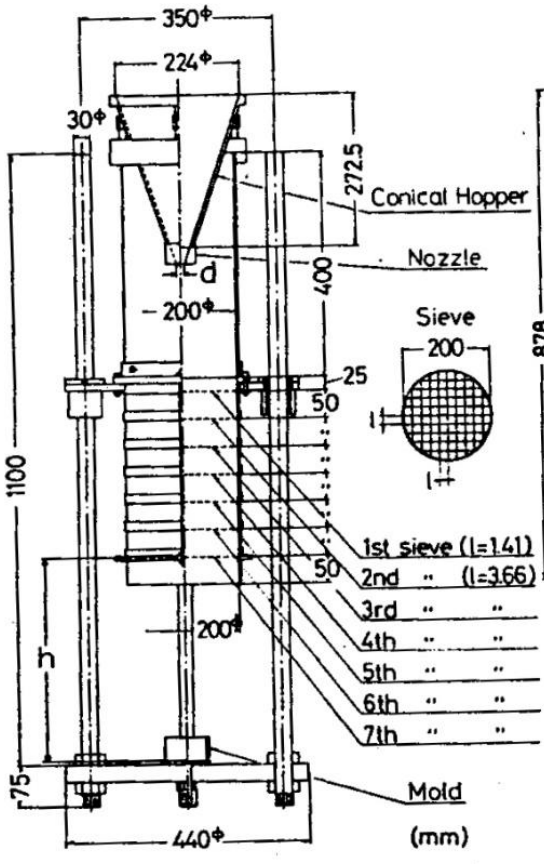

Fig. 3.1: General view of multiple sieving pluviation apparatus (Miura and Toki, 1982)

Fig. 3.2: Sand discharge bowl with 3.5mm diameter holes

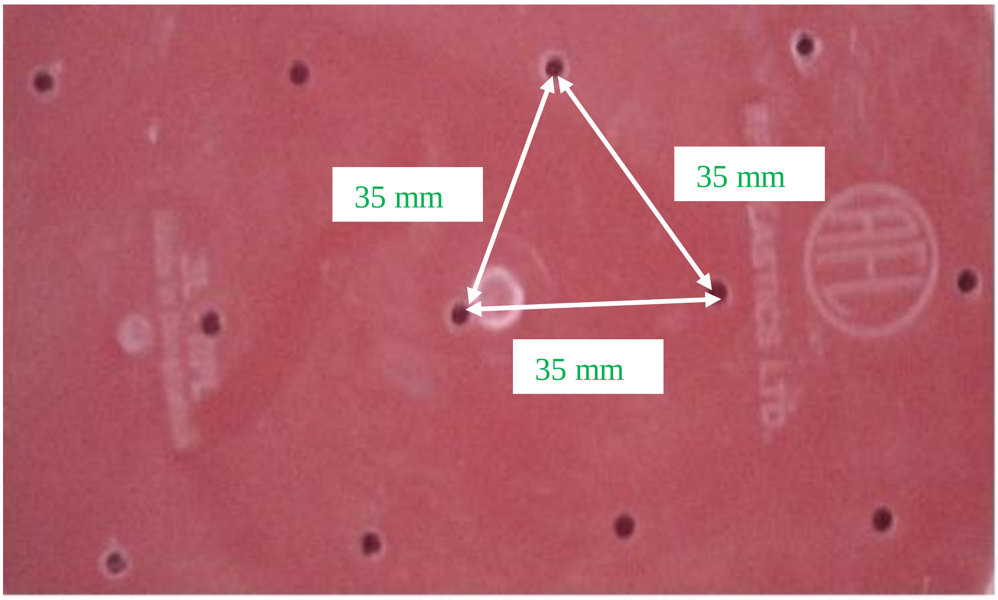

Fig. 3.3: Spacing and pattern of holes of discharge bowls

Fig. 3.4: Air pluviation method

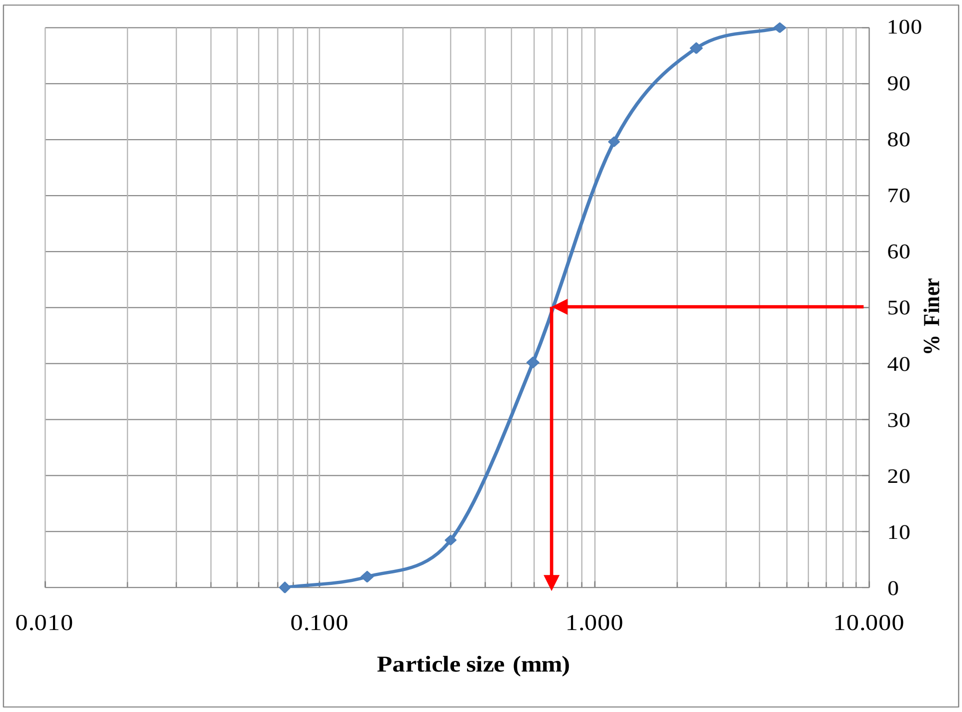

Fig. 3.5: Grain size distribution curve of sand having mean diameter (D_{50}) is 0.70 mm that used in the study

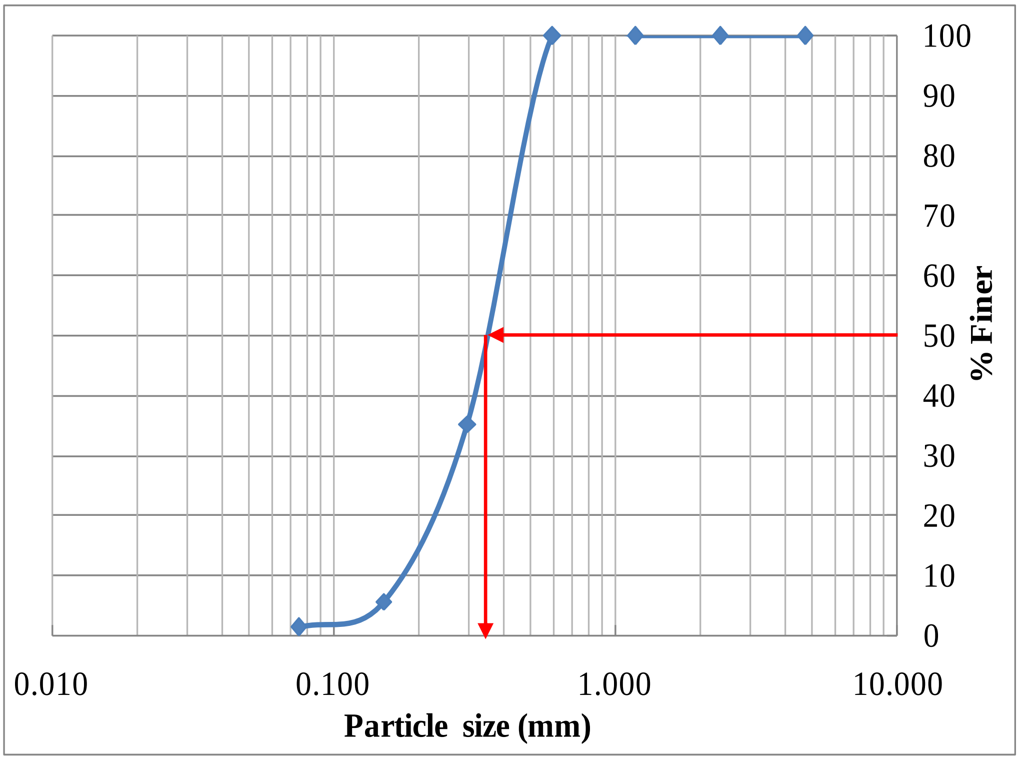

Fig. 3.6: Grain size distribution curve of sand having mean diameter (D_{50}) is 0.35 mm that used in the study

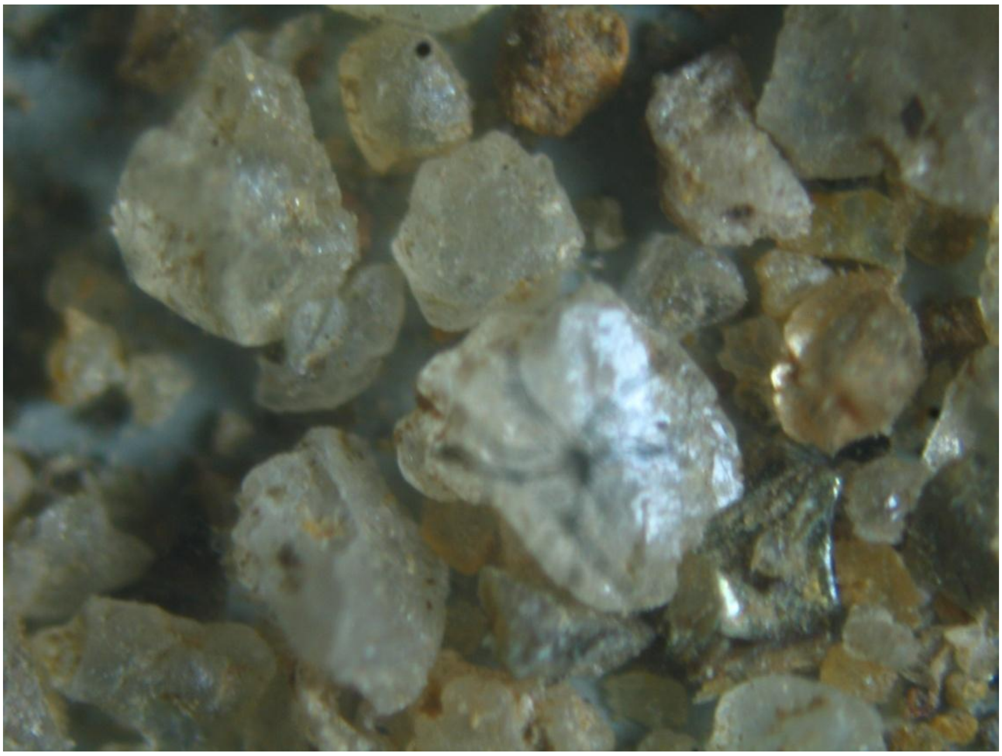

Fig. 3.7: Scanning electro microscopic view sand having mean diameter is 0.70 mm

Fig. 3.8: Scanning electro microscopic view sand having mean diameter is 0.35 mm

Fig. 3.9: Dry deposition into calibration chamber from discharging bowl maintaining a constant height of fall (Azad, A.K., 2008)

Fig. 3.10: Filling of calibration chamber in progress (Azad, A.K., 2008)

Fig. 3.11: Initial reading of the scale before starting DCP

Fig. 3.12: Hydraulic jack (Capacity =50 tonnes)

Fig. 3.13: Deflectometer (Divisions= 0.01mm)

Fig. 3.14: Hydraulic pump and jack gauge

Fig. 3.15: Load column (Capacity=500 kN) (Model No. 1052-12-1085)

Fig. 3.16: Hydraulic jack calibration by using load column (Capacity= 500 kN)
(Model No. 1052-12-108)

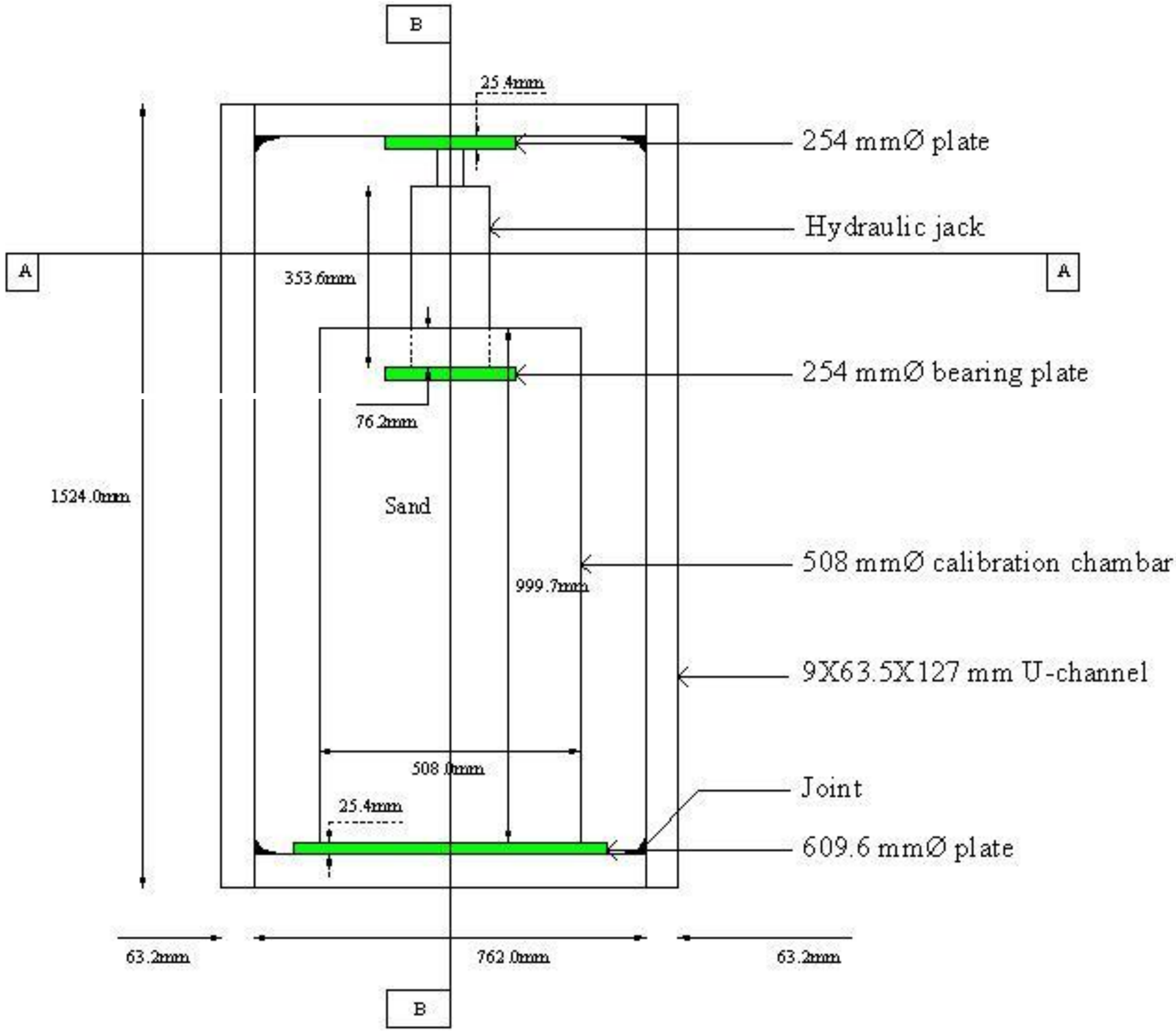

Fig. 3.17: Front view of load frame with hydraulic jack

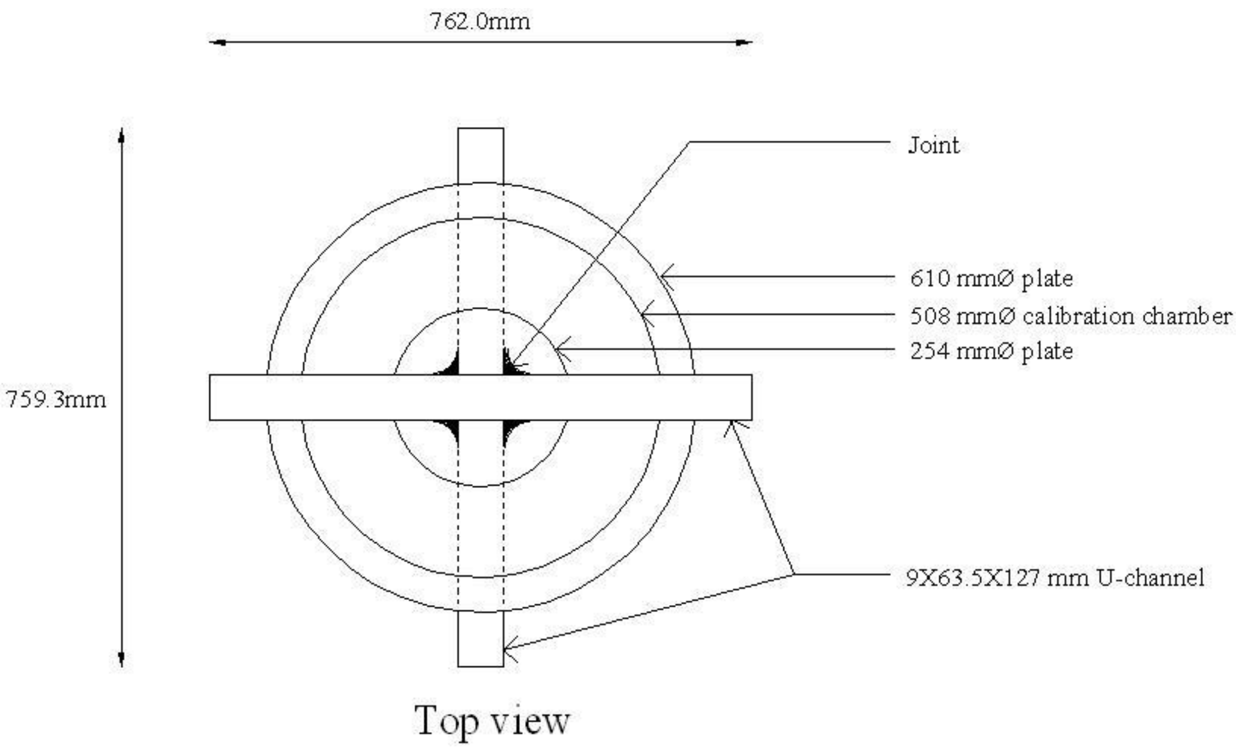

Fig. 3.18: Top view of load frame

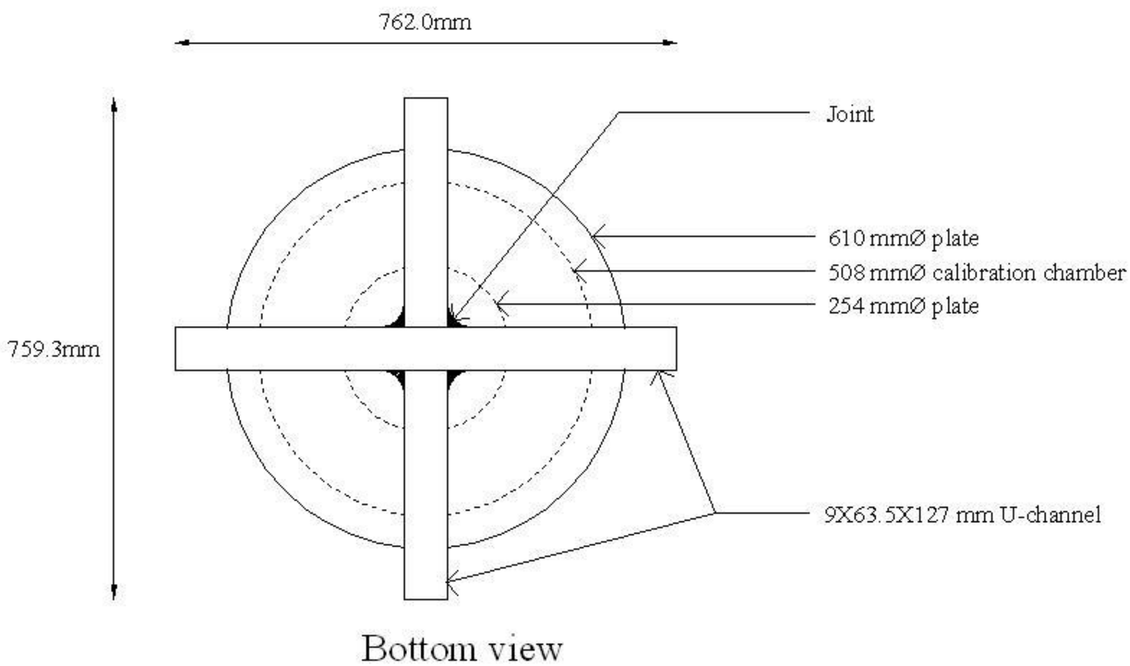

Fig. 3.19: Bottom view of load frame

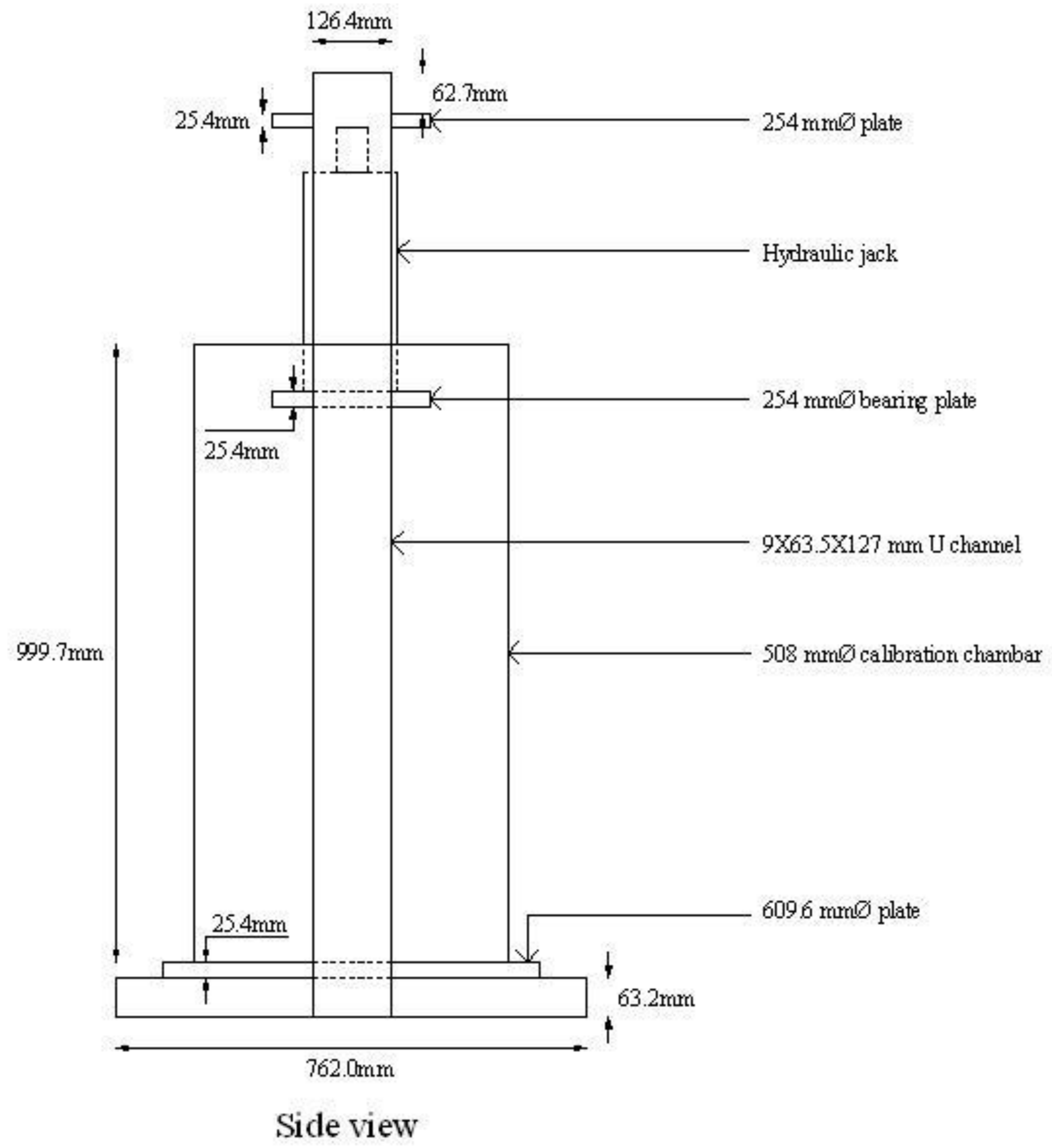

Fig. 3.20: Side view of load frame with hydraulic jack

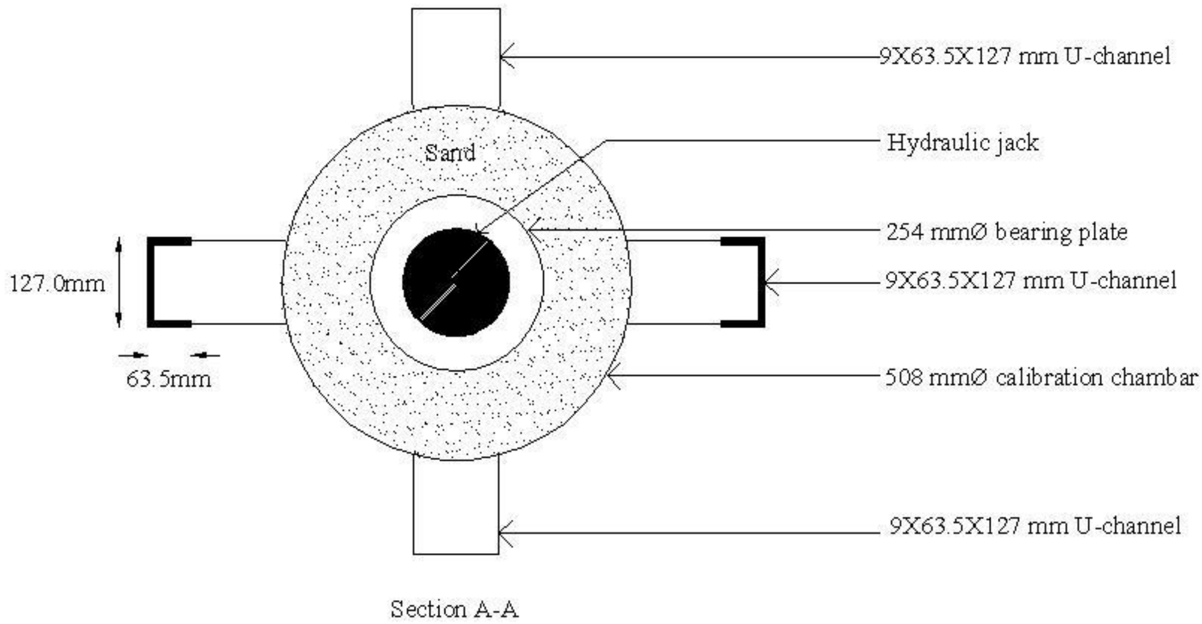

Fig. 3.21: Section A-A of load frame

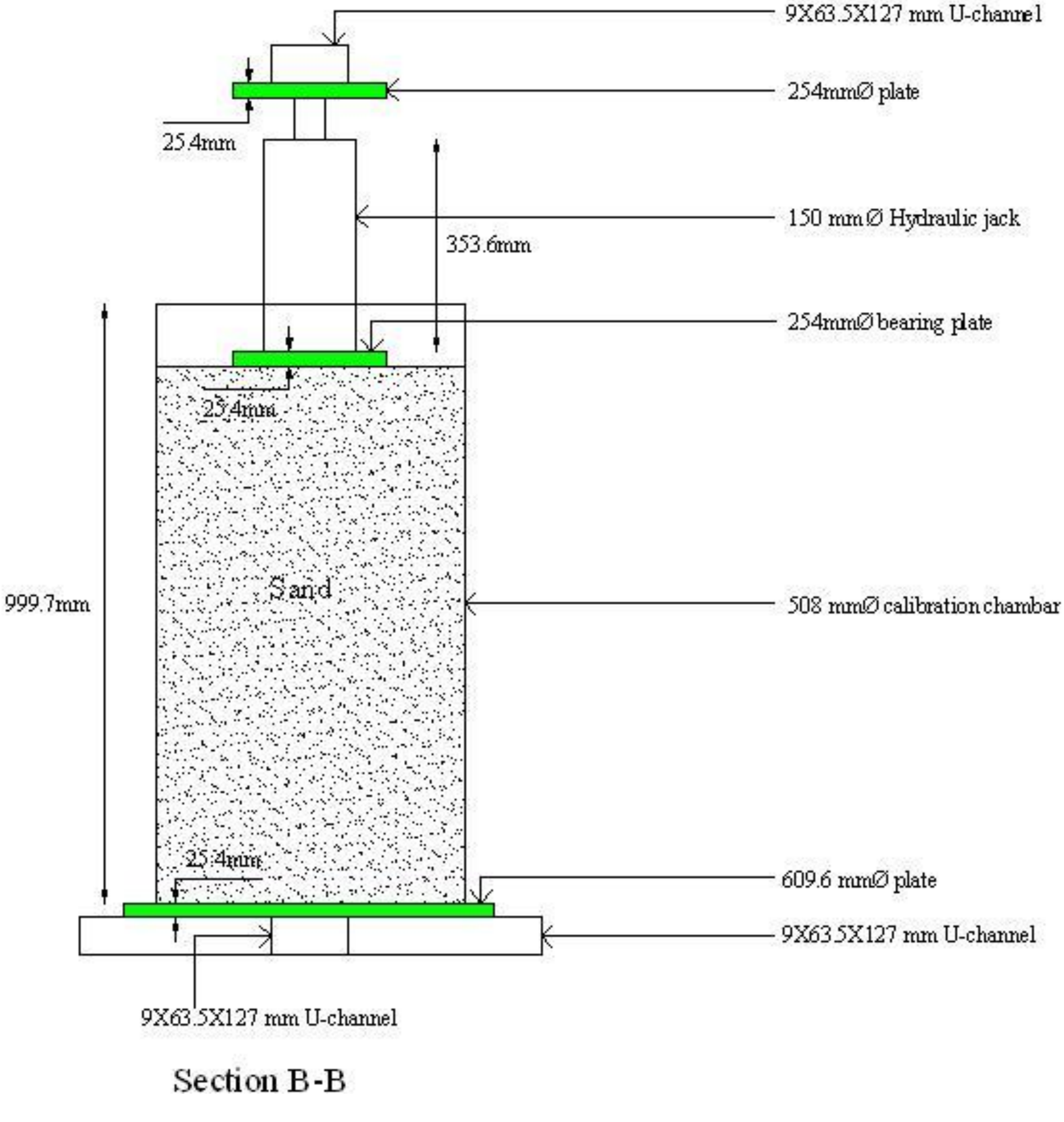

Fig. 3.22: Section B-B of load frame

Fig. 3.23: Load frame with chamber

Fig. 3.24: Load frame with bottom plate (Plate thickness= 1 inch)

Fig. 3.25a: Load column frame with hydraulic jack at loading condition

Fig. 3.25b: Load column frame with hydraulic jack at loading condition

CHAPTER 4
RESULTS AND DISCUSSIONS

4.1 General

In this chapter the results of the experimental program are presented which include the calibration of air pluviation method for sand having mean diameter D_{50} value of 0.35 mm and 0.70 mm and DCP, DPL and Plate Load test results in calibration chamber and field.

4.2 Calibration of Air Pluviation Method

The plot of Relative Density against height of fall for fine sand is presented in Fig. 4.1. Discharge bowls with 5.0 mm and 6.0 mm opening were used for sand of mean diameter is 0.70 mm. Figure 4.2 is the plot of Relative Density against height of fall for sand of mean diameter is 0.35 mm. Discharge bowls with 3.5 mm and 4.0 mm openings were used for sand having mean diameter was 0.35 mm. From Fig. 4.1 to 4.2 it is seen that for a certain diameter of hole of discharge bowl the Relative Density of sand increases with increase of height of fall. For a specific sand type and a fixed height of fall, Relative Density decreases with increase of opening size of discharge bowl (Fig. 4.1 and 4.2). That means if the rate of discharge of sand decreases, Relative Density increases for a constant height of fall. To prepare sand deposit of known Relative Density, Figs. 4.1 to 4.2 were used to find the height of fall required for that Relative Density.

4.3 Result of DCP and DPL in Calibration Chamber

Sand deposit of uniform density was prepared in calibration chamber and then one DCP and one DPL test was performed on prepared sand deposit. Determination of P_{index}, N_{10}, Relative Density and correlation between P_{index} and Relative Density of sand of mean diameter is 0.35 mm and 0.70 mm are presented in the following sections.

4.3.1 Determination of P_{index} and N_{10}

Sand deposit of desired Relative Density was prepared in calibration chamber, then one DCP and one DPL tests were performed in the chamber. Then recorded cumulative numbers of blows were plotted against depth. Figure 4.3shows such plots for sand of Relative Density49.40 % having mean diameter value is 0.70 mm. Some unreliable data points up to depth of 30 cm were eliminated because of presence of very low confining pressure on top of sand deposit. It is observed that cumulative number of blows increases linearly with depth after this elimination. Fig. 4.4 and 4.5indicates uniform density of sand from top to bottom of sand deposit. P_{index} was calculated from the average slope of the cumulative number of blow vs depth plot, as shown in Fig. 4.3**.** Then N_{10} value was calculated as 100/P_{index}. Fig.4.3to 4.10shows typical DCP and DPL test results for two type of sand that having mean diameter is 0.35 mm and 0.70 mm.

It was difficult to obtain Relative Density more than 75% by air pluviation method so by using concrete vibrator we prepare sand deposit of Relative Density 90.21%. DCP and DPL test result on fine sand of Relative Density 86.92% are shown in Fig. 4.5, 4.9and4.11**.** From these figures it was seen that sand deposit was almost uniform throughout the depth. All other test results of DCP and DPL are presented in Appendix A.

4.3.2 Development of correlation between relative density and P_{index}

To calculate the density of sand in calibration chamber all the sands were removed from the chamber and weighed after completion of DCP and DPL on prepared sand deposit. Then the Relative Density was calculated from the density. Following the procedure described in the previous section, P_{index} and N_{10} value for DCP and DPL was determined. To get a generalized correlation, P_{index} value is multiplied by $D_{50}^{0.75}$ of sand where D_{50} is in mm. Then Relative Density vs. $P_{index}D_{50}^{0.75}$ is plotted in Fig. 4.16 and Fig. 4.17. Generalized correlation for DCP is expressed as

$$\mathrm{D_r}\ (\%) = -1.036 P_{index} D_{50}^{\ 0.75} + 94.99 -------------------------- 4.1$$

Generalized correlation for DPL is expressed as

$$D_r\ (\%) = -5.219 P_{index} D_{50}^{\ 0.75} + 101.3 ------------------------- 4.2$$

Where,

D_r = Relative Density,

P_{index} = Penetration Index (mm/blow)

D_{50} = Mean diameter of sand particles in mm

Normalization of P_{index} by multiplying $D_{50}^{0.75}$ was found to be appropriate to make generalized correlation for clean sands of any particle size.

4.4 Result of Plate Load Test (PLT) in Calibration Chamber

The plate load test result was collected by the following procedure that describes below.

4.4.1 Calibration of hydraulic jack

Before starting the plate load test, calibration of hydraulic jack was prepared in the solid mechanics lab of BUET. Figure 4.19 show the relationship between actual load in kN and gauge pressure in kg/cm^2 of hydraulic jack.

4.4.2 Determination of initial tangent modulus ($E_{PLT(i)}$) & subgrade modulus (K_S)

In stress deflection curve of plate load test, initial tangent modulus was drawn. From the curves, based on the initial tangent line corresponding stress and deflection was taken into account to determine the initial tangent modulus and subgrade modulus by using equation. Figs. 4.20 to 4.24 show the stress deflection curve at different relative density for mean diameter (D_{50}) of sand.

4.4.3 Development of correlation among $E_{PLT(i)}$, D_r and $P_{index.}$

To find out the density of sand in calibration chamber all the sands were removed from the chamber and weighed after completion of DCP, DPL and PLT on prepared sand deposit. Then the Relative Density was calculated from the density. Following the procedure described in the previous section, P_{index} and N_{10} value for DCP and DPL was determined, initial tangent modulus was determined based on Plat Load Test (PLT). To get a generalized correlation, D_{50} value is multiplied by $D_{50}^{0.20}$ of sand where D_{50} is in mm. Then Initial tangent Modulus vs.$D_rD_{50}^{0.20}$ is plotted in Fig. 4.25.

$$\mathrm{E}_{\mathrm{PLT(i)}} = 0.615 D_r(\%) D_{50}^{\;0.20} + 5.797 ------------------------ 4.3$$

To get a generalized correlation for DCP, D_{50} value is multiplied by $D_{50}^{0.80}$ of sand where D_{50} is in mm. Then Initial tangent Modulus vs. $P_{index}D_{50}^{0.80}$ is plotted in Fig. 4.27.

Developed correlation for DCP is expressed as

$$\mathrm{E}_{\mathrm{PLT(i)}} = -0.267 P_{index} D_{50}^{\;0.80} + 51.19 ------------------------ 4.4$$

To get a generalized correlation for DPL, D_{50} value is multiplied by $D_{50}^{0.80}$ of sand where D_{50} is in mm. Then Initial tangent Modulus vs.$P_{index}D_{50}^{0.80}$ is plotted in Fig. 4.29.

Developed correlation for DPL is expressed as

$$\mathrm{E}_{\mathrm{PLT(i)}} = -1.13 P_{index} D_{50}^{\;0.80} + 53.04 ------------------------ 4.5$$

4.4.4 Development Correlation among Ks, D_r and P_{index}

Same procedure was followed that is describes in Article 4.4.3. To get a generalized correlation to determine subgrade modulus, D_{50} value is multiplied by $D_{50}^{0.20}$ of sand where D_{50} is in mm. The subgrade modulus vs.$D_rD_{50}^{0.20}$ is plotted in Fig. 4.31.

$$\mathrm{K}_s (MN/m^3) = 3.116\, D_R (D_{50})^{0.20} + 6.447 ------------------------ 4.6$$

To get a generalized correlation for DCP, D_{50} value is multiplied by $D_{50}^{0.60}$ of sand where D_{50} is in mm. Then Initial tangent Modulus vs.$P_{index}D_{50}^{0.60}$ is plotted in Fig. 4.31.

Developed correlation for DCP is expressed as

$$K_s(MN/m^3) = -1.351P_{index(DCP)}(D_{50})^{0.60} + 241.5 ------------------ 4.7$$

To get a generalized correlation for DPL, D_{50} value is multiplied by $D_{50}^{0.80}$ of sand where D_{50} is in mm. Then Initial tangent Modulus vs.$P_{index}D_{50}^{0.80}$ is plotted in Fig. 4.33. Developed correlation for DPL is expressed as

$$K_s(MN/m^3) = -4.304P_{index(DPL)}(D_{50})^{0.50} + 241.5 ------------------- 4.8$$

4.5 Verification of Correlation from Field Data

After establishing generalized correlation between Relative Density and P_{index} from the test results in calibration chamber, the correlation was verified by the field test data at Bashundhra Site, Jamuna Site and Pangaon Site. Figure 4.11 shows a typical plot of number of blows vs. depth of DPL test in Pangaon Site. This type of plot is useful to identify the layers of sand deposit. In the graph shown here clearly identified three distinct layers of sand. Uniform slope indicates a distinct layer. Slope changes where at the interface of the two layers. Penetration Index at any depth was calculated as an average penetration rate (mm/blow) of cone in five blows around that depth. A typical plot of depth vs. Penetration Index is shown in Fig. 4.37. Using generalized correlation mentioned in Equation 4.1 and 4.2, Relative Density was calculated from Penetration Index which is shown in Fig. 4.36.

Field dry density at various depths of the same location where DCP and DPL test was performed was determined using Sand Cone Method. After determination of maximum and minimum index density of that sand, Relative Density was calculated from the field dry density obtained from Sand Cone Method. Relative Density thus obtained from DCP and DPL at various locations was compared with that obtained from Sand Cone Method which is shown in Fig. 4.39. It shows that DCP and DPL give less Relative Density than Sand Cone Method. Two reasons were assumed to be the cause of these differences between results from DCP-DPL and Sand Cone Method. One is the depth and another is fines content. At shallow depth and ground surface, DPL and DCP encounter less resistance of penetration due to zero to very low confining pressure. On the other hand, during calibration of DCP and DPL in calibration chamber the sand was clean sand. In field fines content is about 5% which increases the density of the deposit without increasing cone resistance. Therefore two correction factors were introduced in Equation 4.9 and 4.10, one is correction factor for depth (R_d) and another is correction factor for fines content (R_{FC}). Generalized equation for DCP can expressed as

$$D_r\,(\%) = [-1.036 P_{index} D_{50}{}^{0.75} + 94.99] R_d R_{FC} \text{ ---------------------- } 4.9$$

Developed equation for DPL can be expressed as

$$D_r\,(\%) = [-5.219 P_{index} D_{50}{}^{0.75} + 101.3] R_d R_{FC} \text{ ---------------------- } 4.10$$

Where,

$$R_d = \left(\frac{0.8}{d}\right)^{0.01} \text{ ------------------------------------ } 4.11$$

$$R_{FC} = 1 + 0.003 F_c \text{ ------------------------------------ } 4.12$$

R_d = Correction factor for depth

R_{FC} = Correction factor for fines content

d = Depth (m)

F_c = Fines content (%)

Equations 4.1 and 4.2 are valid for clean sand having no fines content. Equation 4.9 and 4.10 are valid for sand having fines content 0 to 15%. Equations 4.11 and 4.12 for correction factors are established using trial and error method. These two equations should be modified based on more experimental results in sand having fines content.

Using Equations 4 .9 and 4.10, Relative Density at various locations and depth were determined from Penetration Index of DCP and DPL and compared with Relative

Density from Sand Cone Method in Fig. 4.40 and 4.41. It is clear that Relative Density from DCP and DPL are in good agreement with the Relative Density from Sand Cone Method. Relative Density at various locations determined from DCP, DPL and Sand Cone Method are plotted against depth and shown in Fig.4.42 to 4.49. It is proved that instead of Sand Cone Method, DCP and DPL can be successfully used to determine Relative Density of sand deposit.

4.6 Findings

The following are the findings discussed in the previous sections:

i. A generalized correlation between Relative Density and $P_{index}D_{50}^{0.75}$ was established for sizes of sand having fines content less than 15%, which was successfully applied in three dredge fill sites.

ii. The larger the particle size greater be the resistance to penetration for a certain Relative Density of sand. Denser sand gives more resistance for a specific type of sand. Resistance of sand increases exponentially with Relative Density.

iii. Air pluviation method can produce sand deposit of uniform and known Relative Density.

iv. Denser send gives more Initial Tangent Modulus and Subgrade Modulus for a specific type of sand. Initial Tangent Modulus and Subgrade Modulus increase exponentially with relative density and $P_{index.}$

v. The larger particle size sand gives more Initial Tangent Modulus and Subgrade Modulus value than smaller size particle.

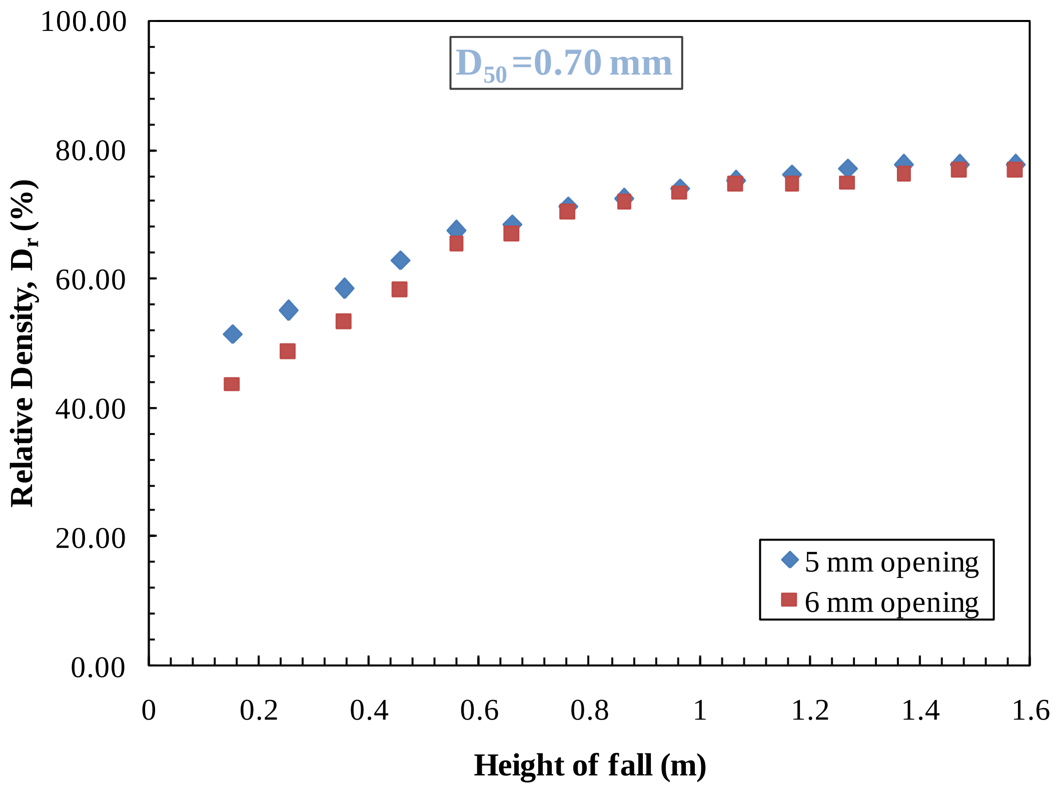

Fig. 4.1: Relative Density vs. height of fall for sand having D_{50}= 0.70 mm

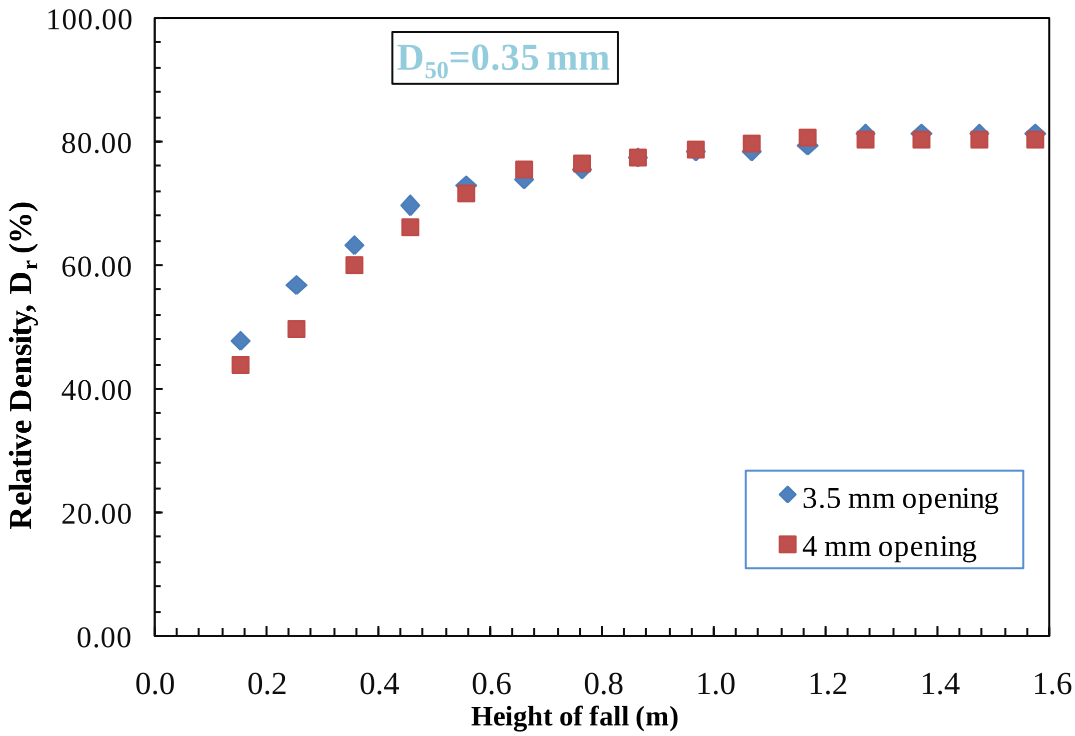

Fig. 4.2: Relative Density vs. height of fall for sand having D_{50}= 0.35 mm

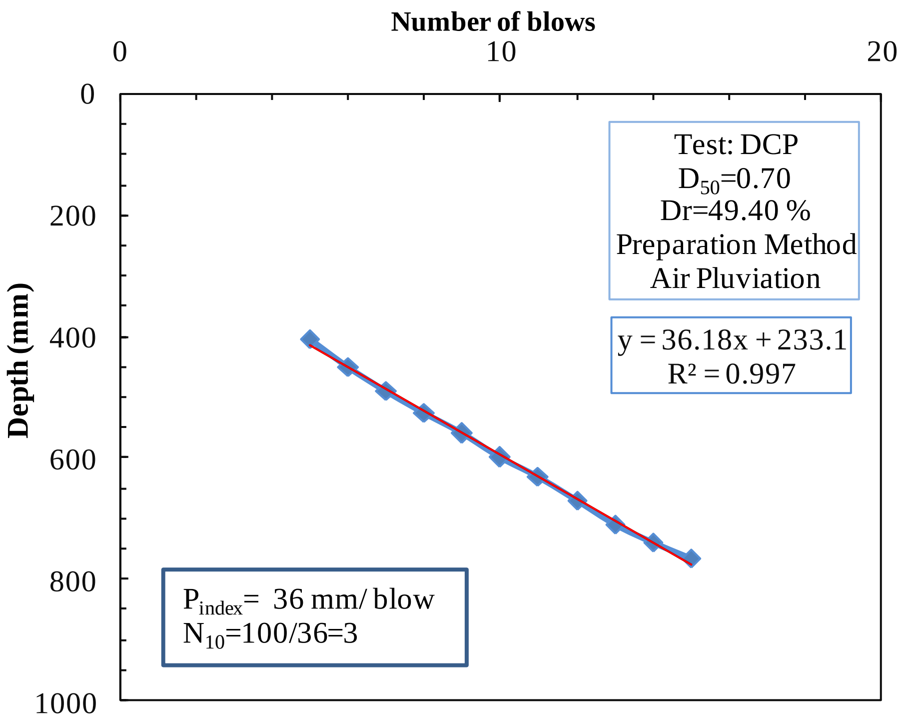

Fig. 4.3: Typical plot of number of blows vs. depth for sand having D_{50}= 0.70 mm at D_r= 49.40% in calibration chamber using DCP

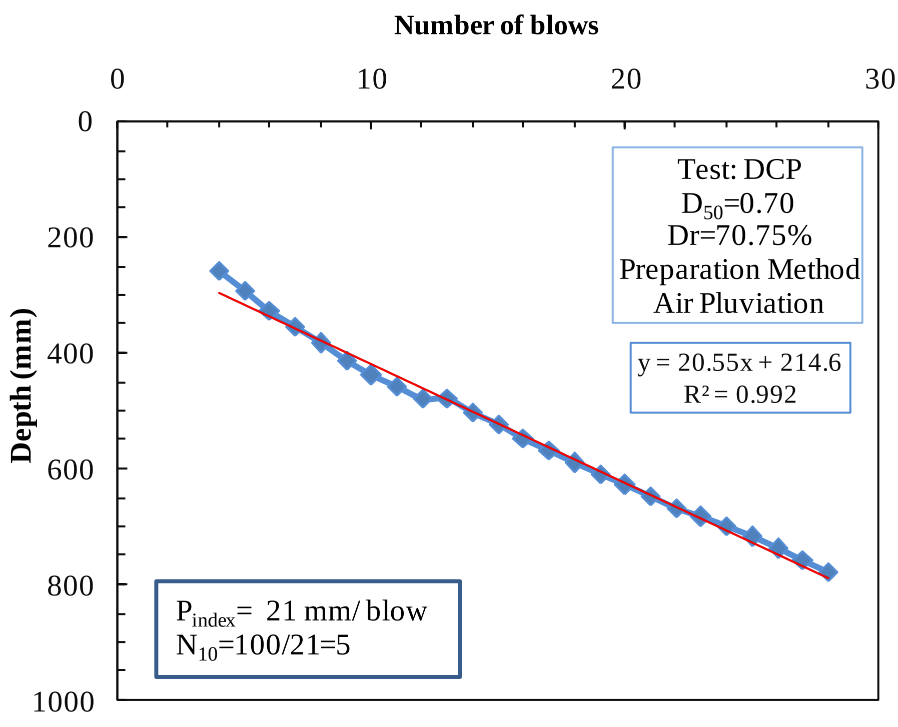

Fig. 4.4: Typical plot of number of blows vs. depth for sand having D_{50}= 0.70 mm at D_r= 70.75% in calibration chamber using DCP

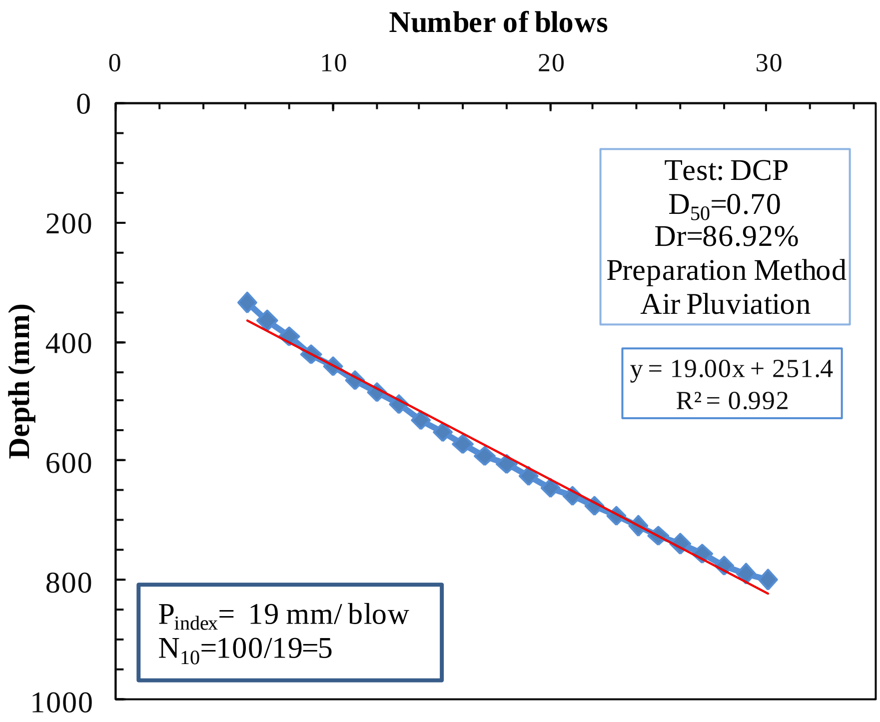

Fig. 4.5: Typical plot of number of blows vs. depth for sand having D_{50}= 0.70 mm at D_r= 86.92% in calibration chamber using DCP

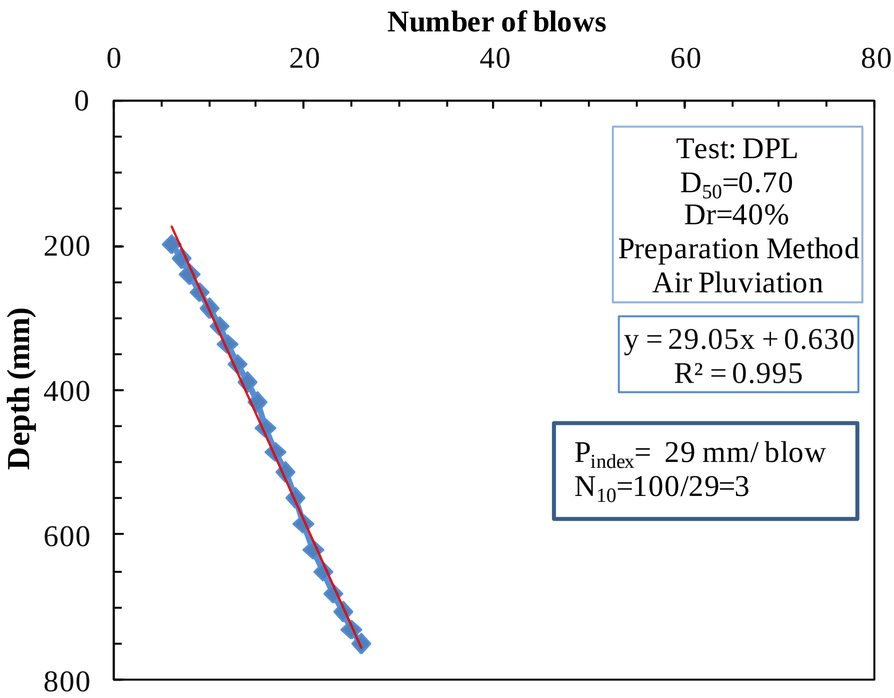

Fig. 4.6: Typical plot of number of blows vs. depth for sand having D_{50}= 0.70 mm at D_r= 40 % in calibration chamber using DPL

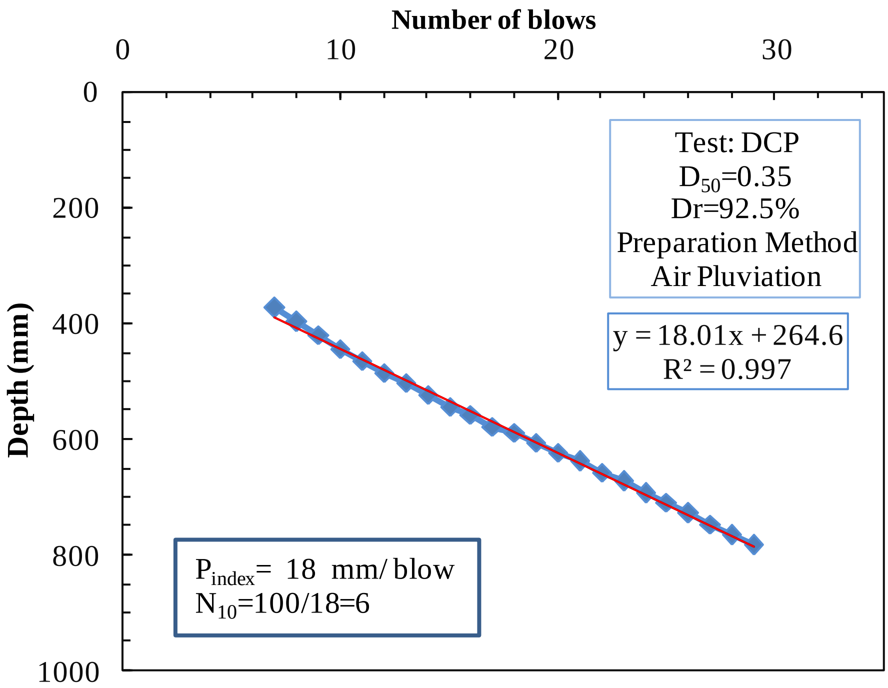

Fig. 4.7: Typical plot of number of blows vs. depth plot for sand having D_{50}= 0.70 mm at D_r= 92.5% in calibration chamber using DCP

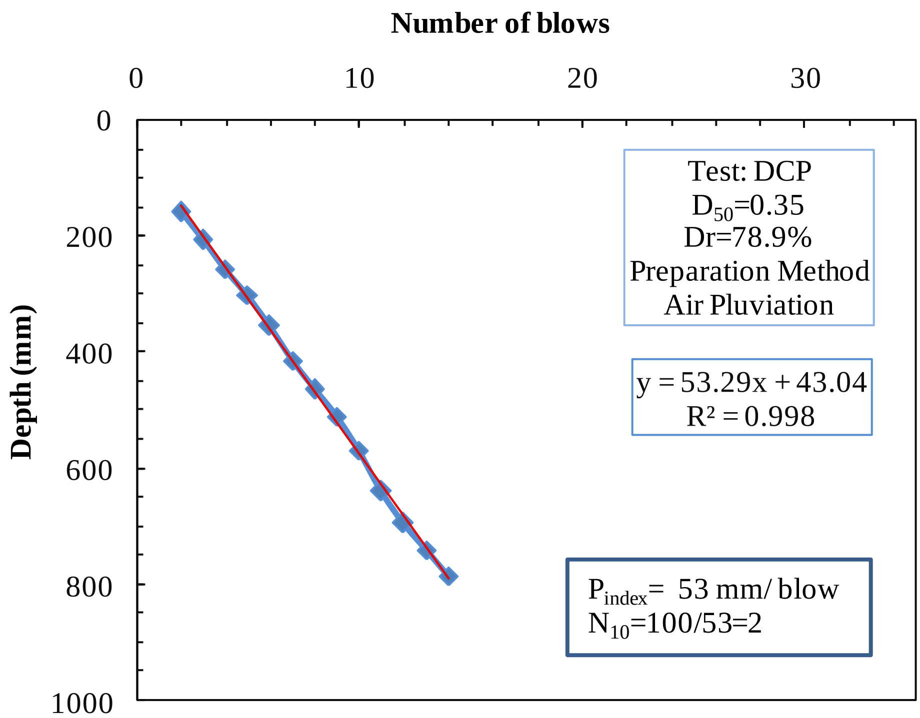

Fig. 4.8: Typical plot of number of blows vs. depth for sand having D_{50}= 0.35 mm at D_r= 78.9% in calibration chamber using DCP

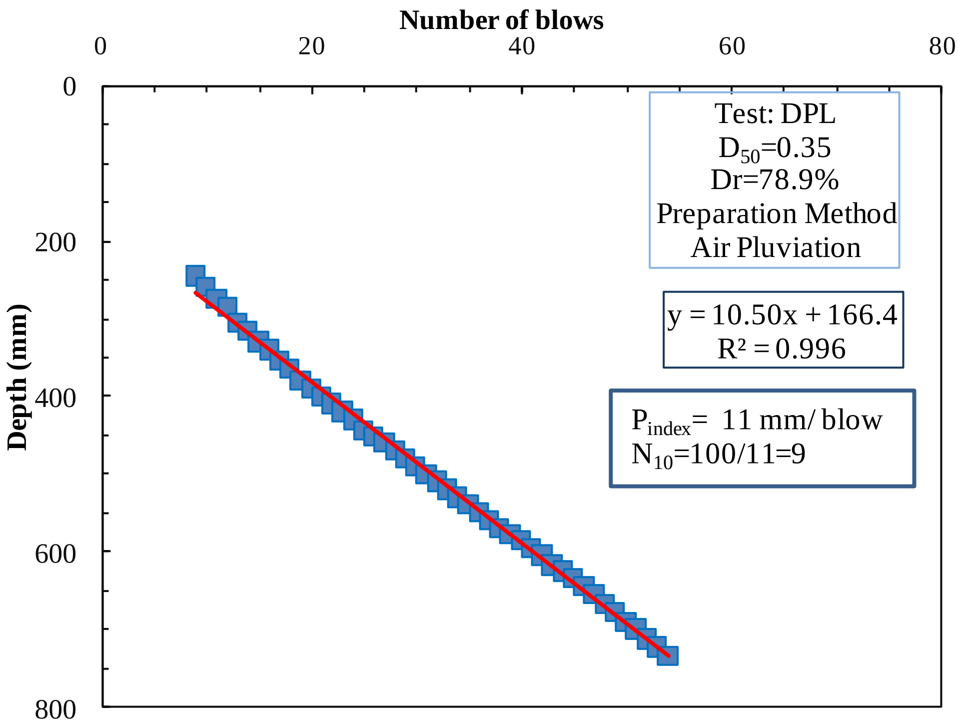

Fig.4.9: Typical plot of number of blows vs. depth for sand D_{50}= 0.35 mm at D_r= 78.9 % in calibration chamber using DPL

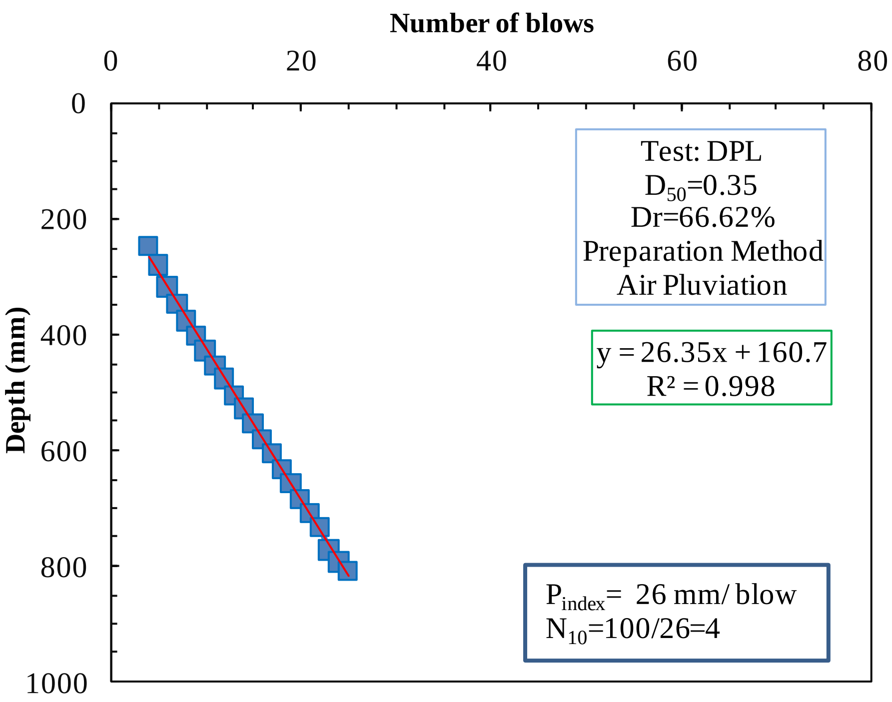

Fig. 4.10: Typical plot of number of blows vs. depth for sand having D_{50}= 0.35 mm at D_r= 66.62 % in calibration chamber using DPL

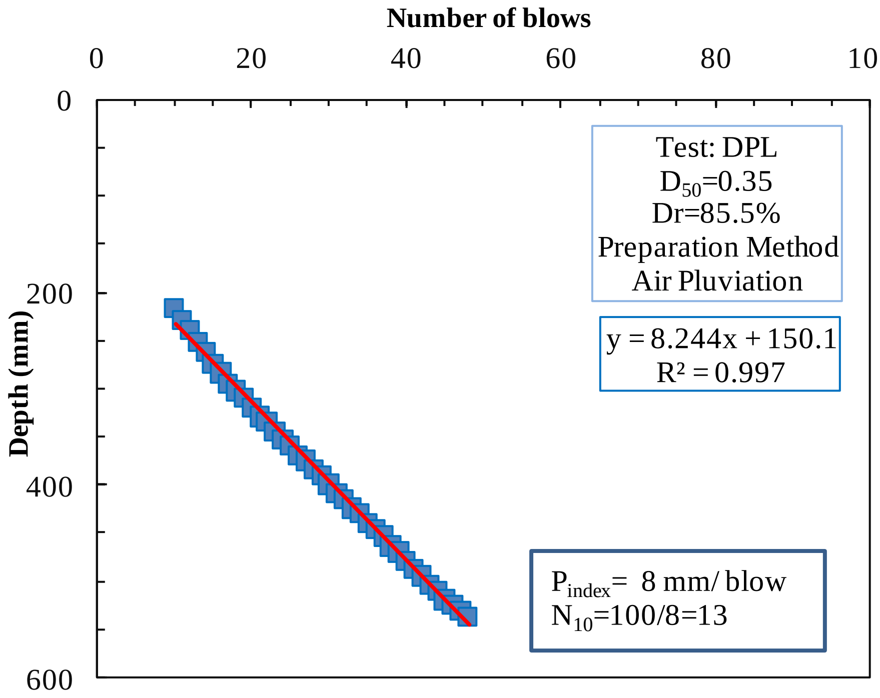

Fig. 4.11: Typical plot of number of blows vs. depth plot for sand having D_{50}= 0.35 mm at D_r= 85.5 % in calibration chamber using DPL

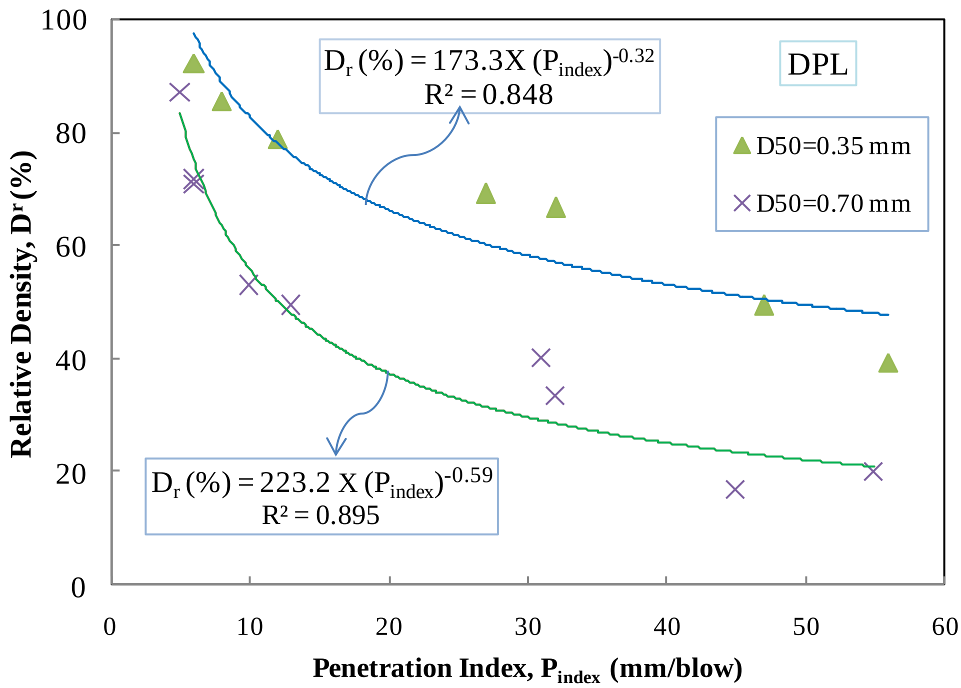

Fig. 4.12: Correlation between Relative Density and P_{index} in DPL for two types (D_{50}=0.70 mm & 0.35 mm) sand. (Non linear scale)

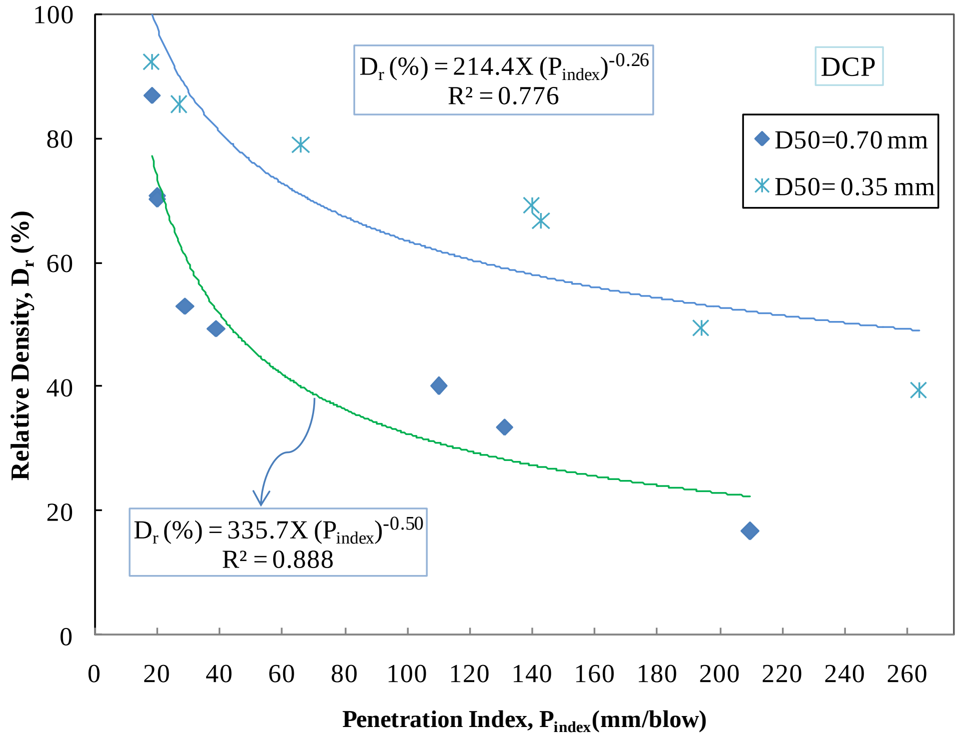

Fig. 4.13: Correlation between Relative Density and P_{index} in DCP for two types (D_{50}=0.70 mm & 0.35 mm) sand. (Non linear scale)

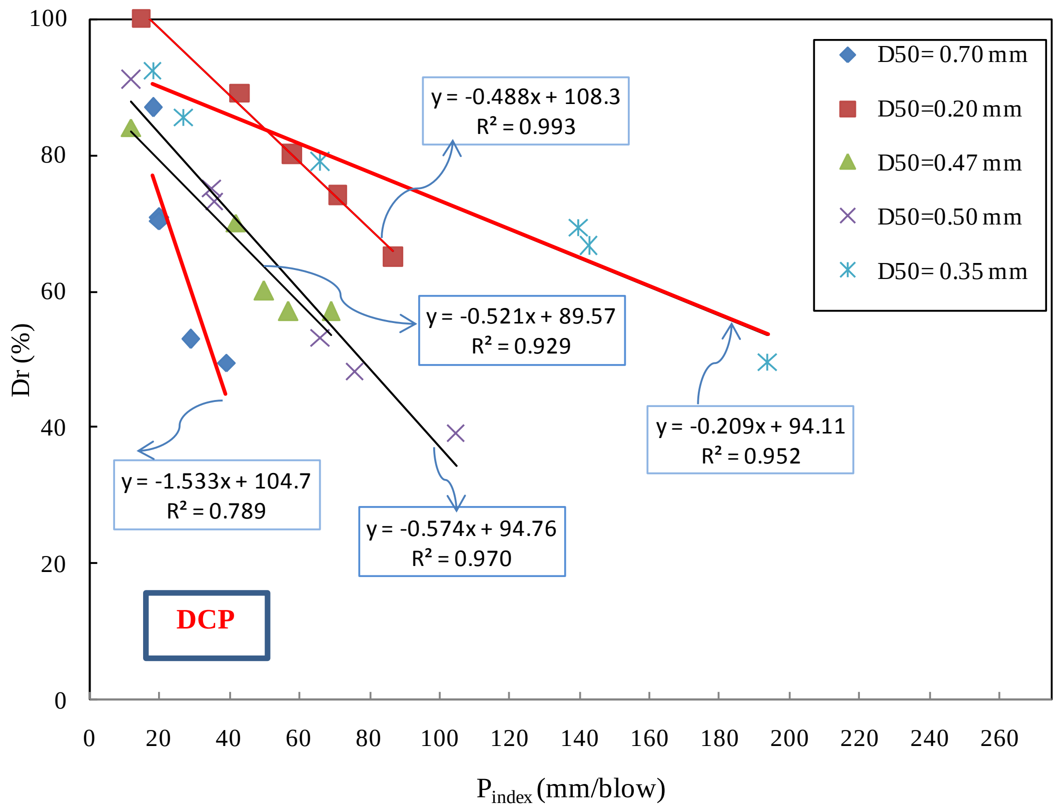

Fig. 4.14: Correlation between Relative Density and P_{index} in DCP for sand of different mean diameter. (Linear scale)

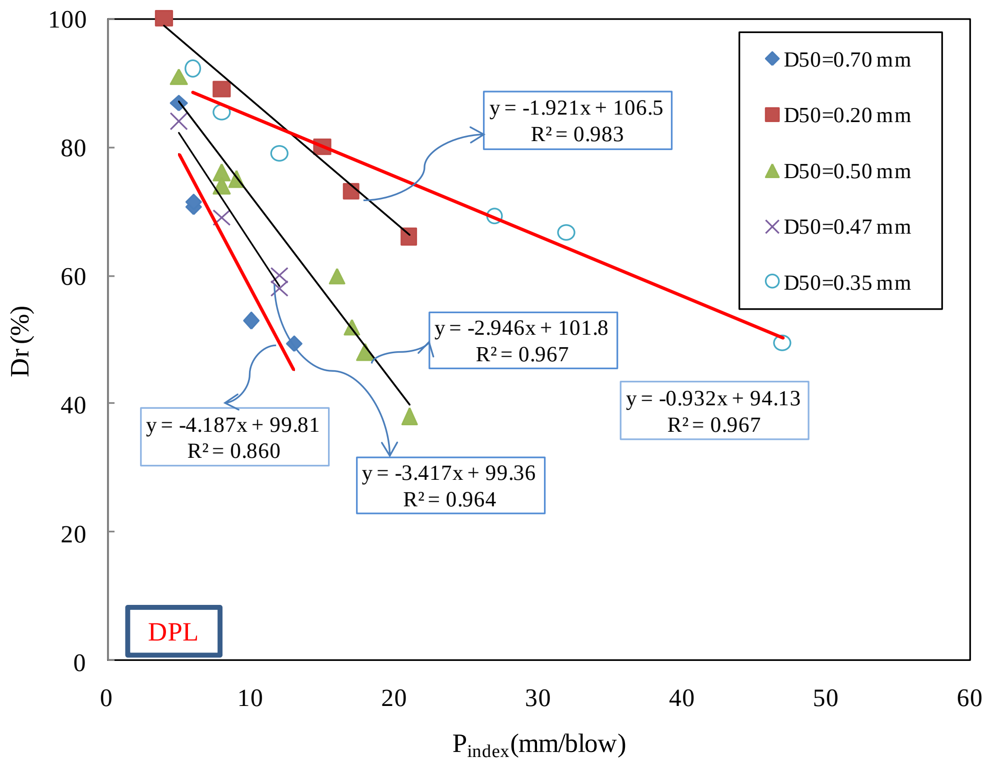

Fig. 4.15: Correlation between Relative Density and P_{index} in DPL for sand of different mean diameter (Linear scale)

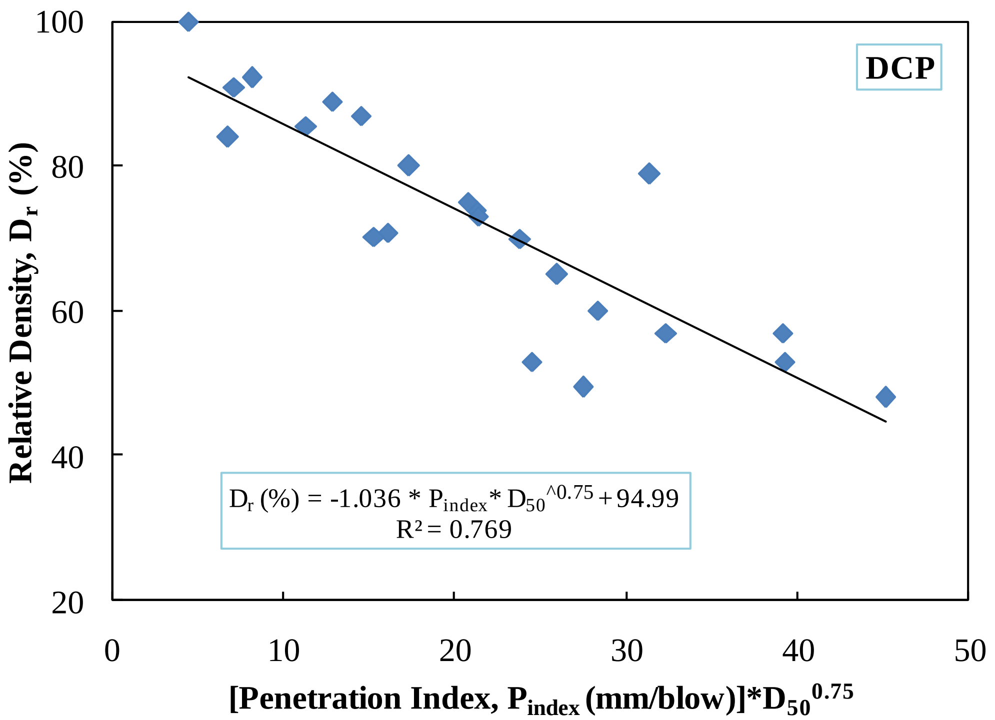

Fig. 4.16: Correlation between Relative Density and $P_{index}D_{50}^{0.75}$ in DCP for sand (Linear scale)

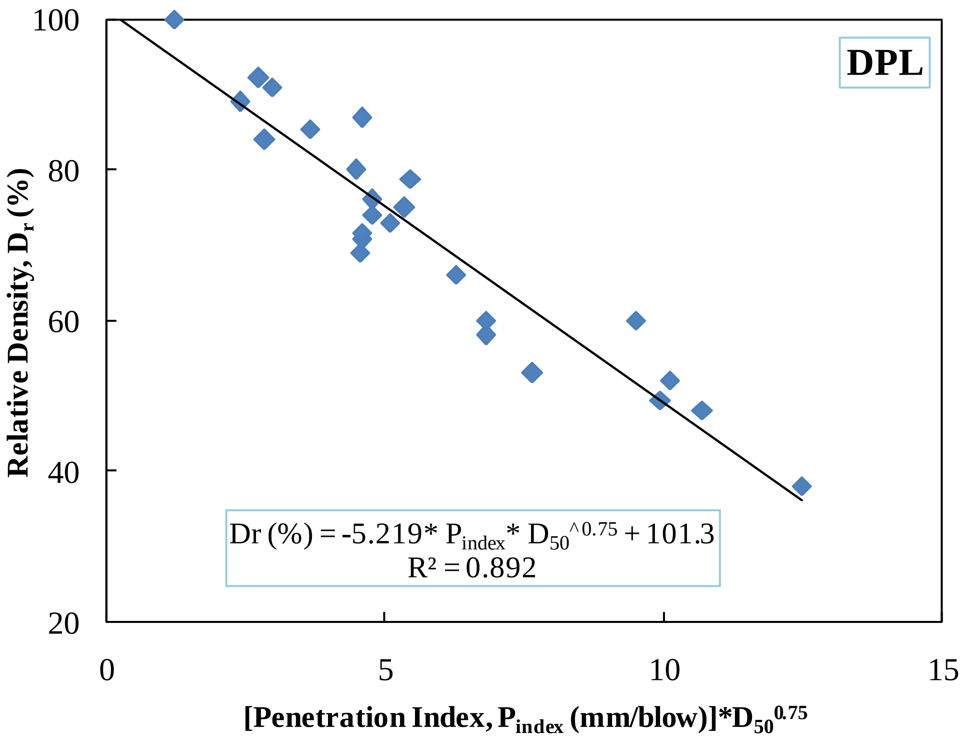

Fig. 4.17: Correlation between Relative Density and $P_{index}D_{50}^{0.75}$ in DPL for sand (Linear scale)

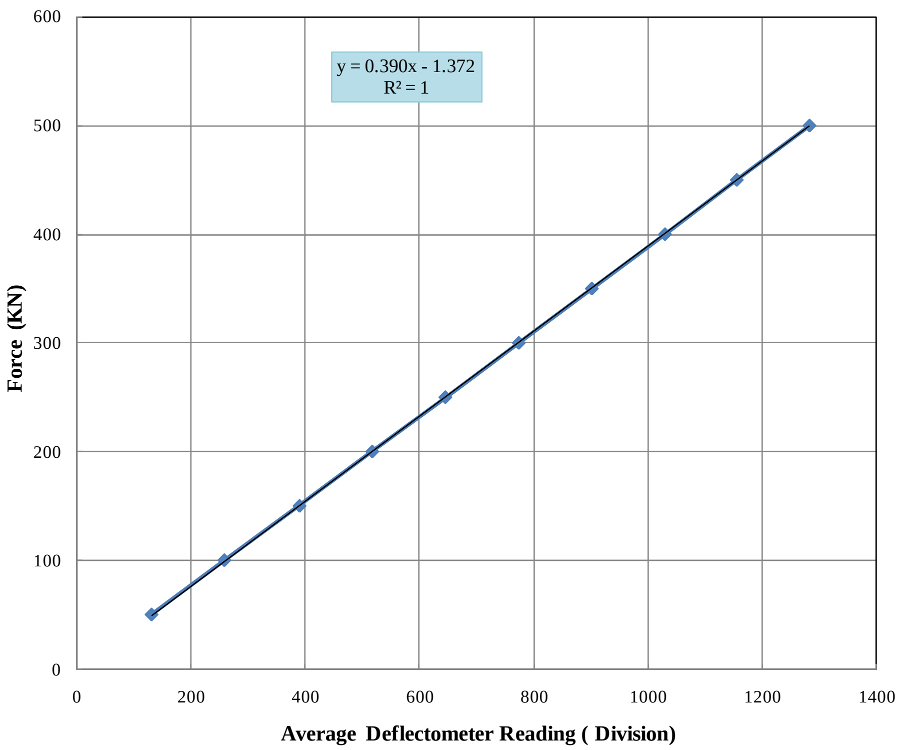

Fig. 4.18: Correlation between Force and average deflectometer reading of load column

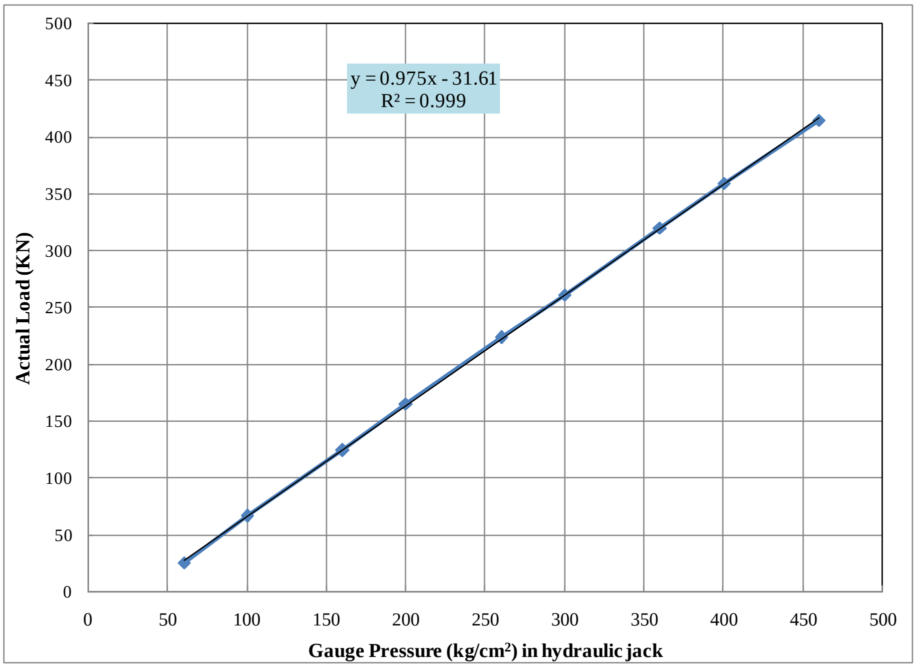

Fig. 4.19: Correlation between actual load and gauge pressure reading in hydraulic jack (Capacity =50 tones)

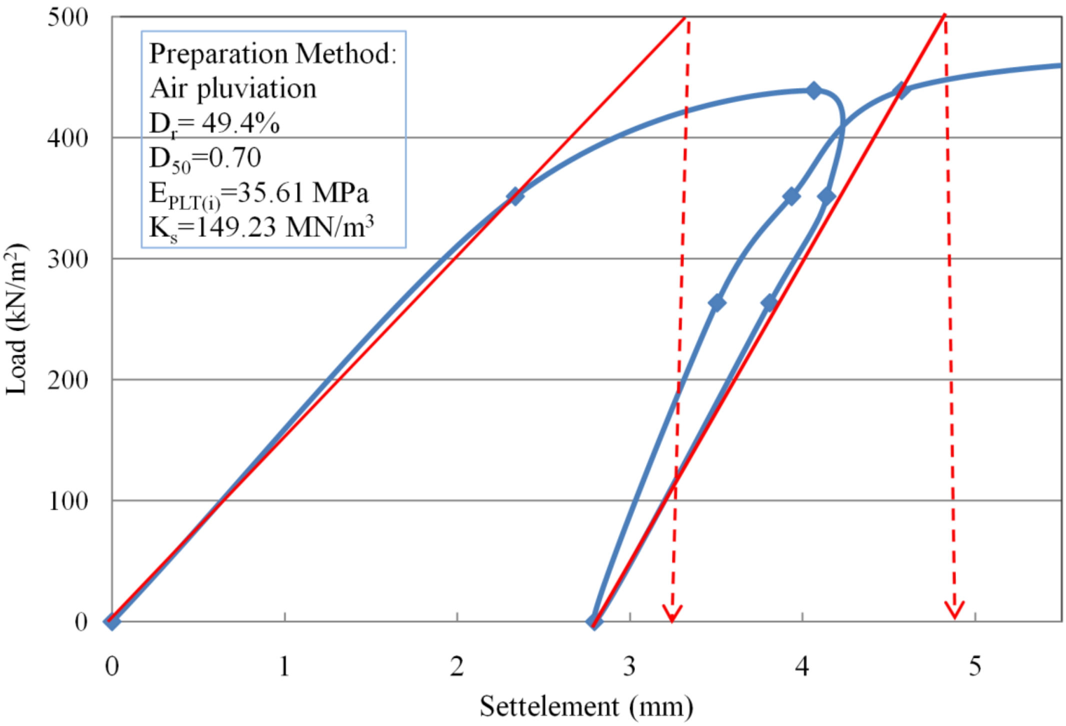

Fig. 4.20: Correlation between normal stress and settlement at Dr=49.40% of D_{50}=0.70 mm

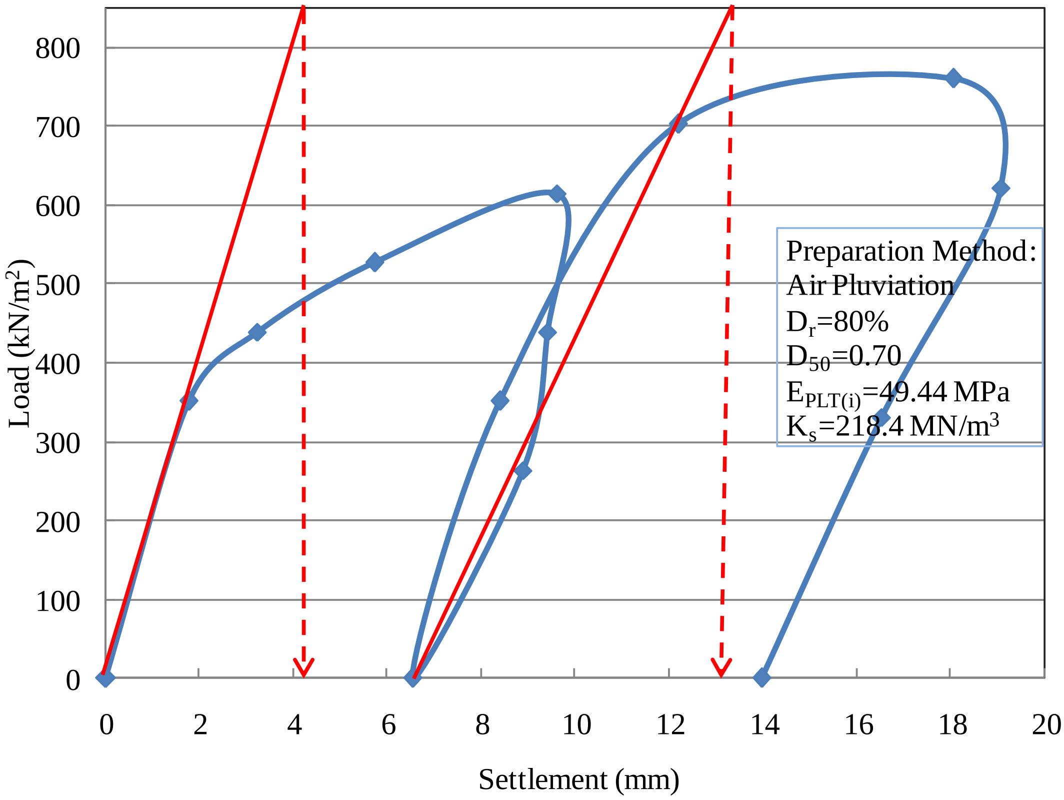

Fig. 4.21: Correlation between normal stress and settlement at D_r=80%of D_{50}=0.70mm

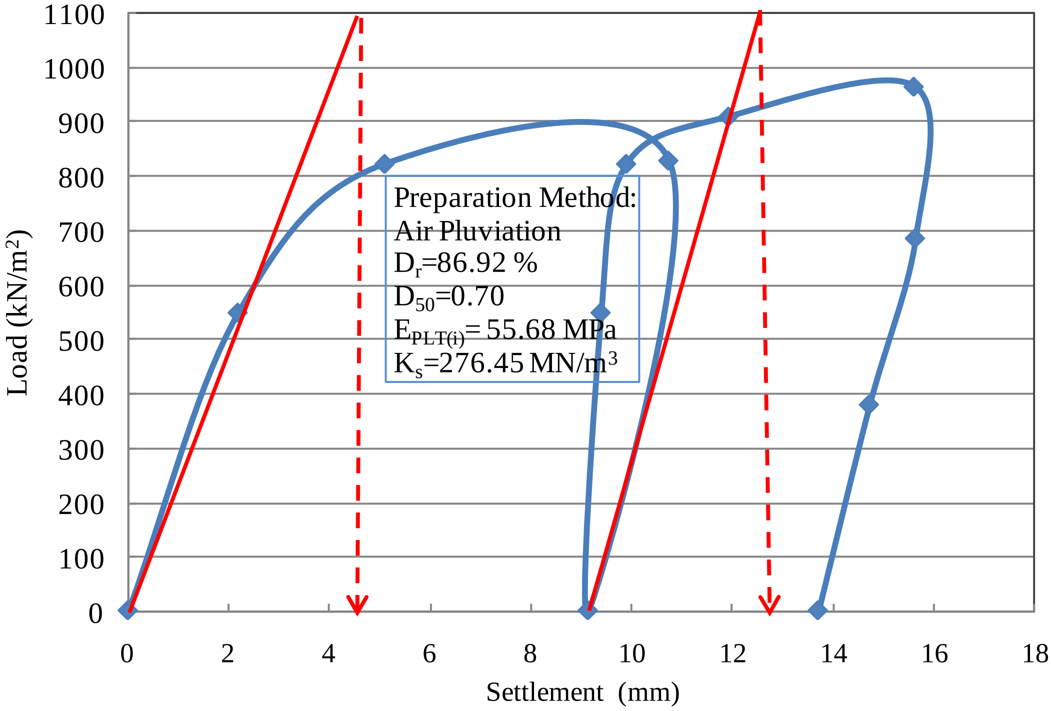

Fig. 4.22: Correlation between normal stress and settlement at D_r=86.92% of D_{50}=0.70 mm

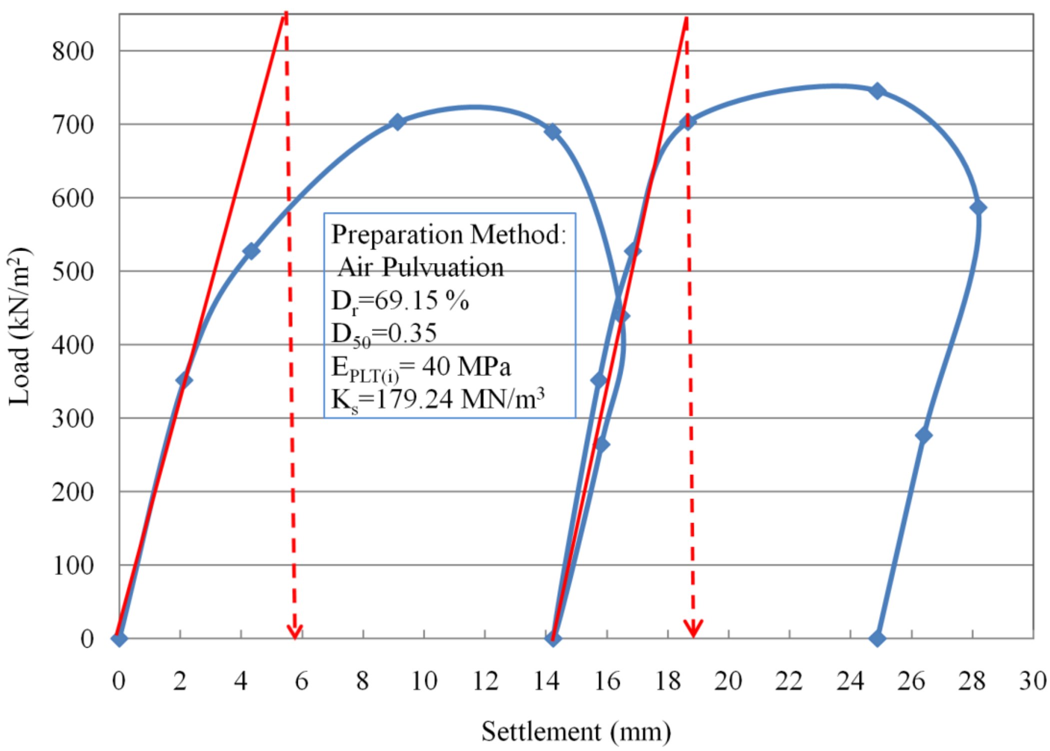

Fig. 4.23: Correlation between normal stress and settlement at D_r=69.15% of D_{50}=0.35 mm

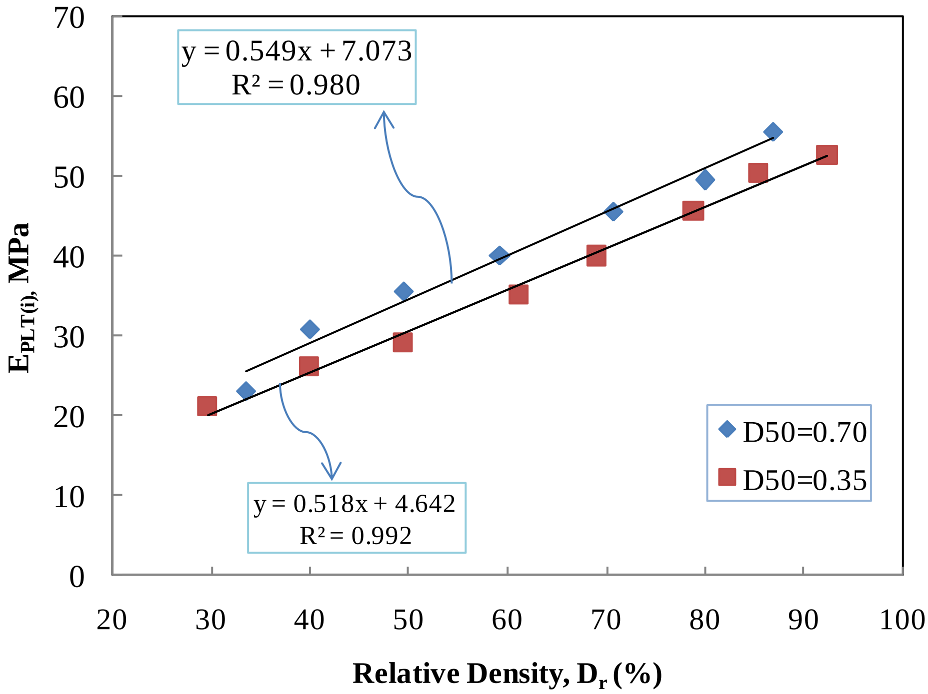

Fig. 4.24: Correlation between initial tangent modulus vs. Relative Density

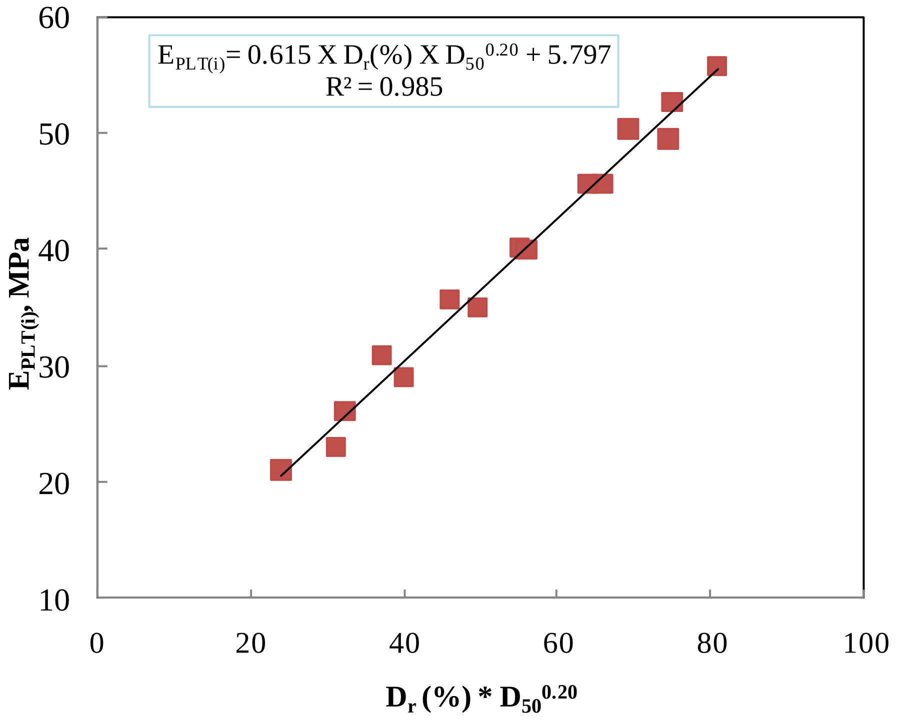

Fig. 4.25: Correlation between initial tangent modulus vs. $D_rD_{50}^{0.20}$

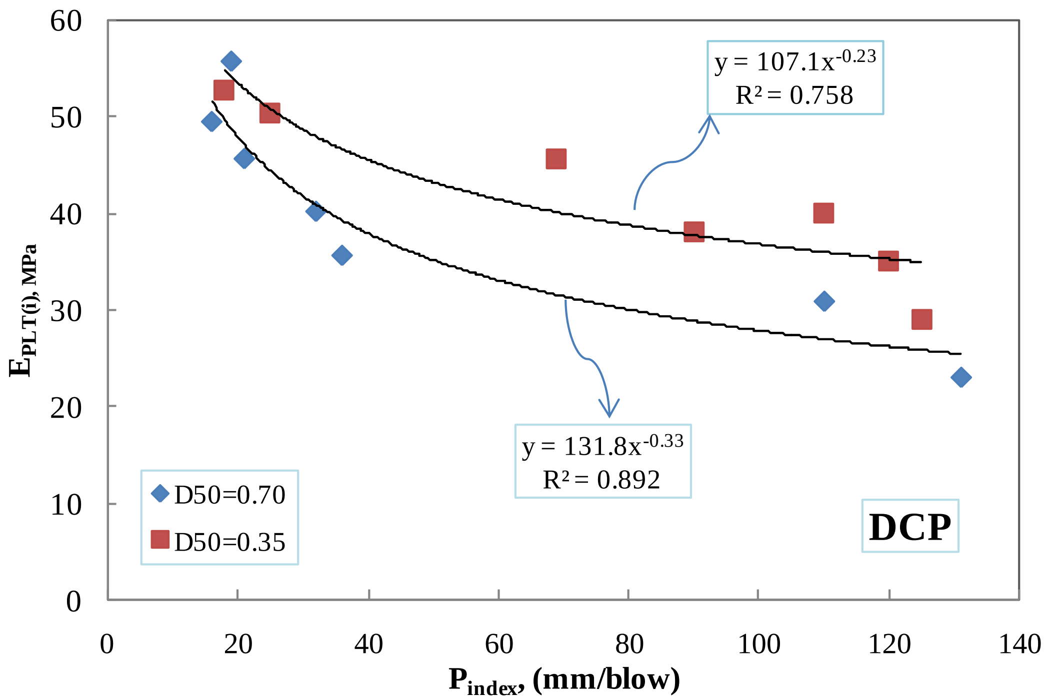

Fig. 4.26: Correlation between initial tangent modulus vs. $P_{index(DCP)}$

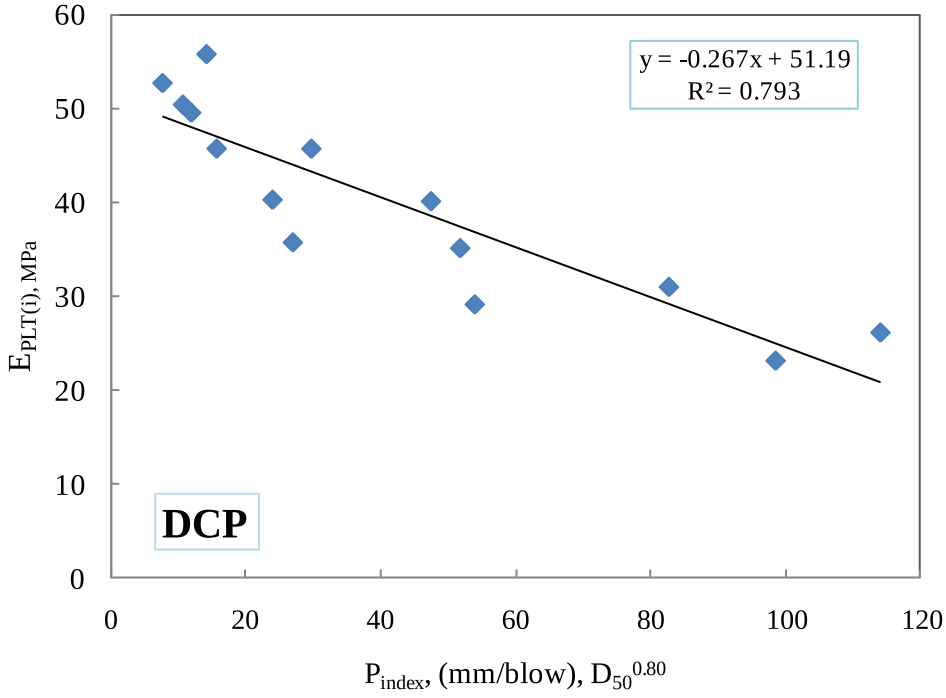

Fig. 4.27: Correlation between initial tangent modulus vs. $P_{index(DCP)}D_{50}^{0.8}$

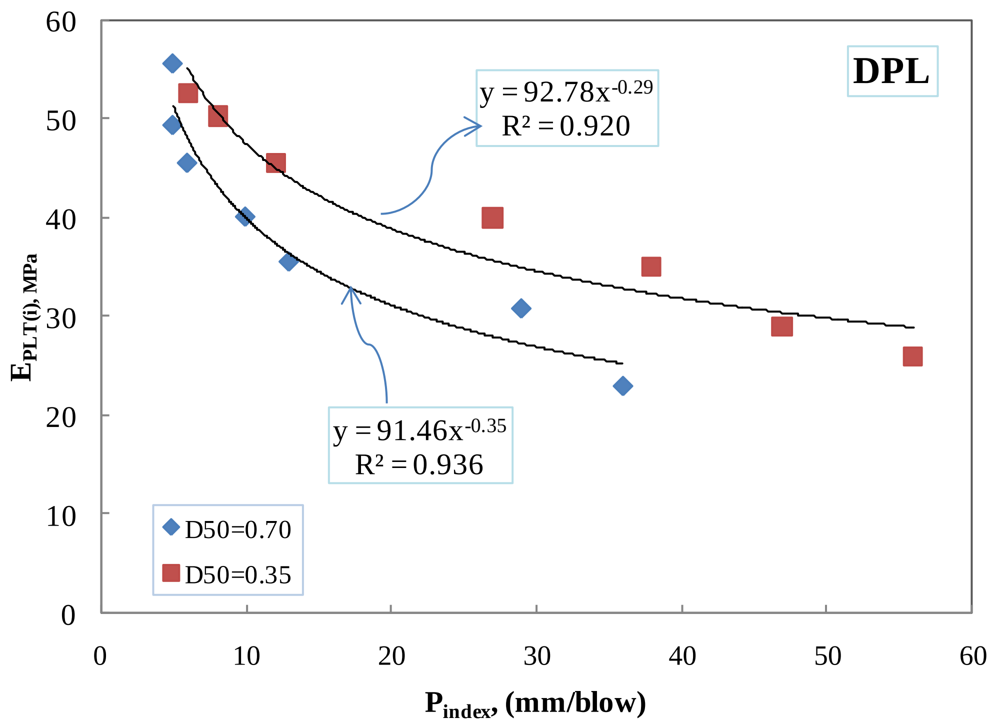

Fig. 4.28: Correlation between initial tangent modulus vs. penetration index (DPL)

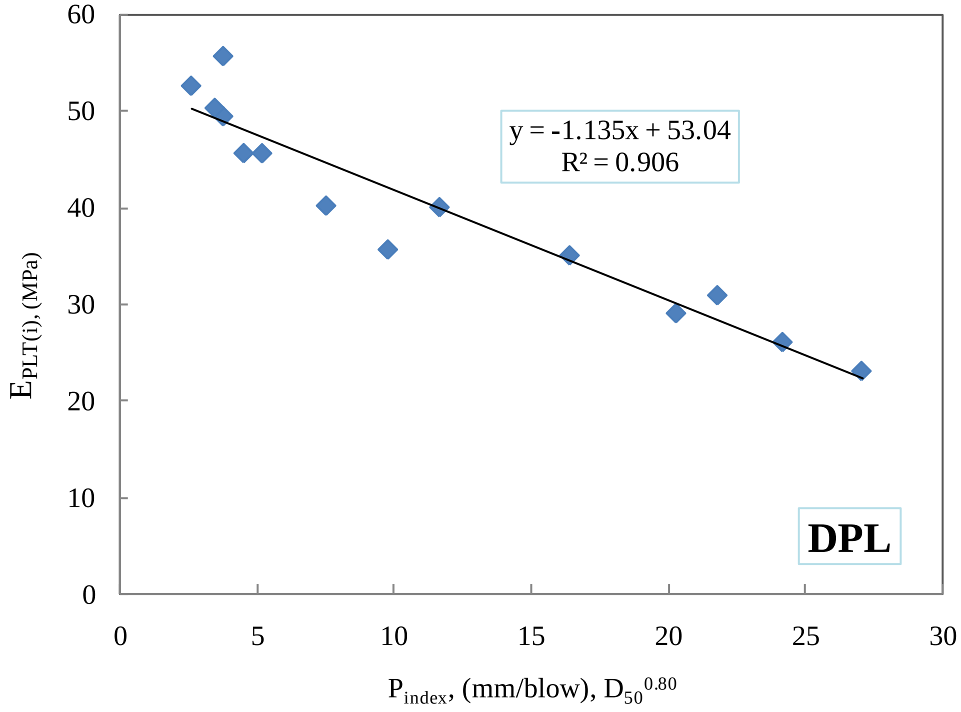

Fig. 4.29: Correlation between initial tangent modulus vs. $P_{index\ (DPL)}\ D_{50}^{0.80}$

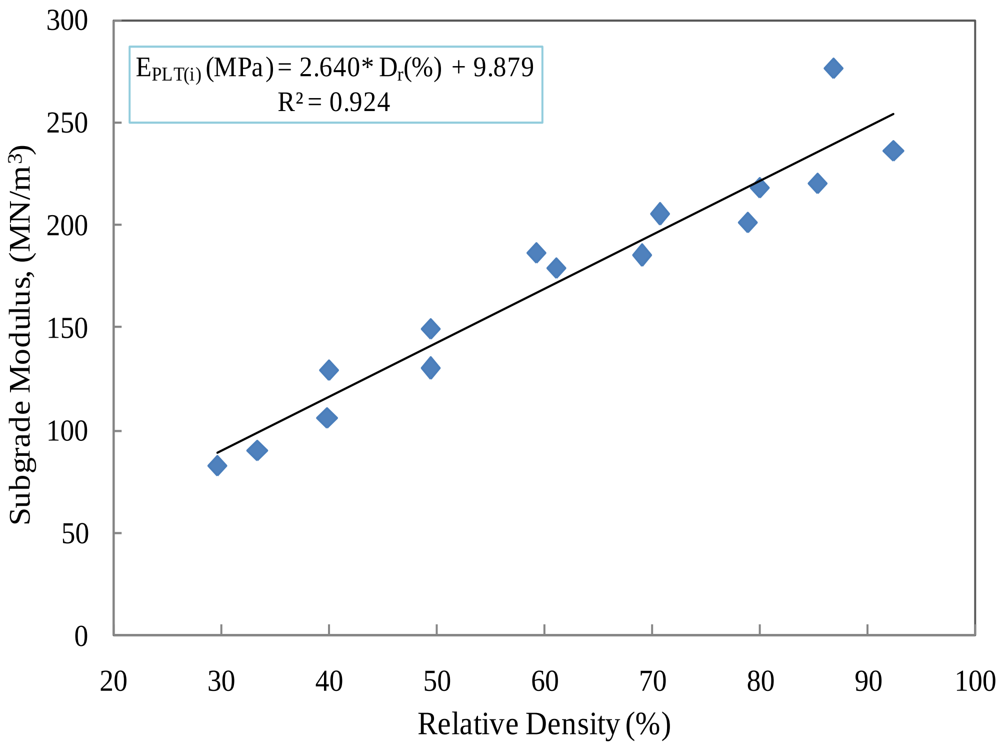

Fig. 4.30: Correlation between subgrade Modulus and Relative Density

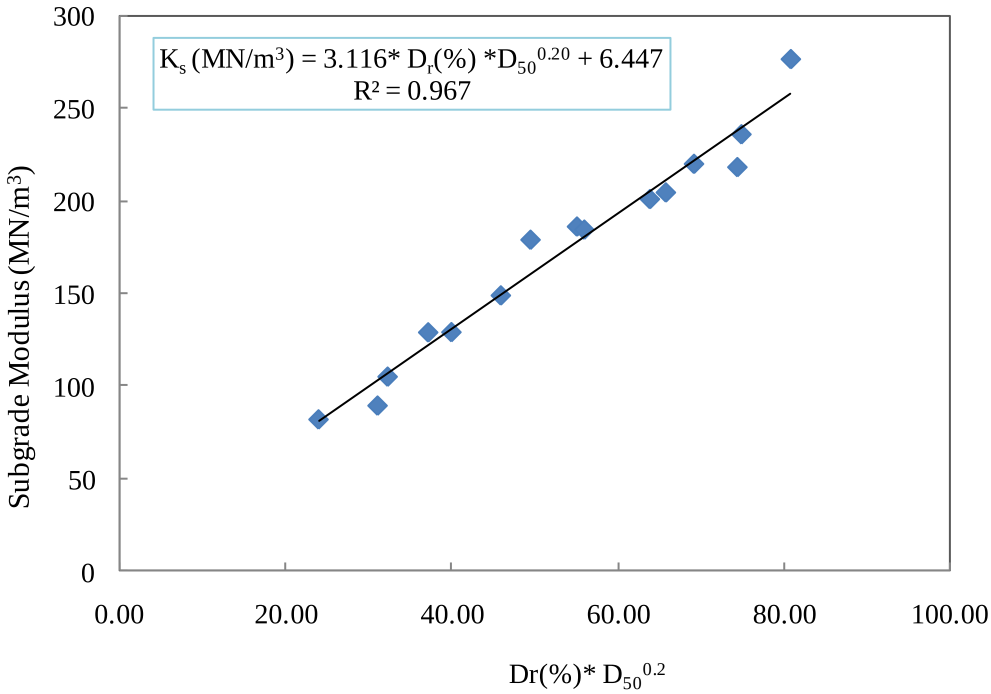

Fig. 4.31: Correlation between Ks and $D_rD_{50}^{0.20}$

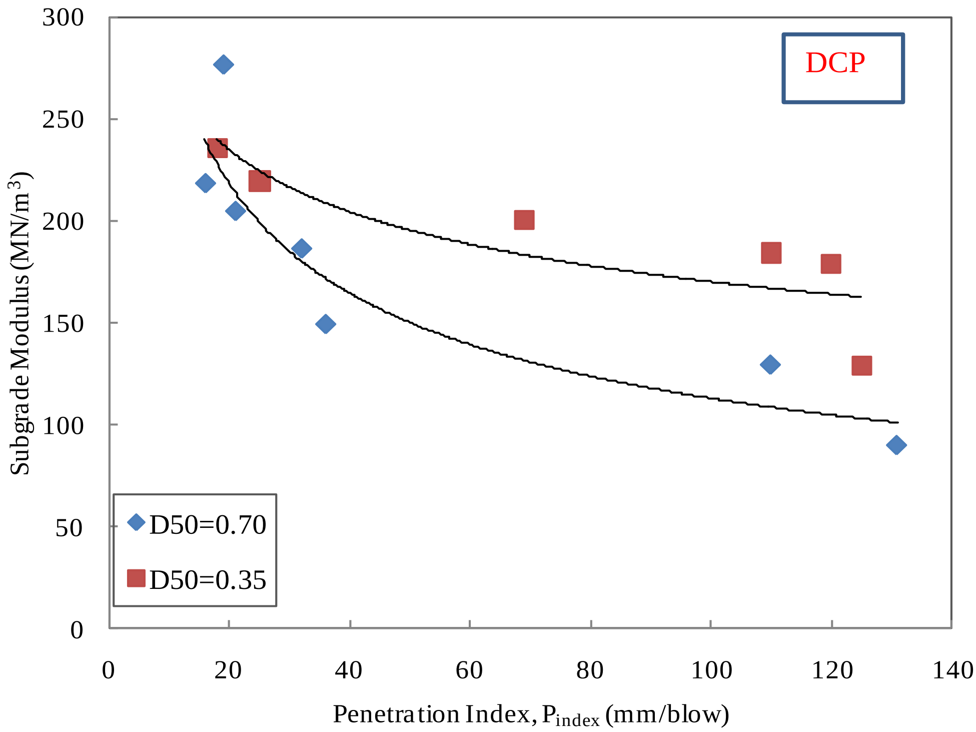

Fig. 4.31: Correlation between Subgrade Modulus and $P_{index\ (DCP)}$

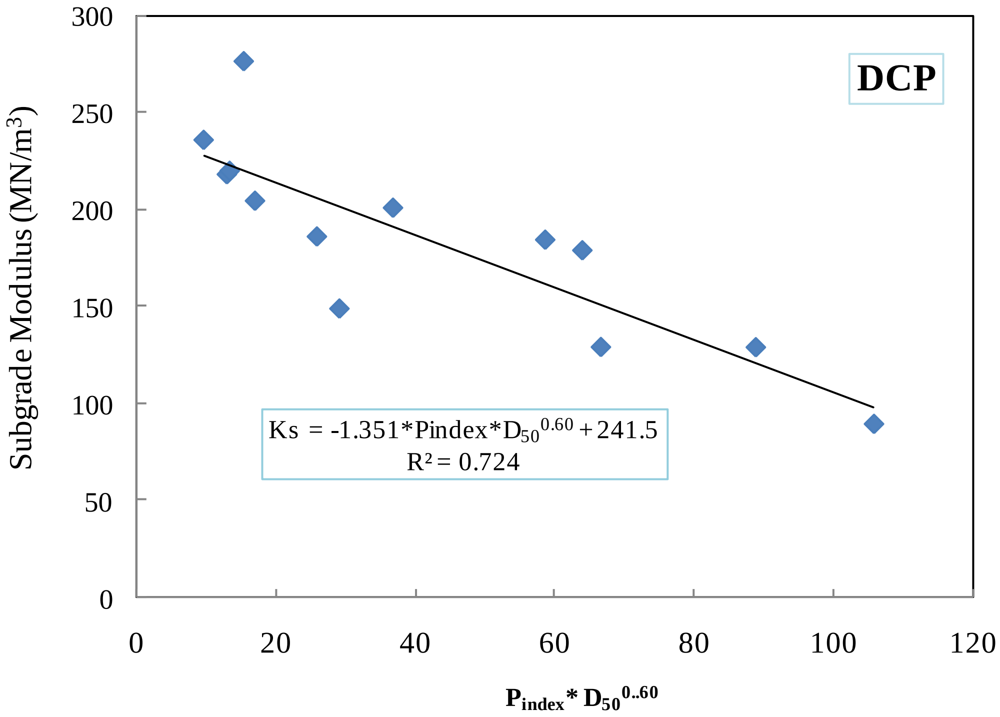

Fig. 4.31: Correlation between Subgrade Modulus and $P_{index(DCP)}D_{50}^{0.60}$

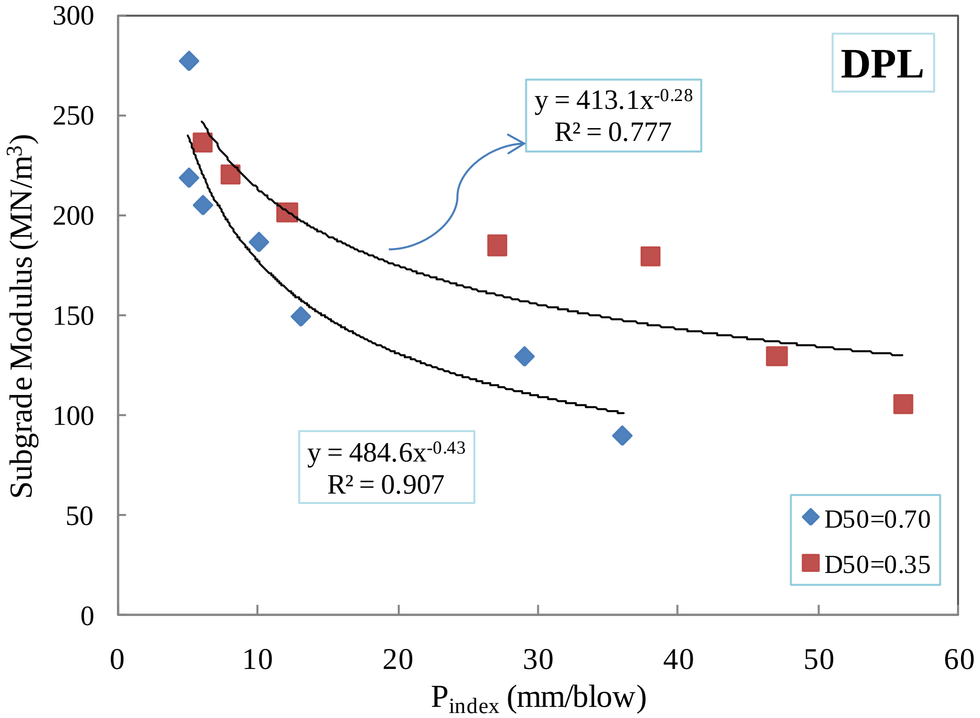

Fig. 4.32: Correlation between Subgrade Modulus and $P_{index\ (DPL)}$

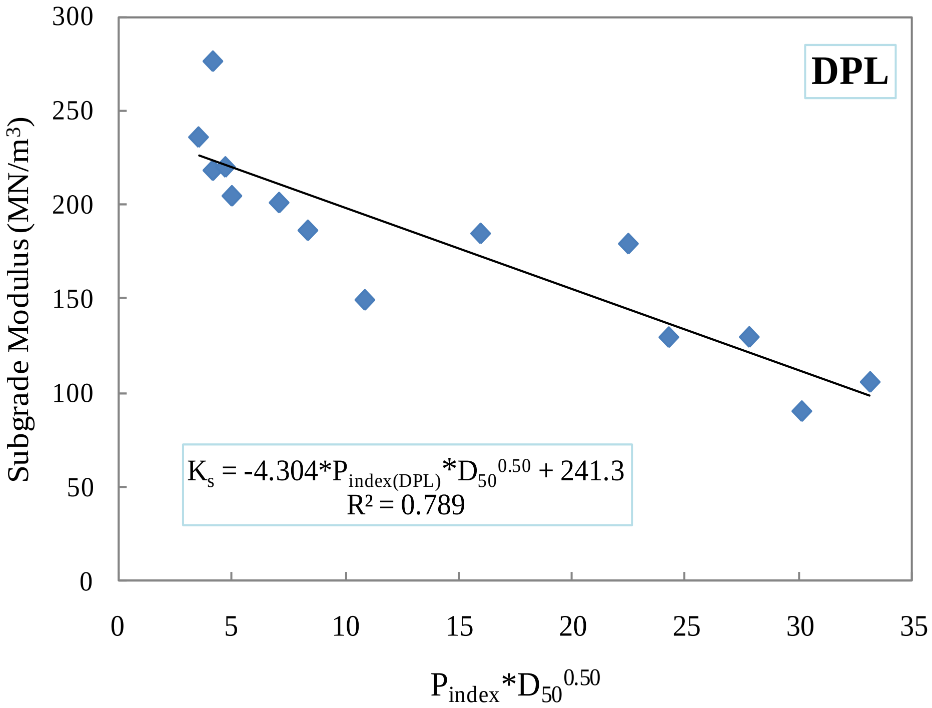

Fig. 4.33: Correlation between Subgrade Modulus and $P_{index\ (DPL)}\ D_{50}^{0.50}$

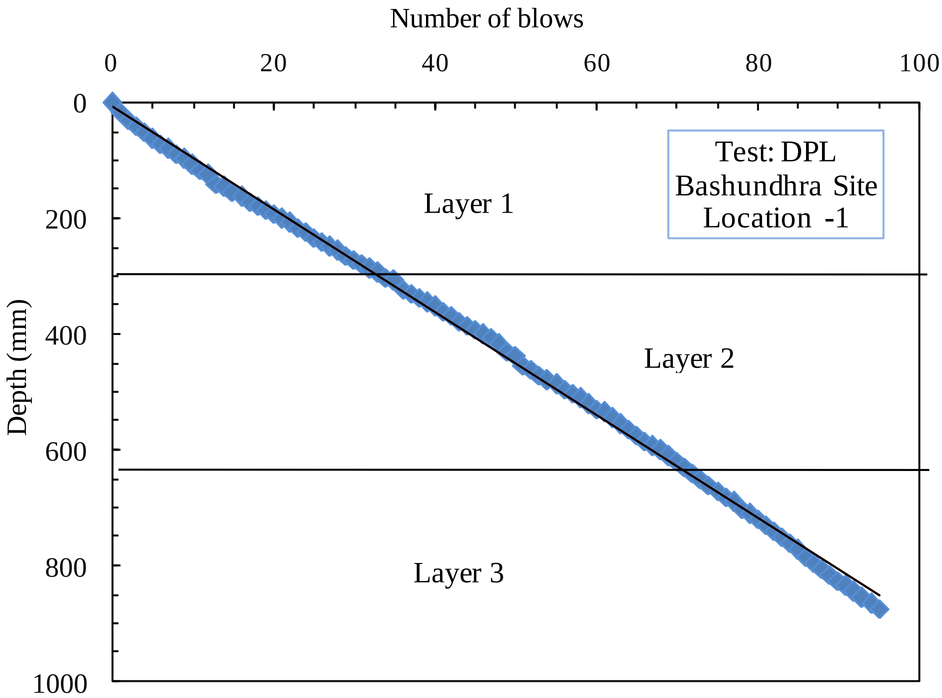

Fig. 4.34: Typical plot of number of blows vs. depth of DPL test in Bashundhara Site (Location 1)

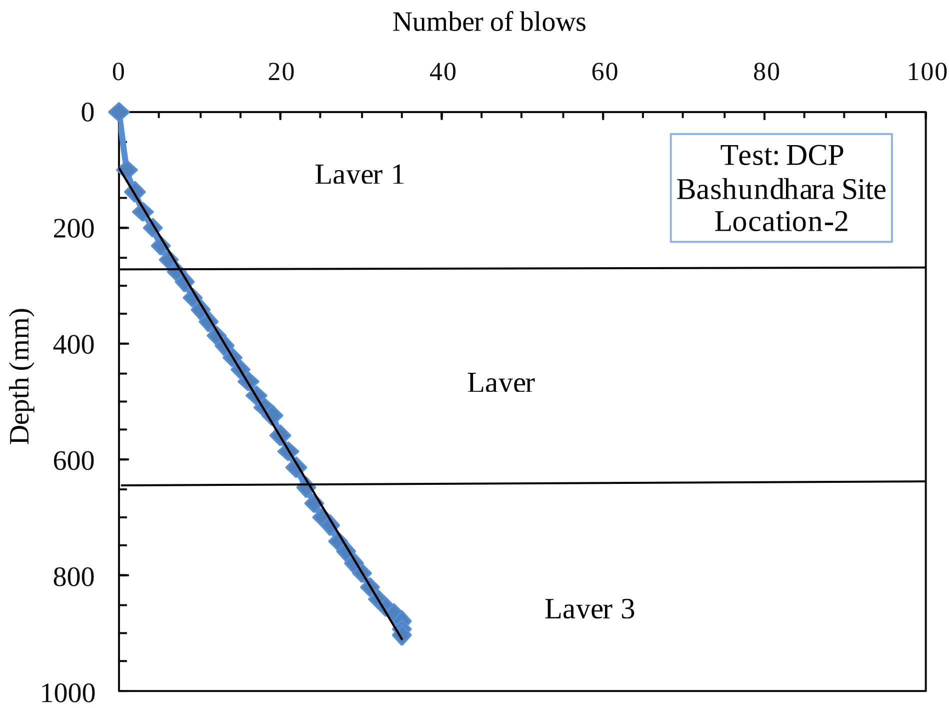

Fig. 4.35: Typical plot of number of blows vs. depth of DCP test in Bashundhara Site (Location 2)

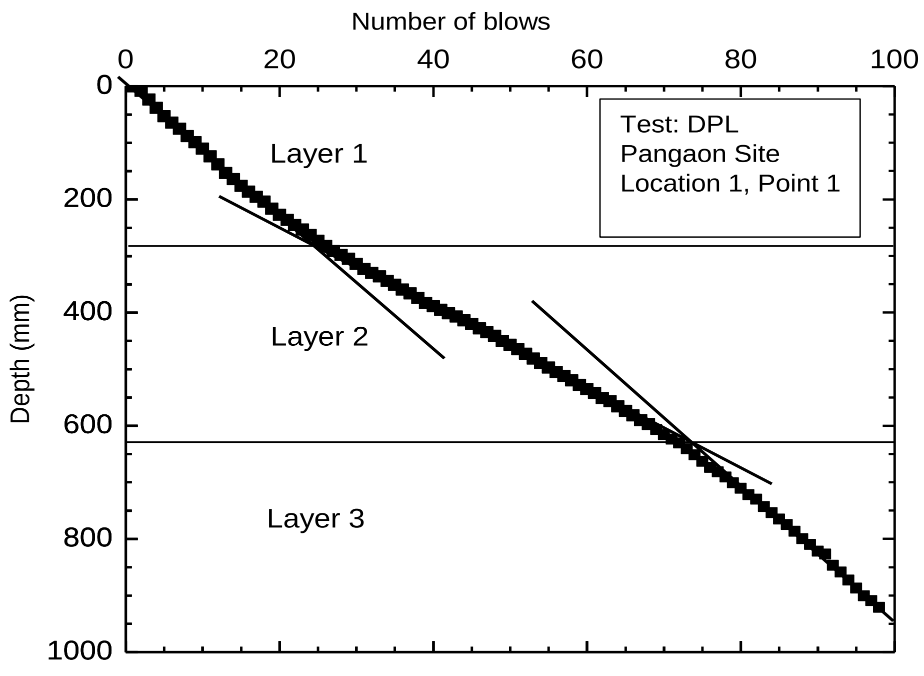

Fig. 4.36: Typical plot of number of blows vs. depth of DPL test in Pangaon Site

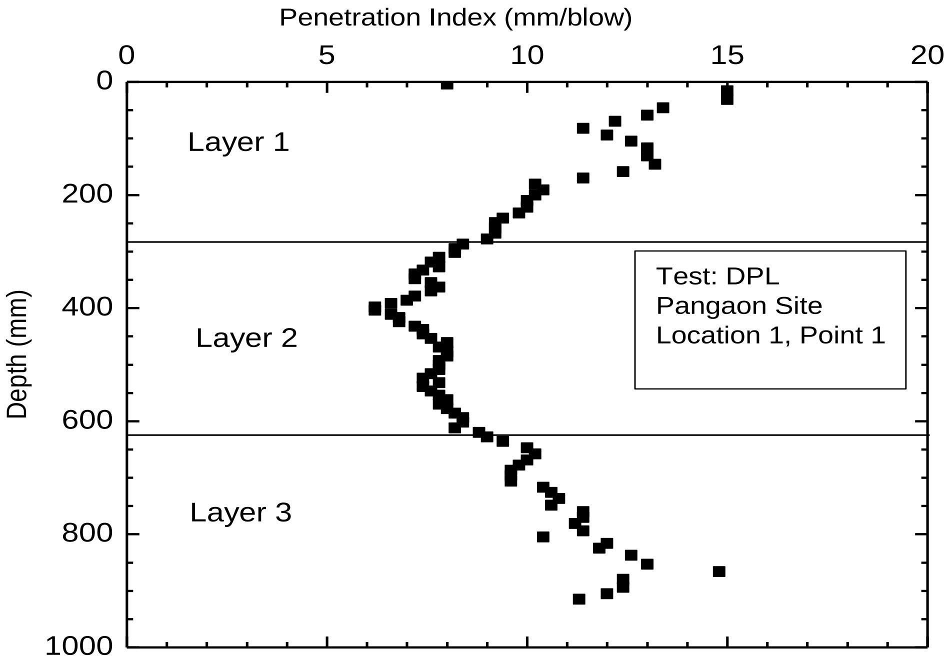

Fig.4.37: Typical plot of Penetration Index vs. depth of DPL test in Pangaon Site

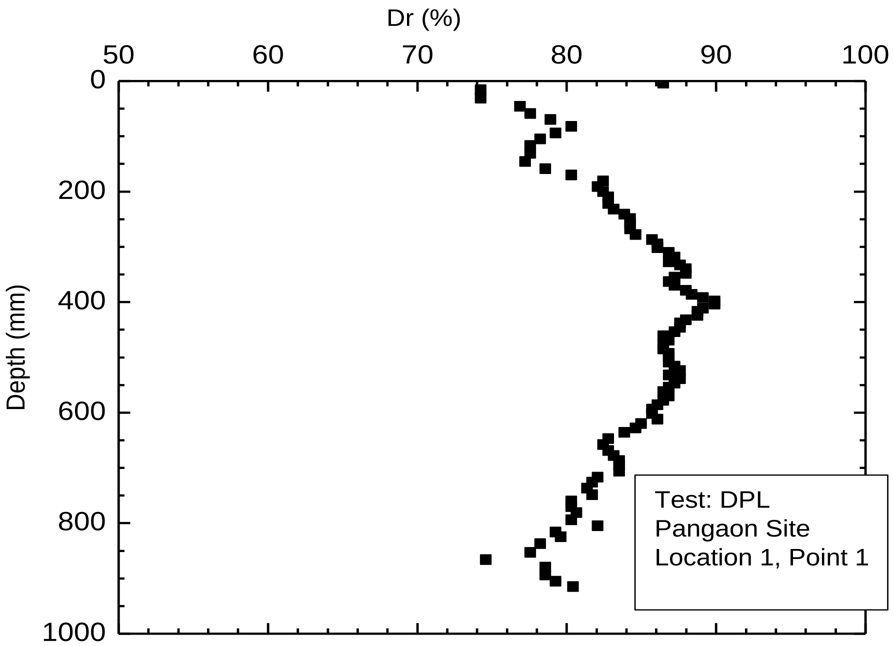

Fig.4.38: Typical plot of Relative Density vs. depth obtained from DPL test in Pangaon Site

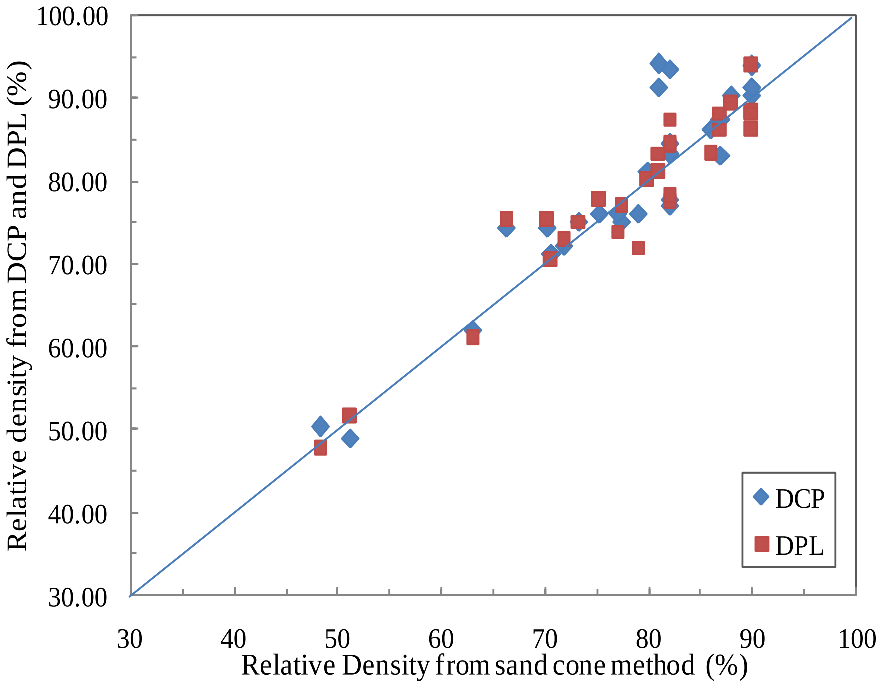

Fig. 4.39: Comparison of Relative Density obtained from DCP and DPL test and Sand Cone Method after introduction of correction factor

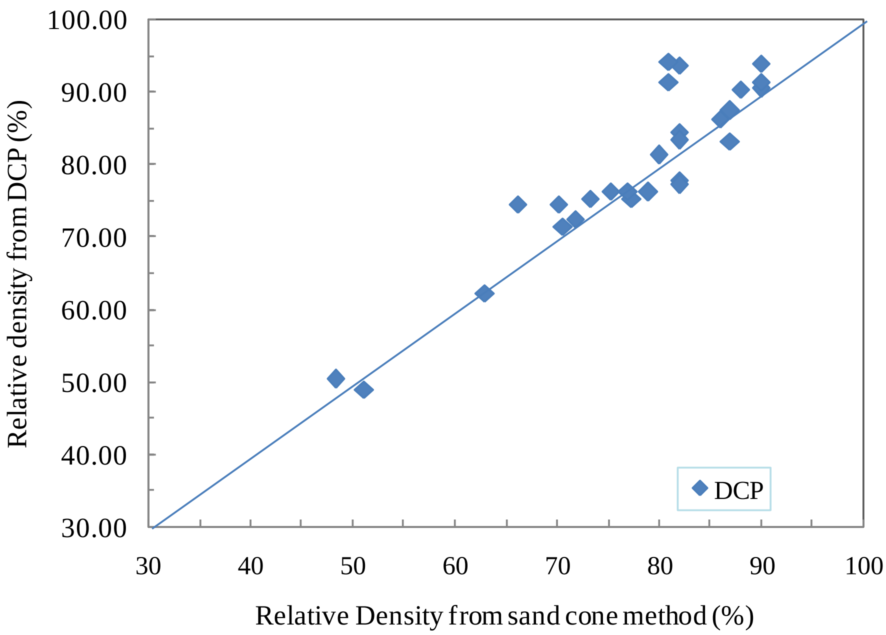

Fig. 4.40: Comparison of Relative Density obtained from DCP test and Sand Cone Method after introduction of correction factor

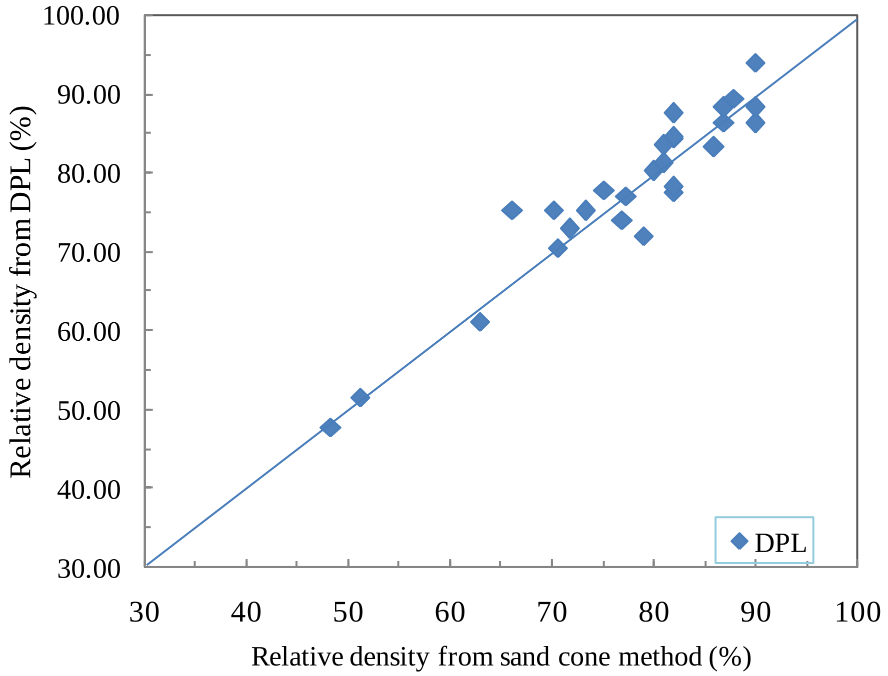

Fig. 4.41: Comparison of Relative Density obtained from DPL test and Sand Cone Method after introduction of correction factor

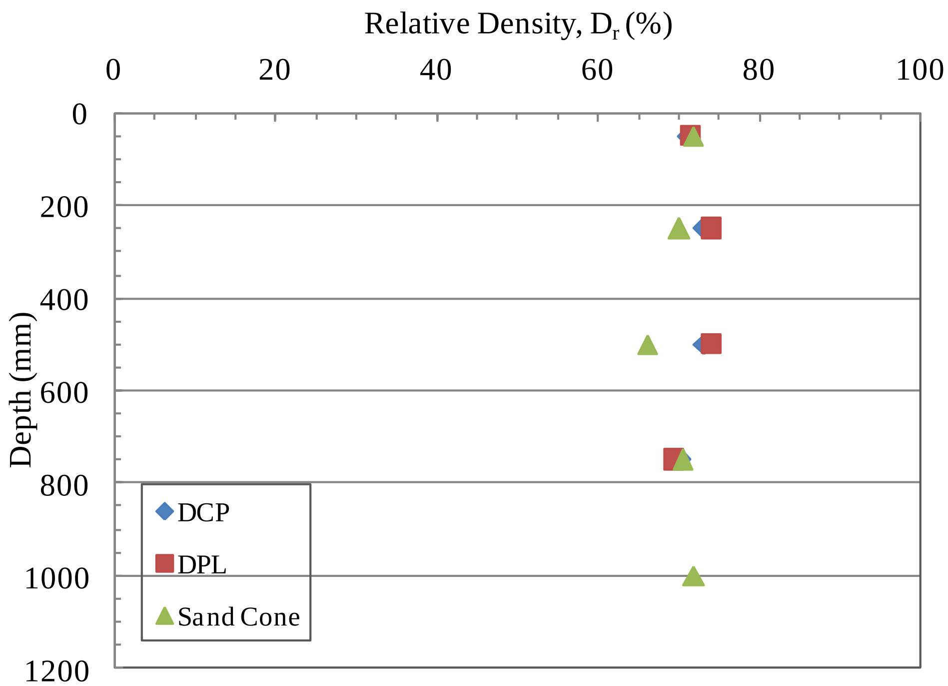

Fig. 4.42: Relative Density vs. depth obtained from DCP, DPL and Sand Cone Method (Location 1, Bashundhara site)

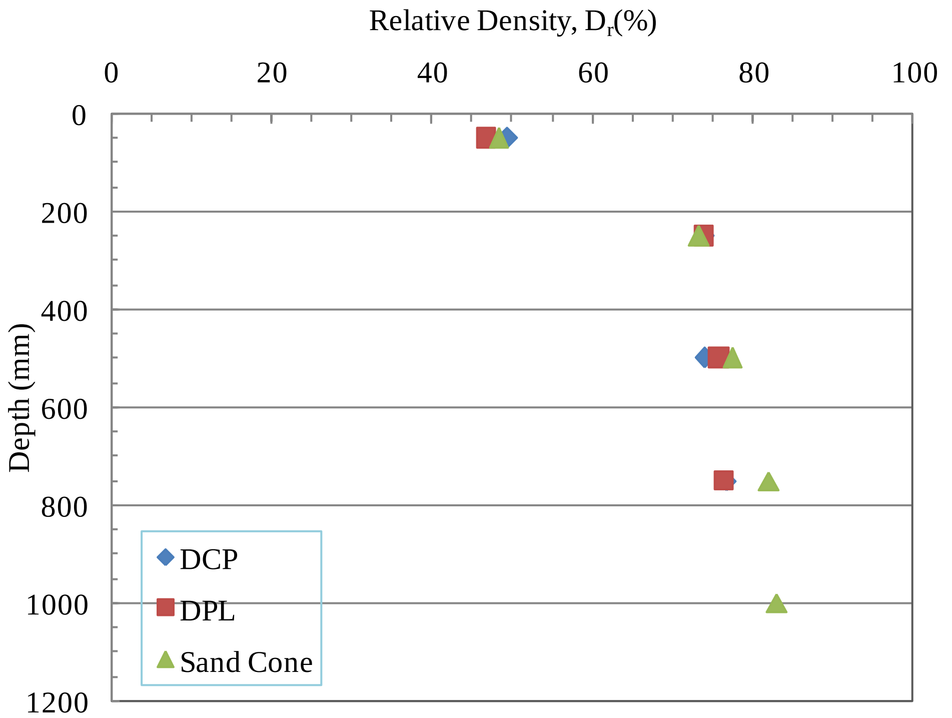

Fig. 4.43: Relative Density vs. depth obtained from DCP, DPL and Sand Cone Method (Location 2, Bashundhara Site)

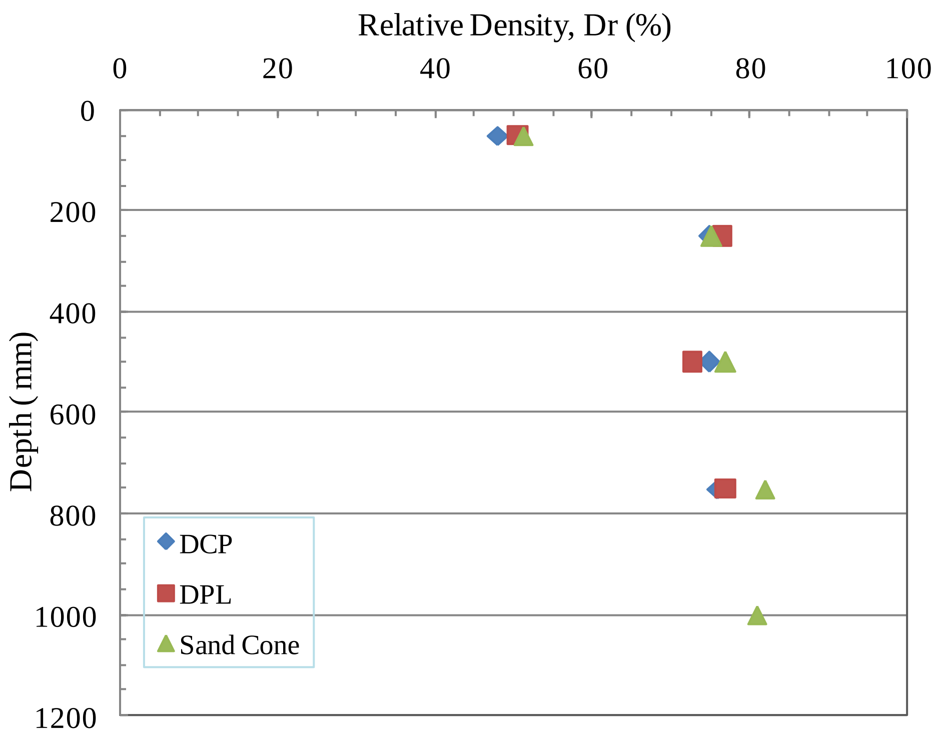

Fig. 4.44: Relative Density vs. depth obtained from DCP, DPL and Sand Cone Method (Location 3, Bashundhara site)

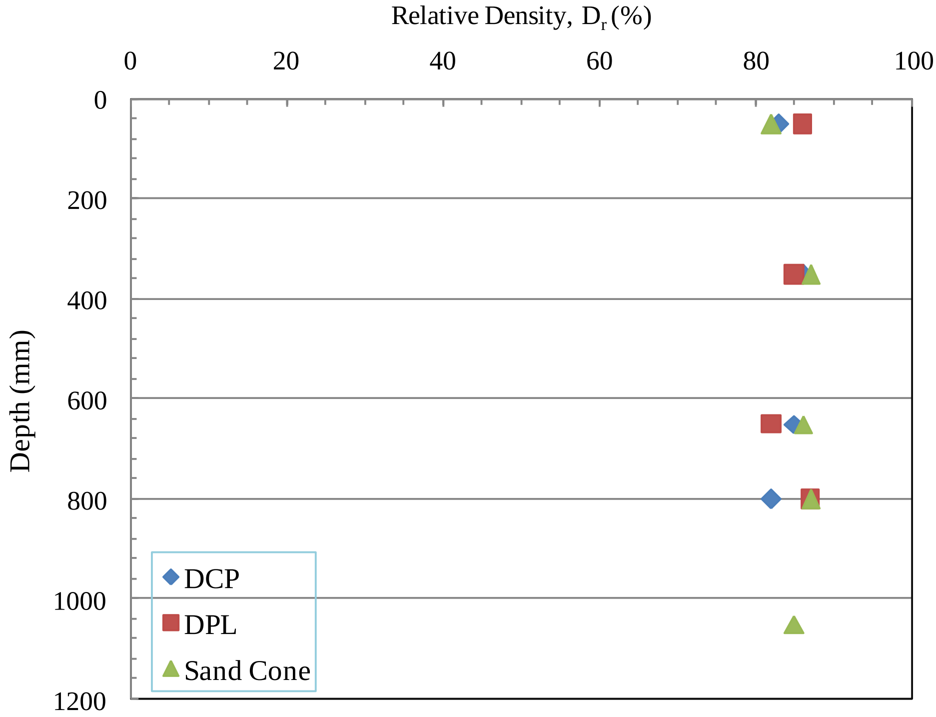

Fig. 4.45: Relative Density vs. depth obtained from DCP, DPL and Sand Cone Method (Location 1, Point 1, Jamuna site)

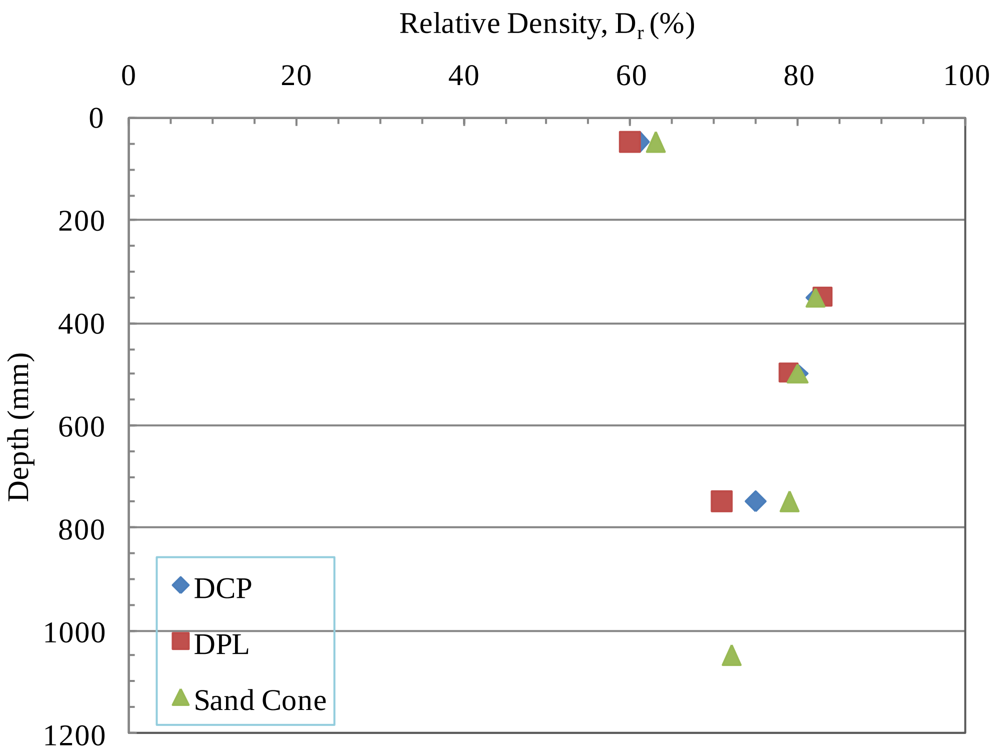

Fig. 4.46: Relative Density vs. depth obtained from DCP, DPL and Sand Cone Method (Location 2, Point 1, Jamuna site)

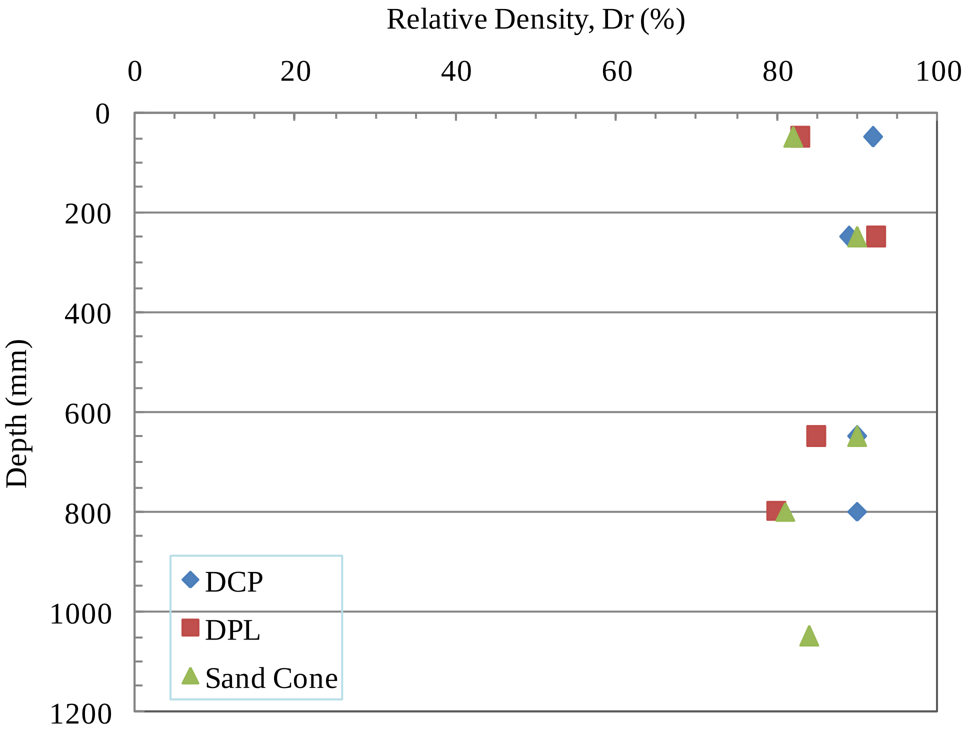

Fig.4.47: Relative Density vs. depth obtained from DCP, DPL and Sand Cone Method (Location 1, Point 1, Pangaon site)

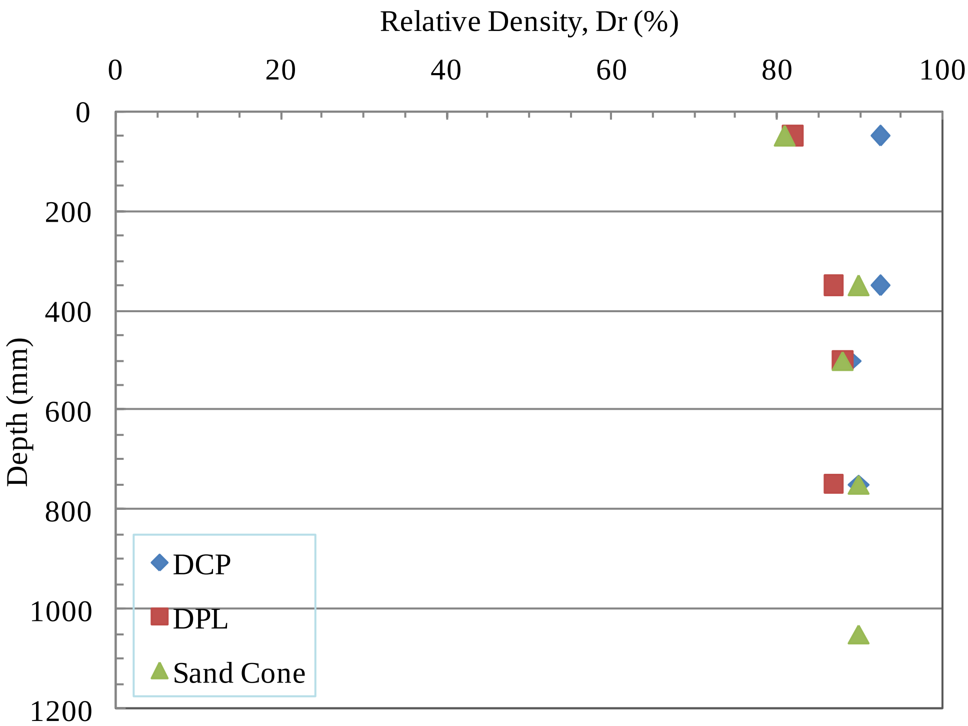

Fig. 4.48: Relative Density vs. depth obtained from DCP, DPL and Sand Cone Method (Location 2, Point 1, Pangaon site)

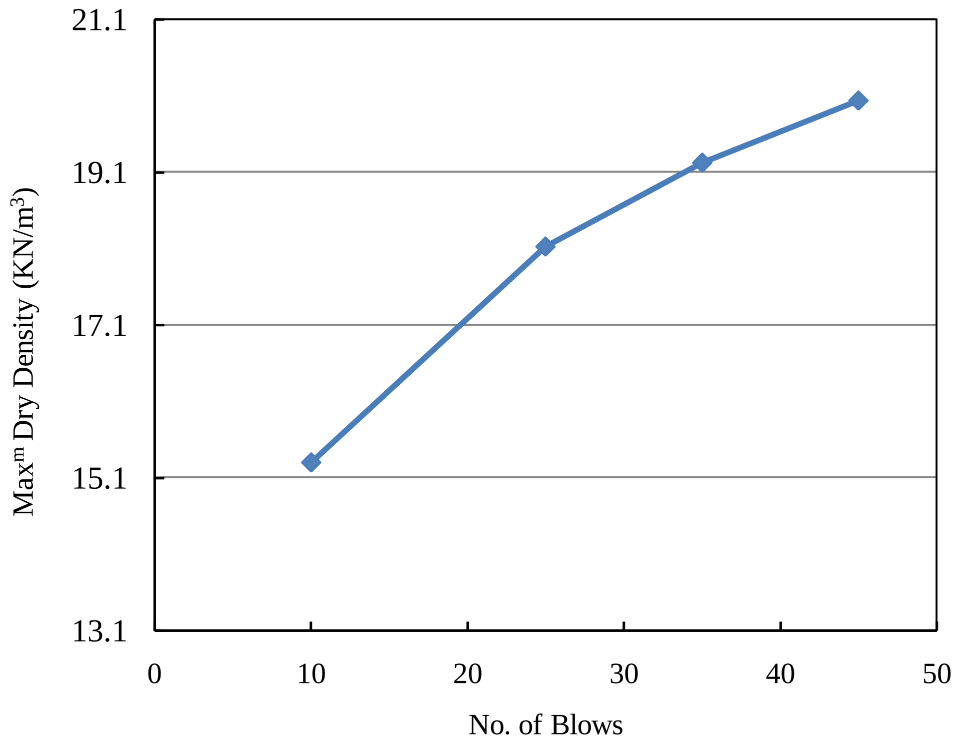

Fig. 4.49: Variation between Max^{m} dry density and No. of blows at Location 1 (Bashundhra site)

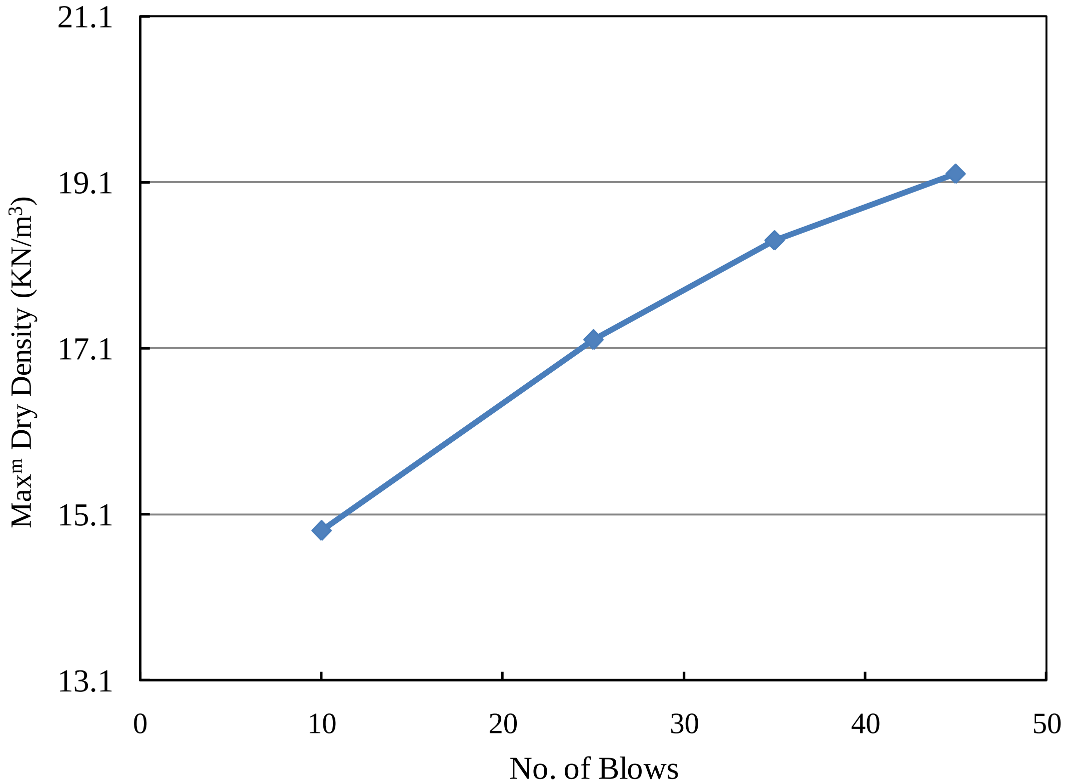

Fig. 4.50: Variation between dry density and No. of blows at location 3 (Bashundhra Site)

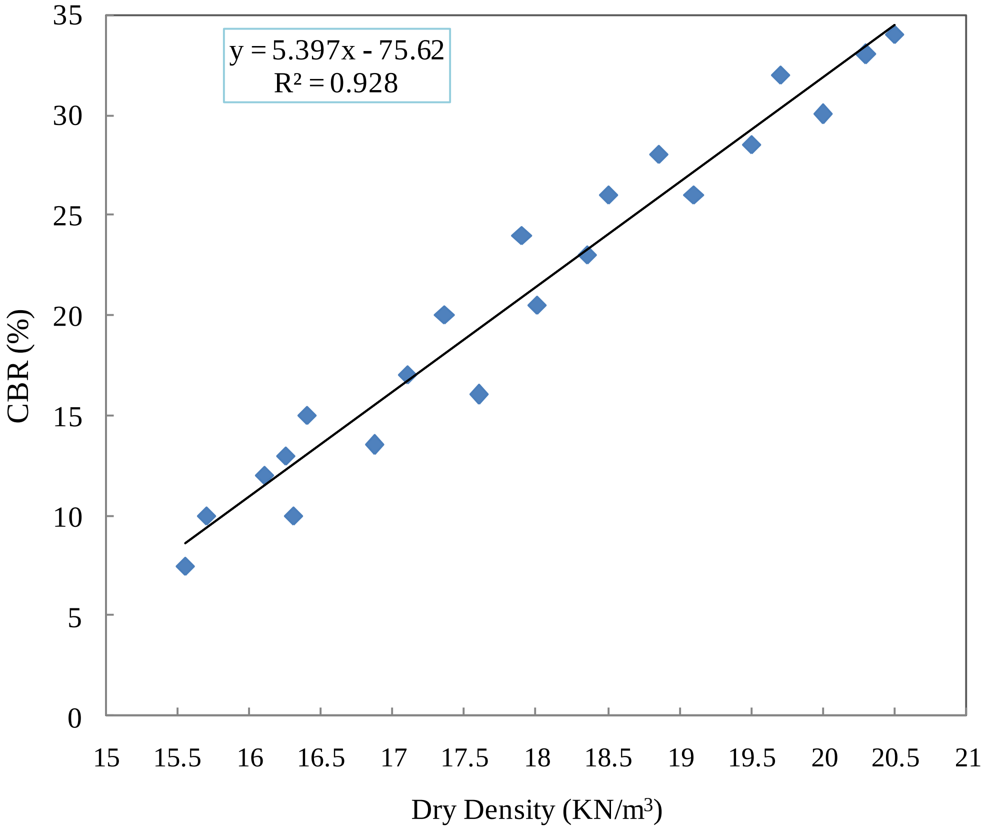

Fig. 4.51: Relationship between CBR (%) value and dry density

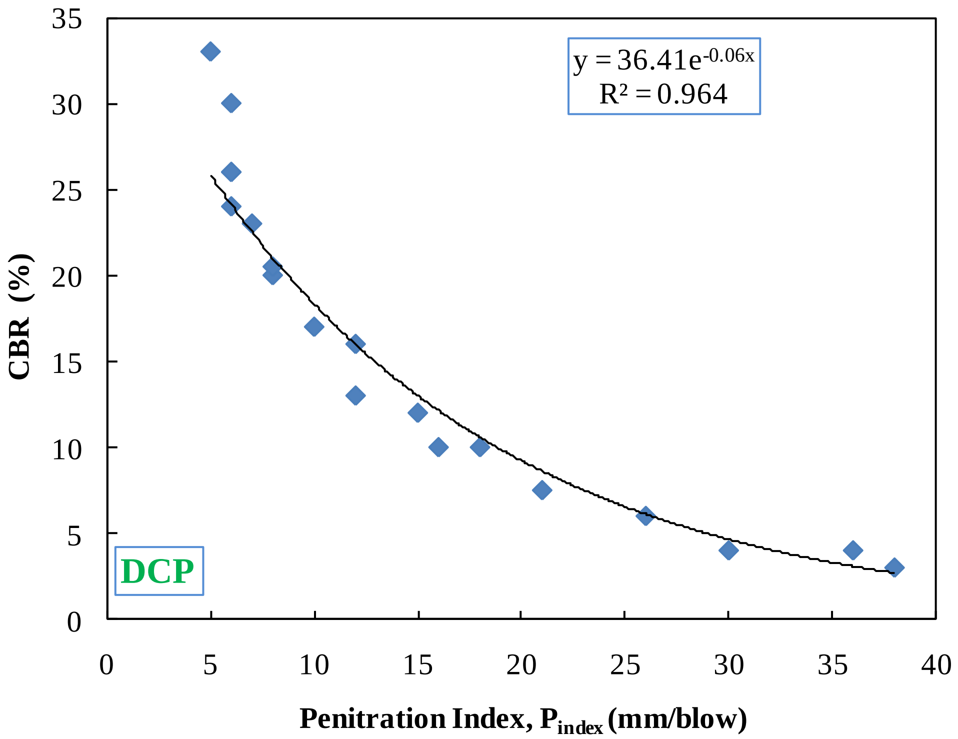

Fig. 4.52: Correlation between DCP Penetration Index (P_{index}) and CBR (%)

CHAPTER 5
REGRESSION MODELS

5.1 General

Based on the laboratory result and using SPSS 16.0 software a linear regression model was developed which correlates the measured Relative Density (D_r) and calculated relative density from developing equation. To depict the validity of the measured D_r and model was developed and then calculate the value of $D_r$and analyzed.

$$D_r\ (\%) = a_1 + a_2(P_{index}) + a_3(D_{50}) + a_4(DCP\ or\ \ DPL) ---------------5.1$$

Where a_1, a_2, a_3 and a_4 are coefficient of regression line and

P_{index}= Penetration index (mm/blow),

D_{50}=Mean diameter of particle size (mm) and

DCP/DPL= Type of instrument used.

The reliability and accuracy of the model were checked by comparing the predicted values of Relative Density from this model and the measured values, and computing the correlation coefficient. The red dot (----) line in the figure represents the line of perfect equality. The correlation coefficient R^2 at 95% confidence interval all values are nearly same.

In order to obtain a more accurate regression model the DCP/DPL was left out as a descriptor variable in the regression equation. The model that gives the best correlation is of the following from again.

$$D_r\ (\%) = a_1 + a_2(P_{index}) + a_3(D_{50}) -------------------------5.2$$

In this study, penetration index (P_{index})in mm/ blow and mean diameter of particle size (D_{50}) in mm are consider as independent variables, measured Relative Density (D_r) are consider as a dependent variable. Based on multiple regressions, the following input and output are shown in below for DCP and DPL.

5.2 Regression Model for Relative Density and Penetration Index based on DCP Used

For regression analysis, penetration index and mean diameter of particle size are consider as independent variables, while, the measured Relative Density are consider as a dependent variableis evident in Table 5.1. Moreover, to depict the validity of the measured relative density against the computed relative density values, the following Equation 5.3, was developed using the unstandardized coefficients as presented in Table 5.2.

Table 5.1: Independent and dependent variables for SPSS analysis

DCP.sav [DataSet1] - SPSS Data Editor

	DR_density	P_Index	D50_value	var	var	var	var
1	65.00	87.00	0.20				
2	74.00	71.00	0.20				
3	80.00	58.00	0.20				
4	89.00	43.00	0.20				
5	100.00	15.00	0.20				
6	57.00	69.00	0.47				
7	57.00	57.00	0.47				
8	60.00	50.00	0.47				
9	70.00	42.00	0.47				
10	84.00	12.00	0.47				
11	16.68	180.00	0.70				
12	33.45	131.00	0.70				
13	40.00	110.00	0.70				
14	49.40	36.00	0.70				
15	52.92	32.00	0.70				
16	70.75	21.00	0.70				
17	86.92	19.00	0.70				
18	70.31	20.00	0.70				

Table 5.2: Unstandardized coefficients for developed model

Coefficients[a]

Model		Unstandardized Coefficients		Standardized Coefficients	t	Sig.
		B	Std. Error	Beta		
1	(Constant)	112.492	5.236		21.485	.000
	D50	-55.346	9.538	-.487	-5.803	.000
	Pindex	-.341	.039	-.736	-8.774	.000

a. Dependent Variable: Dr

$$D_r\,(\%) = 112.492 - 0.341(P_{index}) - 55.346(D_{50}) \text{ ---------------------- } 5.3$$

Figure 5.1 illustrate a plot of the values of computed Relative Density with measured Relative Density values using the linear regression model. The red dot straight line in the figure represents the line of perfect equality, where the values being compared are exactly equal. The correlation coefficient R^2 at 95% confidence interval is 0.922, meaning roughly that 92.2% of the variance in relative density is explained by the model. This value is statistically significant and therefore suggests that the measured and calculated values of relative density are comparable.

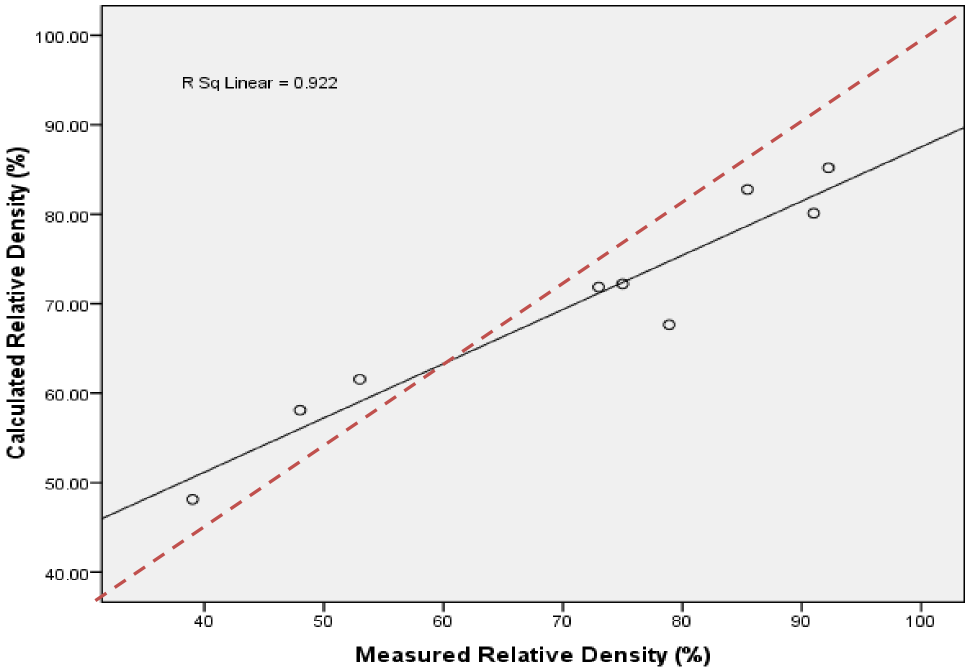

Fig.5.1: Cross plot of computed relative density vs. measured relative density values for DCP using Equation 5.3

5.3 Regression Model for Relative Density and Penetration Index based on DPL Used

Here, it is interesting to note that for regression analysis, penetration index and mean diameter of particle size are consider as independent variables, while, the measured relative density are consider as a dependent variableis evident in Table 5.3. Moreover, to depict the validity of the measured Relative Density against the computed relative density values, the following Equation 5.4, was developed using the unstandardized coefficients as presented in Table 5.4.

Table 5.3: Independent and dependent variables for SPSS analysis

*DPL.sav [DataSet0] - SPSS Data Editor

File Edit View Data Transform Analyze Graphs Utilities Add-ons Window Help

15 :

	Dr_density	PI_Index	D50_Value	var	var
1	66.00	21.00	0.20		
2	73.00	17.00	0.20		
3	80.00	15.00	0.20		
4	89.00	8.00	0.20		
5	100.00	4.00	0.20		
6	58.00	12.00	0.47		
7	69.00	8.00	0.47		
8	84.00	5.00	0.47		
9	60.00	12.00	0.47		
10	49.40	13.00	0.70		
11	52.92	10.00	0.70		
12	70.75	6.00	0.70		
13	86.92	6.00	0.70		
14	71.60	6.00	0.70		

Table 5.4: Unstandardized coefficients for developed model

Coefficients[a]

Model		Unstandardized Coefficients		Standardized Coefficients	t	Sig.
		B	Std. Error	Beta		
1	(Constant)	109.548	5.625		19.477	.000
	D50	-55.424	10.361	-.481	-5.349	.000
	Pindex	-1.079	.131	-.739	-8.208	.000

a. Dependent Variable: Dr

$$\mathrm{D_r}\,(\%) = 109.548 - 1.079\,(P_{index}) - 55.424\,(D_{50}) \quad \text{---------------------} \quad 5.4$$

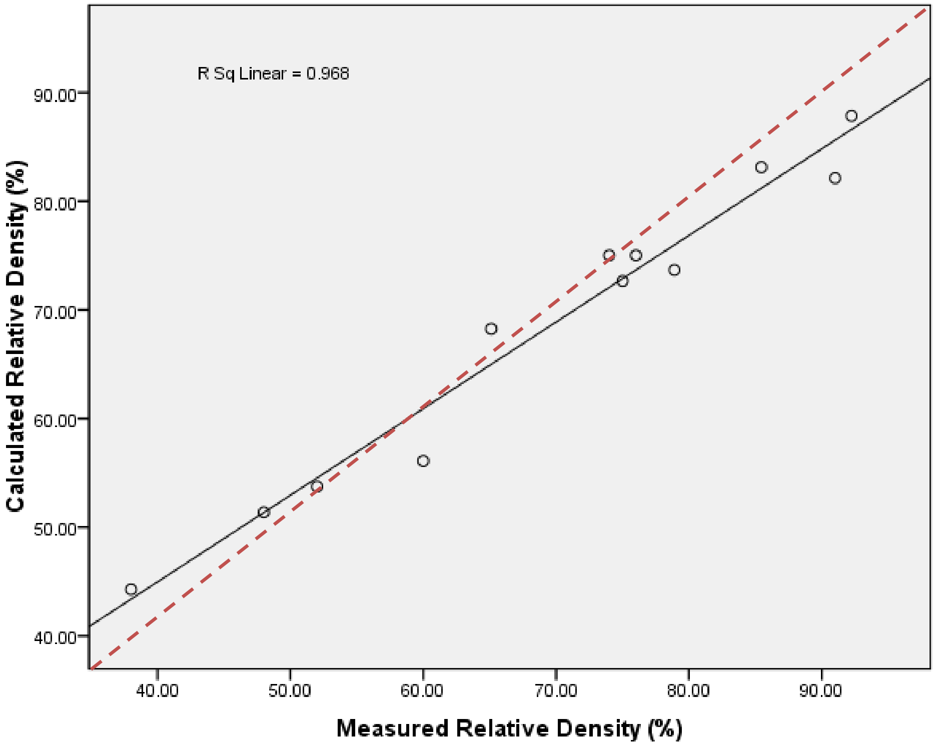

Fig. 5.2: Cross plot of computed relative density vs. measured relative density values for DPL using Equation 5.4

5.4 Comparison between Developed Equation and SPSS Equation for DCP

Based on the DCP test result, Equation 5.5 was developed as a generalized equation and Equation 5.3 was developed based on SPSS analysis. Both equations ware developed to measure the relative density as alternative method of sand cone method. Now to check the accuracy and suitability of both equations for practical purpose, a comparison was made that is shown in Fig. 5.3. Based on the Fig. 5.3, to determine the relative density based on DCP result, Equation 5.3 is more reliable and useable in field.

$$\mathrm{D_r}\ (\%) = 112.492 - 0.341(P_{index}) - 55.346(D_{50}) \text{------------------} 5.3$$

$$\mathrm{D_r}\ (\%) = -1.036 P_{index} D_{50}^{\ 0.75} + 94.99 \text{------------------------} 5.5$$

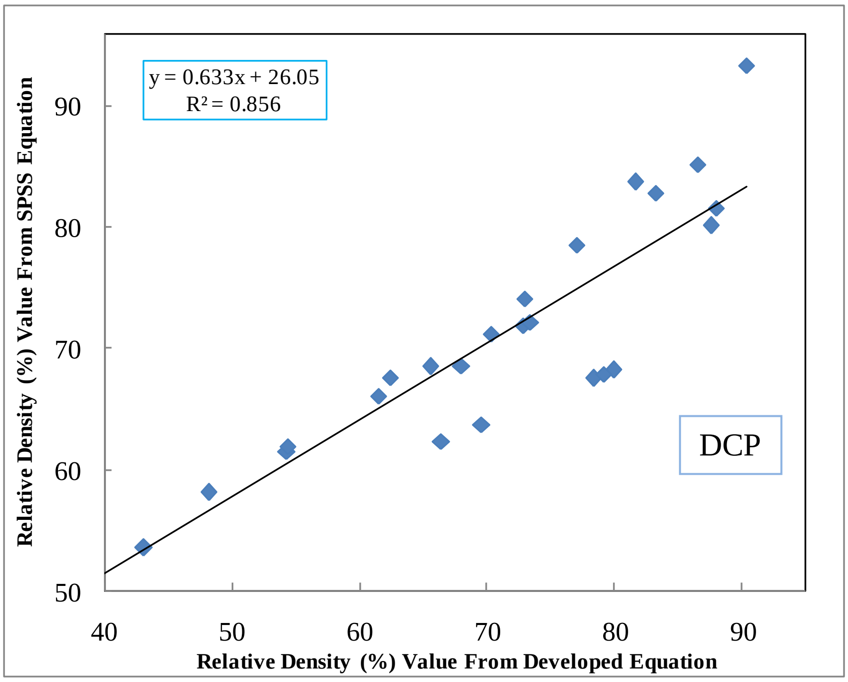

Fig. 5.3: Comparison of measured Relative Density by using SPSS equation and developed equation for DCP

5.5 Comparison between Developed Equation and SPSS Equation for DPL

On the basis of DPL test result, Equation 5.6 was developed as a generalized equation and Equation 5.4 was developed based on SPSS analysis. Both equations ware developed to measure the relative density as alternative method of sand cone method. Now to check the accuracy and suitability of both equations for practical purpose, a comparison was made that is shown in Fig. 5.4. Based on the Fig. 5.4, to determine the relative density based on DPL result, Equation 4.4 is more reliable and useable in field by using DPL.

$$D_r\,(\%) = 109.548 - 1.079\,(P_{index}) - 55.424\,(D_{50}) \text{---------------------} 5.4$$

$$D_r\,(\%) = -5.219 P_{index} D_{50}^{\;0.75} + 101.3 \text{------------------------} 5.6$$

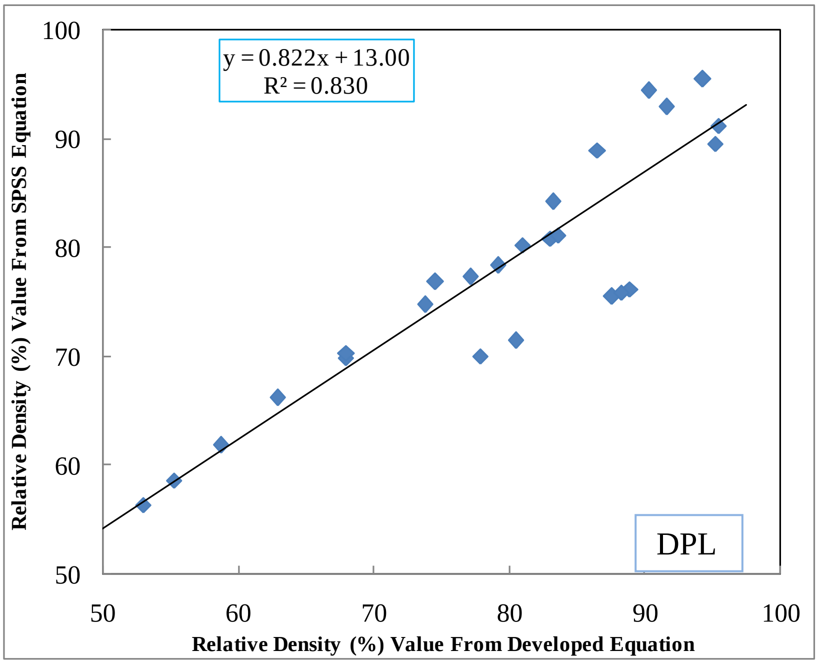

Fig.5.4: Comparison of measured relative density by using SPSS equation and developed equation for DPL

5.6 Regression Model of Initial Tangent Modulus based on DCP used

For regression analysis, Relative Density, penetration index and mean diameter of particle size are consider as independent variables, while, the measured initial tangent modulus are consider as a dependent variable is evident in Table 5.5. To measure the initial tangent modulus values, the following Equation 5.7, was developed using the unstandardized coefficients as presented in Table 5.6.

Table 5.5: Independent and dependent variables for SPSS analysis

	Eplt_Mpa	PI_index	D50_value	var	var
1	52.60	18.00	0.35		
2	55.68	19.00	0.70		
3	50.30	25.00	0.35		
4	49.44	16.00	0.70		
5	45.60	69.00	0.35		
6	45.61	21.00	0.70		
7	40.00	110.00	0.35		
8	35.00	120.00	0.35		
9	40.16	32.00	0.70		
10	35.61	36.00	0.70		
11	29.00	125.00	0.35		
12	30.86	110.00	0.70		
13	26.00	264.00	0.35		
14	23.00	131.00	0.70		

Table 5.6: Unstandardized coefficients for developed model

Coefficients[a]

Model		Unstandardized Coefficients B	Unstandardized Coefficients Std. Error	Standardized Coefficients Beta	t	Sig.
1	(Constant)	60.914	6.294		9.677	.000
	PI_index	-.137	.025	-.927	-5.474	.000
	D50_value	-19.634	9.663	-.344	-2.032	.067

a. Dependent Variable: Eplt_Mpa

$$E_{Plt(i)}(MPa) = 60.914 - 0.137(P_{index}) - 19.634(D_{50}) -------------5.7$$

5.7 Regression Model of Initial Tangent Modulus based on DPL used

For regression analysis based on DPL used, penetration index and mean diameter of particle size are consider as independent variables, while, the measured initial tangent modulus are consider as a dependent variable is evident in Table 5.7. To measure the initial tangent modulus values, the following Equation 5.8, was developed using the unstandardized coefficients as presented in Table 5.8.

Table 5.7: Independent and dependent variables for SPSS analysis

*DPL....sav [DataSet1] - SPSS Data Editor

File Edit View Data Transform Analyze Graphs Utilities Add-ons

17 :

	Eplt_Mpa	PI_index	D50_value	var
1	55.68	5.00	0.70	
2	30.86	29.00	0.70	
3	35.61	13.00	0.70	
4	40.16	10.00	0.70	
5	45.61	6.00	0.70	
6	49.44	5.00	0.70	
7	23.00	36.00	0.70	
8	40.00	27.00	0.35	
9	26.00	56.00	0.35	
10	29.00	47.00	0.35	
11	35.00	38.00	0.35	
12	45.60	12.00	0.35	
13	50.30	8.00	0.35	
14	52.60	6.00	0.35	

Table 5.8: Unstandardized coefficients for developed model

Coefficients[a]

Model		Unstandardized Coefficients		Standardized Coefficients	t	Sig.
		B	Std. Error	Beta		
1	(Constant)	63.905	4.597		13.903	.000
	PI_index	-.601	.072	-1.006	-8.297	.000
	D50_value	-21.320	6.919	-.374	-3.082	.010

a. Dependent Variable: Eplt_Mpa

$$E_{Plt(i)}(MPa) = 63.905 - 0.601(P_{index}) - 21.320(D_{50}) ------------ 5.8$$

5.8 Regression Model of Initial Tangent Modulus based on Dr Value

For regression analysis based on Relative Density value and mean diameter of particle size are consider as independent variables, while, the measured initial tangent modulus are consider as a dependent variable is evident in Table 5.9. To measure the initial tangent modulus values, the following Equation 5.9, was developed using the unstandardized coefficients as presented in Table 5.10.

Table 5.9: Independent and dependent variables for SPSS analysis

relative.....sav [DataSet1] - SPSS Data Editor

File Edit View Data Transform Analyze Graphs Utilities Add-ons Window

21 : D50_value

	Eplt_Mpa	Dr_Density	D50_value	var	var
1	52.60	92.50	0.35		
2	55.68	86.92	0.70		
3	50.30	85.45	0.35		
4	49.44	80.00	0.70		
5	45.60	78.90	0.35		
6	45.61	70.75	0.70		
7	40.00	69.15	0.35		
8	35.00	61.16	0.35		
9	40.16	59.25	0.70		
10	35.61	49.40	0.70		
11	29.00	49.40	0.35		
12	30.86	40.00	0.70		
13	26.00	39.92	0.35		
14	23.00	33.45	0.70		

Table 5.10: Unstandardized coefficients for developed model

Coefficients[a]

Model		Unstandardized Coefficients		Standardized Coefficients	t	Sig.
		B	Std. Error	Beta		
1	(Constant)	-1.851	1.898		-.975	.350
	Dr_Density	.543	.020	1.017	27.355	.000
	D50_value	13.331	2.121	.234	6.285	.000

a. Dependent Variable: Eplt_Mpa

$$E_{Plt(i)}(MPa) = -1.851 + 543(D_r)\% + 13.331(D_{50}) --------------- 5.9$$

CHAPTER 6
CONCLUSIONS

6.1 General

An alternative easy indirect method to determine in situ relative density of sand deposit was developed in this study. For the first time in Bangladesh, DCP and DPL have been used to estimate Relative Density at various depths of sand deposit. DCP and DPL tests were performed on a sand deposit of known Relative Density prepared in a calibration chamber. Azad (2008) calibrated DCP and DPL for two types of sand of Bangladesh. Azad (2008) found good correlations between Relative Density and N_{10} for Jamuna sand and Sylhet sand. He also tried to make a generalized correlation between N_{10} and Relative Density which can be applied for clean sand of any particle size.

The objectives of this study is to evaluate the Plate Load Test (PLT), the Dynamic Cone Penetrometer (DCP) and Dynamic Probing Light (DPL) as potential tests to measure in-situ stiffness of highway materials and embankments.But in practical field in some case these correlations show more than 100% Relative Density of dredge fills sand which is not acceptable. So, in this study improvement of the correlation was made to overcome this limitation. Here, DCP and DPL tests were performed on a sand deposit of known Relative Density prepared in a calibration chamber.

Tests were performed on two types of sand; namely clean sand having mean diameter D_{50} = 0.70 mm and D_{50} = 0.35 mm. Here, generalized correlations between Relative Density and $P_{index}D_{50}^{0.}75$ were made instead of Relative Density was made for DCP and DPL for clean sand of any particle size.

A liner correlation was developed between Relative Density (Dr), Penetration Index (P_{index}) in mm/ blow and mean diameter of particle size (D_{50}) in mm by using SPSS 16.01.To check the suitability of two developed equation for determination of Relative Density (D_r), a comparison was developed between two developed equations. Developed equation by SPSS 16.01 is more reliable then developed equation.

6.2 Conclusions

The following conclusions are drawn with respect to this experimental study:

i. A generalized correlation between relative density and P_{index} were found which is applicable to clean sand of any particle size.

ii. Resistance of sand increases exponentially with relative density. The larger the particle size greater the resistance to penetration for a certain relative density of sand. Denser sand shows higher resistance for a specific type of sand.

iii. Performance of DPL is better than performance of DCP.

iv. The proposed method can be used as an indirect method to determine in situ relative density of sand deposit for upto 2 m depth.

v. Developed equation by using SPSS for determination of relative density is more reliable then developed equation based on DCP and DPL used.

vi. Initial tangent modulus and subgrade modulus of sand increase with increasing relative density and mean diameter of particle value.

6.3 Recommendations for Future Study

The recommendations for future study may be summarized from the lessons of the present study as follows:

i) P_{index} of DCP and DPL can be correlated with SPT value.

ii) To prepare sand deposit in calibration chamber instead of air pluviation method another similar study can be done by using wet tamping method.

iii) The effect of saturation level on dynamic cone resistance can be studied.

iv) DCP and DPL can be correlated with bearing capacity of dredge fill sand.

v) DCP and DPL can be correlated with liquefaction potential for different type of sand.

vi) The effect moisture content can consider to develop more reliable generalized equation for determination of relative density.

vii) The Coefficient of Uniformity (C_u), gradation of sand and confining pressure effect on

viii) The effect of particle shape such as sphericity, elongation and flakiness effect on relative density and dynamic cone resistant can studied.

REFERENCES

American Society of Testing Materials (2003). "Standard Test Method for Use of the Dynamic Cone Penetrometer in Shallow Pavement Applications", ASTM D 6951-03, ASTM International, West Conshohocken, PA.

ASTM D1586 – 99. (2006) "Standard Test Method for Penetration Test and Split-Barrel Sampling of Soils", American Society for Testing and Materials, West Conshohocken, PA19428-2959, USA.

ASTM D4429 – 93. (2006). "Standard Test Method for CBR (California Bearing Ratio) of Soils in Place", American Society for Testing and Materials, West Conshohocken, PA19428-2959, USA.

ASTM D6951– 03. (2006). "Standard Test Method for Use of the Dynamic Cone Penetrometer in Shallow Pavement Applications", American Society for Testing and Materials, West Conshohocken, PA19428-2959, USA.

Abu-Farsakh, M. Y., Al-shibli, K., Nazzal, M. D., and Seyman, E., (2004), "Assessment of in- Situ Test Technology for Construction Control of Base Courses and Embankments" LTRC Project No. 02-1GT, State Project No. 736-02-0995**,** Louisiana Transportation Research Center

Amini, F. (2004). "Dynamic cone penetration in quality control of compaction, state of the Art Report" Geotechnical Engineering for Transportation Projects, GeoTrants 2004, ASCE.

Ayers, M. E., Thompson, M. R., and Uzarski, D. R. (1989). "Rapid Shear Strength Evaluation of In Situ Granular Materials". Transp. Res. Rec. 1227, Transp. Res. Board, pp. 134-146.

Bester, M. D., and Hallat, L. (1977). "Dynamic Cone Penetrometer", University of Pretoria, Pretoria.

Burnham, T. and Johnson, D. (1993). "In Situ Foundation Characterization Using the Dynamic Cone Penetrometer", Study No. 9PR3001, Office of Materials Research and Engineering, Minnesota Department of Transportation, USA.

Burnham, T. R. (1997). “Application of Dynamic Cone Penetrometer to Minnesota Department of Transportation Pavement Assessment Procedures”, Report No. MN/RC. 97/19, Minnesota Department of Transportation, St. Paul, MN. 24

Chan, F. W. K., and Armitage, R. J. (1997). “Evaluation of Flexible Pavements in the Middle East”, Proceedings of the 8th Inter. Conf. on Asphalt Pavements, August, pp. 459-469.

Chen, D. H., Wang, J-N., and Bilyeu, J. (2001). “Application of Dynamic Cone Penetrometer in Evaluation of Base and Subgrade Layers”, Transp. Res. Rec. 1764.

Chen, J., Hossain, M., and LaTorella, T. M. (1999). “Use of Falling Weight Deflectometer and Dynamic Cone Penetrometer in Pavement Evaluation”, Transp. Res. Rec. 1655, Trans. Res. Board, pp. 145-151.

Coonse, J. (1999). “Estimating California Bearing Ratio of Cohesive Piedmont Residual Soil Using the Scala Dynamic Cone Penetrometer”, M.Sc Thesis (MSCE), North Carolina State University, Raleigh, N.C., USA.

Datta, T. (2011). “Correlation between CBR and Index Properties of Soil.” Proceedings of Indian Geotechnical Conference, Paper No. A-350, pp. 131-133.

De Beer, M. (1991). “Use of the Dynamic Cone Penetrometer (DCP) in the Design of Road Structure”, Geotechnics in the African Environment, Blight et al (editors), Balkema, Rotterdam, ISBN 90 5410 0079.

De Beer, M. and Merwe, C. J. (1991). “Use of the Dynamic Cone Penetrometer (DCP) in the Design of Road Structures”, Minnesota Department of Transportation, St. Paul, MN.

Edill, T.B. and Benson, C.H., (2005). “Investigation of the DCP and SSG as Alternative Methodsto Determine Subgrade Stability”, Department of Civil and Environmental Engineering University of Wisconsin-Madison

Ese, Dug, Myre, Jostein, Noss, Per Magne, and Vaernea, Einar. (1994). “The Use of Dynamic Cone Penetrometer (DCP) for Road Strengthening Design in Norway”, Proc. Int. Conf. on Bearing Capacity of Rd. and Airfield, pp. 3-22.

Fredlund, D. G. and Rahardjo, H., (1993), “Soil Mechanics for Unsaturated Soils” John Wiley and Sons, Inc., New York, NY.

Harison, J. R. (1987). “Correlation between California Bearing Ratio and Dynamic Cone Penetrometer Strength Measurement of Soils”, Proc. Instn. of Civ. Engrs., London, Part 2, pp. 83-87.

Hassan, A. (1996). “The Effect of Material Parameters on Dynamic Cone Penetrometer Results for Fine-Grained Soils and Granular Materials”, Ph.D. Dissertation, OklahomaStateUniversity, Stillwater, Oklahoma.

Herath, A., Mohammed, L.N., Gaspard, K., Gudishala, R. and Abu-Farsakh, M. Y., (2005), The Use of dynamic cone penetration to predict resilient modulus of subgrade soils” Advances in Pavement Engineering, ASCE.

Kleyn, E. G. (1975). “The Use of the Dynamic Cone Penetrometer (DCP)”, Rep. No. 2/74. Transval Roads Department, South Africa.

Kleyn, E. G., and Savage, P. E. (1982). “The Application of the Pavement DCP to Determine the Bearing Properties and Performance of the Road Pavements”, International Symposium on Bearing Capacity of Roads and Airfields, Trodheim, Norway.

Konard, J.M., and Lachance, D., (2000). “Mechanical properties of unbound aggregates fromDCP and Plate Load Tests”, Proceedings of the Fifth International Conference onunbound aggregate in roads, Nottingham, United Kingdom.

Livneh, M. (1987). “Validation of Correlations between a Number of Penetration Tests and In Situ California Bearing Ratio Tests”, Transp. Res. Rec. 1219. Transportation Research Board, Washington, D.C., pp. 56-67.

Livneh, M. (2000). “Friction Correction Equation for the Dynamic Cone Penetrometer in Subsoil Strength Testing”, Paper Presented at the 79thTransportation Research Board Annual Meeting, Washington, D.C. 27.

Livneh, M., and Ishai, I. (1988). “The Relationship Between in Situ CBR Test and the Various Penetration Tests”, Proc. First Int. Conf. on Penetration Testing, Orlando, Fl, pp. 445-452.

Livneh, M., and Livneh, N. A. (1994). “Subgrade Strength Evaluation with the Extended Dynamic Cone Penetrometer”, Proc. 7th Int. IAEG Congress.

Livneh, M., Ishai, I., and Livneh, N. A. (1992). “Automated DCP Device Versus Manual DCP Device”, Rd. and Transport Res., Vol. 1, No. 4.

Livneh, M., Ishai, I., and Livneh, N. A. (1995). “Effect of Vertical Confinement on Dynamic Cone Penetrometer Strength Values in Pavement and Subgrade Evaluations”, Transp. Res. Rec. 1473, pp. 1-9.

McElvaney, J., and Djatnika, I. (1991). “Strength Evaluation of Lime-Stabilized Pavement Foundations Using the Dynamic Cone Penetrometer”, Australian Rd. Res., Volume 21, No. 1, pp. 40-52.

McGrath, P. (1989). “Dynamic Penetration Testing”,Proceedings, Field and Laboratory Testing of Soils for Foundations and Embankments, TrinityCollege, Doublin.

McGrath, P. G. et al. (1989). “Development of Dynamic Cone Penetration Testing in Ireland”, Proc. Twelfth Int. Conf. on Soil Mechanics and Foundation Engineering. Rio De Janeiro, pp. 271-276.

Meier, R. W., and Baladi, G. Y. (1988). “Cone Index Based Estimates of Soil Strength”, Theory and User.s Guide for Computer Code CIBESS, Technical Report No. SL-88-11, Waterways Experiment Station, Vicksburg, MS.

Melzer, K. J., and Smoltczyk, U. (1982). “Dynamic Penetration Testing-State of the Art Report”, Proc. Second European Symposium on Penetration Testing, Amsterdam, Netherlands, pp. 191-202.

Mitchell, J. M. (1988). “New Developments in Penetration Tests and Equipment”, Proc. First International Symposium on Penetration Testing. Orlando, FL, pp. 245-262.

Mohammadi, S.D., Nikoudel, M.R., Rahimi, H. and Khamehchiyan, M.,(2008), “Application of the Dynamic Cone Penetrometer (DCP) for Determination of the Engineering Parameters of Sandy Soils” Engineering Geology 101 (2008) 195–203, ELSEVIER. doi:10.1016/j.enggeo.2008.05.006

Murthy, V. N. S. (1993). “A Text Book of Soil Mechanics & Foundation Engineering”, Revised and Enlarged Fourth Edition in SI Units.

Nazzal, M. D., (2003), “Field Evaluation of In-Situ Test Technology for Qc/Qa (quality control/quality assurance) During Construction of Pavement Layers and Embankments” M. Sc Thesis, Department of Civil and Environmental Engineering, Louisiana State University and Agricultural and Mechanical College, Baton Rouge, Louisiana, United States.

Newcomb, D. E., Van-Deusen, D. A., and Burnham, T. R. (1994). “Characterization of Subgrade Soils at the Minnesota Road Research Project”, Report No. MN/RD-94/19, Minnesota Department of Transportation, St. Paul, MN.

OVERSEAS ROAD NOTE 31 (1993). “A guide to the structural design of bitumen-surfaced roads in tropical and sub-tropical countries”. Overseas Centre, Transportation Research Laboratory, Crowthrone, Berkshire, United Kingdom.

Rahim, A and George, K.P.,(2004), Dynamic Cone Penetration Test Resistance of Soils –Theory and Evaluation” Geotechnical Engineering for transportation Projects, GeoTrants 2004, ASCE.

Sahoo, P. K. and Reddy, K. S., (2009), “Evaluation of Subgrade Soils Using Dynamic Cone Penetrometer” International Journal of Earth Sciences and Engineering, ISSN 0974-5904, Vol. 02, No. 04, pp. 384-388.

Scala, A. J. (1956). “Simple Methods of Flexible Pavement Design Using Cone Penetrometers”, New Zealand Engineering, Vol. 11.

Siekmeier, J., Burnham, T., and Beberg, D. (1998). “Mn/DOT.s New Base Compaction Specification Based on the Dynamic Cone Penetrometer”, 46th Geotechnical Engineering Conference, University of Minnesota.

Sowers, G. and Hedges, C. (1966). “Dynamic Cone for Shallow In-Situ Penetration Testing”, Vane Shear and Cone Penetration Resistance Testing of In-Situ Soils, ASTM STP 399, American Society for Testing and Materials, pp. 29.

Truebe M. A., and Evans, G. L. (1995). “Lowell Test Road: Helping Improve Road Surfacing Design”, Proc. 6th Int. Conf. on Low-Volume Roads, Minneapolis, Minnesota, Vol. 2, June.

Tumay, M. T. (1994). "Implementation of Louisiana Electric Cone Penetrometer System (LECOPS) For Design of Transportation Facilities Executive Summary", LouisianaTransportationResearchCenter, Baton Rouge, LA.

Van Vuuren, D. J. (1969). "Rapid Determination of CBR with the Portable Dynamic Cone Penetrometer", The Rhodesian Engineer, Vol. 7, No. 5, pp. 852-854.

Wang, J.N., Chen, D.H and Bilyeu, J.,(2001), "Evaluation of Base and Subgrade Layer Moduli Using Dynamic Cone Penetrometer" Proceeding of the Eastern Asia Society for Transportation Studies, Vol.3,No.1,pp.477-491.

Appendix A

DCP, DPL and PLATE LOAD TEST RESULTS

Test results on sand having mean diameter, D_{50}=0.35 mm in calibration chamber

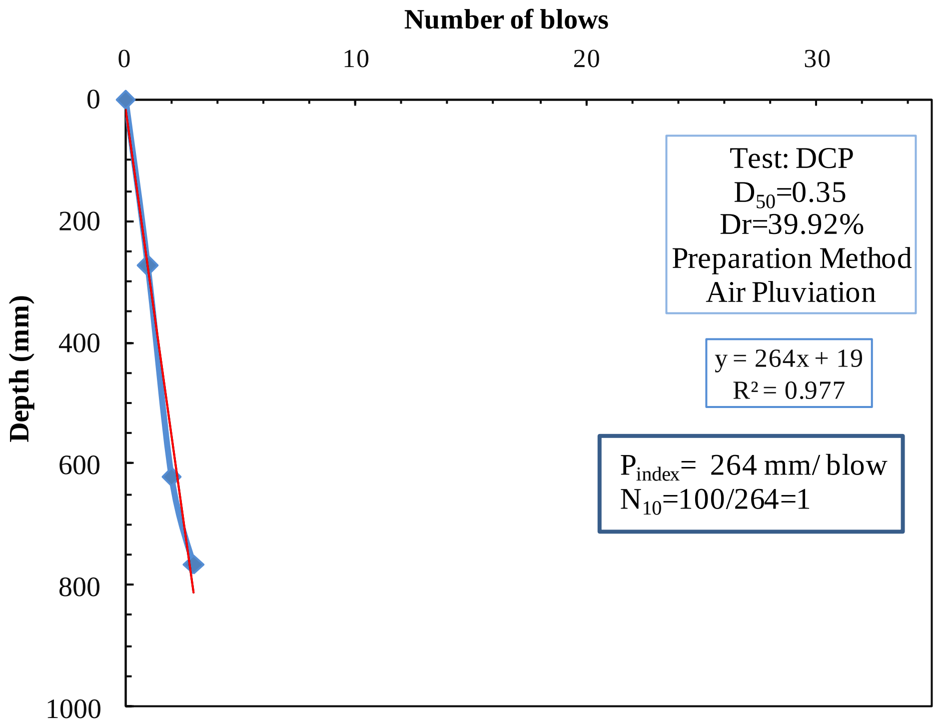

Fig. A.1: Number of blows vs. depth plot of DPC test on sand in calibration chamber having mean diameter, D_{50}= 0.35 mm (Relative Density, D_r = 39.92 %)

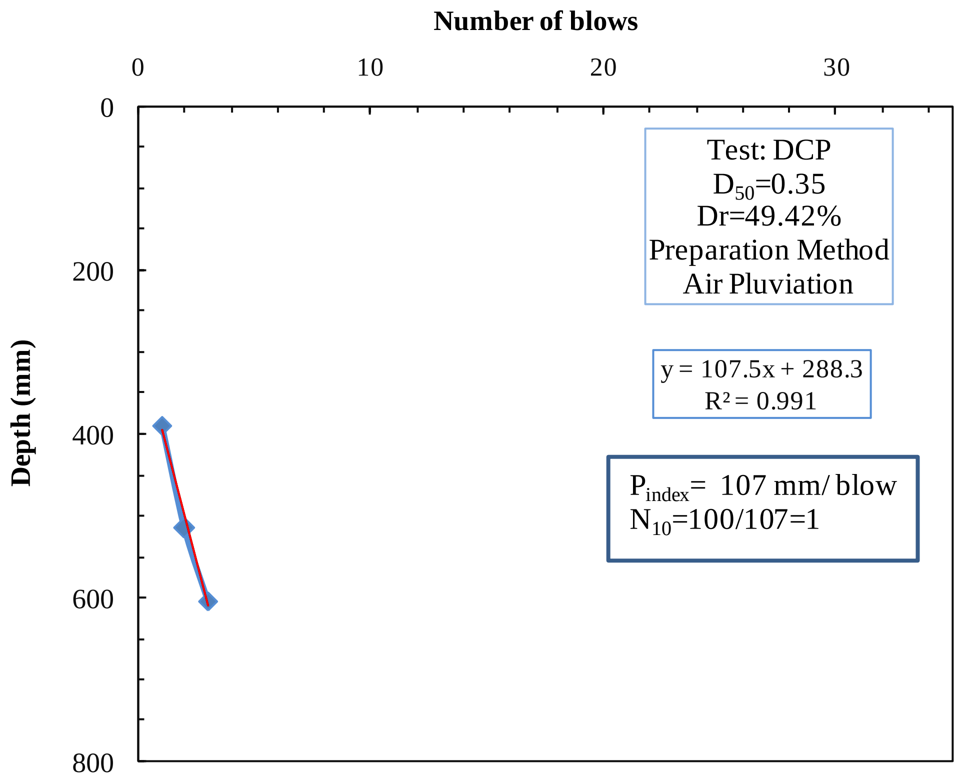

Fig. A.2: Number of blows vs. depth plot of DPC test on sand in calibration chamber having mean diameter, D_{50}= 0.35 mm (Relative Density, D_r = 49.42 %)

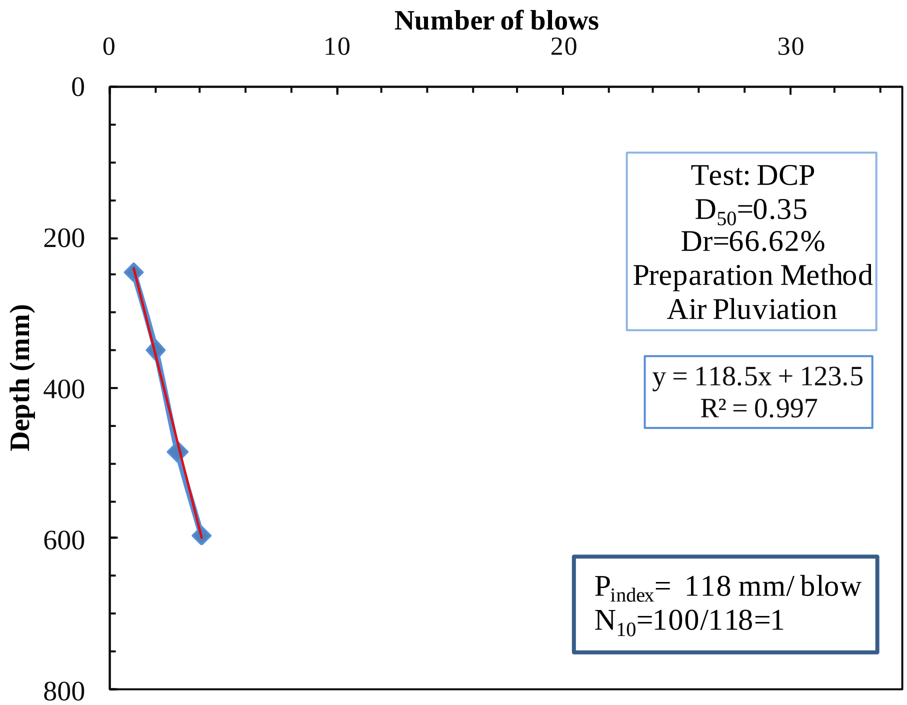

Fig. A.3: Number of blows vs. depth plot of DPC test on sand in calibration chamber having mean diameter, D_{50}= 0.35 mm (Relative Density, D_r = 66.62 %)

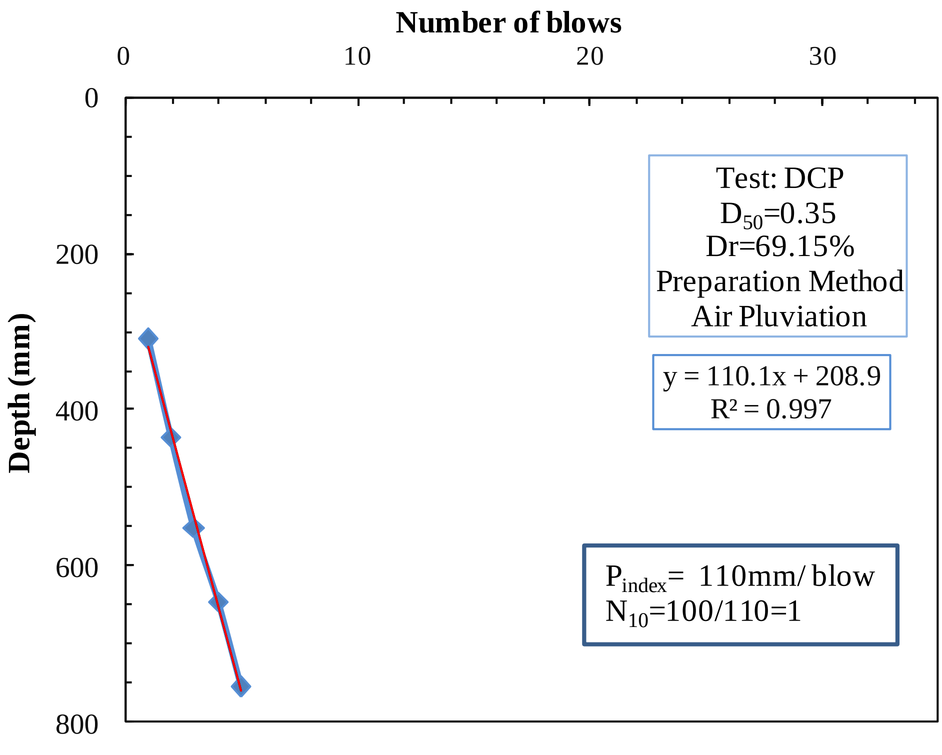

Fig. A.4: Number of blows vs. depth plot of DPC test on sand in calibration chamber having mean diameter, D_{50}= 0.35 mm (Relative Density, D_r = 69.15 %)

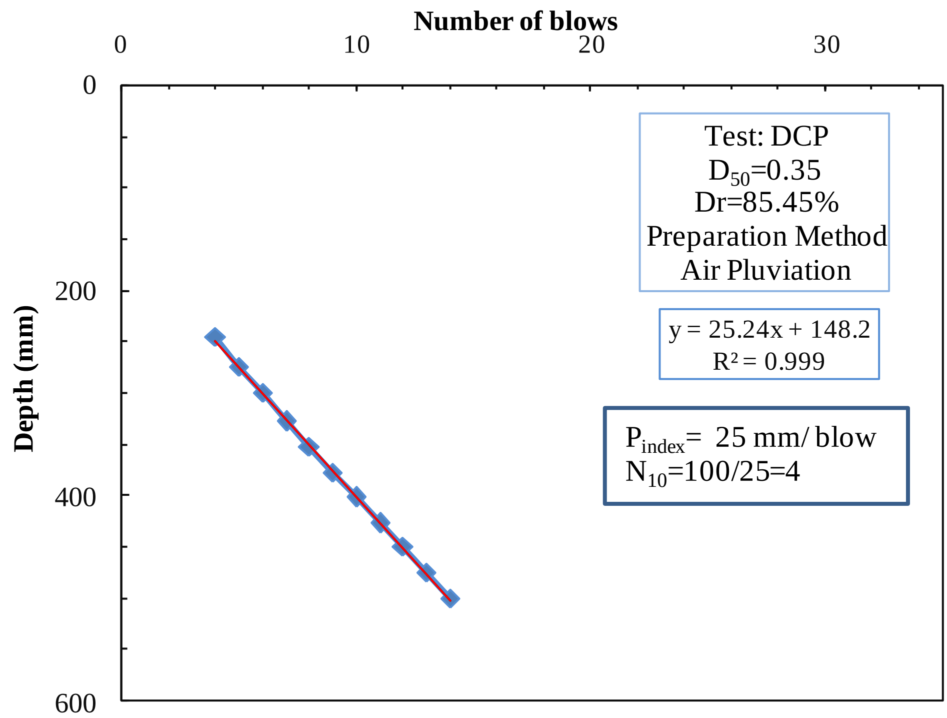

Fig. A.5: Number of blows vs. depth plot of DPC test on sand in calibration chamber having mean diameter, D_{50}= 0.35 mm (Relative Density, D_r = 85.45 %)

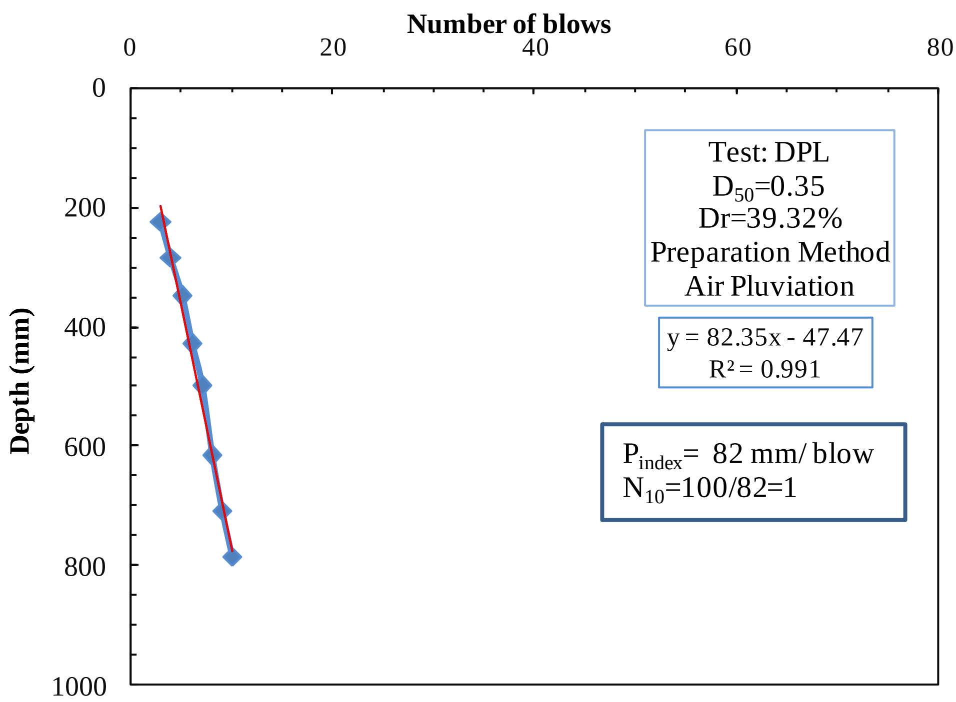

Fig. A.6: Number of blows vs. depth plot of DPL test on sand in calibration chamber having mean diameter, D_{50}= 0.35 mm (Relative Density, D_r = 39.92 %)

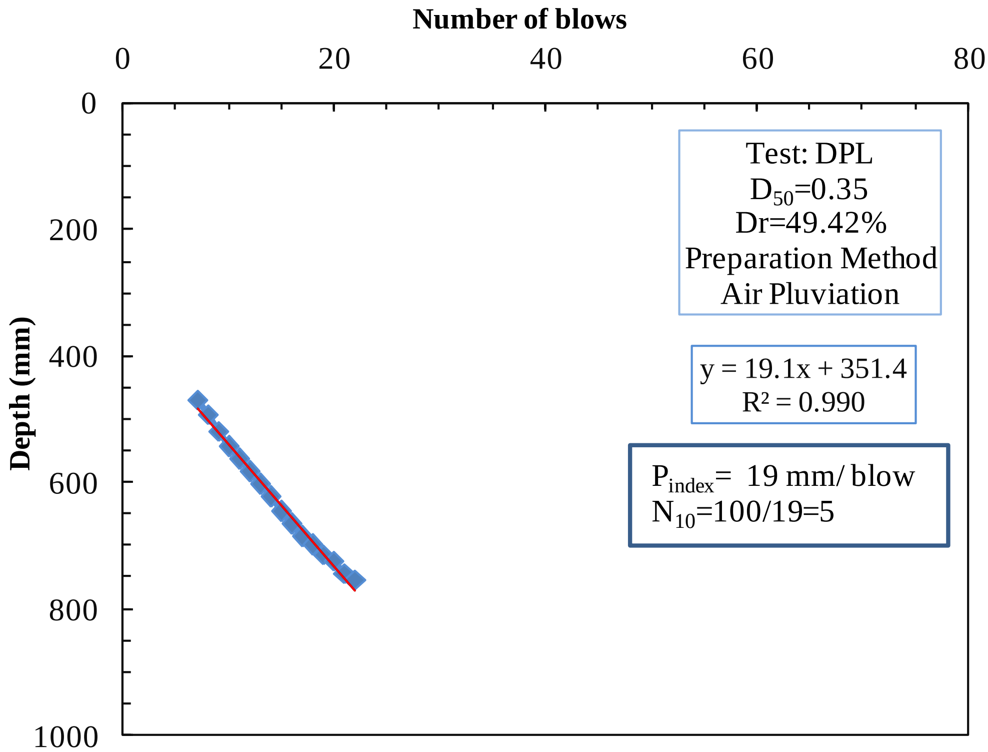

Fig. A.7: Number of blows vs. depth plot of DPL test on sand in calibration chamber having mean diameter, D_{50}= 0.35 mm (Relative Density, D_r = 49.42 %)

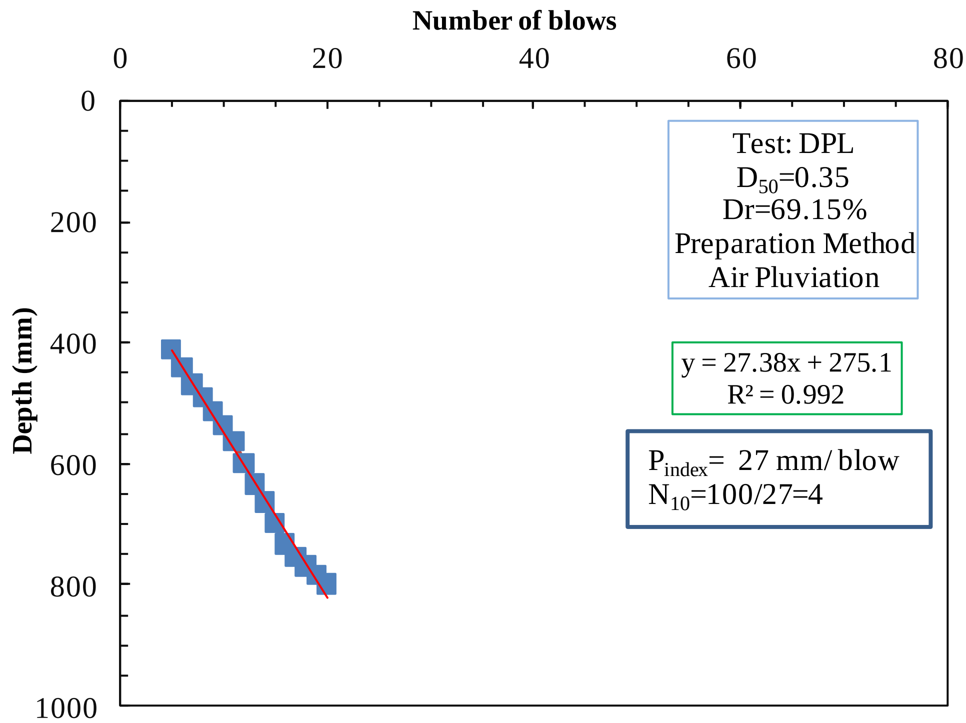

Fig. A.8: Number of blows vs. depth plot of DPL test on sand in calibration chamber having mean diameter, D_{50}= 0.35 mm (Relative Density, D_r = 69.15 %)

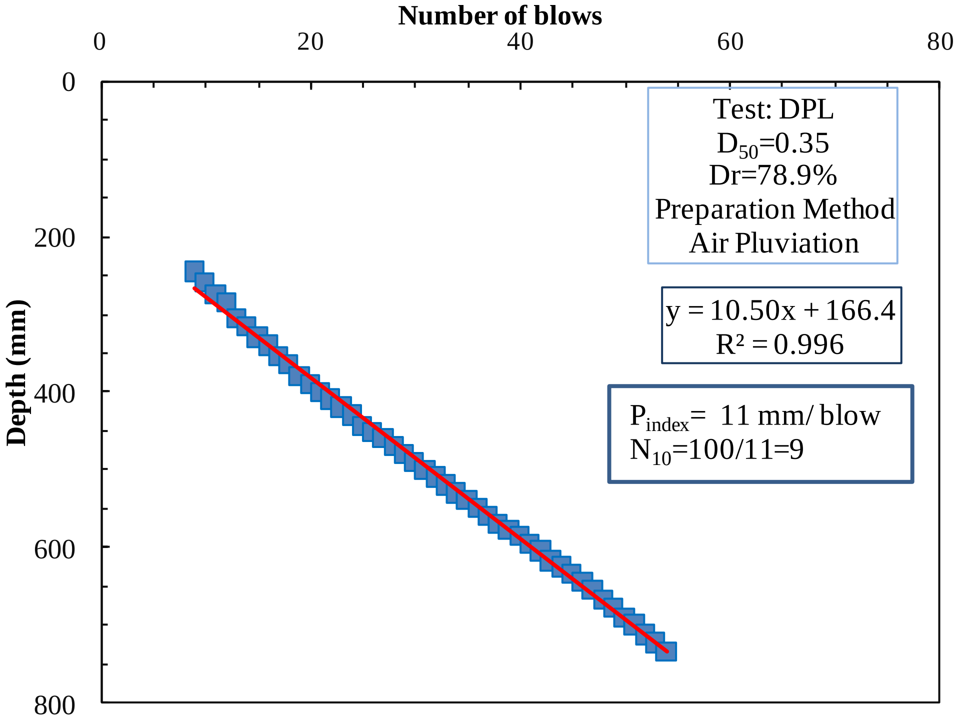

Fig. A.9: Number of blows vs. depth plot of DPL test on sand in calibration chamber having mean diameter, D_{50}= 0.35 mm (Relative Density, D_r = 78.9 %)

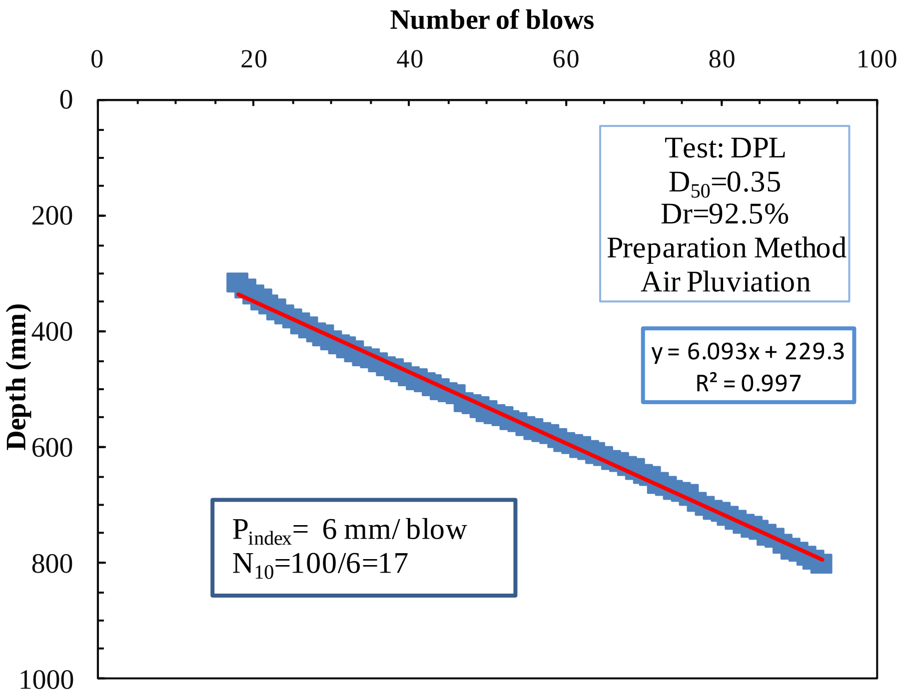

Fig. A.10: Number of blows vs. depth plot of DPL test on sand in calibration chamber having mean diameter, D_{50}= 0.35 mm (Relative Density, D_r = 92.5 %)

Test results on sand having mean diameter, D_{50}=0.70 mm in calibration chamber

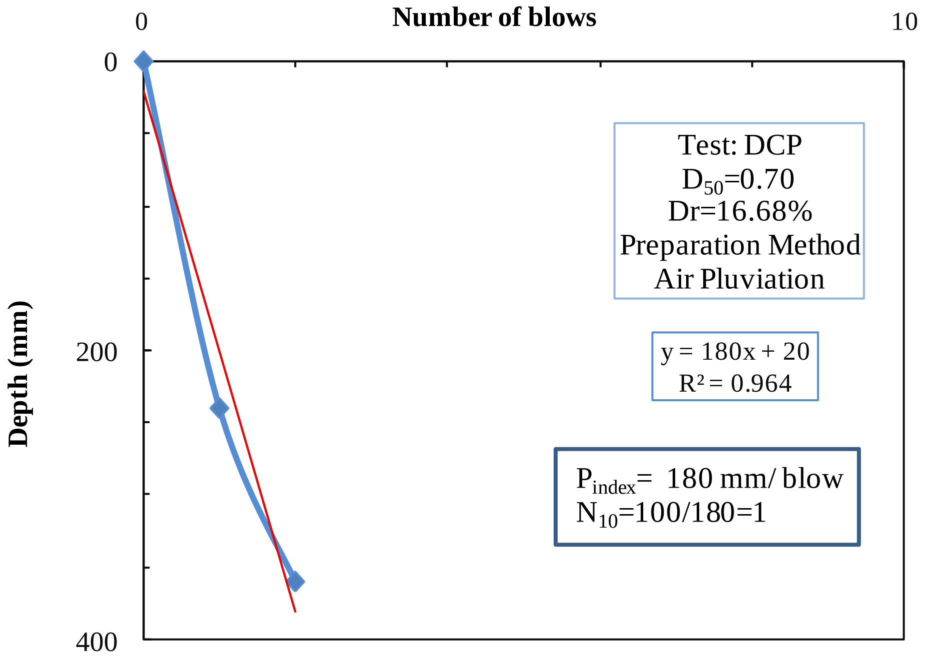

Fig. A.11: Number of blows vs. depth plot of DCP test on sand in calibration chamber having mean diameter, D_{50}= 0.70 mm (Relative Density, D_r = 16.68 %)

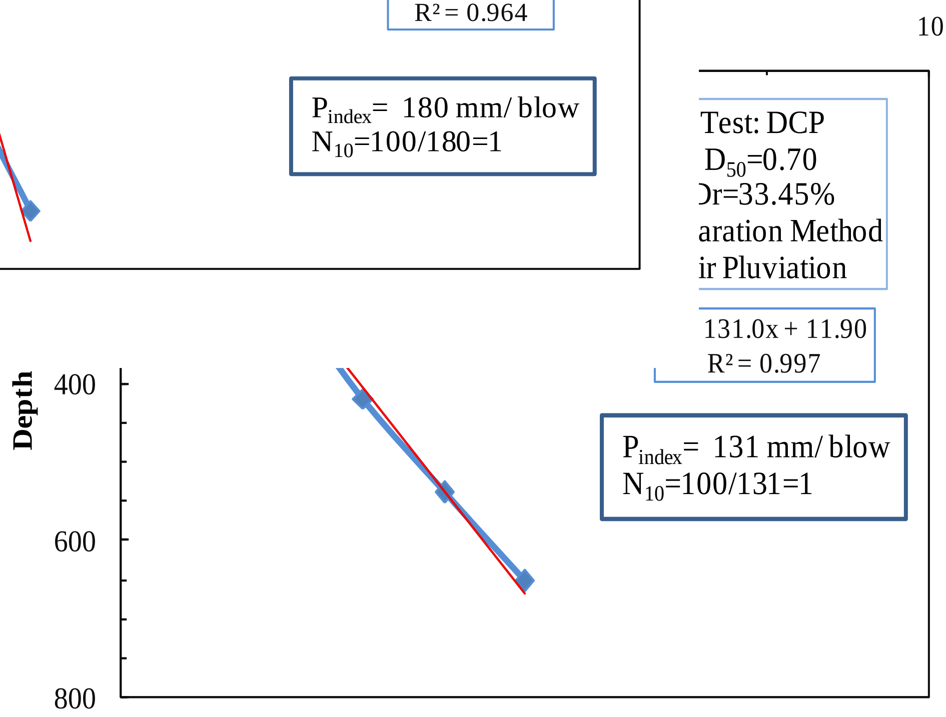

Fig. A.12: Number of blows vs. depth plot of DCP test on sand in calibration chamber having mean diameter, D_{50}= 0.70 mm (Relative Density, D_r = 33.45 %)

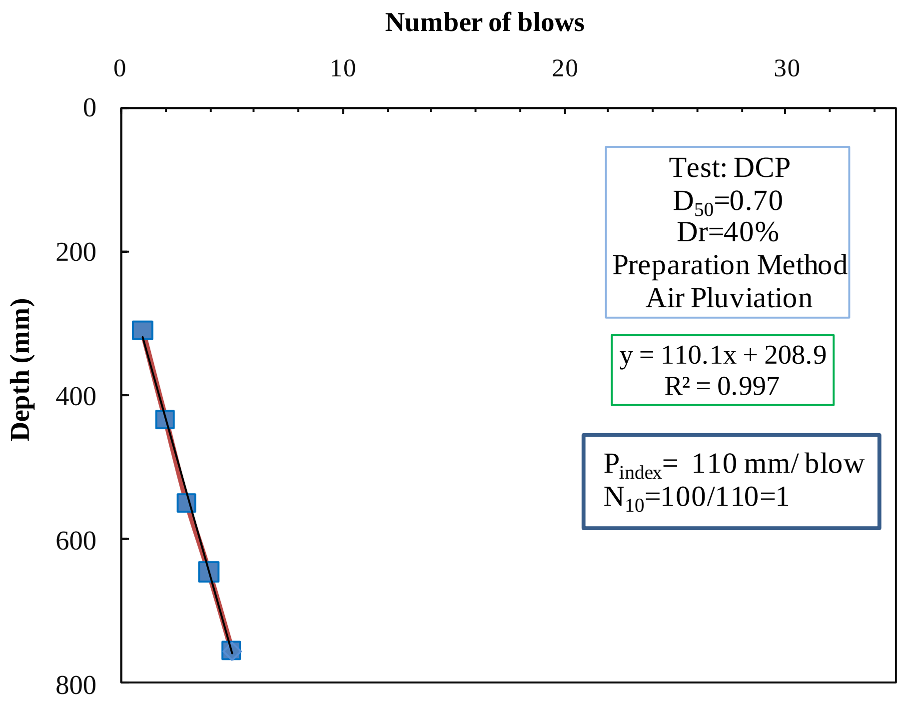

Fig. A.13: Number of blows vs. depth plot of DCP test on sand in calibration chamber having mean diameter, D_{50}= 0.70 mm (Relative Density, D_r = 40 %)

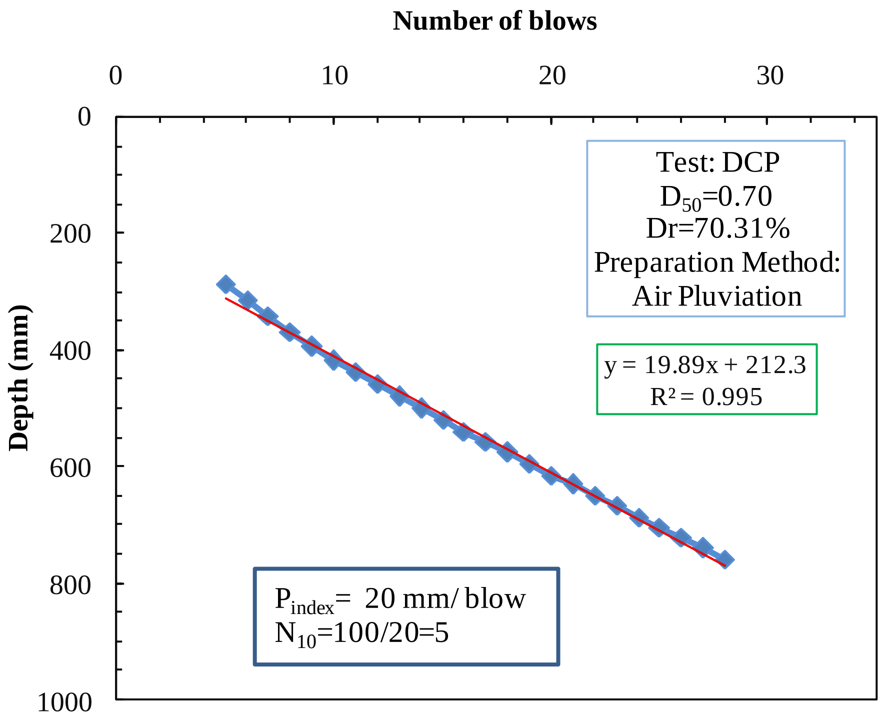

Fig. A.14: Number of blows vs. depth plot of DCP test on sand in calibration chamber having mean diameter, D_{50}= 0.70 mm (Relative Density, D_r = 70.31%)

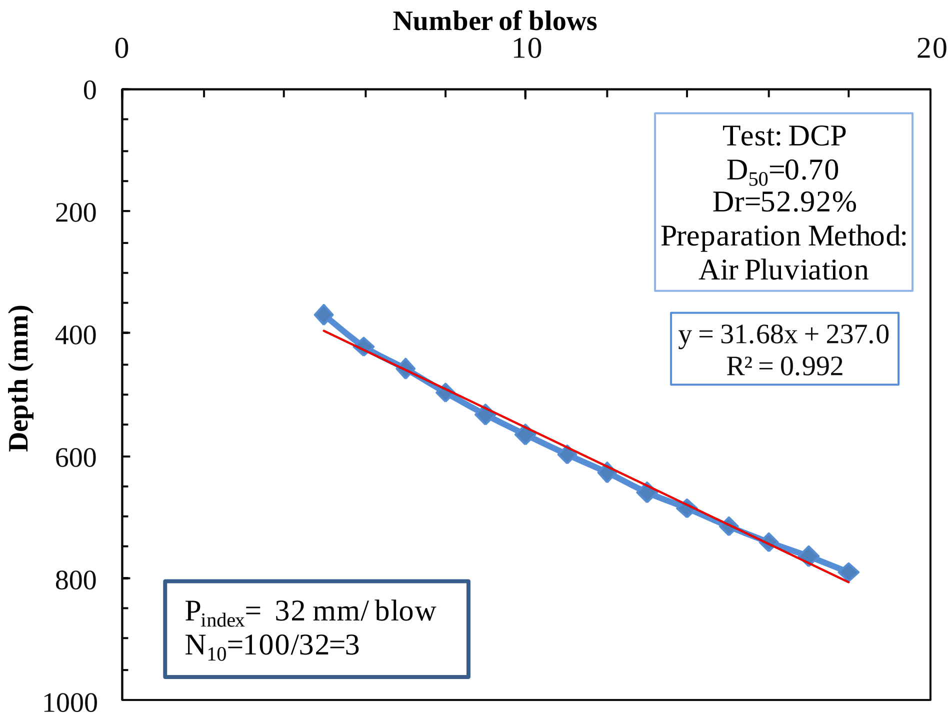

Fig. A.15: Number of blows vs. depth plot of DCP test on sand in calibration chamber having mean diameter, D_{50}= 0.70 mm (Relative Density, D_r = 52.92 %)

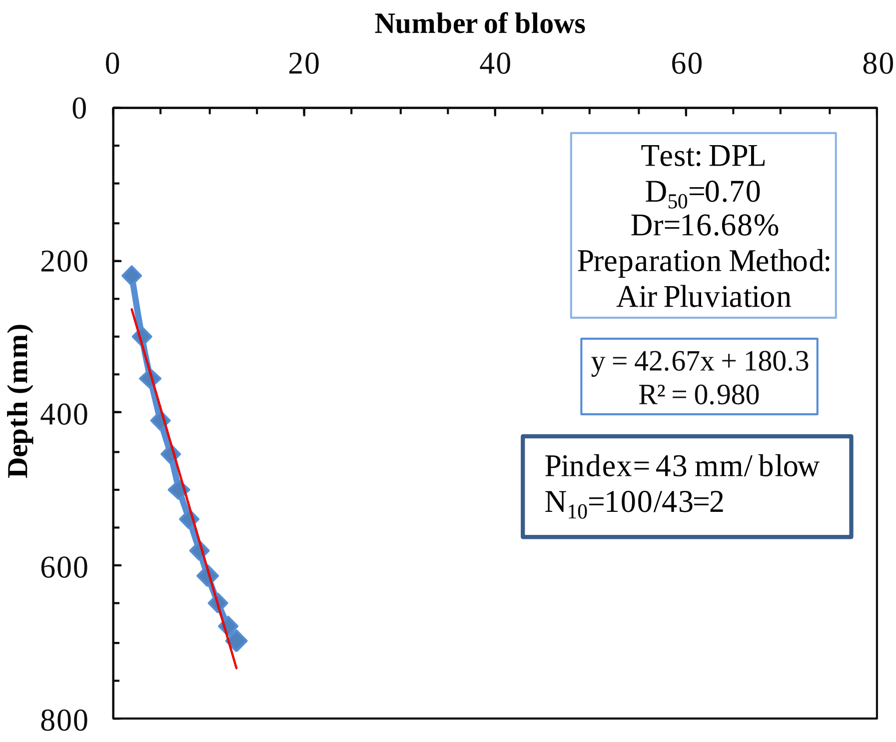

Fig. A.16: Number of blows vs. depth plot of DPL test on sand in calibration chamber having mean diameter, D_{50}= 0.70 mm (Relative Density, D_r = 16.68 %)

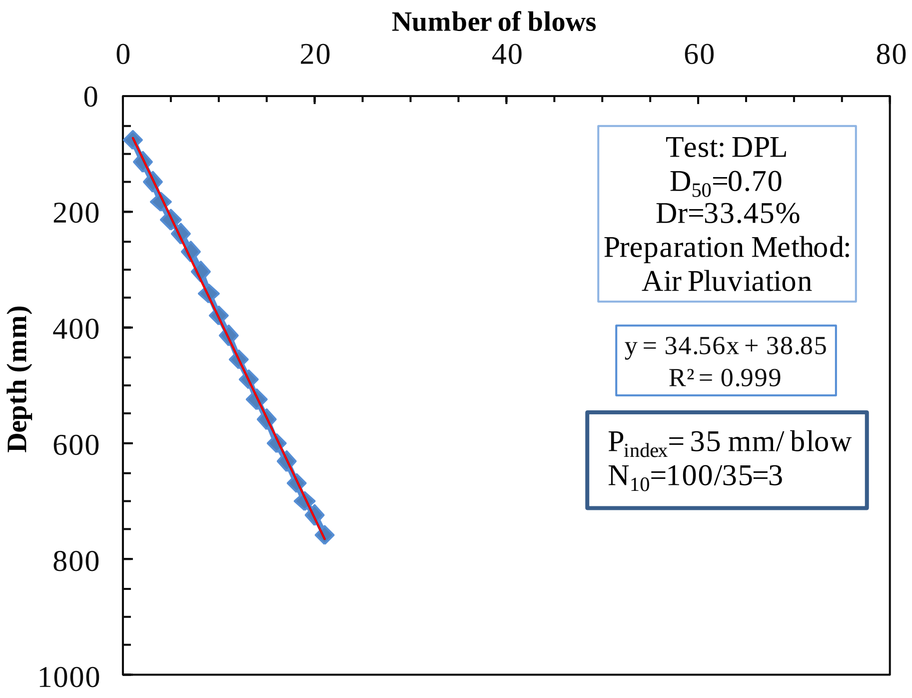

Fig. A.17: Number of blows vs. depth plot of DPL test on sand in calibration chamber having mean diameter, D_{50}= 0.70 mm (Relative Density, D_r = 33.45 %)

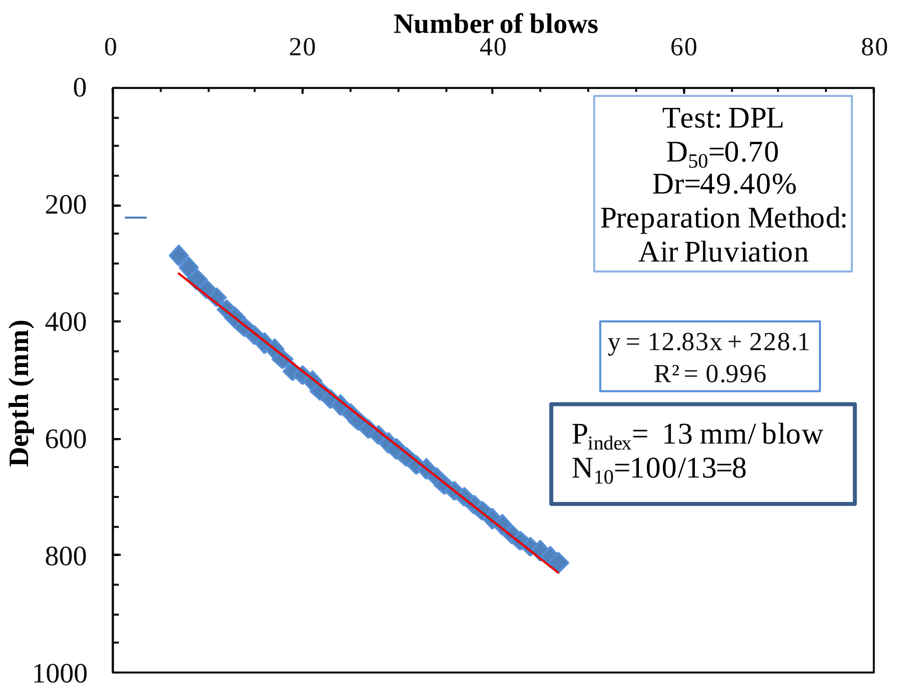

Fig. A.18: Number of blows vs. depth plot of DPL test on sand in calibration chamber having mean diameter, D_{50}= 0.70 mm (Relative Density, D_r = 49.40 %)

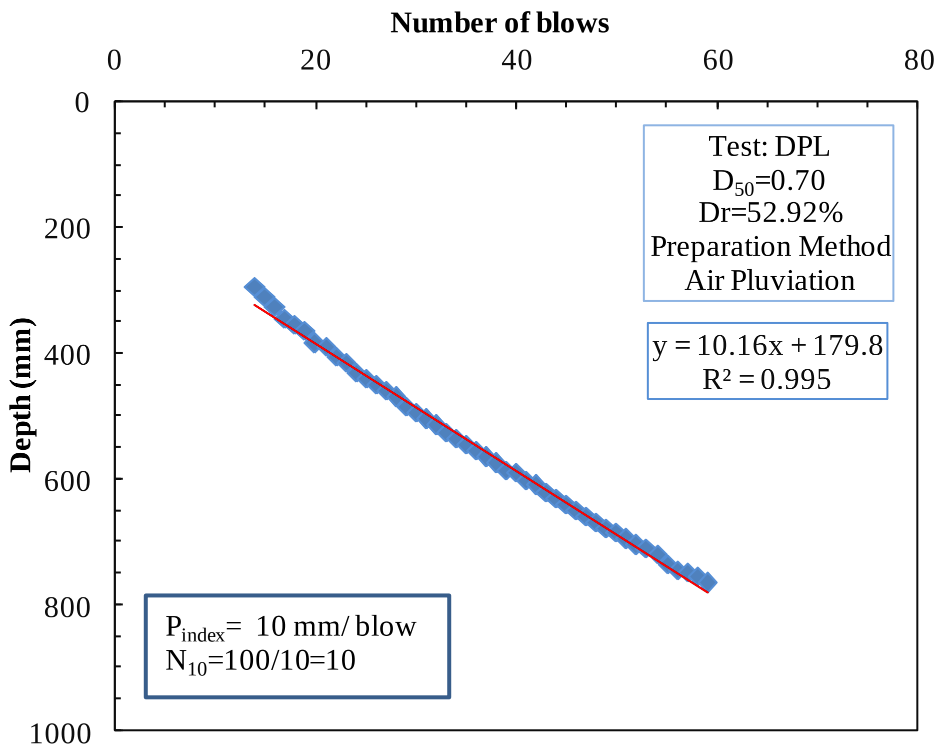

Fig.

A.19: Number of blows vs. depth plot of DPL test on sand in calibration chamber having mean diameter, D_{50}= 0.70 mm (Relative Density, D_r = 52.92 %)

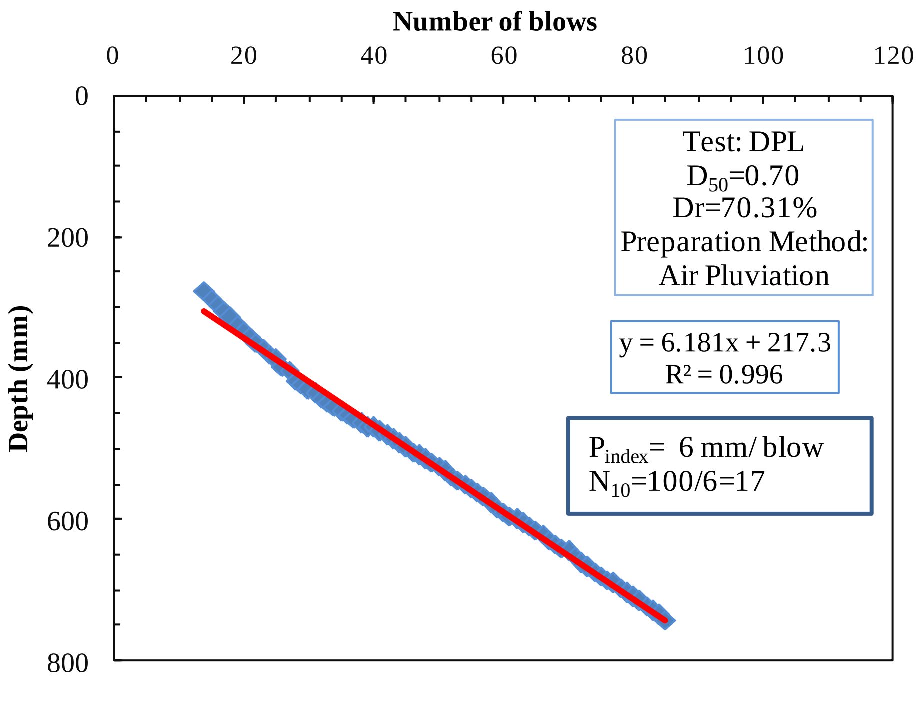

Fig. A.20: Number of blows vs. depth plot of DPL test on sand in calibration chamber having mean diameter, D_{50}= 0.70 mm (Relative Density, D_r = 70.31 %)

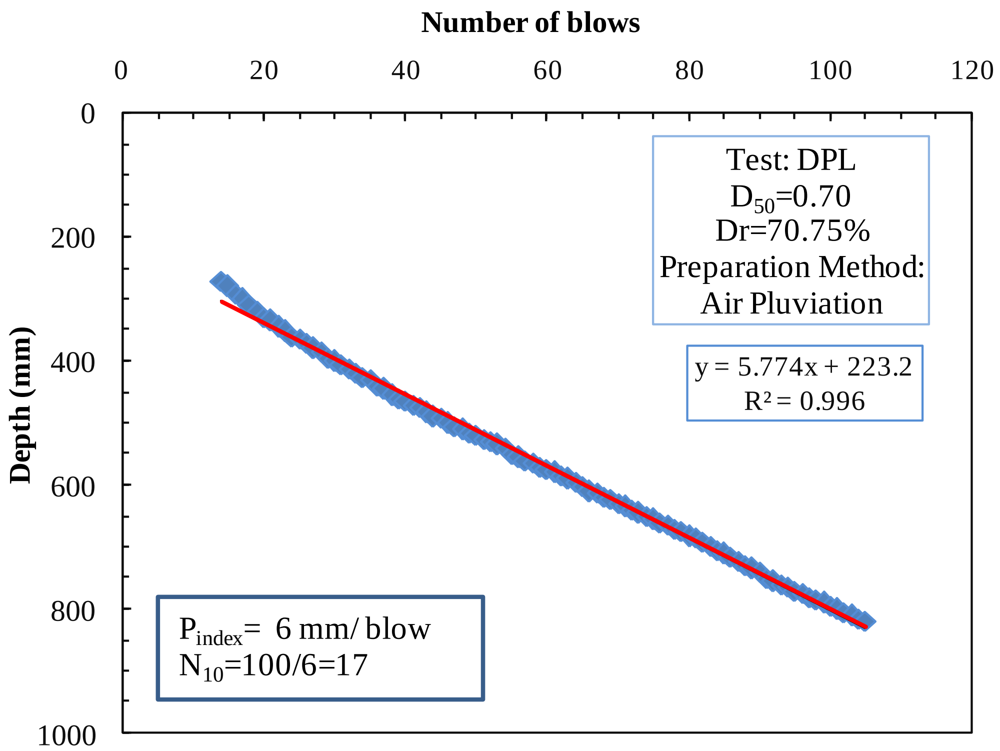

Fig. A.21: Number of blows vs. depth plot of DPL test on sand in calibration chamber having mean diameter, D_{50}= 0.70 mm (Relative Density, D_r = 70.75 %)

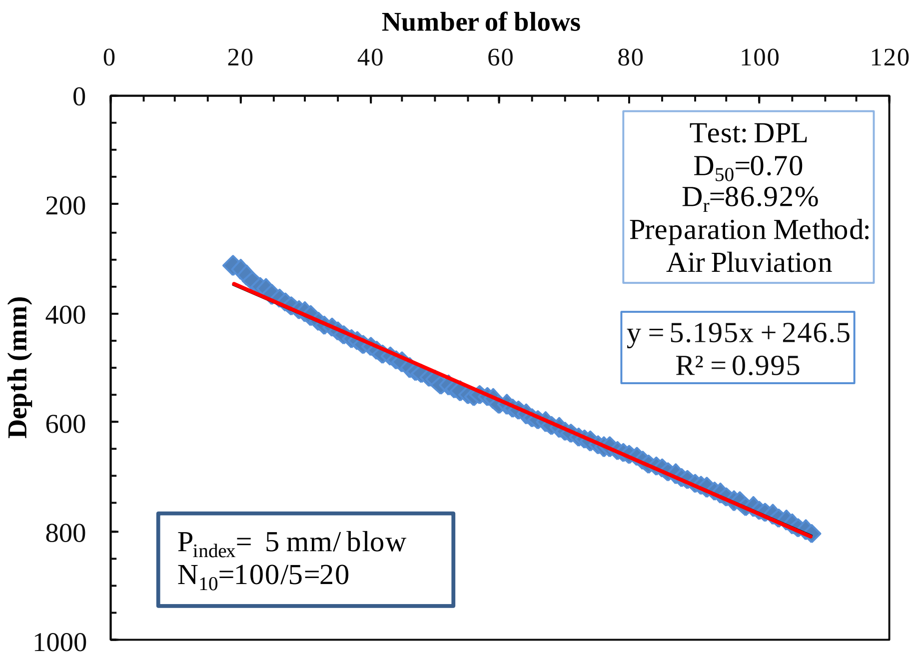

Fig. A.22: Number of blows vs. depth plot of DPL test on sand in calibration chamber having mean diameter, D_{50}= 0.70 mm (Relative Density, D_r = 86.92 %)

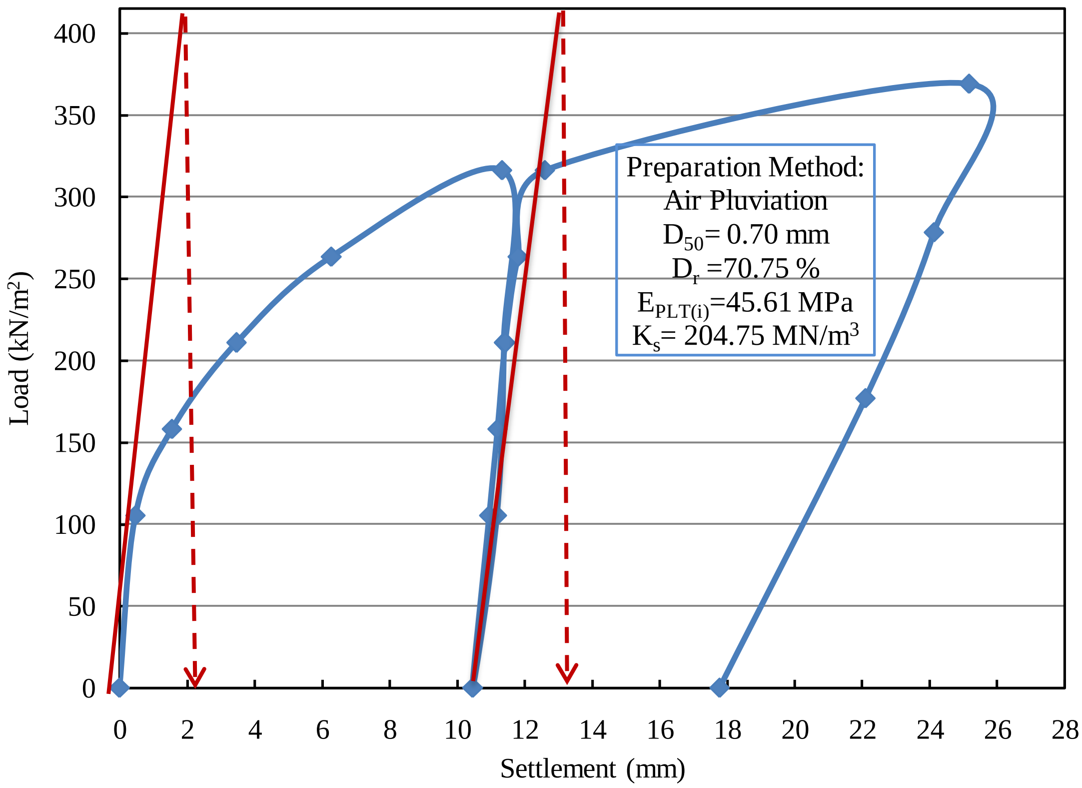

Fig. A.23: Correlation between normal stress and settlement at Dr=70.75% of D_{50}=0.70 mm

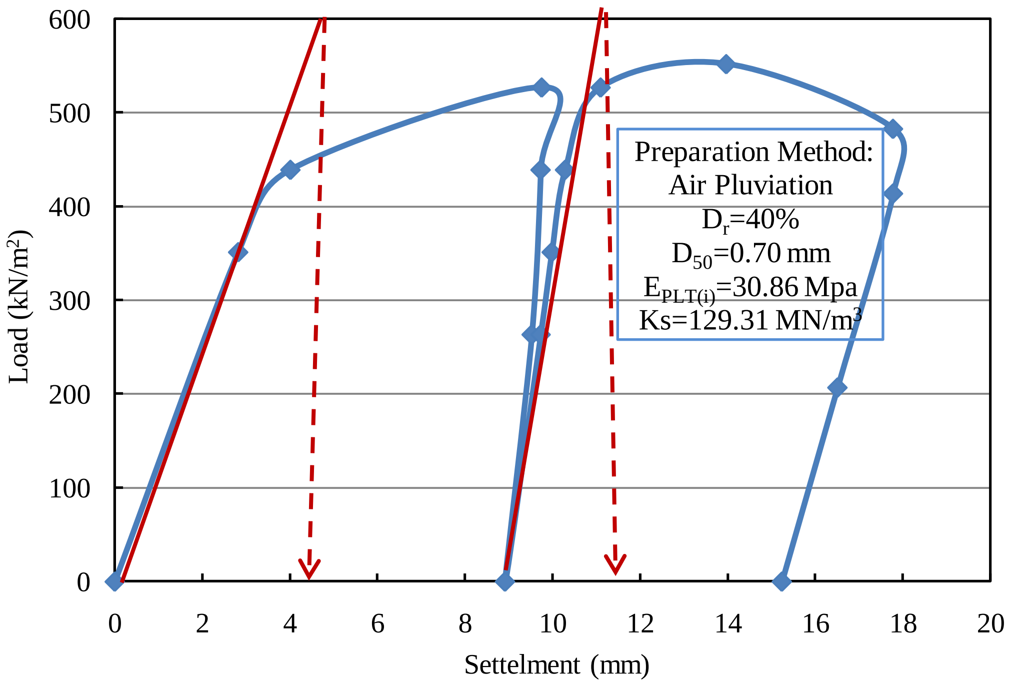

Fig .A.24: Correlation between normal stress and settlement at Dr=40% of D_{50}=0.70 mm

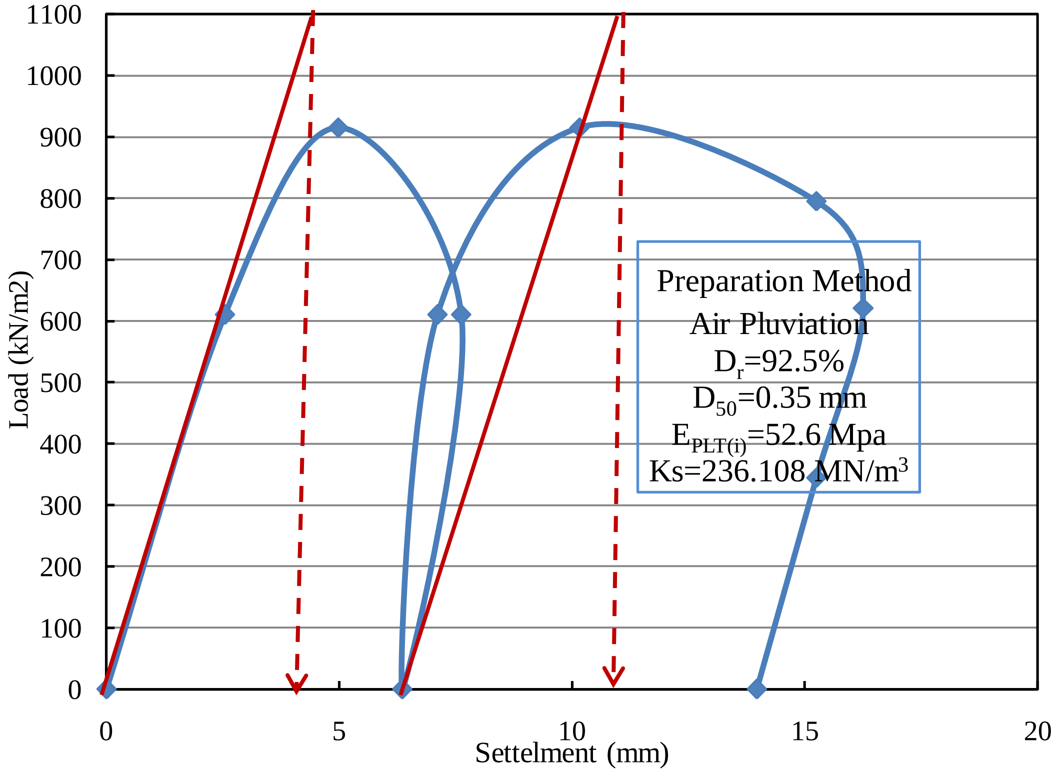

Fig. A.25: Correlation between normal stress and settlement at Dr=92.5% of D_{50}=0.35 mm

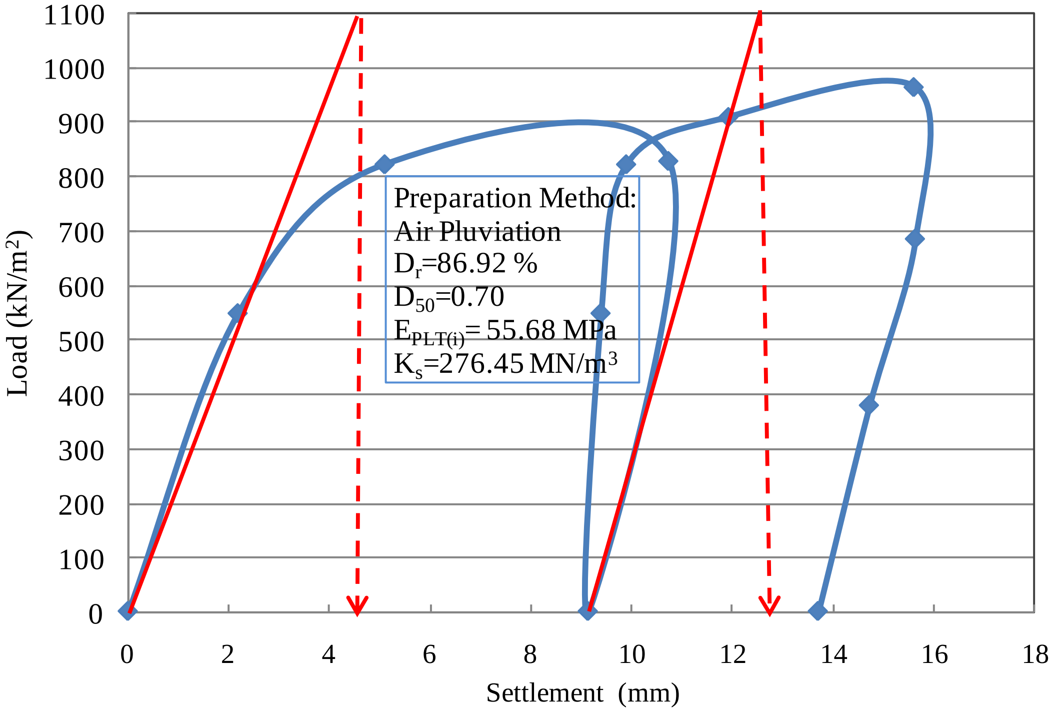

Fig. A.26: Correlation between normal stress and settlement at Dr=86.92 % of D_{50}=0.70 mm

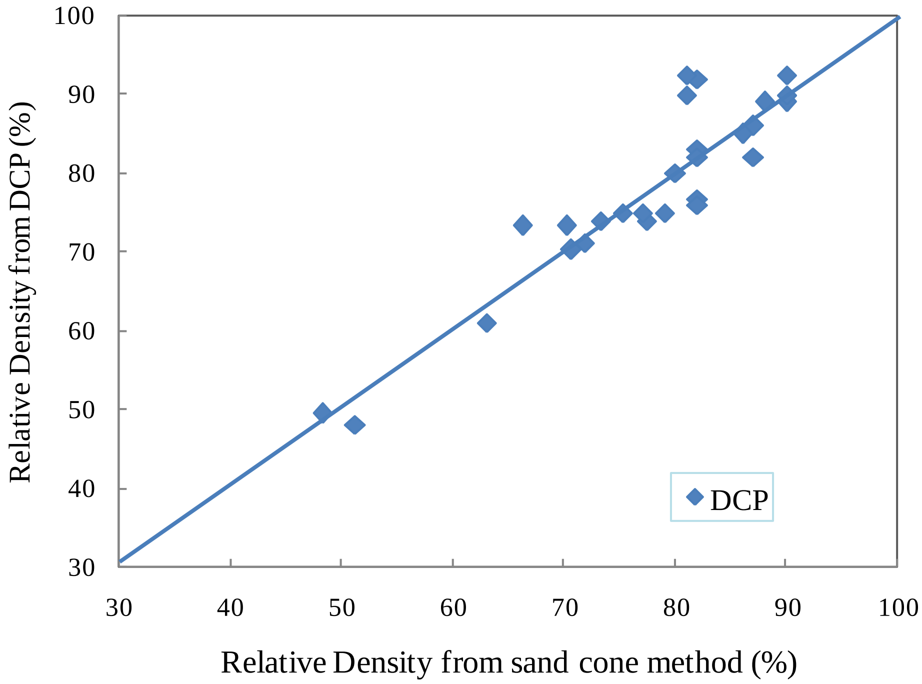

Fig. A.27: Comparison of Relative Density obtained from DCP test and Sand Cone Method before introduction of correction factor

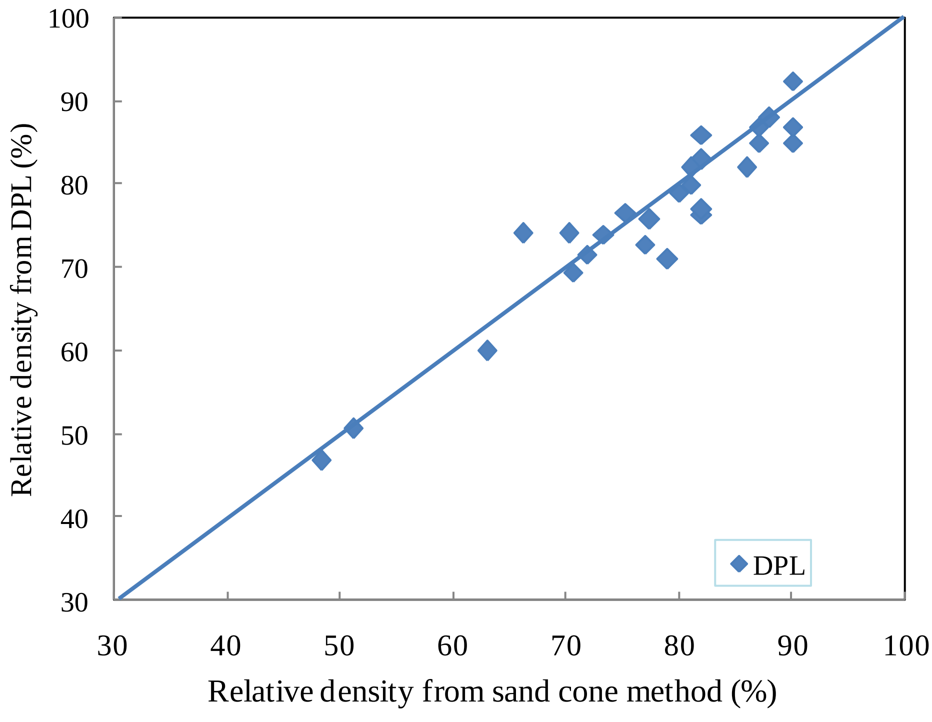

Fig. A.28: Comparison of Relative Density obtained from DPL test and Sand Cone Method before introduction of correction factor

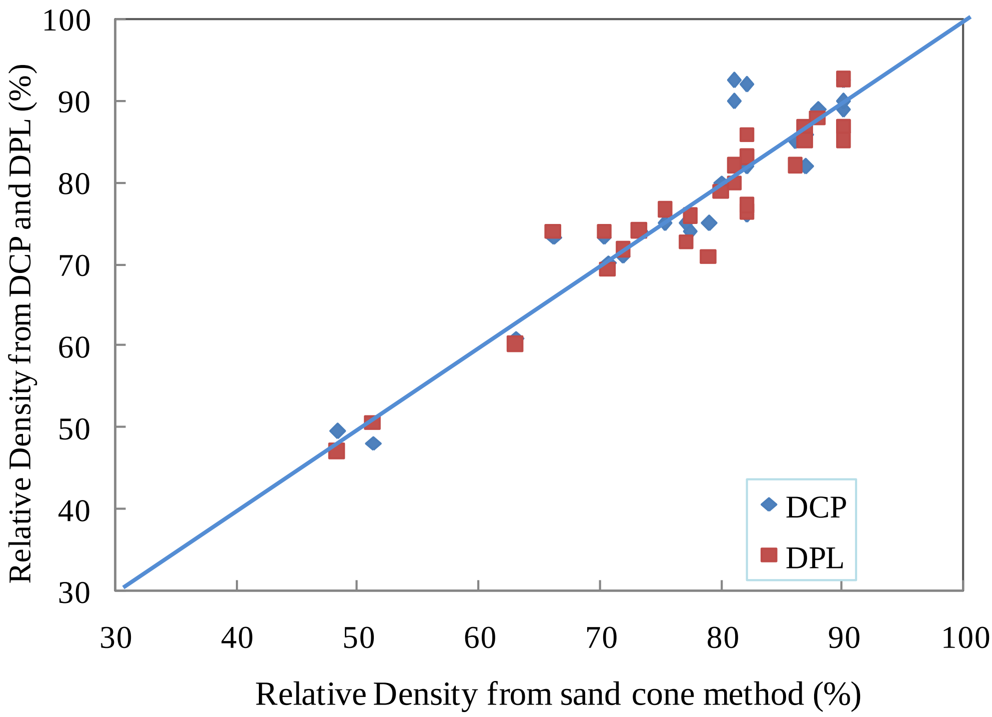

Fig. A.29: Comparison of Relative Density obtained from DCP and DPL test and Sand Cone Method before introduction of correction factor

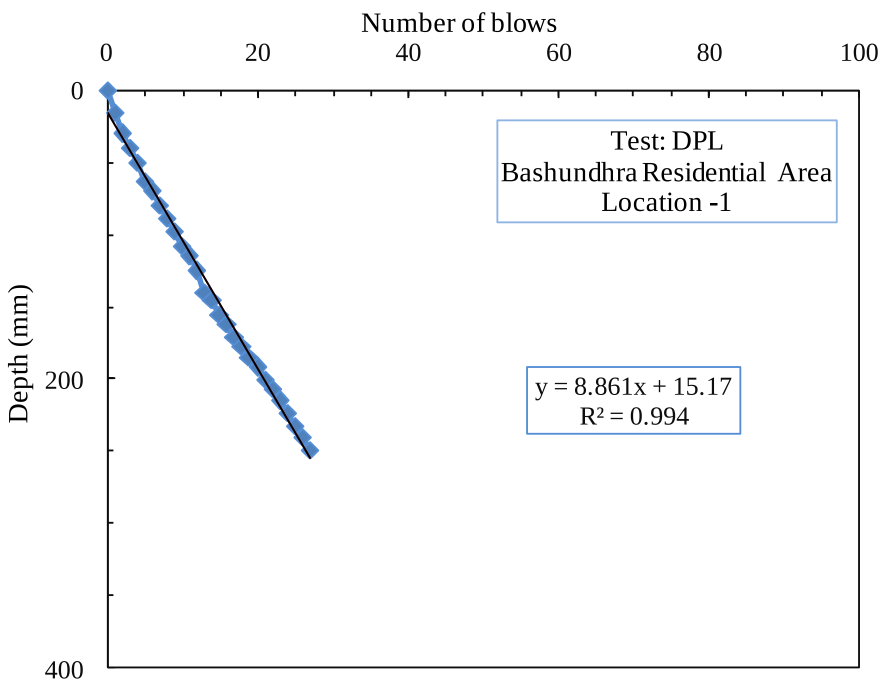

Fig. A.30: Number of blows vs. depth plot of DPL test at location 1 of Bashundhara Residential Area up to depth 250 mm

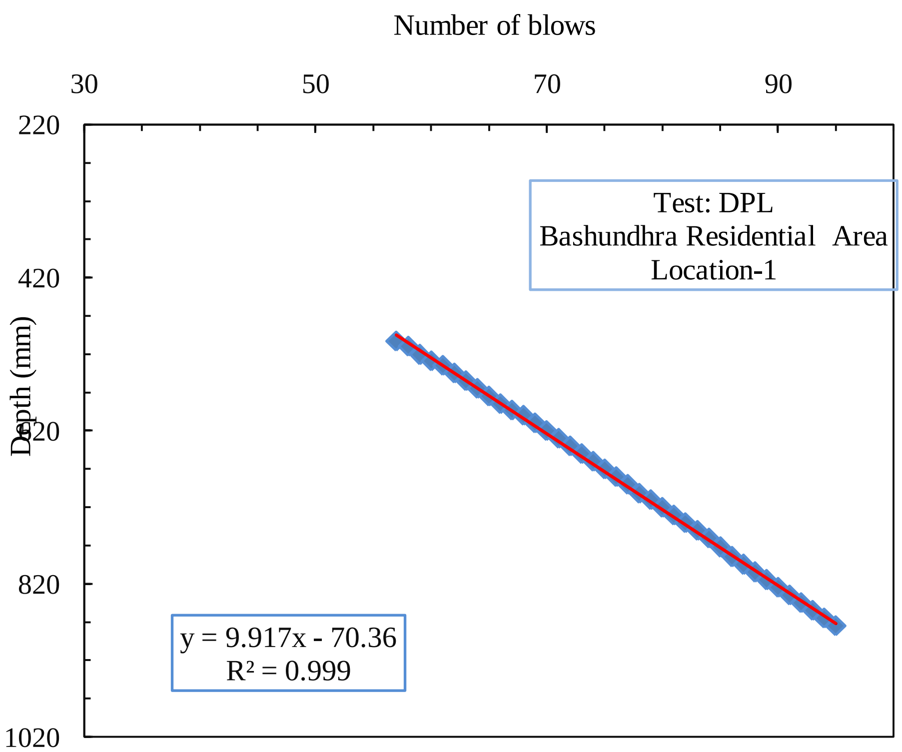

Fig. A.31: Number of blows vs. depth plot of DPL test at location 1 of Bashundhara Residential Area at depth 500 mm to 870 mm

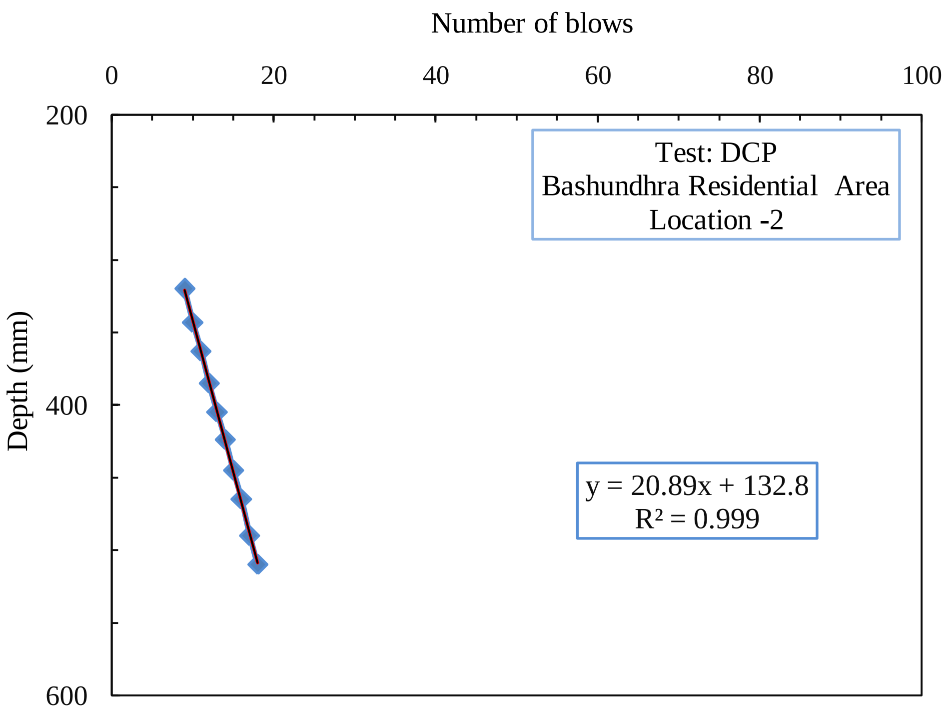

Fig. A.32: Number of blows vs. depth plot of DCP test at location 2 of Bashundhara Residential Area at depth 300 mm to 500 mm

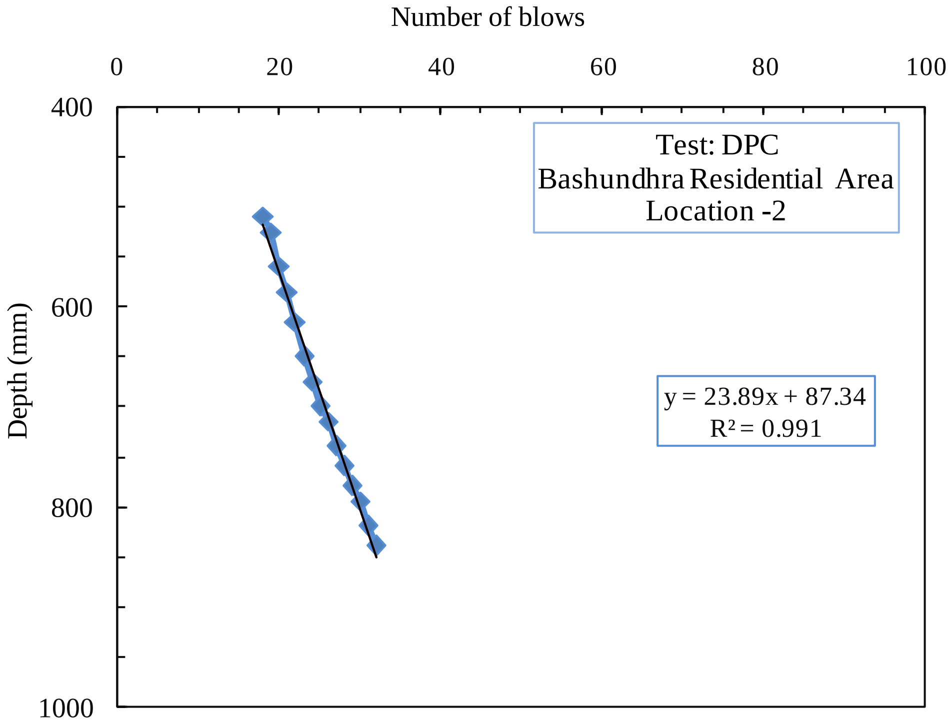

Fig. A.33: Number of blows vs. depth plot of DCP test at location 2 of Bashundhara Residential Area at depth 500 mm to 850 mm

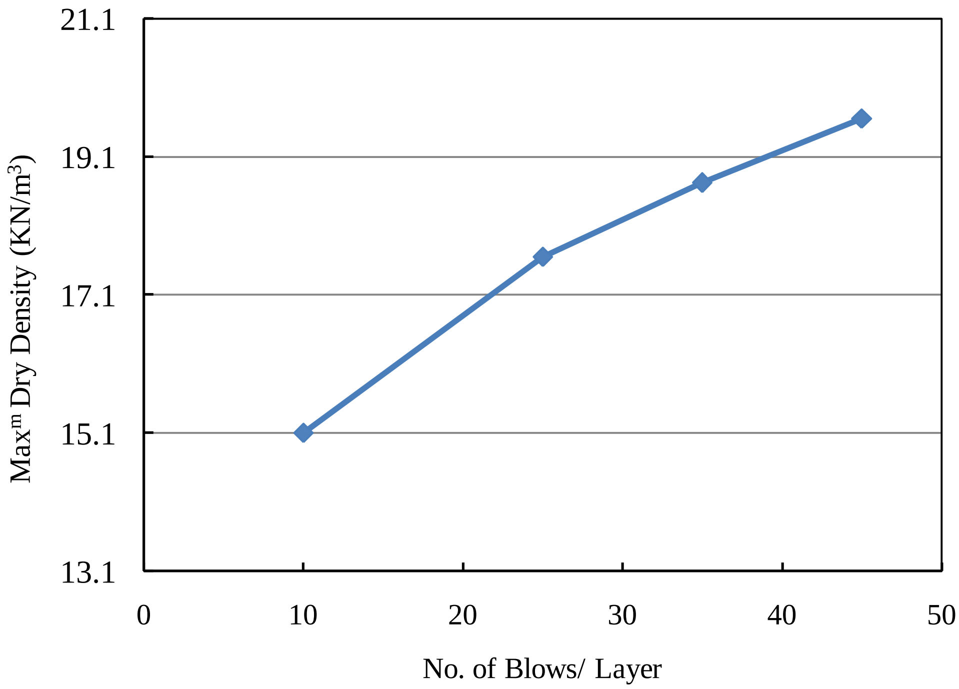

Fig. A.34: Variation between dry density and No. of blows at location 2 (Bashundhra Site)

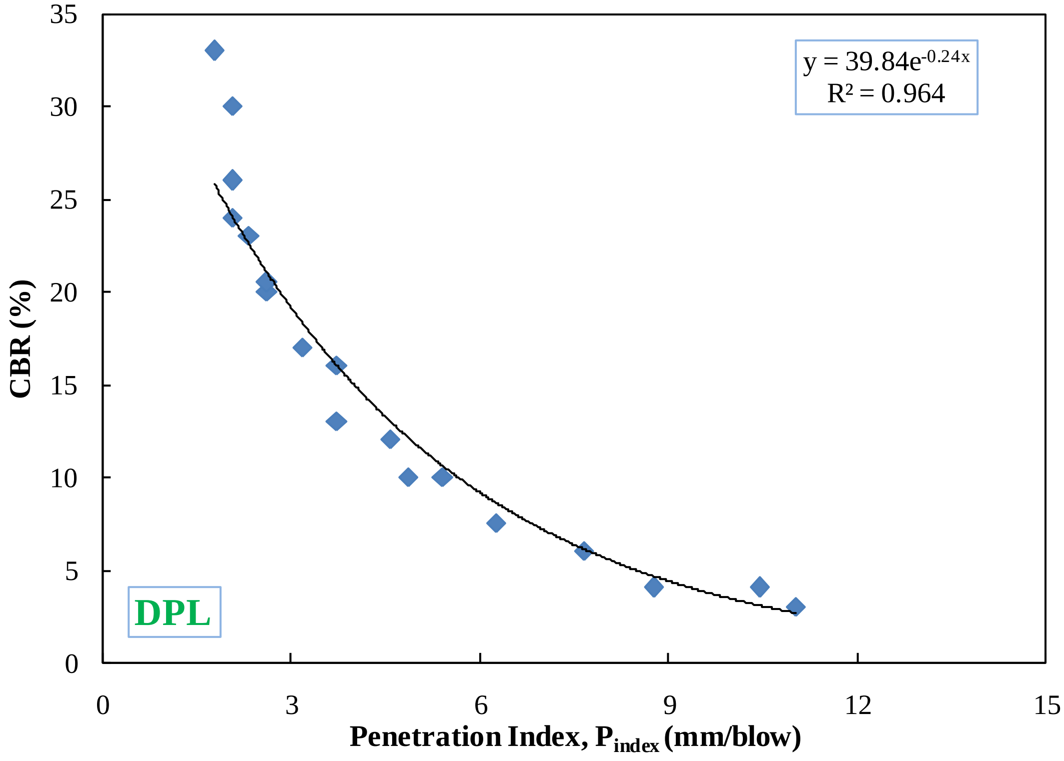

Fig. A.35: Correlation between DPL Penetration Index (P_{index}) and CBR (%)